ZooKeys 925: 1–54 (2020)
doi: 10.3897/zookeys.925.39691
http://zookeys.pensoft.net

RESEARCH ARTICLE

A peer-reviewed open-access journal
ZooKeys
Launched to accelerate biodiversity research

Sitticine jumping spiders: phylogeny, classification, and chromosomes (Araneae, Salticidae, Sitticini)

Wayne P. Maddison[1], David R. Maddison[2], Shahan Derkarabetian[3,4], Marshal Hedin[3]

1 *Departments of Zoology and Botany and Beaty Biodiversity Museum, University of British Columbia, 6270 University Boulevard, Vancouver, British Columbia, V6T 1Z4, Canada* **2** *Department of Integrative Biology, Oregon State University, Corvallis, OR 97331, USA* **3** *Department of Biology, San Diego State University, San Diego, CA 92182, USA* **4** *Department of Organismic and Evolutionary Biology, Harvard University, Cambridge MA 02138, USA*

Corresponding author: Wayne P. Maddison (wayne.maddison@ubc.ca)

Academic editor: J. Miller | Received 4 September 2019 | Accepted 5 February 2020 | Published 8 April 2020

http://zoobank.org/BB966609-0878-49A1-B13C-138C2495E6B7

Citation: Maddison WP, Maddison DR, Derkarabetian S, Hedin M (2020) Sitticine jumping spiders: phylogeny, classification, and chromosomes (Araneae, Salticidae, Sitticini). ZooKeys 925: 1–54. https://doi.org/10.3897/zookeys.925.39691

Abstract

The systematics of sitticine jumping spiders is reviewed, with a focus on the Palearctic and Nearctic regions, in order to revise their generic classification, clarify the species of one region (Canada), and study their chromosomes. A genome-wide molecular phylogeny of 23 sitticine species, using more than 700 loci from the arachnid Ultra-Conserved Element (UCE) probeset, confirms the Neotropical origins of sitticines, whose basal divergence separates the **new subtribe** Aillutticina (a group of five Neotropical genera) from the subtribe Sitticina (five genera of Eurasia and the Americas). The phylogeny shows that most Eurasian sitticines form a relatively recent and rapid radiation, which we unite into the genus *Attulus* Simon, 1868, consisting of the subgenera *Sitticus* Simon, 1901 (seven described species), *Attulus* (41 described species), and *Sittilong* Prószyński, 2017 (one species). Five species of *Attulus* occur natively in North America, presumably through dispersals back from the Eurasian radiation, but an additional three species were more recently introduced from Eurasia. *Attus palustris* Peckham & Peckham, 1883 is considered to be a full synonym of *Euophrys floricola* C. L. Koch, 1837 (not a distinct subspecies). *Attus sylvestris* Emerton, 1891 is removed from synonymy and recognized as a senior synonym of *Sitticus magnus* Chamberlin & Ivie, 1944. Thus, the five native *Attulus* in North America are *Attulus floricola*, *A. sylvestris*, *A. cutleri*, *A. striatus*, and *A. finschi*. The other sitticines of Canada and the U.S.A. are placed in separate genera, all of which arose from a Neotropical radiation including *Jollas* Simon, 1901 and *Tomis* F.O.Pickard-Cambridge, 1901: (1) *Attinella* Banks, 1905 (*A. dorsata*, *A. concolor*, *A. juniperi*), (2) *Tomis* (*T. welchi*), and

(3) *Sittisax* Prószyński, 2017 (*S. ranieri*). All Neotropical and Caribbean "*Sitticus*" are transferred to either *Jollas* (12 species total) or *Tomis* (14 species). *Attinella* (three species) and *Tomis* are both removed from synonymy with *Sitticus*; the synonymy of *Sitticus cabellensis* Prószyński, 1971 with *Pseudattulus kratochvili* Caporiacco, 1947 is restored; *Pseudattulus* Caporiacco, 1947 is synonymized with *Tomis*. Six generic names are newly synonymized with *Attulus* and one with *Attinella*. Two Neotropical species are described as new, *Jollas cupreus* **sp. nov.** and *Tomis manabita* **sp. nov.** Forty-six new combinations are established and three are restored. Three species synonymies are restored, one is new, and two are rejected. Across this diversity of species is a striking diversification of chromosome complements, with X-autosome fusions occurring at least four times to produce neo-Y sex chromosome systems (X_1X_2Y and $X_1X_2X_3Y$), some of which (*Sittisax ranieri* and *S. saxicola*) are sufficiently derived as to no longer preserve the simple traces of ancestral X material. The correlated distribution of neo-Y and a base autosome number of 28 suggests that neo-Y origins occurred preferentially in lineages with the presence of an extra pair of autosomes.

Keywords

Amycoida, karyotype, molecular phylogeny, Salticinae, sex chromosomes

Introduction

The jumping spider species long placed in the genus *Sitticus* Simon, 1901 are well known in both Eurasia and the Americas as prominent members of habitats as diverse as boreal forests, marshes, deserts and human habitations (e.g., Locket and Milledge 1951; Prószyński 1968, 1971, 1973, 1980; Harm 1973; Logunov and Marusik 2001). They belong to the tribe Sitticini, characterized morphologically by the loss of a retromarginal cheliceral tooth, long fourth legs, and an embolus fixed to the tegulum. Phylogenetic studies have suggested that sitticines arose in the Neotropics, dispersed to Eurasia, and radiated there (Maddison and Hedin 2003; Maddison 2015), a breadth of distribution rarely seen in recent lineages of salticids. The Neotropical sitticines (Figs 1–10) show considerable diversity, with some species having males with colourful and fringed courtship ornaments (*Aillutticus* Galiano, 1987; Figs 2, 3), and others with shiny metallic colours (*Jollas geniculatus* group; Figs 7, 113–116). The Eurasian radiation is more sedate in appearance, though there is still diversity in form and markings in *Attulus* Simon, 1868 (Figs 15–47).

This work's three goals are to resolve sitticine phylogeny, to review the taxonomy of sitticines of one region (Canada), and to describe the remarkably diverse chromosomes of sitticines. Our immediate (and urgent) purpose in studying the group's phylogeny is to settle its turbulent generic classification, which has seen, for instance, some well-known species change names three times in two years, for example, from *Sitticus floricola* (C. L. Koch, 1837) to *Sittiflor floricola* (by Prószyński 2017a) to *Calositticus floricola* (by Blick and Marusik 2018) and back to *Sitticus floricola* (by Breitling 2019).

Until the last few years, most sitticines were placed in the single widespread and species-rich genus *Sitticus* Simon, 1901 (e.g., Platnick 2014 listed 84 species). Prószyński, who developed our understanding of north-temperate species in a series

of papers (1968, 1971, 1973, 1980), recently (2016, 2017a) partitioned this diversity into several genera: *Sittipub* Prószyński, 2016, *Sittiflor* Prószyński, 2017, *Sittilong* Prószyński, 2017, *Sittisax* Prószyński, 2017, *Sittiab* Prószyński, 2017, *Attulus*, and *Sitticus*. Prószyński did not intend this classification to be phylogenetic, but rather "pragmatic" (Prószyński 2017b), which is to say, not based on a conceptual justification. If a classification rejects reference to a broader theory, whether about monophyly or adaptive zones or predictivity across many characters, then it is not clear what it means, how it can be tested, or whether it can even be correct, except in its specific statements about the few characters mentioned. Furthermore, Prószyński provides little discussion of the diagnostic characters, indeed arguing against explicitly stating or explaining them (see Prószyński 2017a; Kropf et al. 2019). Thus, both his characters and his taxa remain inscrutable.

Breitling (2019) reversed Prószyński's splitting by synonymizing many of the genera back into *Sitticus*, based on results from the single mitochondrial gene COI. We are fortunate that Breitling followed only a small fraction of the implications of his COI gene tree, for had they been followed more thoroughly they would have yielded taxonomic chaos in sitticines and throughout salticids, given that they scramble many well-supported salticid relationships, splitting (for instance) *Sitticus* sensu lato among five different tribes (discussed below, with our phylogenetic results). That COI is particularly bad at resolving salticid phylogeny has been reported previously (Hedin and Maddison 2001; Maddison et al. 2008, 2014; Bodner and Maddison 2012; Maddison and Szűts 2019). The results from this single mitochondrial gene therefore have given us no secure basis for sitticine taxonomy.

Neither Prószyński's "pragmatic" classification nor Breitling's COI-based classification have promoted taxonomic stability in sitticines. Prószyński's intentionally non-phylogenetic approach is particularly problematical. The great majority of systematists no longer use such "pragmatic" non-evolutionary classifications, as they are not anchored to a broadly predictive external reality: they are subject to the whims of biologists' interests and the character systems they focus on. A taxon delimited for this sense of pragmatism carries with it no promise of meaning or utility, other than the promise it will bear the diagnostic characters chosen. Different choices of diagnostic characters would lead to different classifications, with no basis for selecting among different authors' approaches except the weight of authority – in the end, not as pragmatic as a stable phylogenetic classification, which, by the implications of genetic descent, will predict trait distributions across the genome. Breitling's approach might have dampened the instability, as it is phylogenetic and uses explicit data and analysis, but his choice of the single gene COI, without supporting morphological information, has yielded a classification in which we can have little confidence. Prószyński's and Breitling's reclassifications might have been steps forward had they been done in a group of salticids with almost no previous attention, but the sitticines are reasonably well studied and often mentioned in the literature. These sudden, comprehensive, conflicting, and largely baseless rearrangements of *Sitticus* have yielded taxonomic instability in a well-known group.

Taxonomic instability yields confusion in ecological and other biodiversity literature about the identity of species studied, and damages the reputation of the taxonomic enterprise. We are now sufficiently capable of resolving phylogeny that we do not need to rely on the "pragmatic" choices of one authority or on a single misbehaving gene. Our goal is to provide stronger evidence, explicitly analyzed, for phylogenetic relationships in order to stabilize the classification of sitticines.

Materials and methods

Morphology

Preserved specimens were examined under both dissecting microscopes and a compound microscope with reflected light. Most of the coquille drawings were done in 1977 or 1978 using a reticle grid in a stereomicroscope. Colour drawings were done in 1974 through 1977 with a stereomicroscope and reticle grid. Pen and pencil drawings were made recently using a drawing tube on a Nikon ME600L compound microscope. Because some images were made decades ago, we are unable to supply scale bars on many. Terms used are standard for Araneae. All measurements are given in millimeters. Carapace length was measured from the base of the anterior median eyes not including the lenses to the rear margin of the carapace medially; abdomen length to the end of the anal tubercle. The following abbreviations are used: ALE, anterior lateral eyes; PLE, posterior lateral eyes; PME, posterior median eyes (the "small eyes"); RTA, retrolateral tibial apophysis of the male palp.

Specimens were examined from the collections of the American Museum of Natural History (**AMNH**), the Canadian National Collection of Insects, Arachnids and Nematodes (**CNC**), the Museo Argentino de Ciencias Naturales (**MACN**), the Museum of Comparative Zoology (**MCZ**), the Museum of Zoology, Pontificia Universidad Católica, Quito, Ecuador (**QCAZ**), and the Spencer Entomological Collection of the Beaty Biodiversity Museum (**UBC-SEM**).

Nomenclatural authorities

Authors of nomenclatural acts in this paper vary by rank. For acts affecting the synonymy of genera (viz., reinstatement of *Attinella* and *Tomis*; synonymies of *Sitticus*, *Pseudattulus* and *Sittiab*), the authors are those of the paper itself. For all other acts, the author is W. Maddison. These include the establishment of the Aillutticina, new subtribe, acts that affect the synonymy and placement of species (new synonyms, restored synonyms, new combinations), and new species.

If not otherwise indicated, the authors of species names are given in the Classification section.

Molecular phylogeny

Taxa were sampled to cover a diversity of sitticine species groups from Eurasia, North America, and South America (Table 1). Most were preserved in 95% ethanol, although we attempted to obtain sequences from some species (*Attulus rupicola*, *A. striatus*, *A. cutleri*) available only as 70–80% ethanol preserved specimens. We were unable to obtain sequences from *A. striatus* and *A. cutleri*, leaving us with a total of 23 sitticine species and two outgroups. The outgroups are *Breda*, from the sister group to sitticines, and *Colonus*, from the sister group to remaining amycoids as a whole (see Ruiz and Maddison 2015; Maddison et al. 2017).

For most samples, DNA was extracted from multiple legs using the Qiagen DNeasy Blood and Tissue Kit (Qiagen, Valencia, CA) following manufacturer's protocol. Specimens d491 and d492 of *Attulus rupicola* and d493 of *A. zimmermanni* were extracted using standard phenol-chloroform methods. UCE library preparation followed methods previously used in arachnids (e.g., Starrett et al. 2017; Derkarabetian et al. 2018; Hedin et al. 2018). Target enrichment was performed using the MYbaits Arachnida 1.1K version 1 kit (Arbor Biosciences; Faircloth 2017) following the Target Enrichment of Illumina Libraries v. 1.5 protocol (http://ultraconserved.org/#protocols). Libraries were sequenced with an Illumina HiSeq 2500 (Brigham Young University DNA Sequencing Center) with 150 bp paired end reads. Raw demultiplexed reads were processed with Phyluce (Faircloth 2016), quality control and adapter removal was conducted with the Illumiprocessor wrapper (Faircloth 2013), and assemblies were created with Velvet (Zerbino et al. 2008) at default settings. The *Sittilong longipes* ARV4504 sample was sequenced on a NovaSeq 6000 at the Bauer Core Facility at Harvard University with 150 bp paired end reads, and was assembled with Trinity (Grabherr et al. 2011) with default settings. Contigs were matched to probes using minimum coverage and minimum identity values of 80. UCE loci were aligned with MAFFT (Katoh and Standley 2013) and trimmed with Gblocks (Castresana 2000; Talavera and Castresana 2007), using -- b1 0.5, --b2 0.5, --b3 10, --b4 4 settings in the Phyluce pipeline.

In the resulting set of loci, most taxa have over 100,000 base pairs of sequence data, but some are less thoroughly sequenced. The less thoroughly sequenced taxa are: *J. leucoproctus* d478 (13,943 bp), *Attulus rupicola* d491 (46,660 bp), *Attulus rupicola* d492 (65,500 bp), and *A. zimmermanni* d493 (68,285 bp). The last species is represented by an alternative well-sequenced specimen, the others by well-sequenced close relatives. Although we did analyses with the entire set of taxa ("All Taxa"), we were concerned that the weakly sequenced taxa would disrupt resolution. Therefore, we rely primarily on analyses (and bootstrap values) that exclude these and use only the remaining well-sequenced taxa ("Core Taxa"). The Core Taxa dataset also excludes the less thoroughly sequenced of the two specimens of *Jollas cupreus* (d473, 92,549 bp).

This pipeline therefore resulted in two collections of genes, one of 968 loci for all the taxa ("All Taxa"), the other of 957 loci for the core set of well-sequenced taxa

Table 1. Specimens from which UCE sequence data gathered. "UCE loci" indicates number of loci from Phyluce. "Reads Pass QC" indicates number of reads retained after quality control and adapter removal via Illumiprocessor.

Species	Specimen	sex	Locality	Reads Pass QC	Contigs	UCE loci
Ailluticus nitens	d475	f	Uruguay: Canelones: -34.867, -56.009	946351	207743	434
Attinella dorsata	d490	m	U.S.A.: California: 37.2834, -120.8515	1617332	360661	480
Attulus ammophilus	d482	m	Canada: British Columbia: 49.7963, -119.5338	1471891	351670	588
A. burjaticus	RU18-7302	f	Russia: Tuva: 50.205, 95.135	529905	151897	627
A. distinguendus	RU18-6432	f	Russia: Tuva: 50.746, 93.142	406186	90846	626
A. fasciger	d487	m	Canada: Ontario: 43.35074, -79.75928	1370738	299273	564
A. finschi	d480	m	Canada: British Columbia: 49.0261, -114.0611	1489551	303924	579
A. floricola	d488	m	Canada: Saskatchewan: 52.4898, -107.3843	1466702	303612	606
A. inexpectus	RU18-6799	m	Russia: Tuva: 50.669, 92.9844	261947	60612	653
A. longipes	ARV4504	m	Italy: Stilfs	16385503	42677	515
A. mirandus	RU18-7308	f	Russia: Tuva: 50.205, 95.135	468358	110900	649
A. pubescens	d483	m	Canada: British Columbia: 49.2, -123.2	1316697	279173	503
A. rupicola	d491	m	Poland: Cisna near Lesko	187507	58418	312
A. rupicola	d492	m	Poland: Bukowksa Kopa	418777	137114	397
A. saltator	d512	m	Germany: Saxony: 51.607, 12.711	416618	113416	591
A. sylvestris	d489	m	U.S.A.: California: 36.3646, -121.5544	1289981	278727	506
A. terebratus	RU18-5346	m	Russia: Novosibirsk Oblast: 53.73, 77.866	306744	72547	668
A. zimmermanni	d493	m	Poland: Grabarka 52.417, 23.005	338718	113167	408
A. zimmermanni	RU18-5156	m	Russia: Novosibirsk Oblast: 53.721, 77.726	435654	93640	627
Breda bicruciata	d471	f	Uruguay: Lavalleja: -34.426, -55.195	646088	248616	549
Colonus hesperus	d472	m	U.S.A.: Arizona: 34.5847, -112.5707	1015130	250378	448
Jollas cellulanus	d479	f	Argentina: Neuquén: -37.0679, -69.7566	981935	268639	497
J. cupreus	d473	m	Ecuador: Orellana: -0.526, -77.418	1419103	289905	469
J. cupreus	d474	m	Ecuador: Orellana: -0.526, -77.418	3513351	723782	607
J. leucoproctus	d478	f	Uruguay: Maldonado: -34.94, -54.95	121131	61298	109
Sittisax ranieri	d481	m	U.S.A.: Oregon: 44.0322, -121.6722	1529835	322636	536
Tomis manabita	d476	m	Ecuador: Manabí: -1.5497, -80.8104	2524270	710859	651
T. palpalis	d477	m	Ecuador: Napo: -0.1996, -77.7023	1211674	256367	582

("Core Taxa"). A filter of occupancy was then applied, eliminating all loci which had sequences for fewer than seven of the 20 well-sequenced taxa of the ingroup (*Jollas*, *Attinella*, *Tomis*, *Sittisax*, *Attulus*), resulting in 810 loci in the All Taxa dataset and 803 in the Core Taxa dataset. Preliminary analyses of these loci revealed some whose gene trees strongly suggested two paralogs or chimeras were included: a single very long branch isolating a few taxa (which for all other considerations and subsequent analyses showed no indication of being so distinctive or related to one another), whose sequences differed from the others extensively and consistently. Out of caution we chose to discard a locus if its preliminary gene tree (RAxML 8.2.8, Stamatakis 2014, single search, default settings) had the longest branch at least five times longer than the second longest branch. Inspection of the results indicated this matched approximately our subjective judgment of a strong suspicion of paralogy. This filter left 749 loci in the All Taxa dataset and 757 loci in the Core Taxa dataset.

Maximum likelihood phylogenetic analyses were run using IQ-TREE version 1.6.7.1 (Nguyen et al. 2015), run via the Zephyr package (version 2.11, Maddison and Maddison 2018a) of Mesquite (Maddison and Maddison 2018b). The data were analyzed both without partitions ("unpartitioned") and partitioned by locus, allow-

ing the possibility of separate rates and substitution models (Kalyaanamoorthy et al. 2017). We ran 50 separate search replicates for the maximum likelihood tree for the concatenated analysis. We performed a standard bootstrap analysis with 1000 replicates and the same model and partition settings.

A separate small phylogenetic analysis was done to explore the distinction in *Attulus floricola* between hemispheres, using data of other specimens in Genbank and BOLD (boldsystems.org), to blend with our data. Insofar as only COI barcode data are available online, and this gene struggles to reconstruct salticid phylogeny (Hedin and Maddison 2001; Maddison et al. 2008, 2014; Bodner and Maddison 2012; Breitling 2019; Maddison and Szűts 2019), we provided a skeletal constraint tree of our UCE specimens from which we could obtain COI data, so that the gene's burden would be only to place the extra COI-only *floricola* group specimens on this skeleton. We obtained COI data for our UCE taxa by mining the UCE reads for COI-alignable bycatch. A local database was assembled in Geneious v11.0.4 comprising labeled Velvet UCE contigs for all sequenced taxa, then published *A. striatus* sequences (voucher BIOUG14302-A06) were used to query this local database using BLASTN (max e value of 1×10^{-10}). Retaining only high-coverage sequences, we recovered COI bycatch for all taxa except for *A. saltator*, *A. inexpectus*, and *A. rupicola*. For *A. saltator* and *A. rupicola* we substituted COI data from Genbank from another geographically proximate specimen. The constraint tree was set to match Figure 48 in topology. Then, we added and aligned COI sequences of *A. floricola* from scattered locations, as well as specimens of *A. caricis* (from the Netherlands) and *A. sylvestris* (from Canada). (The latter were identified in BOLD as *A. rupicola*, but inspection of genitalic photographs courtesy of G. Blagoev shows they are *A. sylvestris*.) The gene tree was recontructed by RAxML (Stamatakis 2014), with codon positions as separate partitions, and using Figure 48 as a skeletal (partial) constraint tree.

Sequence reads are deposited in the Sequence Read Archive (BioProject submission ID PRJNA605426, http://www.ncbi.nlm.nih.gov/bioproject/605426). Alignments and trees are deposited in the Dryad data repository (https://doi.org/10.5061/dryad.cjsxksn2q).

Chromosomes

Chromosomes were studied in 17 taxa of Sitticina. The specific identity of the specimen labelled "*A. rupicola*/*floricola*" is ambiguous because the voucher specimen has not been located, and the first author is not confident he was able to distinguish the two species in the 1980s. Although its specific identity is not known, it can be confidently placed within the *floricola* group, and so can play a role in phylogenetic interpretation.

Meiotic chromosomes were observed in testes of adult and subadult males using Feulgen staining, following the methods of Maddison (1982), except that no colchicine was used. Most preparations of Nearctic material were done between 1980 and 1989, and scored for autosome number and form and sex chromosome system soon thereafter. In the years since, some of the slides have faded considerably, and even

with phase contrast they can no longer be scored. For most species we were able to confirm the old scores through re-examination (in an Olympus BX51 phase contrast microscope), except as noted in Chromosome observations. Because of the long history of this study, our photographs are of varied ages and qualities. We recognize that chromosome scoring of some species has uncertainty, and that future studies should be directed to confirming or correcting our intepretations. Nonetheless, the broad patterns we describe are supported even taking the uncertainty into account.

Evidence for scoring chromosome complement of each species is described in Chromosome observations. Most chromosome scoring was done from meiotic nuclei in first metaphase or diakinesis showing chromosomes that are well separated, or, if overlapping, easily interpretable. Although well-spread mitotic nuclei would have added useful data, we judge meiotic chromosomes to be sufficient as they show distinctive features, e.g. when they are oriented by the centromere pulling toward the pole on the metaphase plate. Metacentrics show an obvious bend at the centromere where the second arm hangs loose like a dog's ear (Fig. 130), while acrocentrics show an opposite bend more distally (at chiasmata), or no bend (if chiasmata are terminal), and a narrower neck to the centromere stretched pole-ward (Figs 131, 140, 143, 147, 154, 156, 164). In most specimens, multiple nuclei contributed to the scoring. In other salticids (e.g., Maddison 1982), the Xs of the X_1X_20 sex chromosome system have distinctive behaviour during meiosis. At first metaphase they typically lie toward one pole, side by side and without chiasmata. They are heteropycnotic, condensing early, but by first metaphase slightly decondensed, and in second prophase condensed. We use this behaviour as evidence for interpreting chromosomes as Xs, or for interpreting portions of chromosomes as representing ancestral X material. For several species additional evidence came from metaphase II counts, and for one (*Sittisax ranieri*) female mitosis in subadult digestive glands was examined.

In describing chromosome complements, we use "a" and "m" to indicate one-armed (acrocentric/telocentric) and two-armed (metacentric/submetacentric) chromosomes respectively. Thus, "26a+XaXa0" would mean "26 acrocentric autosomes plus two X's, both of which are acrocentric". In all cases, the multiple Xs of a male are interpreted as not being homologous, and therefore it would be more proper to refer to the systems as X_1X_20, X_1X_2Y, or $X_1X_2X_3Y$ rather than as XX0, XXY, or XXXY. However, the "1", "2", "3" will be left implicit, omitted for ease of reading, to avoid overly complex labels like $Xa_1Xa_2Xa_3Ym$.

Phylogenetic results

The maximum likelihood tree from the UCE data is shown in Figure 48, which incorporates results from both partitioned and unpartitioned analyses. As seen in previous results from fewer genes (Ruiz and Maddison 2015), *Aillutticus* Galiano, 1987 is the sister group to all other sitticines sampled. *Aillutticus* is the only sampled representative of what is likely a large radiation of little-studied Neotropical sitticines with high, rounded carapaces and unusual genitalia, currently including five genera (Galiano

1987; Ruiz and Brescovit 2005, 2006). As described under classification, we propose the name Aillutticina, new subtribe, for the *Aillutticus* group of genera, and the name Sitticina for the remaining sitticines.

The phylogeny of Sitticina shows two major groups, the *Jollas-Tomis* clade and *Attulus*. The *Jollas-Tomis* clade is distributed entirely in the Americas except for the two species of *Sittisax*; *Attulus* is entirely Eurasian except for 8 species in North America. The only previously published comprehensive phylogeny of sitticines, of Prószyński (1983), is substantially similar in placing *Sittisax* and *Attinella* outside of the major clade of the *floricola*, *distinguendus* and *penicillatus* species groups. The most notable differences between his arrangement and ours are the placements of *Attulus pubescens* and *A. dzieduszycki*. Prószyński's more recent (2017a) classification into genera, however, is discordant in many respects with our results, as can be seen in the many combinations that we establish or reinstate below in order to achieve monophyly of genera and subgenera. This discord may have arisen partly because Prószyński was not attempting to create a taxonomy that reflected phylogenetic relationships, but rather the distribution of a few diagnostic characters (Prószyński 2017b).

Our UCE phylogeny differs in several respects from Breitling's (2019) COI phylogeny. Ours places *Sittisax ranieri* next to *Tomis*, distant from the Eurasian Radiation, while his places it next to *Attulus finschi*. The other disagreements are not visible in the isolated portion of the tree shown in Breitling's figure 9B, but are visible in his more complete supplemental figure "Salticidae". It places *Attinella concolor* sister to the euophryine *Sidusa*, *Attulus fasciger* among the plexippines, *Tomis manabita* ("*Sitticus* sp. MCH–2003") as sister to the asemoneine *Asemonea*, and *Jollas cupreus* as sister to the lapsiine *Thrandina* – thus mixing the sitticines among three different subfamilies and 5 tribes. Given our far stronger data (hundreds of loci, multiple linkage groups, many times more nucleotide sites), inclusion of more Neotropical sitticines, more efficient analysis (likelihood as opposed to neighbour joining), and concordance with morphological traits uniting the sitticines, we consider Breitling's phylogeny to be in error. The startling scrambling of established clades in Breitling's supplemental figures is in accord with previous studies in salticids, which have shown the COI gene to be particularly error-prone in reconstructing phylogeny (Hedin and Maddison 2001; Maddison et al. 2008, 2014; Bodner and Maddison 2012; Maddison and Szűts 2019). However, our phylogeny agrees with one important result from Breitling's study: the close relationship of *A. pubescens* with *A. terebratus* (though, as noted above, their close relative *A. fasciger* is placed in another tribe).

Although *Attulus* includes some Nearctic members, it is considerably more species-rich in Eurasia, and is most parsimoniously interpreted as having radiated there. The few Nearctic members of this clade are likely recent returns from the Palearctic, insofar as they are Holarctic (*Attulus floricola*, *A. cutleri*, *A. finschi*), close relatives of Eurasian species (*A. sylvestris* within the *A. floricola* group, *A. striatus* close to *A. rivalis*), or recent introductions (*A. ammophilus*, *A. fasciger*, *A. pubescens*: see Prószyński 1976, 1983 and Cutler 1990). Our results thus support Prószyński's (1983) hypothesis of a Palearctic radiation of *Sitticus* sensu lato, although we differ in concluding that only one subgroup diversified in Eurasia, *Attulus*, arising from an earlier Neotropical diversification.

The deep branches of the Eurasian Radiation are short, suggesting the group diversified rapidly. Nonetheless, the monophyly of subgenus *Sitticus* is well supported

by a bootstrap percentage of 100 in our primary Core Taxa analysis (Fig. 48). The monophyly of subgenus *Attulus* has weak bootstrap support in the partitioned analysis (72%), although good support in the unpartitioned analysis (95%). As well, the major subgroup of subgenus *Attulus* excluding *A. saltator* and *A. mirandus* is well supported (92% or 96%). Despite its weak support in the partitioned analysis, monophyly of subgenus *Attulus* as a whole is consistent across multiple analyses, for example, when the filter for loci present in at least seven core taxa is changed from seven to four or ten. Analyses (following the same methods described above) without *A. longipes* gave 99.6% bootstrap support to subgenus *Attulus*.

The relationships among *Attulus* species are concordant with morphological expectations with one exception: the placement of *A. burjaticus* with *A. zimmermanni*, suggesting that the longer embolus of *A. zimmermanni* and the *floricola* group are convergent. Otherwise, the *floricola* group holds together, as do the morphologically similar pairs of *A. ammophilus*/*distinguendus* and *mirandus*/*saltator*. The placement of *A. pubescens* nested within the *terebratus* group indicates that the very short embolus of the former is a derivation from the very long embolus of the latter.

Jollas and *Tomis* together form a Neotropical radiation and share (typically) an RTA that appears displaced basally, so as to appear to arise closer to the patella, as well as anteriorly placed epigynal openings.

Classification

The phylogenetic results lead us to revise the generic division of sitticines. Unless we are to put all Sitticina into a single genus, perhaps palatable for the shallow-diverging Eurasian fauna, but not for the deep Neotropical lineages, then *Tomis* must be restored for many of the Neotropical species. Given that, *Sittisax* must be separated from *Attulus*/*Sitticus*, rejecting Breitling's synonymy of this taxon with *Sitticus*. These choices are relatively easy. The more difficult choices concern the Eurasian Radiation.

Here we give a taxonomic review of the tribe, focussing especially on the species in Canada, and the two new species used in the molecular phylogeny (*Jollas cupreus* and *Tomis manabita*). In order to faciliate the use of figures for identification and comparison of species in North America, the sequence of taxa in figures will be different from that in the text, with a series of standardized plates placing images of all of the Canadian species in a block (Figs 49–103).

Tribe Sitticini Simon, 1901

Amycoid salticids with fourth legs much longer than third and retromarginal cheliceral tooth lacking. Ancestrally they were ground-dwellers in the Neotropics, later diversifying in Eurasia to include species that live on tree trunks (e.g., *A. finschi*) and up in vegetation (e.g., *Attulus floricola*).

Eleven genera are here recognized in the Sitticini, including one (*Semiopyla* Simon, 1901) whose placement is unclear, and thus remains *incertae sedis* within the tribe. Two genera are in Eurasia (*Attulus* and *Sittisax*), while a disjunct set of eight genera are in South America (the five aillutticines, plus *Tomis*, *Jollas*, and *Semiopyla*). This geographical partitioning matches a phylogenetic division approximately, but not precisely, for the Holarctic *Sittisax* is phylogenetically a member of the Neotropical radiation. North America has four genera, one arising from the Eurasian radiation (*Attulus*), and three from the Neotropical radiation (*Attinella*, *Sittisax*, and *Tomis*).

Despite the synonymy of *Sitticus* with *Attulus*, the names Sitticini and Sitticina can persist (ICZN Article 40.1).

Subtribe Aillutticina W. Maddison, new subtribe
http://zoobank.org/4DBE8F82-300A-4AE0-9A11-7A0DC55D7099
Figures 1–4

Type genus. *Aillutticus* Galiano, 1987

Diagnosis. This group of five Neotropical genera was first recognized by Ruiz and Brescovit (2005, 2006), who characterize it as sharing "a high, broad carapace, laterally rounded behind the posterior lateral eyes, and the slightly convex dorsal surface of the cephalic region". The contained genera are:

Aillutticus Galiano, 1987
Amatorculus Ruiz & Brescovit, 2005
Capeta Ruiz & Brescovit, 2005
Gavarilla Ruiz & Brescovit, 2006
Nosferattus Ruiz & Brescovit, 2005

Subtribe Sitticina Simon, 1901

There are no known morphological synapomorphies of this subtribe, but the molecular data show clearly that the five genera listed here form a clade. There are two major subgroups according to the UCE phylogeny: the genus *Attulus*, a primarily Eurasian radiation, and the *Jollas-Tomis* clade (*Attinella*, *Jollas*, *Sittisax*, *Tomis*), a primarily Neotropical radiation. We divide the taxonomy below into those two major groups, and under each discuss the genera, describe the Canadian species and two new Ecuadorian species used in the molecular work.

Genus *Attulus* Simon, 1868, restored (to respect its priority over *Sitticus*)

Attulus Simon, 1868 (type species *Attus helveolus* Simon, 1871)
Sitticus Simon, 1901 (type species *Araneus terebratus* Clerck, 1757)

Figures 1–14. Subtribe Aillutticina (**1–4**) and the *Jollas-Tomis* clade of the subtribe Sitticina (**5–14**) **1–4** *Aillutticus nitens*, Uruguay (-34.877, -56.023): **1–3** male **4** female **5, 6** *Tomis palpalis* male and female, Ecuador (-0.1996, -77.7023) **7, 8** *Jollas* species: **7** *J. cupreus* male, Ecuador (-0.675, -76.397) **8** *Jollas* sp. female, Ecuador (-0.7223, -77.6408) **9** *J. leucoproctus*, Uruguay (-34.94, -54.95) **10** *J. flabellatus*, Uruguay (-34.426, -55.195) **11–14** *Attinella dorsata* male (**11–13**) and female (**14**), Canada (48.870, -123.379). Also included in the *Jollas-Tomis* clade is *Sittisax* (Figs 99–103). Additional members of the *Jollas-Tomis* clade can be seen in Figs 108–128.

Sitticulus F. Dahl, 1926 (type species *Attus saltator* O. Pickard-Cambridge, 1868), syn. nov.
Calositticus Lohmander, 1944 (type species *Attus caricis* Westring, 1861), syn. nov.
Hypositticus Lohmander, 1944 (type species *Aranea pubescens* Fabricius, 1775), syn. nov.
Sittipub Prószyński, 2016 (type species *Aranea pubescens* Fabricius, 1775), syn. nov.
Sittiflor Prószyński, 2017 (type species *Euophrys floricola* C.L. Koch, 1837), syn. nov.
Sittilong Prószyński, 2017 (type species *Attus longipes* Canestrini, 1873), syn. nov.

We unite the primary Eurasian radiation under the single genus *Attulus* because of the recency of the radiation, the very short phylogenetic branches separating the subgroups, and the clade's morphological homogeneity. The total phylogenetic depth of *Attulus* is far less than that of its sister group (Fig. 48), but more importantly, the deepest branches of *Attulus* are very short. This suggests a rapid radiation, and that any subgroups will have only limited predictive value about traits, as most of the divergence occurred since the initial radiation. The monophyly of the major subgroups is to some extent uncertain, and so any generic division could be unstable. The morphological diversity encompassed by *Attulus* (e.g. variation in narrowness of carapace, leg length, embolus length, position of epigynal openings) is arguably less than that of other stable genera like *Pellenes* and *Habronattus*; the subgenera we recognize are comparable to species groups in *Habronattus* (Maddison and Hedin 2003) or subgenera in *Pellenes* (Logunov et al. 1999). By considering *Attulus* as a single genus with subgenera, we also simplify identifications by ecologists and others. A Eurasian salticid, even a juvenile, can easily be keyed to *Attulus* based on the long fourth legs and absence of retromarginal cheliceral teeth, except only for the exclusion of *Sittisax*.

Our choice to consider all but two Eurasian species as belonging to *Attulus* is informed partly by their phylogenetic context among Neotropical salticids. From a Palearctic perspective, the Eurasian radiation of sitticines may seem to represent a lineage of salticids so distinctive and species-rich that they deserve splitting into many genera, especially since the sister group of sitticines among the Old World salticids is the huge clade Salticoida (Maddison 2015), which is divided into hundreds of genera. From the Americas, though, the Eurasian sitticine radiation appears as a shallow expatriate lineage, the tip of the iceberg of a large and deeply diverging Neotropical radiation (the Sitticini, and more broadly, the Amycoida). If more generic subdivision is needed, it will be in the much more divergent and poorly explored sitticine fauna of South America.

The appropriate name for this unified genus is *Attulus*, as it is far older than *Sitticus*, and has been used continuously, though for only a few species. Two proposals have been made to ignore priority and instead use *Sitticus*, the generic name used for most of the species until Prószyński's (2016, 2017) splitting. Prószyński himself had proposed to the ICZN in 2008 suppression of *Attulus* in favour of *Sitticus*, but in 2018 apparently withdrew that proposal (ICZN 2018). Breitling (2019) also proposed that the younger name *Sitticus* be used. We argue that priority in general should be respected unless it would disrupt a long-stable name against a little-used alternative. In this case, *Sitticus* has already been destabilized, *Attulus* has been used more or less continuously, and most species have already been moved to *Attulus* by Prószyński. The World Spider Catalog (WSC 2019) and other resources (Metzner 2019) have already begun to use *Attulus* for most species. Abandoning nomenclatural rules to avoid facing the consequences of new information will over the long term likely lead to instability or to classifications based on the weight of authority, just as with abandoning monophyly. Thus, the least disruptive choice is to use the name "*Attulus*".

However, there is value in offering a weaker recognition of three subgroups of *Attulus*, as subgenera, given that there are names available: *Attulus*, *Sitticus*, and *Sittilong*. Our results support reciprocal monophyly of the subgenera *Attulus* and *Sitticus*, and

a placement of *Sittilong* outside of both. Monophyly of subgenus *Attulus* has variable bootstrap support (72% to 95%, Fig. 48), although the clade's presence is consistent across various alternative analyses (when *Sittilong* is not included; when the filter for loci present in at least seven core taxa is changed to four or ten). Even if subgenus *Attulus* falls apart with more data, the bulk of the subgenus would likely hold together, as there is high bootstrap support for the large subclade including the type species *A. distinguendus*. The low bootstrap support for the subgenus as a whole (in the partitioned analysis) derives from the weakness of inclusion of the unusual *penicillatus* group (represented by *A. saltator* and *A. mirandus*; see Logunov 1993), which might eventually need a separate subgenus (for which a name, *Sitticulus* F. Dahl 1926, is available).

The three subgenera have subtle but mostly consistent morphological differences. *Attulus s. str.* tends to have smaller and more compact bodies, with roundish carapaces (Figs 15–38). *Sitticus* have a narrower carapace and longer legs (Figs 39–47), and (except in *A. relictarius*) a large sweeping retrolateral tibial apophysis (Figs 74, 79, 84). *Sittilong* is notable for its long first legs.

Attulus includes 49 species in three subgenera:

Subgenus *Attulus* Simon, 1868, with 41 species:

Attulus (*Attulus*) *albolineatus* (Kulczyński, 1895), comb. nov., transferred from *Sitticus*
Attulus (*Attulus*) *ammophilus* (Thorell, 1875)
Attulus (*Attulus*) *ansobicus* (Andreeva, 1976)
Attulus (*Attulus*) *atricapillus* (Simon, 1882), comb. nov., transferred from *Calositticus*
Attulus (*Attulus*) *avocator* (O. Pickard-Cambridge, 1885)
Attulus (*Attulus*) *barsakelmes* (Logunov & Rakov, 1998), comb. nov., transferred from *Sitticus*
Attulus (*Attulus*) *burjaticus* (Danilov & Logunov, 1994)
Attulus (*Attulus*) *caricis* (Westring, 1861), comb. nov., transferred from *Calositticus*
Attulus (*Attulus*) *clavator* (Schenkel, 1936)
Attulus (*Attulus*) *cutleri* (Prószyński, 1980), comb. nov., transferred from *Calositticus*
Attulus (*Attulus*) *damini* (Chyzer, 1891)
Attulus (*Attulus*) *distinguendus* (Simon, 1868) (= type species *Attus helveolus* Simon, 1871)
Attulus (*Attulus*) *dubatolovi* (Logunov & Rakov, 1998)
Attulus (*Attulus*) *dudkoi* (Logunov, 1998), comb. nov., transferred from *Calositticus*
Attulus (*Attulus*) *dzieduszyckii* (L. Koch, 1870), comb. nov., transferred from *Sittisax*
Attulus (*Attulus*) *eskovi* (Logunov & Wesolowska, 1995), comb. nov., transferred from *Sitticus*
Attulus (*Attulus*) *floricola* (C. L. Koch, 1837), comb. nov., transferred from *Calositticus*
Attulus (*Attulus*) *goricus* (Ovtsharenko, 1978)
Attulus (*Attulus*) *hirokii* Ono & Ogata, 2018
Attulus (*Attulus*) *inexpectus* (Logunov & Kronestedt, 1997), comb. nov., transferred from *Calositticus*
Attulus (*Attulus*) *inopinabilis* (Logunov, 1992)
Attulus (*Attulus*) *karakumensis* (Logunov, 1992)

Attulus (*Attulus*) *kazakhstanicus* (Logunov, 1992)
Attulus (*Attulus*) *mirandus* (Logunov, 1993)
Attulus (*Attulus*) *monstrabilis* (Logunov, 1992), comb. nov., transferred from *Calositticus*
Attulus (*Attulus*) *nenilini* (Logunov & Wesolowska, 1993)
Attulus (*Attulus*) *nitidus* Hu, 2001, comb. nov., transferred from *Sitticus*
Attulus (*Attulus*) *niveosignatus* (Simon, 1880)
Attulus (*Attulus*) *penicillatus* (Simon, 1875)
Attulus (*Attulus*) *penicilloides* (Wesolowska, 1981)
Attulus (*Attulus*) *pulchellus* (Logunov, 1992), comb. nov., transferred from *Calositticus*
Attulus (*Attulus*) *rivalis* (Simon, 1937), comb. nov., and removed from synonymy with *A. striatus* (Emerton).
Attulus (*Attulus*) *rupicola* (C. L. Koch, 1837), comb. nov., transferred from *Calositticus*
Attulus (*Attulus*) *saltator* (O. Pickard-Cambridge, 1868)
Attulus (*Attulus*) *sinensis* (Schenkel, 1963)
Attulus (*Attulus*) *striatus* (Emerton, 1911), comb. nov., transferred from *Calositticus*
Attulus (*Attulus*) *sylvestris* (Emerton, 1891), comb. nov., transferred from *Sitticus*, removed from synonymy with *A. palustris*
Attulus (*Attulus*) *talgarensis* (Logunov & Wesolowska, 1993)
Attulus (*Attulus*) *vilis* (Kulczyński, 1895)
Attulus (*Attulus*) *zaisanicus* (Logunov, 1998)
Attulus (*Attulus*) *zimmermanni* (Simon, 1877), comb. nov., transferred from *Calositticus*

Subgenus *Sitticus* Simon, 1901, with seven species:
Attulus (*Sitticus*) *fasciger* (Simon, 1880), comb. nov., transferred from *Sitticus*
Attulus (*Sitticus*) *finschi* (L. Koch, 1879), comb. nov., transferred from *Sitticus*
Attulus (*Sitticus*) *godlewskii* (Kulczyński, 1895), comb. nov., transferred from *Sitticus*
Attulus (*Sitticus*) *pubescens* (Fabricius, 1775), comb. nov., transferred from *Sitticus*
Attulus (*Sitticus*) *relictarius* (Logunov, 1998), comb. nov., transferred from *Sitticus*
Attulus (*Sitticus*) *tannuolana* (Logunov, 1991), comb. nov., transferred from *Sitticus*
Attulus (*Sitticus*) *terebratus* (Clerck, 1757) (type species of *Sitticus*), comb. nov., transferred from *Sitticus*

Subgenus *Sittilong* Prószyński, 2017, with one species:
Attulus (*Sittilong*) *longipes* (Canestrini, 1873) (type species of *Sittilong*), comb. nov., transferred from *Sittilong*

Subgenus *Attulus* Simon, 1868

Figures 15–38, 49–73

Attulus Simon, 1868 (type species *Attus helveolus* Simon, 1871).
Sitticulus F. Dahl, 1926 (type species *Attus saltator* O. Pickard-Cambridge, 1868).
Calositticus Lohmander, 1944 (type species *Attus caricis* Westring, 1861).
Sittiflor Prószyński, 2017 (type species *Euophrys floricola* C.L. Koch, 1837).

Body generally more compact than in subgenus *Sitticus*, with a wider carapace. The spermatheca is a simple tube, folded near the middle. From the point at which the copulatory ducts enter the spermatheca, the spermatheca extends medially to the fertilization duct, but also laterally and then posteriorly (*floricola* group) or medially (most others) to a separate posterior lobe. Most *Attulus* (*Attulus*) have the embolus short, arising near the basal prolateral corner of the bulb, and the tegulum with basal edge more or less straight (not rounded). Several species have a rounder bulb and longer embolus, representing two or three lineages: the *floricola* group (*A. caricis*, *A. floricola*, *A. inexpectus*, *A. rupicola*, *A. sylvestris*), the *striatus* group (*A. striatus*, *A. rivalis*, *A. cutleri*, *A. dudkoi*) and the *zimmermanni* group (*A. zimmermanni*, *A. atricapillus*). These also have the folded spermathecae rotated slightly compared to the other *Attulus*, with the posterior lobe pointing posteriorly, rather than medially. The placement of *A. niveosignatus* in *Attulus* (*Attulus*) is somewhat doubtful, as the position of the tibial apophysis and the anterior medial epigynal openings both resemble those of *Sittisax* and *Attulus* subgenus *Sittilong*. We are reluctant to move it, however, until it is better studied.

Five species of *Attulus* (*Attulus*) are known from North America, all of which occur in Canada, as follows.

Attulus (*Attulus*) *ammophilus* (Thorell, 1875)

Figures 27–30, 69–73

Attus ammophilus Thorell, 1875

Remarks. *Attulus ammophilus* is part of the species-rich *distinguendus* group that is otherwise unrepresented in North America. We have collected it from rocks on the ground in Ontario, British Columbia, and Utah, on litter among marsh plants along the edge of a lake in Siberia, and occasionally from buildings. It was introduced into North America during the 20th century (Prószyński 1976, 1983).

Material examined (all in UBC-SEM): Canada: Ontario: Hamilton (69 males, 35 females), Oakville (4 males, 3 females), Toronto (1 male), Windsor (1 male, 2 females); British Columbia: 49.7963, -119.5338 (1 male, 2 females), 49.95, -119.401 (3 males, 2 females); U.S.A.: Utah: 40.7482, -112.1856 (5 males, 7 females), 40.7672, -112.1575 (2 males).

Attulus (*Attulus*) *floricola* (C.L. Koch, 1837)

Figures 33–35, 49–53

Euophrys floricola C. L. Koch, 1837.

Attus palustris Peckham & Peckham, 1883 (specimens in MCZ labelled as types, examined, but see below).

Attus morosus Banks, 1895 (synonymized by Prószyński 1980; confirmed here by examination of holotype female in MCZ from Olympia, Washington).

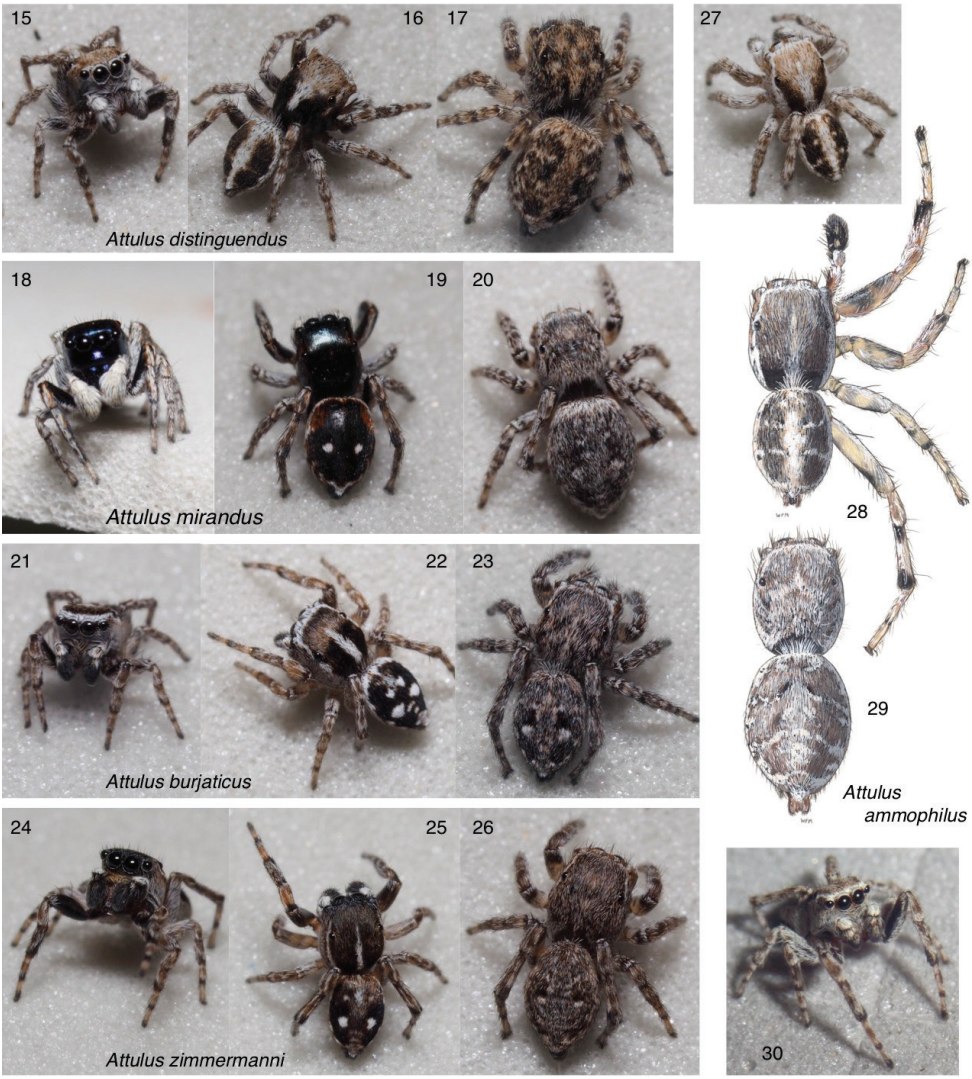

Figures 15–30. *Attulus* subgenus *Attulus* **15–17** male and female *A. distinguendus*, Tuva (50.746, 93.142) **18–20** male and female *A. mirandus*, Tuva (50.205, 95.135) **21–23** *A. burjaticus*: **21** male, Tuva (50.68, 92.99) **22** male, Tuva (50.205, 95.135) **23** female, Tuva (50.68, 92.99) **24–26** *A. zimmermanni*: **24, 25** male Novosibirsk Oblast (53.721, 77.726) **26** female Novosibirsk Oblast (53.730, 77.865) **27–30** *A. ammophilus*: **27** male Tuva (50.6690, 92.9844) **28** male Ontario, Oakville **29** female Ontario, Hamilton **30** male British Columbia (49.08, -119.52). For additional images of *A. ammophilus*, see Figs 69–73. For additional images of *Attulus* (*Attulus*), see Figs 31–38, 49–73.

Remarks. A widespread Holarctic species often found in retreats in dry flower heads in wetter areas such as marshes, *A. floricola* is distinctive for the sharp white lines around the eyes of males, forming an apparent mask (Fig. 34). *Attulus floricola* has often been confused in the past with its close relatives, but the distinctions have been clarified considerably by Prószyński (1980) and Logunov and Kronestedt (1997).

We treat the North American populations as full *floricola*, not a distinct subspecies. While Nearctic populations were long recognized as a separate species *palustris*, Prószyński (1980) suggested they are conspecific with the Eurasian populations. He maintained them as a distinct subspecies, but he expressed doubt as to whether even that distinction was warranted. We concur with his skepticism. If any consistent differences exist between the continents, they are no more visible than any differences that might exist between the Eurasian and North American populations of other species for which we don't recognize subspecies such as *Sittisax ranieri*, *Attulus cutleri*, *Dendryphantes nigromaculatus* (Keyserling, 1885), *Pellenes ignifrons* (Grube, 1861), and *Pellenes lapponicus* (Sundevall, 1833).

The results of our COI analysis of Palearctic and Nearctic *floricola* group (Fig. 104) show all *floricola* to be close on the gene tree, with the New World specimens in two clades (not clearly related to one another) and the German specimens in a third clade. This suggests that *A. floricola* is not cleanly or deeply divided between the Nearctic and Palearctic. The molecular and morphological evidence leads us to fully synonymize *palustris* into *floricola*.

Within North America, the characterization of *A. floricola* has been muddied by confusion with a second species, *A. sylvestris*. *Attulus sylvestris*, long synonymized with *palustris*, is a distinctively different species. *Attulus floricola* is larger-bodied, has a much more contrasting colour pattern, and longer legs. *Attulus floricola* has a different angle of the spermaphore loop (subtle but consistent; Fig. 49 vs. Fig. 54), and in females the darkness of the spermathecal lobe is visible through the anteriormost portion of the epigynal atrium (Fig. 50 vs. Fig. 55). *Attulus sylvestris* has genitalia more similar to those of the Eurasian *A. caricis*, *A. rupicola*, and *A. inexpectus*, as noted below. The synonymy of *sylvestris* with *palustris* was originally proposed by Peckham and Peckham (1909), after which Kaston (1948) may have stirred confusion by choosing to illustrate *palustris* using Emerton's (1891) figure of *sylvestris*.

A more serious confusion apparently occurred with the labelling of type specimens of *Attus palustris*. The description by Peckham and Peckham (1883) refers without doubt to the common white-striped species long known as *Sitticus palustris* (Fig. 34): males dark brown, reddish toward eyes, marked with white lines, including those around the eyes, and palp with some white hairs on several segments of the palp. As well, the habitat suggested by the name "*palustris*" is marsh or swamp, more typical for *A. floricola* than *A. sylvestris*. However, the specimens labelled as the types of *Attus palustris* in the MCZ are clearly specimens of the less common dusty brown species (i.e., Emerton's *sylvestris*, Fig. 32). These specimens, we argue, are mislabelled: they do not match the Peckhams' description, and thus are not the type specimens of *A. palustris*. That the Peckhams viewed the white-striped form as typical *palustris* can be judged not only from their 1883 description, but also from their implicitly distinguishing two forms in their 1909 statement "Mr. Emerton agrees with us that the form which he described as *sylvestris* is a variety of *palustris*, with the leg a little shorter and stouter." The label of the holotype does not appear to be in the handwriting of either George or Elizabeth Peckham, and it is possible that these "types" were so labelled after 1883.

Figures 31–38. *Attulus* subgenus *Attulus*, continued (*floricola* group) **31, 32** *Attulus sylvestris*: **31** male, Ontario, Ottawa **32** male, Maryland, Dorchester Co **33–35** *A. floricola*: **33** male, Ontario, Port Cunnington **34** male, Ontario (46.9300, -79.7268) **35** male, Ontario, Gravenhurst **36–38** *A. inexpectus*: **36, 37** male, Tuva (50.6690, 92.9844) **38** female, Tuva (51.316, 94.495). For additional images of the *floricola* group, see Figs 49–58.

At stake is not the name used for the common white-striped species (which would be *floricola* regardless), but the name for the uncommon dusty brown species, which would be *palustris* were we to accept these specimens as its types. However, as argued above, they are not the types. We therefore treat *palustris* as a synonym of *floricola*, and *sylvestris* as the name for the dusty brown species. To settle the mislabelling properly, a male specimen of the white-striped species from Wisconsin (the type locality) should be designated as the neotype or lectotype of *palustris*. We have not yet done so as we

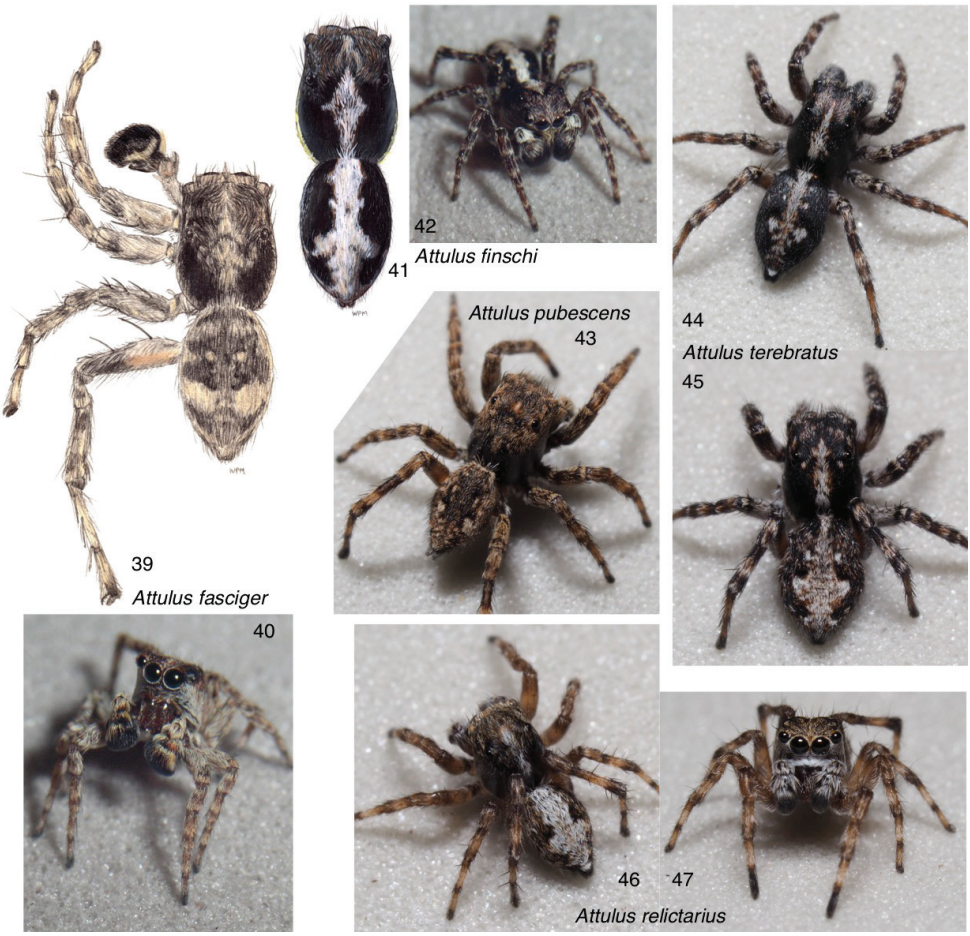

Figures 39–47. *Attulus* subgenus *Sitticus* **39, 40** *A. fasciger*, male, Ontario (43.3508, -79.7593) **41, 42** *A. finschi*: **41** male, Saskatchewan (55.31, -105.11) **42** male body, Ontario, 4 miles S of Wawa **44, 45** *A. terebratus*: **44** male, Novosibirsk Oblast (53.730, 77.865) **45** female, Novosibirsk **46, 47** *A. relictarius* male, Stavropol Krai, (43.88, 42.70). For additional images of *Attulus* (*Sitticus*), see Figs 74–88.

await reexamination of the full Peckham collection in case specimens can be located that might be identifiable as from the true type series.

Material examined. Canada: British Columbia: Richmond (2 females), 49.66, -114.73 (1 female), 49.45, -115.08 (3 males, 6 females); Alberta: 52.46, -113.94 (1 male); Ontario: Richmond (2 males, 1 female), Gravenhurst (3 males), Port Cunnington (1 female); Dwight (2 males, 5 females), Batchawana Bay (1 female), Woodstock (3 females), 46.9300, -79.7268 (2 males, 1 female), 42.53, -80.12 (1 female), 43.2626, -80.5636 (1 male), 49.0852, -81.3237 (1 female); Quebec: Touraine (1 male); Nova ScotiA: 44.4318, -64.6075 (1 male); U.S.A.: Washington: 46.43, -123.86 (2 males); Colorado: Jackson Lake State Rec. Area (1 male); Nebraska: 41.88, -103.09 (1 female).

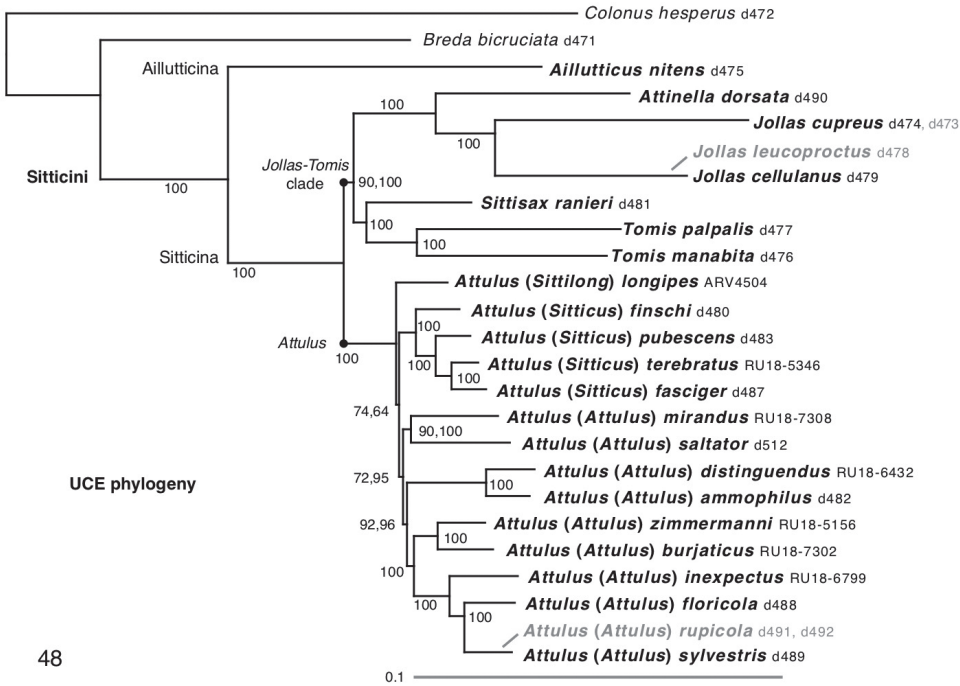

Figure 48. Maximum likelihood phylogeny from 757 concatenated UCE loci (average 113231 base pairs/taxon) analyzed primarily for the 23 Core Taxa in black (IQ-TREE, partitioned by locus). Topology is identical in unpartitioned analyses, with nearly identical branch lengths. Bootstrap percentage values from 1000 replicates shown for each clade. Where two numbers are shown, the first is the bootstrap percentage for the partitioned analysis, the second for the unpartitioned analysis. Where one number is shown, both analyses yielded the same percentage. An analysis of the All Taxa dataset, including the weakly-sequenced taxa in grey, yielded the same topology.

Attulus (*Attulus*) *sylvestris* (Emerton, 1891), restored (removed from synonymy with *S. floricola*)

Figures 31, 32, 54–58

Attus sylvestris Emerton, 1891 (Holotype male in MCZ from Beverly, Massachusetts, examined).

Sitticus magnus Chamberlin & Ivie, 1944, syn. nov.

Sitticus rupicola – Prószyński, 1980, figs 58, 59 (misidentification), specimen from Texas.

Remarks. A widespread but little-known Nearctic species, *A. sylvestris* can be found on partially shaded ground where the males stand out for their tiny bouncing bright white spots (the white tuft of setae on the palp's tibia). We have found them on rocks and leaf litter along a forest edge in Ontario, on the ground at the edge of a creek in a forest in California, and on forest leaf litter in Maryland. See discussion under *A. floricola*

about why we judge *A. sylvestris* to be the proper name of this species, at issue because of confusion over the type specimens of *Attus palustris*.

Both males and females have shorter legs and less contrasting markings than in *A. floricola*, but the distinction of markings is most notable in the male, which lacks the high-contrast white stripes on dark brown seen in *A. floricola*. The white setae on the male's palp are concentrated on just the tibia and end of the femur. The bulb of the palp is rotated slightly more than in *A. floricola*, and thus the spermophore's path shows an upturn (i.e., the loop is angled to point distally instead of basally as in *floricola*), and the female's copulatory ducts arrive further to the posterior before looping back anteriorly to enter the spermathecae. In these regards the genitalia resemble those of the Eurasian *A. rupicola*, *A. caricis*, and *A. inexpectus* (Logunov and Kronsestedt 1997). *Attulus sylvestris* is most similar to *A. caricis* in appearance (low-contrast brown markings), in having a small loop of the copulatory duct, and small body size, but differs in brighter markings on the palp, a more anteriorly-placed junction where the ducts enter the spermatheca, a larger epigynal RTA coupling pocket, and a more distinctly swollen bulb of the spermatheca. (They are also distinct on the COI tree, Fig. 104.) The synonymy of *magnus* can be determined by its original description and Prószyński's (1980) excellent drawing of the vulva of the holotype female. The female from Texas tentatively identified by Prószyński (1980: 15, figs 58, 59) as *S. rupicola* is considered here to be *S. sylvestris* based on his clear drawings showing the loop of the copulatory duct slightly bigger than typical, but not reaching nearly as far to the posterior as in *S. rupicola*.

Material examined (all in UBC-SEM except as indicated): Canada: Ontario: Ottawa, Britannia Bay, 45.374, -75.796 (26 males, 3 females), Long Point, 42.53, -80.12 (2 females); U.S.A.: Maryland: Dorchester Co. (1 male 1 female, MCZ); Colorado: Morgan Co., Fort Morgan (1 female); California: Smith Redwoods State Reserve (1 male), 36.3907, -121.5951 (2 females), 36.3742, -121.5614 (1 male, 4 females).

Attulus (*Attulus*) *striatus* (Emerton, 1911)

Figures 59–63

Sitticus striatus Emerton, 1911

Remarks. *Attulus striatus* is a small-bodied Northern species with distinctively striped males, from sphagnum bogs. Although we were unable to obtain molecular data for it or the similar *A. rivalis* and *A. cutleri*, these three species can be placed into subgenus *Attulus* with some confidence, based on their boxy carapaces (resembling the other *Attulus* (*Attulus*) rather than *Attulus* (*Sitticus*)), and the genitalic similarities with subgenus *Attulus*, including the two small posterior openings of the epigyne on either side of a narrow triangular RTA coupling pocket. Prószyński (1980) considered them close to the *floricola* group in particular.

We reinstate *S. rivalis* Simon, 1937 as a distinct species (contra Prószyński 2017a), accepting Logunov's (2004) clear evidence for their distinction (primarily, in the rotation of the bulb of the palp). *Attulus rivalis* is known from France, also from sphagnum bogs.

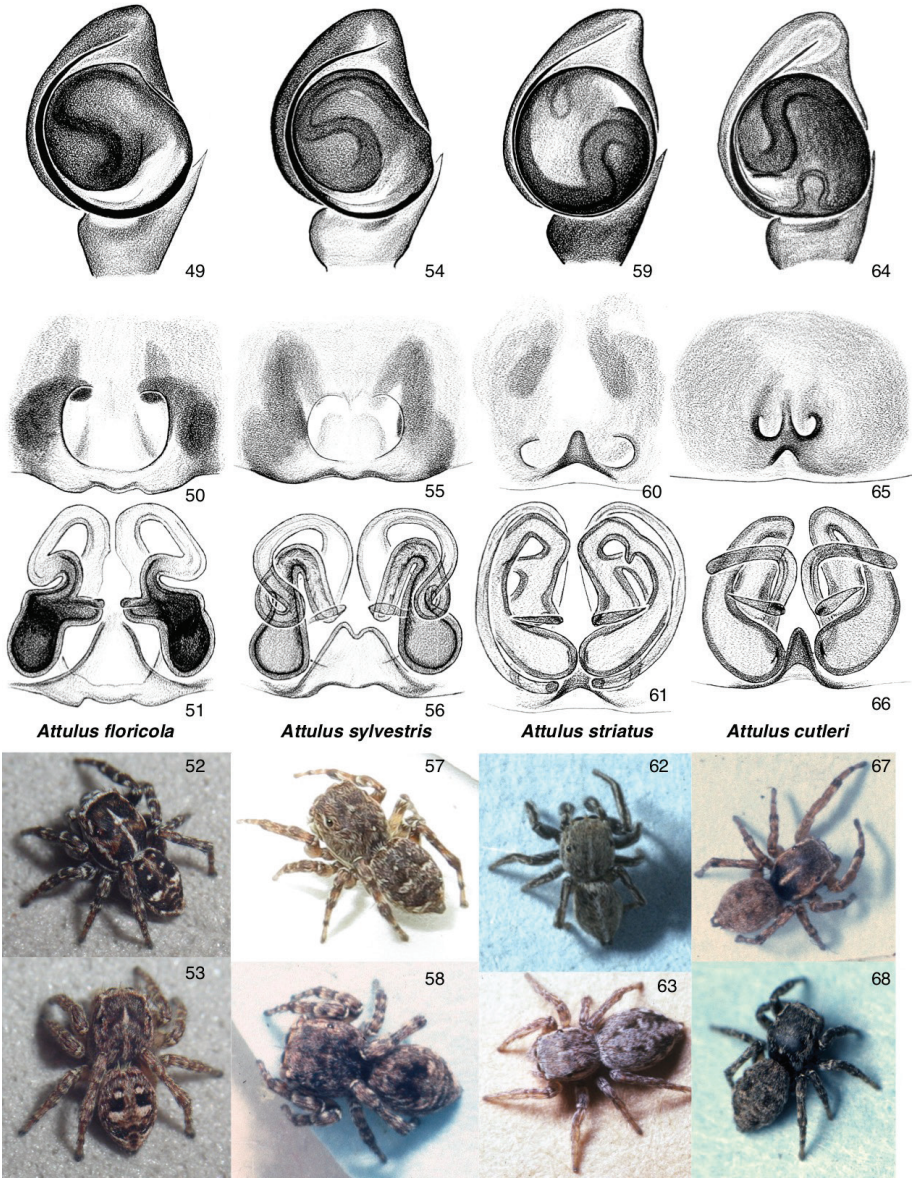

Figures 49–68. Sitticines of Canada: *Attulus* subgenus *Attulus* (for *A. ammophilus*, see Figs 69–73) **49–53** *Attulus floricola*: **49** palp (Ontario, Gravenhurst) **50, 51** ventral view of epigyne, dorsal view of cleared vulva (Ontario, Gravenhurst) **52** male (Ontario, 46.9300, -79.7268) **53** female (Ontario, 46.9300, -79.7268) **54–58** *Attulus sylvestris*: **54** palp (Ontario, Ottawa) **55, 56** ventral view of epigyne, dorsal view of cleared vulva (Ontario, Ottawa) **57** male (California, 36.3646, -121.5544) **58** female (Ontario, 42.55, -80.13) **59–63** *Attulus striatus*: **59** palp (Ontario, 45.1453, -75.8467) **60, 61** ventral view of epigyne, dorsal view of cleared vulva (Ontario, 45.1453, -75.8467) **62** male (Ontario, 45.1453, -75.8467) **63** female (New Hampshire, Ponemah Bog) **64–68** *Attulus cutleri*: **64** palp (Northwest Territories, Wrigley) **65, 66** ventral view of epigyne, dorsal view of cleared vulva (Northwest Territories, Wrigley) **67** male (Northwest Territories, Inuvik) **68** female (Yukon, 67.57, -139.67). For habitus of other *Attulus* species, see Figs 15–38.

Material examined (all UBC-SEM): Canada: Alberta: S. Islay (3 female), Beaverhill Lake (1 female); Ontario: 48.3260, -76.8365 (1 female); 3 km S. Richmond (6 males, 2 females); New Brunswick: Chipman (1 male, 1 female); U.S.A.: New Hampshire: Ponemah Bog (1 female).

Attulus (*Attulus*) *cutleri* (Prószyński, 1980)
Figures 64–68

Sitticus cutleri Prószyński, 1980
Sitticus gertschi Prószyński, 1980

Remarks. A Sibero-American boreal species that is little collected, resembling closely *A. striatus* but differing in having less striped legs, a less rotated bulb of the male palp, more medially placed epigynal openings. Collected on "leaf litter under small *Salix* just above stream" (D. Maddison, June 1981, Inuvik).

Material examined. Canada: Northwest Territories: Wrigley (1 female, CNC), Inuvik (1 male, UBC-SEM).

Subgenus *Sitticus* Simon, 1901
Figures 39–47, 74–88

Sitticus Simon, 1901 (type species *Araneus terebratus* Clerck 1757)
Hypositticus Lohmander, 1944 (type species *Aranea pubescens* Fabricius, 1775)
Sittipub Prószyński, 2016 (type species *Aranea pubescens* Fabricius, 1775)

The species placed here, despite having palpi with very different embolus lengths, share a similarly narrow and high body with relatively long legs (Figs 39–47), and (except for *A. relictarius*) a dramatically large RTA, broadly arising from the tibia and sweeping diagonally to the retrolateral and distal (Figs 74, 79, 84). Several species have a long embolus and correspondingly long and convoluted copulatory ducts, though *A. pubescens* and *A. relictarius* have among the shortest in sitticines. The species of *Sitticus* are Palearctic or Holarctic; the following three are found in Canada.

Attulus (*Sitticus*) *finschi* (L. Koch, 1879)
Figures 41, 42, 79–83

Attus finschii L. Koch, 1879
Euophrys cruciatus Emerton, 1891

Remarks. The natty contrasting black-and-white markings distinguish *Attulus finschi* from the closely related *A. fasciger*. *Attulus finschi* is the only *Sitticus* that has likely

been in the Americas for thousands of years; it also lives in Siberia. It is found in boreal habitats on tree trunks.

Material examined (all UBC-SEM): Canada: Saskatchewan: 55.31, -105.11 (1 male, 1 female), 55.27, -105.19 (1 female); Ontario: Wawa (1 male), Nipigon (1 female), 48.9143, -80.9446 (2 females); New Brunswick: Doaktown (1 male).

Attulus (*Sitticus*) *fasciger* (Simon, 1880)

Figures 39, 40, 74–78

Attus fasciger Simon, 1880

Remarks. This species, introduced to North America apparently in the middle of the 20th century (Cutler 1990), is typically found on buildings. The large male palp and spaghetti-like copulatory ducts distinguish it from other species in North America except the differently-coloured *A. finschi*.

Material examined (all in UBC-SEM): Canada: Ontario: Burlington (3 males, 6 females), 43.35074, -79.75928 (25 males, 14 females); U.S.A.: Missouri: Dogtown (3 males, 4 females); Massachusetts: Cambridge (1 female).

Attulus (*Sitticus*) *pubescens* (Fabricius, 1775)

Figures 43, 84–88

Aranea pubescens Fabricius, 1775

Remarks. Although closely related to *A. fasciger* and *A. terebratus*, which have among the longest emboli and copulatory ducts in sitticines, *Attulus pubescens* has among the shortest known in sitticines. The very large RTA is distinctive. Introduced to North America in the 20th century (Cutler 1990).

Material examined (All in UBC-SEM): Canada: British Columbia: Vancouver (1 male 1 female); U.S.A.: Massachusetts: Cambridge (3 males, 3 females), Boston (2 males), Milton (2 males), Arlington (1 female).

Subgenus *Sittilong* Prószyński, 2017

Sittilong Prószyński, 2017 (type species *Attus longipes* Canestrini, 1873)

The single species *Attulus* (*Sittilong*) *longipes* of the European Alps is peculiar for its flat body and long first legs in the male, as well as its genitalia. Like *Sittisax* and other members of the *Jollas-Tomis* clade, the RTA is offset basally, and the epigynal openings are anterior and medial. The little-studied *Attulus niveosignatus* has somewhat similar genitalia and may also belong in *Sittilong*.

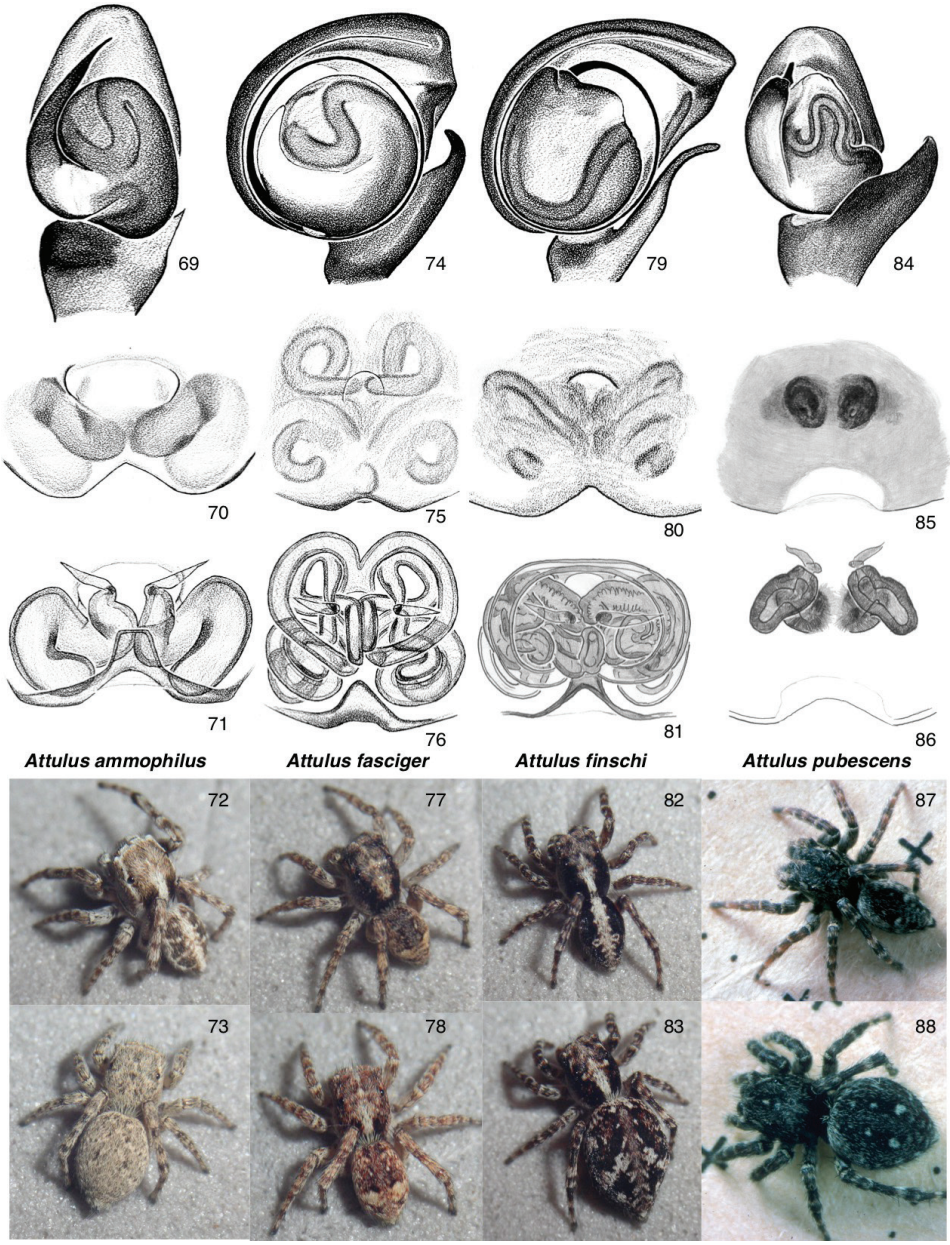

Figures 69–88. Sitticines of Canada: *Attulus*, continued **69–73** *Attulus* (*Attulus*) *ammophilus*: **69** palp (Ontario, Oakville) **70, 71** ventral view of epigyne, dorsal view of cleared vulva (Ontario, Hamilton) **72** male (British Columbia, 49.08, -119.52) **73** female (British Columbia, 49.08, -119.52) **74–78** *A.* (*Sitticus*) *fasciger* (Ontario, 43.3508, -79.7593): **74** palp **75, 76** ventral view of epigyne, dorsal view of cleared vulva **77** male **78** female **79–83** *A.* (*S.*) *finschi*: **79** palp (Ontario, Wawa) **80, 81** ventral view of epigyne, dorsal view of cleared vulva (Saskatchewan, 55.31, -105.11) **82** male (Saskatchewan, 55.31, -105.11) **83** female (Saskatchewan, 55.27, -105.19) **84–88** *A.* (*S.*) *pubescens*: **84** palp (Massachusetts, Milton) **85, 86** ventral view of epigyne, dorsal view of cleared vulva (Massachusetts, Arlington) **87** male (Massachusetts, Cambridge) **88** female (Massachusetts, Cambridge). For other images of *Attulus* (*Sitticus*), see Figs 39–47.

The *Jollas-Tomis* clade

We have chosen not to subdivide the Neotropical Sitticina more finely than into two genera, *Tomis* and *Jollas*, primarily because the fauna is poorly enough known that it is as yet unclear what coarseness of division would be most useful. We might have synonymized their respective Nearctic offshoots (*Sittisax* into *Tomis*, and *Attinella* into *Jollas*), but by retaining them as distinct, we facilitate the eventual splitting of both *Tomis* and *Jollas* as their species become better known. We choose splitting in the *Jollas-Tomis* clade, in contrast to lumping with *Attulus*, because the phylogenetic divergences are so much deeper in the former compared to the latter.

The *Jollas-Tomis* clade includes four genera with 31 species:

Attinella Banks, 1905, with three species:
- *Attinella concolor* (Banks, 1895), comb. nov.**,** transferred from *Sitticus*
- *Attinella dorsata* (Banks, 1895), combination restored, transferred from *Sitticus* (type species)
- *Attinella juniperi* (Gertsch & Riechert, 1976), comb. nov., transferred from *Sittiab*

Jollas Simon, 1901, with 12 species:
- *Jollas amazonicus* Galiano, 1991
- *Jollas cellulanus* (Galiano, 1989), comb. nov., transferred from *Sitticus*
- *Jollas cupreus* W. Maddison, sp. nov.
- *Jollas flabellatus* (Galiano, 1989), comb. nov., transferred from *Sitticus*
- *Jollas geniculatus* Simon, 1901 (type species)
- *Jollas hawkeswoodi* Makhan, 2007
- *Jollas leucoproctus* (Mello-Leitão, 1944), comb. nov., transferred from *Sitticus*
- *Jollas manantiales* Galiano, 1991
- *Jollas paranacito* Galiano, 1991
- *Jollas pompatus* (Peckham & Peckham, 1894)
- *Jollas puntalara* Galiano, 1991
- *Jollas richardwellsi* Makhan, 2009

Sittisax Prószyński, 2017, with two species:
- *Sittisax ranieri* (Peckham & Peckham, 1909)
- *Sittisax saxicola* (C. L. Koch, 1846) (type species)

Tomis F.O. Pickard-Cambridge, 1901, with 14 species
- *Tomis canus* Galiano, 1977, combination restored, transferred from *Sitticus*
- *Tomis kratochvili* (Caporiacco, 1947), comb. nov., transferred from *Pseudattulus*
- *Tomis manabita* W. Maddison, sp. nov.
- *Tomis mazorcanus* (Chamberlin, 1920), comb. nov., transferred from *Sitticus*
- *Tomis mona* (Bryant, 1947), comb. nov., transferred from *Sidusa*
- *Tomis palpalis* F. O. Pickard-Cambridge, 1901, combination restored, transferred from *Sitticus* (type species)
- *Tomis pavidus* (Bryant, 1942), comb. nov., transferred from *Sidusa*
- *Tomis phaleratus* (Galiano & Baert, 1990), comb. nov., transferred from *Sitticus*
- *Tomis pintanus* (Edwards & Baert, 2018, comb. nov., transferred from *Sitticus*

Tomis tenebricus (Galiano & Baert, 1990), comb. nov., transferred from *Sitticus*
Tomis trisetosus (Edwards & Baert, 2018), comb. nov., transferred from *Sitticus*
Tomis uber (Galiano & Baert, 1990), comb. nov., transferred from *Sitticus*
Tomis vanvolsemorum (Baert, 2011), comb. nov., transferred from *Sitticus*
Tomis welchi (Gertsch & Mulaik, 1936), comb. nov., transferred from *Sitticus*

Genus *Attinella* Banks, 1905, restored (removed from synonymy with *Sitticus*)

Attinella Banks, 1905 (type species *Attus dorsatus* Banks, 1895)
Sittiab Prószyński, 2017 (type species *Sitticus absolutus* Gertsch & Mulaik, 1936), syn. nov.

Small species from southern North America, related to the *Jollas* of South America. Except for the thin longitudinal stripes of *A. dorsata*, their bodies are more or less unmarked. Like many other members of the *Jollas-Tomis* clade, the RTA is long and thin, paralleling the axis of the palp, the tibia is robust, and the embolus is fairly short. The first leg's trochanter is unusually long in at least some males (note angles in Fig. 12), though less so than in *Jollas*. The epigynal openings are anterior, with the ducts (intially fused) leading to the posterior and to fairly small spermathecae. As noted below under *A. dorsata*, the synonymy of *Sitticus absolutus* with *Attus dorsatus* leads to *Sittiab* being a junior synonym of *Attinella*. Two species of *Attinella* reach Canada.

Attinella concolor (Banks, 1895)

Figures 89–93

Attus concolor Banks, 1895 (holotype examined; see Maddison 1996: 270)
Sittacus cursor Barrows, 1919, synonymy restored
Sitticus floridanus Gertsch & Mulaik, 1936

Remarks. A small unmarked leaf litter species, known best from the southeastern United States, but recently reported from Canada in the BOLD barcode database (Ratnasingam and Hebert 2007, 2013), from the extreme southern point in Ontario (Point Pelee National Park, specimens PPELE142-11, PPELE183-11, CNPPE2332-12, PPELE666-11, PPELE644-11).

Prószyński (2017a) rejected Maddison's (1996) synonymy of *cursor* with *concolor* on the basis of "lack of documentation", an extra specimen inside the type vial, and the fact that it was published in a revision of *Pelegrina*. However, Maddison (1996) indicated clearly the evidence that identified the holotype within the vial (by its location, labeling, and match to Banks's description), and the features that matched the specimen to *Sittacus cursor* Barrows; that the nomenclatural act was published in a revision of a different salticid genus has no bearing on the validity of the act. Maddison's synonymy, therefore, is reaffirmed here as valid.

Material examined. U.S.A.: Florida: Gainesville (1 male, 1 female, UBC-SEM).

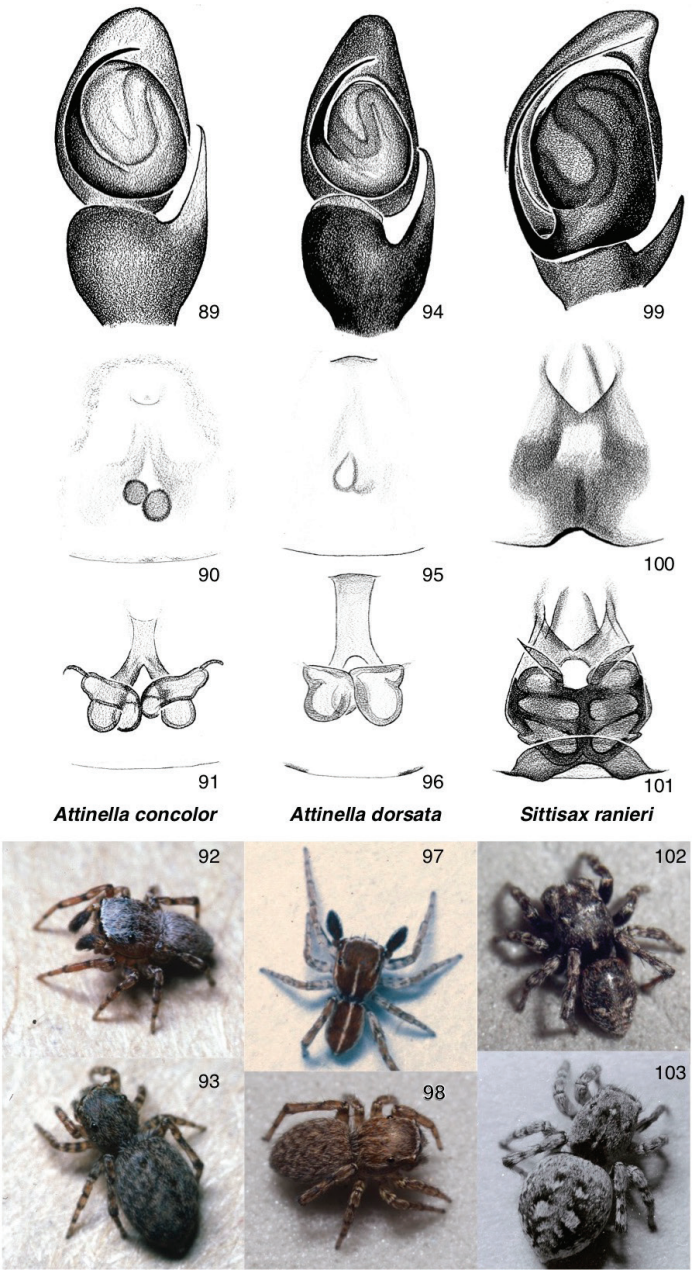

Figures 89–103. Sitticines of Canada: the *Jollas-Tomis* clade, represented by the genera *Attinella* and *Sittisax* **89–93** *Attinella concolor*: **89** palp (Florida, Gainesville) **90, 91** ventral view of epigyne, dorsal view of cleared vulva (Florida, Gainesville) **92** male (Texas, 30.10, -97.25) **93** female (Texas, 30.10, -97.25) **94–98** *Attinella dorsata*: **94** palp (California, San Diego County) **95, 96** ventral view of epigyne, dorsal view of cleared vulva (British Columbia, Nanaimo) **97** male (California, Siskiyou County) **98** female (British Columbia, 48.870, -123.379) **99–103** *Sittisax ranieri*: **99** palp (Northwest Territories, Tuktoyaktuk) **100, 101** ventral view of epigyne, dorsal view of cleared vulva (Nunavut, Baffin Island) **102** male (Saskatchewan, 55.27, -105.19) **103** female (Ontario, Old Woman Bay).

Attinella dorsata (Banks, 1895)
Figures 11–14, 94–98, 105

Attus dorsatus Banks, 1895 (holotype female in MCZ from California: Los Angeles, examined)
Sitticus absolutus Gertsch & Mulaik, 1936, synonymy restored
Sitticus callidus Gertsch & Mulaik, 1936, synonymy restored

Remarks. While females of this small Southwestern desert-dwelling species are indistinctly unmarked, males tend to be reddish with a narrow central longitudinal stripe (Figs 11–14). Prószyński (2017a) rejected Richman's (1979) synonymy of *Attinella dorsata* (Banks, 1895) with *Sitticus absolutus*, saying that *dorsata* is unidentifiable. That statement is false, given that the type specimen is in the MCZ and in good condition. The specimen (examined) has a relatively wide carapace with single thin longitudinal pale line dorsally, long fourth leg, no retromarginal cheliceral tooth, and epigyne (Fig. 105) with a single anterior opening that leads posteriorly through a single duct that splits before the spermathecae, which are visible as two small medial pear-shapes flanked by slightly larger chambers. In these respects, it clearly falls within our current concept of *Sitticus absolutus* as a common, widespread, and relatively uniform species from Texas to California north to Canada (see illustrations by Gertsch and Mulaik 1936, Prószyński 1973). Even if future work were to show that the Californian populations (type locality of *dorsatus*) and Texan populations (type locality of *absolutus*) represent distinct species, they are extremely closely related, certainly congeneric. *Attus dorsatus* is a member of these Californian populations, and for this reason the synonymy of *Sittiab* (type species *Sitticus absolutus*) with *Attinella* (type species *Attus dorsatus*) is assured.

Material examined. Canada: British Columbia: Summerland (1 male, CNC), Galiano Island (2 males, 3 females, UBC-SEM), Nanaimo (1 female). U.S.A.: CALIFORNIA: Humboldt Co., Orleans (1 male, UBC-SEM), Siskyou Co., Beaver Creek and Klamath River (1 male, UBC-SEM), San Diego Co., Johnson Canyon (1 male 1 female, UBC-SEM), El Dorado Co., Camino (1 female, UBC-SEM), Inyo Co., Gilbert Summit (1 female, UBC-SEM); Utah: Millard Co., Sevier Lake (1 male, UBC-SEM); Colorado: Morgan Co., Jackson Lake (1 male, UBC-SEM), Jefferson Co., Golden (2 females, UBC-SEM); Texas: Jim Hogg Co., Guerra (1 female, UBC-SEM), Pecos Co., Fort Stockton (1 female, UBC-SEM).

Genus *Jollas* Simon, 1901
Figures 7–10, 108–119

Jollas Simon, 1901 (type species *Jollas geniculatus* Simon, 1901)
Oningis Simon, 1901 (type species *Neon pompatus* Peckham & Peckham, 1893)

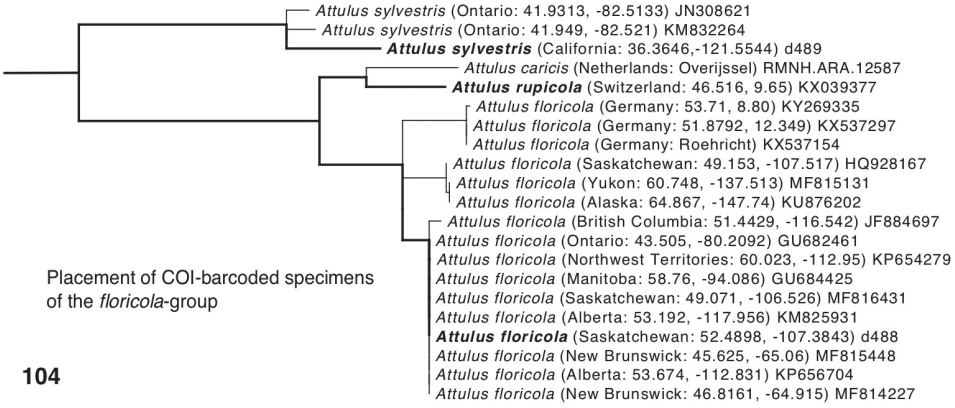

Figure 104. Relationships among *Attulus floricola* mitochondrial COI sequences in the context of the *floricola* group. Specimens in bold had their relationships constrained by the UCE phylogeny of Fig. 48; not shown are the relationships outside the *floricola* group, which are fixed to match the UCE phylogeny. The placement of non-bold specimens on this constrained skeletal tree was inferred by maximum likelihood (RAxML, codon positions as separate partitions).

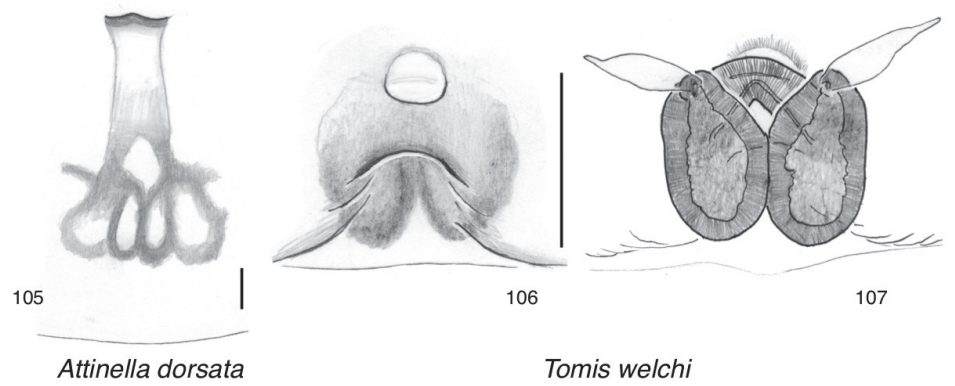

Figures 105–107. Epigynes of *Attinella dorsata* and *Tomis welchi* **105** holotype of *Attus dorsatus* Banks, 1895, epigyne, ventral view **106, 107** holotype of *Sitticus welchi* Gertsch & Mulaik, 1936 **106** epigyne, ventral view **107** cleared vulva, dorsal view.

A Neotropical group, consisting of two species groups, the small glabrous or shiny *geniculatus* group (Galiano 1991b), and the typically grey *leucoproctus* group (Galiano 1989). The male's first trochanter is relatively long, approximately as long as the coxa (Galiano 1989). Typically, the male's first tibia and patella are marked by dark lines on the prolateral face. Epigynal openings are medial, with ducts proceeding toward the lateral. Most species have a long thin RTA, though that is also seen in many *Tomis* and *Attinella*.

***Jollas cupreus* W. Maddison, sp. nov.**
http://zoobank.org/68F87DD6-8C31-4D0B-A349-245B9B201CF3
Figures 7, 108–111, 113–119

Type material. Male holotype and 2 male, 3 female paratypes from Ecuador: Orellana: Río Bigal Reserve, main camp area. 0.5251, -77.4177. 950 m elev. 1–5 November 2010. W & D Maddison, M Vega, M Reyes. WPM#10-041c. The holotype (specimen ECU2010-2060) pertains to the Museum of Zoology, Pontificia Universidad Católica, Quito, Ecuador (QCAZ), but is currently held in the Spencer Entomological Collection at the Beaty Biodiversity Museum, University of British Columbia (UBC-SEM).

Etymology. Refers to the copper colour of males.

A species common in eastern Ecuador on disturbed open grassy ground. It was used in the molecular phylogenetic study of Maddison and Hedin (2003) under the name "*Jollas* sp." (voucher S162) from Sucumbios, Ecuador.

Diagnosis. Differs from the very similar *Jollas puntalara* Galiano, 1991 in the thinner and straighter RTA and the angle at which the embolus arises. The RTA is more or less straight until a curl at the tip, but it narrows dramatically for its terminal three quarters (Fig. 109), whereas in *J. puntalara* (Galiano, 1991b: fig. 26) it bends at the midpoint and thins much less dramatically. The embolus of *J. cupreus*, as it arises, proceeds directly to the prolateral, thus generating an angle in the retrolateral-basal corner of the bulb (like a chin pointing to the retrolateral), while the embolus of *J. puntalara* emerges angled toward the basal, leaving the bulb more rounded (arrow in Fig. 112). These differences are small but consistent, insofar as all Ecuadorian specimens show the distinct "chin" at the base of the embolus and the narrower RTA. It might usually be conservative to leave such close forms as a single species, but given that there is considerable data (molecular phylogenetic and chromosome) attached to the Ecuadorian form, it is safer to name it and thus provide an unambiguous anchor for these data. (Cristian Grismado kindly supplied photographs of Galiano's (1991b) holotype of *Jollas puntalara* to facilitate our comparison, although these differences can be seen as well in her figures 26 and 29.)

Description. Male (holotype). Carapace length 1.37; abdomen length 1.16. ***Carapace*** orange with a black ocular area, mostly glabrous, with only a few scattered setae. ***Clypeus*** orange-brown. ***Chelicerae*** vertical, orange. ***Palp*** orange-brown except for dark brown cymbium, with dark setae except brilliant white patch of setae dorsally on patella. ***Legs*** long, especially the first and fourth. Legs honey coloured to orange-brown except for a strong black line on prolateral-ventral face of first patella, tibia and metatarsus. ***Embolus*** arises at ca. 5 o'clock and curls half-way around bulb. Tibia somewhat bulbous, broad, with bases of setae on retrolateral side forming row of tubercles. RTA begins broad but then narrows abruptly at ca. one quarter its length, from which point it proceeds straight until just before the tip, where it curls. ***Abdomen*** orange-brown, with black scalloped patch covering dorsum, covered with metallic scales. A patch of bright white setae sits above the anal tubercle.

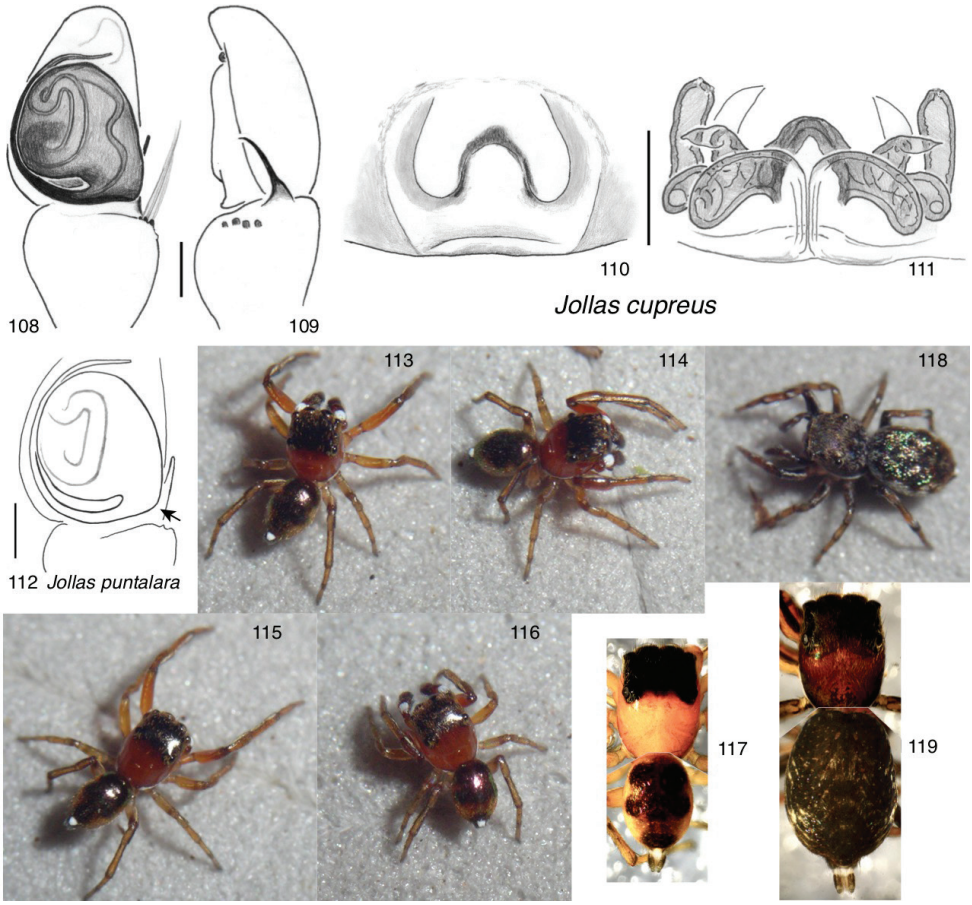

Figures 108–119. *Jollas cupreus*, sp. nov. (except **112**, *J. puntalara*) **108, 109** Left palp of holotype **108** ventral view **109** retrolateral view **110** ventral view of epigyne of paratype **111** dorsal view of same, cleared **112** palp of holotype of *J. puntalara* Galiano **113–115** holotype male **116** male from Yasuní, Ecuador (-0.675, -76.397) **117** holotype male in alcohol **118, 119** paratype female.

Female (paratype). ***Carapace*** length 1.36; ***abdomen*** length 1.89. Much darker than the male in body and appendages (Figs 130, 131). ***Carapace*** dark brown, black in ocular area, sparsely covered with paler scales. ***Clypeus*** and ***chelicerae*** brown, more or less glabrous. ***Chelicerae*** brown, more or less. ***Palps*** and ***legs*** honey coloured but with strongly contrasting black markings: annulae at joints, black stripes or patches on front and back faces of femora, and black stripe on front face of first and second tibiae. Abdomen black but with reflective metallic scales. ***Epigyne*** (Figs 110, 111) with distinctive dark inverted "V" in which are the narrow openings into the copulatory ducts, though lateral pockets may lead the embolus to the openings.

Additional material. 22 males and 6 females from: Ecuador: Napo: Tarapoa. 23 June – 1 July 1988 W. Maddison WPM#88-002 (1 male); Ecuador: Napo: bridge

over Rio Cuyabeno on road to Tipishca. 25–30 June 1988 W. Maddison WPM#88-004 (1 male 1 female); Ecuador: Napo: bridge over Rio Cuyabeno on road to Tipishca. 29–30 July 1988 W. Maddison WPM#88-018 (4 males 2 females); Ecuador: Napo: Reserva Faunistica de Cuyabeno, Laguna Grande, Sendero La Hormiga. 2–5 August 1988 W. Maddison WPM#88-023 (2 males); Ecuador: Napo: Reserva Faunistica de Cuyabeno, Laguna Grande, PUCE field station. 1–7 August 1988 W. Maddison WPM#88-025 (1 male); Ecuador: Napo: bridge over Rio Cuyabeno on road from Lago Agrio to Tipishca. 8–9 August 1988 W. Maddison WPM#88-027 (1 male); Ecuador: Sucumbios: Reserva Faunistica Cuyabeno, Laguna Grande, PUCE field station. 0.002, -76.172. 21–29 July 1989 W. Maddison WPM#89-032 (1 male); Ecuador: Sucumbios: bridge over Rio Cuyabeno on road between Tarapoa and Tipishca, 0.025, -77.308. 29 July 1989 W. Maddison WPM#89-036 (1 male); Ecuador: Sucumbios: Reserva Faunistica Cuyabeno, Nuevo Mundo cabins along Rio Cuyabeno at jcn with Lago Agrio-Tipishca HWY 19–29 April 1994 W. Maddison WPM#94-021 (3 males); Ecuador: Sucumbios: Reserva Faunistica Cuyabeno, Nuevo Mundo cabins, jcn Rio Cuyabeno & Lago Agrio-Tipishca HWY tree trunks 19–29 April 1994 W. Maddison WPM#94-023 (1 male); Ecuador: Morona Santiago: km 3 from Limón towards Gualaceo. 2.9663, -78.4209; 1250 m el. 12 July 2004 Maddison, Agnarsson, Iturralde, Salazar. WPM#04-030 (1 male 2 females); Ecuador: Morona Santiago: km 4 from Limón towards Gualaceo. 2.9808, -78.4414; 1380 m el. 12 July 2004 Maddison, Agnarsson, Iturralde, Salazar. WPM#04-031 (2 males); Ecuador: Orellana: Yasuní Res.Stn.area, Station area 0.675, -76.397 210–280 m elev. 26 July – 13 Aug 2011 Maddison/Piascik/Vega WPM#11-015 (2 males); Ecuador: Orellana: Yasuní Res.Stn.area, Station area 0.674, -76.397 210–280 m elev. Clearings, forest edge 8–9.Aug.2011 Maddison/ Piascik/Vega. WPM#11-104 (1 male); Ecuador: Orellana: Río Bigal Reserve, boundary along road. 0.541, -77.424. 970 m elev. 5 November 2010. M Vega, D & W Maddison, M Reyes. WPM#10-048 (1 female). (Note: the province Sucumbios was established after 1988; the 1988 localities listed as Napo Province would now all be in Sucumbios.).

Genus *Sittisax* Prószyński, 2017, restored (removed from synonymy with *Sitticus*)

Sittisax Prószyński, 2017 (type species *Euophrys saxicola* C.L. Koch, 1846)

Breitling's (2019) synonymy of *Sittisax* with *Sitticus* is here rejected based on our phylogenetic results, which strongly support it as the sister group of *Tomis*. According to the phylogeny, this lineage of two species arrived from the New World to Eurasia independently from *Attulus*, and retains a few features more similar to the other members of the *Jollas-Tomis* clade: the RTA is offset basally, and the epigynal openings are placed anteriorly and medially.

***Sittisax ranieri* (Peckham & Peckham, 1909)**
Figures 99–103

Attus lineolatus Grube, 1861 (junior homonym)
Sittacus ranieri Peckham & Peckham, 1909

Remarks. The Holarctic *Sittisax ranieri* is a widespread boreal species, which in North America follows the high elevations of the Western Cordillera to the south, living on rocks and litter. It is dark in colour, large-bodied, and with distinctive genitalia.

Material examined. Canada: Northwest Territories: Tuktoyaktuk (1 male); Nunavut: Baffin Island (1 female); British Columbia: Downton Creek (2 males 2 females), 49.026, -114.061 (1 male), 59.8, -127.5 (1 male), Pink Mountain (1 male); Yukon: km 72 Dempster Highway (2 males, 2 females); km 75.6 Dempster Highway (1 female); Saskatchewan: 55.27, -105.19 (2 males), Ontario: Old Woman Bay (1 female); New Brunswick: 65.336, -69.4 (6 males, 3 females); U.S.A.: Washington: Spray Park (1 males, 2 females); Oregon: 45.261, -117.178 (1 female); Colorado: 39.803, -105.782 (1 male).

Genus *Tomis* F.O. Pickard-Cambridge, 1901, restored (removed from synonymy with *Sitticus*)
Figures 5, 6, 106, 107, 120–128

Tomis F.O. Pickard-Cambridge, 1901 (type species *Tomis palpalis* F.O. Pickard-Cambridge, 1901)
Pseudattulus Caporiacco, 1947 (type species *Pseudattulus kratochvili* Caporiacco, 1947), syn. nov.

A Neotropical group whose male spermophore (with some possible exceptions) has a "shortcut loop". That is, the large loop of the spermophore that normally occupies much of the visible face of the tegulum, and which points basally in many sitticines (e.g., Fig. 89), is incomplete, instead diving into the subtegulum, and thus not returning terminally to complete the loop on the surface of the tegulum (e.g., Fig. 120; Galiano 1991a: fig. 13).

The phylogeny strongly places *T. palpalis*, *T. manabita*, and *Sittisax ranieri* together. Although the phylogeny gives us the freedom to synonymize *Sittisax* into *Tomis*, this deep clade will eventually deserve at least two genera, and so we tentatively retain the boundary between the Neotropical *Tomis* and the Holarctic *Sittisax*, based on the apparent difference in spermophore loops. The other species are included in *Tomis* because of their apparent relationship with *T. palpalis* and *T. manabita*. The *palpalis* group (*T. palpalis*, *T. canus*, *T. mazorcanus*, *T. phaleratus*, *T. vanvolsemorum*, and *T. uber*) is delimited by a flattened cymbium (Galiano, 1991a) and well-separated epigy-

nal openings. The remaining species all are known from coastal areas of the Caribbean or South America, and at least some live on beaches. They might not form a monophyletic group, as some show a long thin RTA, others not. *T. pavidus* and *T. mona* appear especially close to *T. manabita* by similarities in the palps. The others can be tentatively included in *Tomis* because they share with *T. palpalis* and *T. manabita* the shortcut spermophore loop.

The placement of *Sitticus welchi* Gertsch & Mulaik, 1936 in *Tomis* is tentative. The holotype female (AMNH, examined) lacks most of its legs and setae, but is nonetheless identifiable as a sitticine through the absence of a retromarginal cheliceral teeth and a very long leg that appears to be (it is disarticulated) of the fourth pair. The single anteriorly-placed epigynal opening (Figs 106, 107) indicates it belongs in the *Jollas-Tomis* clade. What suggests placement in *Tomis* in particular is the deep incision from the epigastric furrow toward the epigynal opening (Fig. 106). Such an incision as seen also in *Tomis mona* (Bryant 1947: fig. 6), which itself is placed in *Tomis* by the close similarity between its palp and that of *T. manabita*.

We synonymize *Pseudattulus* (see Ruiz et al. 2007) based on its shortcut spermophore loop and flattened cymbium, which suggest close relationship to (or membership in) the *palpalis* group. We accept (and thus re-assert) Ruiz et al.'s (2007) synonymy of *Sitticus cabellensis* Prószyński, 1971 with *Pseudattulus kratochvili*. Prószyński (2017a) had rejected their synonymy, but we see no basis for this, as Ruiz et al. had explained it well. Although we suspect *Pseudattulus* will eventually be reinstated, keeping it separate now would most likely yield a non-monophyletic genus *Tomis*. For many species (e.g., those from the Galapagos) we have no basis for choosing whether to assign them to *Pseudattulus* or to *Tomis*, and so either or both genera, if separated, would likely be non-monophyletic. Uniting them solves this until we have better phylogenetic information.

Tomis manabita **W. Maddison, sp. nov.**

http://zoobank.org/4C656386-8B15-4B5C-BF3F-27805897C65F
Figures 120–128

Type material. Male holotype, 10 male and 8 female paratypes from Ecuador: Manabí: Puerto Rico, Cabañas Alandaluz 5 May 1994 W. Maddison WPM#94-031. The holotype (specimen UBC-SEM AR00217) pertains to the Museum of Zoology, Pontificia Universidad Católica, Quito, Ecuador (QCAZ), but is currently held in the Spencer Entomological Collection at the Beaty Biodiversity Museum, University of British Columbia (UBC-SEM).

Etymology. Based on the type locality; the form is the adjective in Spanish (masculine or feminine).

A species on the beaches of coastal Ecuador, resembling *Attulus* in habitus. It was used in the molecular phylogenetic study of Maddison and Hedin (2003) under the name "*Sitticus* sp." (voucher S220) from Manabí, Ecuador.

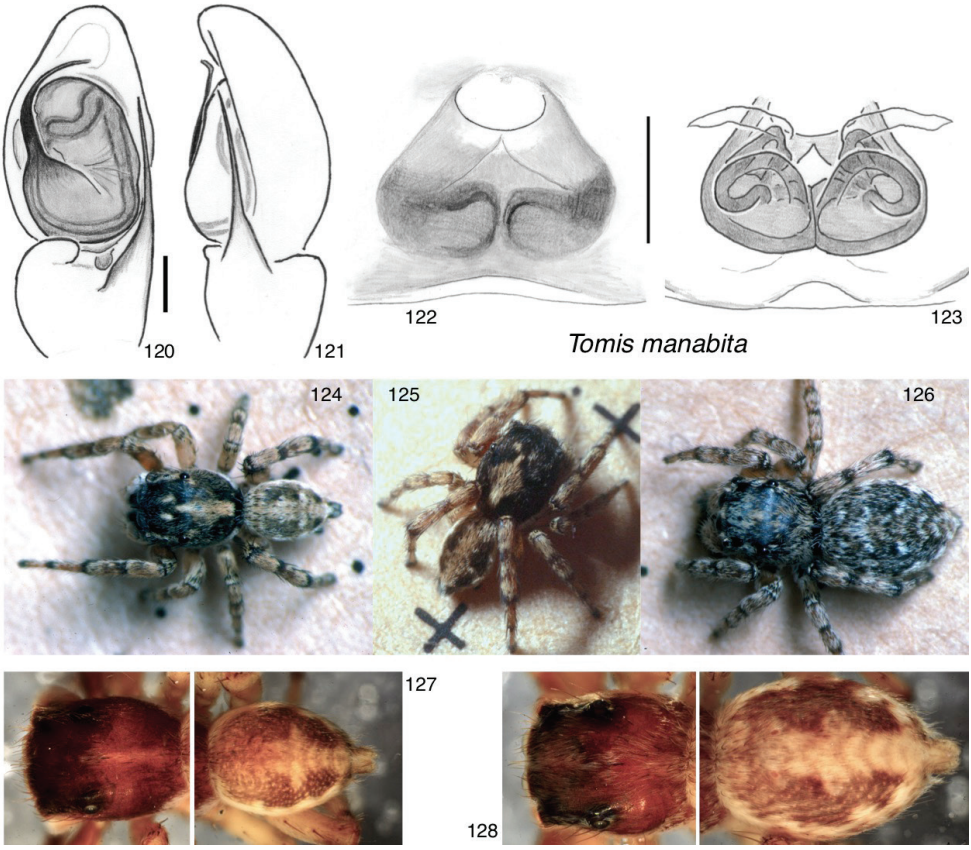

Figures 120–128. *Tomis manabita*, sp. nov. **120, 121** Left palp of holotype **120** ventral view **121** retrolateral view **122** ventral view of epigyne of paratype **123** dorsal view of same, cleared **124–128** specimens from type locality **124** male **125** male **126** female **127** male holotype **128** female paratype.

Diagnosis. Palp closely resembles that of *Tomis pavidus*, from which it differs in the smaller tibia and longer RTA.

Description. Male (holotype). Carapace length 1.58; abdomen length 1.51. ***Carapace*** (Figs 124, 127) medium brown with recumbent brown setae except for thin medial longitudinal band of white setae on thorax, two spots of pale setae in ocular area, and a marginal band of white setae that is broad on the thorax but narrows to the anterior, disappearing before the clypeus is reached. ***Clypeus*** brown, with a few brownish setae. ***Chelicerae*** vertical, with a few pale setae near the clypeus. Retromarginal chelicerial teeth lacking. ***Palp*** clothed with white setae dorsally, but prolaterally with darker integument and setae from tip of femur to cymbium; cymbium mostly dark brown. ***Embolus*** (Fig. 120) arises broadly, more centrally beneath bulb (and less peripherally) than is typical, then narrows abruptly at ca. 9 o'clock. RTA extremely long and thin, parallel to axis of the palp. ***Legs*** honey-coloured, with notably darker annulae at the

tarsus-metatarsus joints, and black stripe on prolateral-ventral face of first patella and tibia. ***Abdomen*** (Figs 124, 127) brown with two lateral and one median longitudinal bands of paler setae, the medial band less distinct, wavy, and accompanied by a lateral extension that forms a cross.

Female (paratype # UBC-SEM AR00218). ***Carapace*** length 1.76; ***abdomen*** length 2.22. ***Carapace*** (Figs 126, 128) brown, covered unevenly with recumbent cream-coloured setae. ***Clypeus*** with white setae, longest at midline where they overhang the chelicerae. Chelicerae brown, with a few setae near clypeus. ***Palps*** and ***legs*** honey coloured, with weak annulae. ***Abdomen*** brown, marked as in male except bands are less distinct (Figs 126, 128). ***Epigynum*** with an anterior atrium from which short copulatory ducts lead diagonally to the spermathecae (Figs 122, 123).

Additional material. 15 males and 7 females from Ecuador: Manabí: Machalilla National Park, Salaite, between HWY and coast 6 May 1994 W. Maddison WPM#94-032 (4 males, 2 females); Ecuador: Manabí: Machalilla National Park, Salaite, 1 km inland along trail from HWY. 6 May 1994 W. Maddison WPM#94-033 (3 males); Ecuador: Manabí: Machalilla National Park, trail between Agua Blanca & San Sebastien 50–400 m dry forest 7 May 1994 W. Maddison WPM#94-034 (1 male); Ecuador: Manabí: Crucita. 30 August 1988 W. Maddison WPM#88-040 (2 males 4 females); Ecuador: Del Oro: Jambelí 13 August 1989 W. Maddison WPM#89-040 (3 males); Ecuador: Manabí: Puerto Lopez. 1.5497, -80.8104; 5 m el. 1–5 August 2004 W. Maddison. WPM#04-067 (2 males 1 female).

Species misplaced as sitticines

The following species are not sitticines, indicated by the presence of retromarginal cheliceral teeth (lacking in the Sitticini, a synapomorphy) or characteristic euophryine genitalia.

The following three are members of the Euophryini. They are left within sitticine genera because it is unclear to which genus they should be transferred.

Jollas armatus (Bryant, 1943)

Jollas crassus (Bryant, 1943)

Jollas minutus (Petrunkevitch, 1930)

The following two species described in *Sitticus* are also euophryines (see Prószyński 2017a). They are tentatively placed in a likely genus, *Chinophrys*:

Chinophrys taiwanensis (Peng & Li, 2002), comb. nov.

Chinophrys wuae Peng, (Tso & Li, 2002), comb. nov.

The following species can be moved out of *Sitticus* to their appropriate genera. The type specimens of both, in the MCZ, have been examined.

Heliophanus designatus (Peckham & Peckham, 1903), comb. nov. – bears the stridulatory apparatus characteristic of chrysillines (Maddison 1987), as well as the body form, markings and epigynum typical of *Heliophanus*.

Mexigonus peninsulanus (Banks, 1898), comb. nov. – appears as a typical *Mexigonus* with euophryine genitalia.

Chromosome diversity and evolution

Chromosome observations

Table 2 summarizes the chromosome complements of the 18 sitticines studied along with those reported in the literature (Hackman 1948, Kumbiçak et al. 2014). Except in *Attinella concolor*, all autosomes are acrocentric. Eight species have the usual chromosome complement for male salticids, 13 pairs of acrocentric autosomes and X_1X_20 sex chromosomes. Three taxa (*A. burjaticus*, *A. floricola*, *A. finschi*) have the standard XX0 sex chromosomes but an extra pair of autosomes to make 28a+XaXa0. Of the remaining species, six have neo-Y systems of varied forms, while the seventh, *Attinella concolor*, has apparently completed a series of Roberstonian fusions to generate all metacentrics and halve the chromosome number to male 14m + Xm0. The following account of our observations, species by species, gives the basis for our interpretation of chromosome complements.

Chromosomes of the *Jollas-Tomis* clade

Attinella concolor: 14m+Xm0 (Figs 129, 130): Nuclei of first meiotic metaphase show clearly seven pairs of metacentric autosomes and one metacentric X chromosome (Figs 129, 130). The metacentric autosomes appear strikingly different from the usual acrocentrics typical of spiders. Most of the bivalents are held together by just one arm at first metaphase, the other free.

Attinella dorsata: 26a+XaXa0 (uncertain). Scored as 26a+XaXa0 in notes from the 1980s, the slides are too faded and degraded for precise re-count, but re-examination shows they have at least 13 acrocentric bivalents, and what looks like XX0. Although we might have abandoned the score entirely, we include it here to show that it is at least similar to the typical salticid complement, and not at all what is seen in the close relative *Attinella concolor*.

Jollas cupreus: 26a+XaXa0. One first division nucleus appears clearly as 13 autosomal bivalents plus two acrocentric Xs, while two more show the typical Xs side by side.

Sittisax ranieri: 24a+XmXaYm (Figs 132–136). The distinctive chromosome complement is confirmed by many clear nuclei. The sex chromosomes (Figs 132–136) appear as a rabbit's head (the Y) with two ears (the Xs), one of which is floppy (a metacentric with an unpaired arm). The two arms of the metacentric Y and one of each X meet together at a single point, a junction of four arms. That the "head" and "ears" segregate to opposite poles is confirmed by second metaphase counts (nine nuclei with 12 acro.+1 meta.; five nuclei with 13 acro.+ 1 meta.). That the "head" is a Y and the "ears" are Xs is indicated by counts of 26 acrocentrics and two metacentrics in mitotic metaphase of two young females from Wawa, Canada (47.79N, 84.90W) (2 complete, countable nuclei found in each female, scored in 1986; now faded). Unlike *Habronattus* (Maddison, 1982) and most other species

Table 2. Chromosome complements observed for males of 17–18 species of sitticines. The autosomal counts represent diploid complement, and thus 26a means 13 pairs of acrocentric autosomes. In the chromosome counts, a = acrocentric (one-armed), m = metacentric (two-armed). Exx. is the number of specimens; nuc. is the number of nuclei showing the full chromosome complement; +nuc sex is the number of additional nuclei showing the sex chromosomes (though not clearly the autosomes). Uncertainties about scoring, in particular about *Attinella dorsata*, *Attulus burjaticus* and the specimen labelled "*Attulus rupicola/floricola*" are explained under Chromosome observations.

Species	Autosomes	♂ Sex chrom.	Y present	Locality	exx	nuc	+nuc sex
***Jollas-Tomis* clade**							
Attinella concolor	14m	Xm0	no	U.S.A.: Gainesville, 29.63, -82.37	1	6	2
A. dorsata	26a?	XaXa0?	?	U.S.A.: Dillon Cr., 41.57, -123.54	3	11	
Jollas cupreus	26a	XaXa0	no	Ecuador: Tarapoa, -0.12, -76.34	1	2	1
Sittisax ranieri	24a	XmXaYm	yes	Canada: Leguil Creek, 59.8, -127.5	2	10	1
				Canada: Inuvik, 68.31, -133.49	1		1
				Canada: Wawa, 47.79, -84.90	2	8	
				U.S.A.: Mt. Monadnock, 42.87, -72.11	1	3	
Sittisax saxicola	24a	XaXaXaYm or XmYaYaYa	yes	Switzerland: Flims, 46.9, 9.2	3	14	10
Tomis manabita	26a	XaXa0	no	Ecuador: Crucita, -0.9, -80.5	1	3	2
Attulus							
Attulus (*Attulus*) *ammophilus*	26a	XaXa0	no	Canada: Toronto, 43.65, -79.32	3	9	1
				Russia: Uvs Nuur, 50.6690, 92.9844	2	11	6
A. (*A.*) *burjaticus*	? (28a?)	XaXa0	no	Russia: Uvs Nuur, 50.677, 92.99	1	1	7
A. (*A.*) *caricis*	26a	XaXa0	no	38.6, 34.8 (Kumbiçak et al. 2014)	–		
A. (*A.*) *cutleri*	26a	XaXaYa	yes	Canada: Inuvik, 68.35, -133.70	1	3	4
A. (*A.*) *floricola*	28a	XaXa0	no	Canada: Barrie, 44.43, -79.65	1	7	7
				U.S.A.: Naselle, 46.43, -123.86	1	2	
A. (*A.*) *rupicola/floricola*	24a?	XaXaXaYm?	yes	Switzerland: Flims, 46.9, 9.2	1	3	5
A. (*A.*) *inexpectus*	26a	XaXa0	no	Russia: Uvs Nuur, 50.6690, 92.9844	2	13	5
A. (*A.*) *striatus*	24a	XaXaXaYm	yes	U.S.A.: Ponemah, 42.82, -71.58	1	5	6
Attulus (*Sitticus*) *fasciger*	26a	XaXa0		Canada: Burlington, 43.351, -79.759	3	16	
A. (*S.*) *finschi*	28a	XaXa0	no	Canada: Nipigon, 49.01, -88.16	1	4	
				Canada: Sault Ste. Marie, 46.94, -84.55	1	1	
				Canada: Chinook L., 49.67, -114.60	1	8	3
A. (*S.*) *pubescens*	26a	XaXmYa	yes	U.S.A.: Cambridge, 42.38, -71.12	4	10	9
A. (*S.*) *terebratus*	26a	XaXa0	no	Russia: Karasuk, 53.730, 77.866	1	9	14
	26a	XaXa0		Hackman (1948)	–		

of sitticines, no heteropycnosis or achiasmate meiotic pairing was noted in the sex chromosomes of *S. ranieri* which would have indicated ancestral X material. We thus have no account for how this structure evolved, and what parts of it represent ancestral X versus autosome material.

Sittisax saxicola: 24a+XaXaXaYm or 24a+XmYaYaYa (good quality, though ambiguous in interpretation; Figs 137–139). The sex chromosome system in *Sittisax saxicola* is at least superficially similar to that in *S. ranieri* except that the "rabbit" has three straight "ears". The many metaphase I nuclei observed show 12 clear autosomal acrocentric bivalents plus the sex chromosomes, while two mitotic nuclei had clear counts of 28 chromosomes, one of which is notably longer than the others, possibly the metacentric. The acrocentric "ears" of the sex chromosomes are always oriented together toward one pole at metaphase I, the metacentric "head" to the other, indicating either a XXXY or XYYY sex chromosome system. Consistent

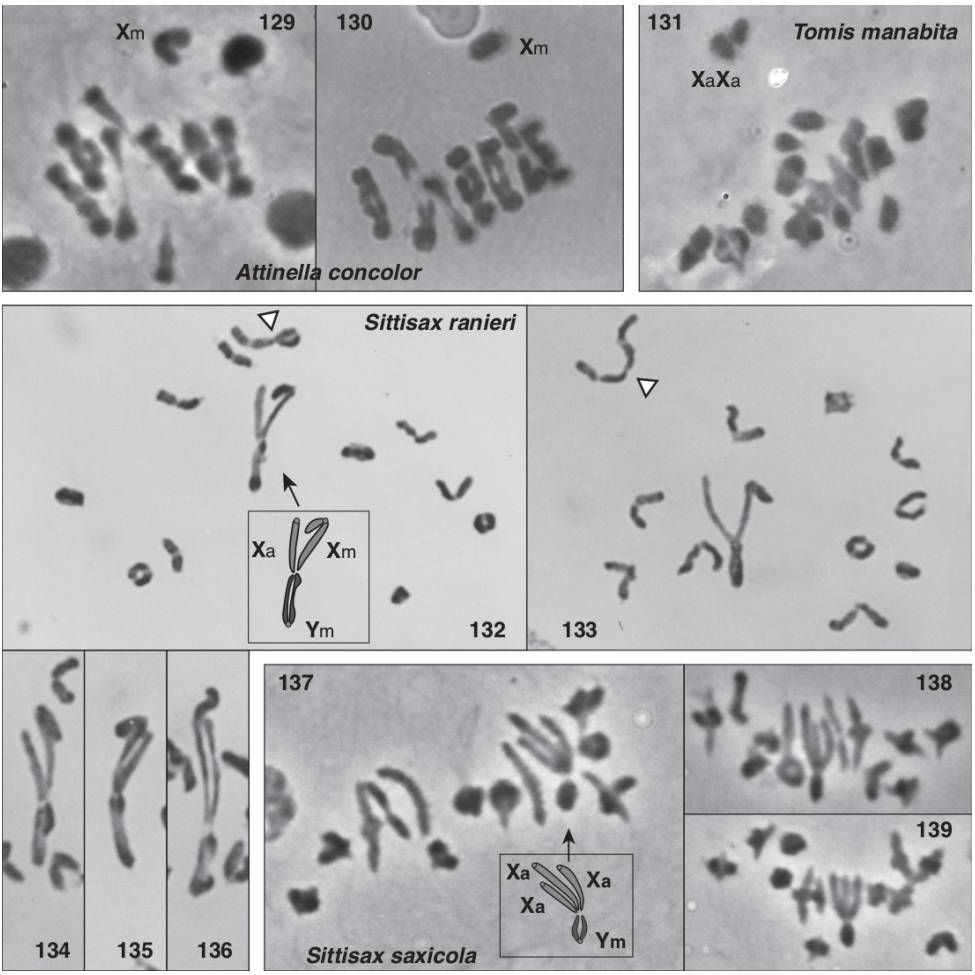

Figures 129–139. Chromosomes of first meiotic division in males of the *Jollas-Tomis* clade **129, 130** *Attinella concolor*, with only seven pairs of autosomes, but each two-armed, 14m+Xm0, Florida (29.63N, 82.37W) **131** *Tomis manabita*, showing the two Xs off to one pole, and 13 acrocentric bivalents on the metaphase plate, Ecuador (0.9S, 80.5W) **132–136** *Sittisax ranieri*, whose distinctive XmXaYm appears as a rabbit head with a droopy ear. White triangles show points where two bivalents are apparently linked together **134–136** details of XXY of *S. ranieri* **137–139** *Sittisax saxicola*, with sex chromsomes, interpreted tentatively as XaXaXaYm, appearing as a rabbit head with three ears, Switzlerland (46.9N, 9.2E).

with this are three observations of second division nuclei with 15 acrocentrics, and one observation with 12 acrocentrics and a metacentric. There is no clear evidence from heteropycnosis, and no female karyotype, to indicate whether the "ears" are the Xs or the Ys. We might invoke parsimony to suggest the metacentric is the Y and the ears the Xs, as in *S. ranieri*, but will resist this, and treat the sex chromosomes as ambiguous, either XXXY or XYYY.

All four sex chromosomes of *S. saxicola* come together in a quintuple junction. This and the quadruple junction of *S. ranieri* are unusual, possibly formed because

mutual translocations or repeated sequences generate a knit pattern of pairing. White (1965) postulated that a similar triple terminal junction in a mantid is formed by chiasmata joining the three arms on triple pairing segments and subsequently terminalizing. There is evidence that different autosomes in *Sittisax* might also have common terminal segments. In all males of *S. ranieri*, autosomal bivalents with proximal chiasmata are often joined together into tetravalent and sometimes hexavalent chains, via the terminal ends of one chromosome of each bivalent (see white triangles in Figs 132, 133). The terminal ends of the autosomes appear to have small satellites.

Tomis manabita: 26a+XaXa0 (Fig. 131). Although there are only a few nuclei, they show 13 autosomal bivalents plus two acrocentric Xs. In three nuclei, the two acrocentric Xs are side by side and off to one pole.

Chromosomes of *Attulus*

Attulus (*Attulus*) *ammophilus*: 26a+XaXa0 (Figs 140, 141). Many clear nuclei show the classical 13 acrocentric bivalents and two acrocentric X's off toward one pole.

Attulus (*Attulus*) *burjaticus*: ?+XaXa0 (autosome count uncertain; Fig. 142). One clear and isolated meiotic nucleus in metaphase I shows 15 figures, one of which is presumably be the XX, suggesting that it may have 28a+XX0. Six nuclei show a typical pair of XaXa toward one pole. The interpretation of XX0 seems reasonably secure, but the autosome count is not.

Attulus (*Attulus*) *cutleri*: 26a+XaXaYa (Figs 152, 153). There are a few clear nuclei, and several more in which the sex chromosomes are clear (but the autosome counts are not). Interpretation of the sex chromosomes seems fairly clear. They are interpreted to be XXY because two elements are seen side by side and slightly decondensed (the Xs). The third chromosome is small, paired terminally with the more condensed end of the larger X, and thus interpreted as a Y. There is no hint of a centromere in the larger X, and so all appear to be acrocentrics.

Attulus (*Attulus*) *floricola*: 28a+XaXa0, with one autosome much smaller (Figs 143–146). In addition to the clear division I nuclei showing the classic pair of X's lying side by side, counts of second division nuclei show either 14 acrocentric chromosomes (six clear nuclei) or 16 chromosomes (five clear nuclei). All of the second division nuclei show one chromosome much smaller than the others. Those with 16 chromosomes show two of the chromosomes appearing larger and distinct in appearance, consistent with their being the Xs, pointing to an XaXa0 sex chromosome system.

Attulus (*Attulus*) *rupicola/floricola* (Switzerland): 24a+XaXaXaYm (uncertain in details, though the presence of at least one Y is secure; Figs 150, 151). The presence of a Y chromosome is well supported, but the details of the sex chromosome system are uncertain. No single nucleus shows both the chromosome count and the sex chromosome system convincingly. The total number of chromosomes (27 acrocentrics and one metacentric) can be seen in two mitotic nuclei, and in a few first division

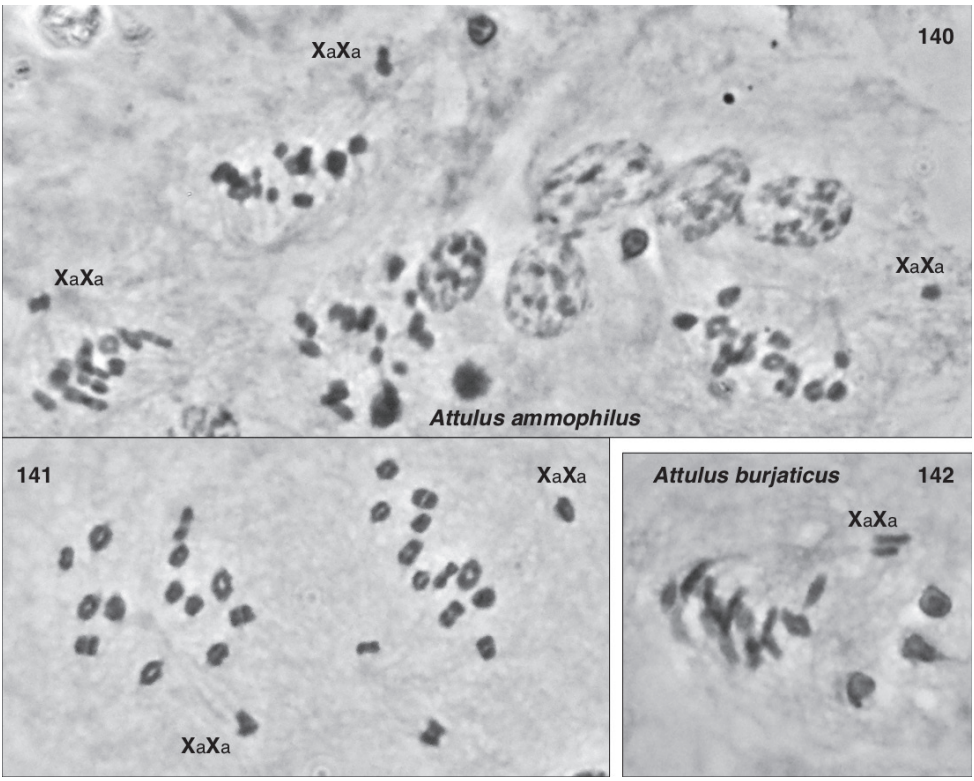

Figures 140–142. Chromosomes of first meiotic division of *Attulus* subgenus *Attulus* **140, 141** *Attulus ammophilus*, Tuva (50.6690N, 92.9844E): **140** four nuclei, three showing the two X chromosomes toward one pole **141** two nuclei showing two Xs and thirteen pairs of acrocentric autosomes **142** *Attulus burjaticus*, showing the two X chromosomes toward one pole, Tuva (50.677N, 92.99E). The three large spots to the lower right are spermatids.

meioses. Although at least 20 nuclei show the V-shaped trivalent of metacentric (point of the "V") and two acrocentrics (distal arms of the "V"), interpreted as the Y and two Xs, only three show the fourth member, an acrocentric, lying near one of the Xs. This achiasmate association leads us to intepret the system as XaXaXaYm rather than XmYaYaYa, but the evidence is weak, as there are no female counts, heteropycnosis is not obvious, and most often the fourth member is lying distant from the trivalent, usually not obviously directed to the same pole as the two acrocentrics, though not apparently oriented against it either.

Attulus (*Attulus*) *inexpectus*: 26a+XaXa0 (Figs 147–149). Several very clear first division nuclei show 13 acrocentric bivalents and the two acrocentric Xs, heteropycnotic and lying side by side, off of the metaphase plate. Three second division counts are consistent with an XX0 sex chromosome system (two counts of 13 acrocentrics; one count of 15).

Attulus (*Attulus*) *striatus*: 24a+XaXaXaYm. The slides are too faded to score now even under phase contrast, and so for this we rely entirely on notes from 1985. Those

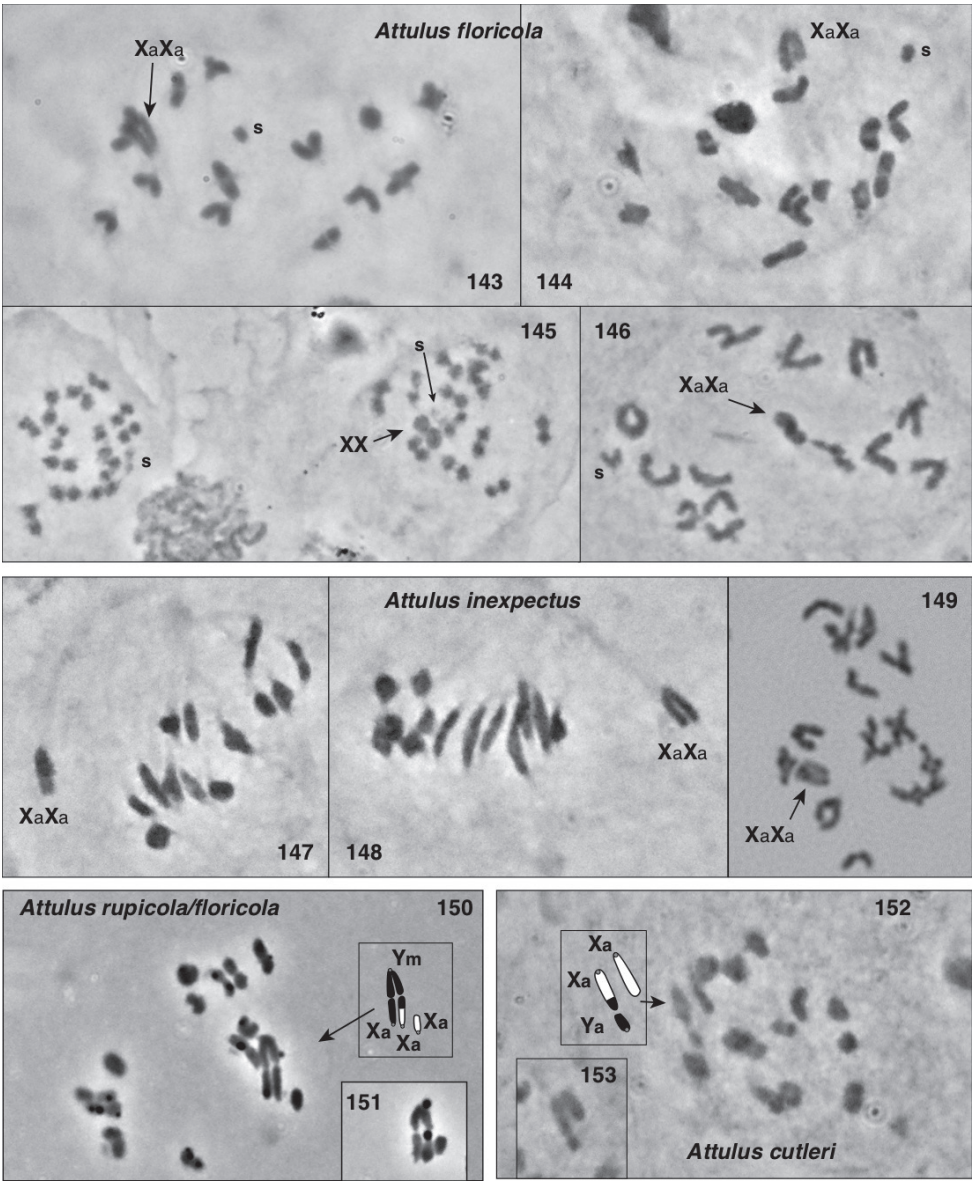

Figures 143–153. Chromosomes of meiosis of *Attulus* subgenus *Attulus*, continued **143–146** *Attulus floricola*, with an extra small bivalent (**s**) to make 28a+XaXa0, Ontario (44.43, -79.65): **143, 144** first metaphase **145** second division, showing one nucleus with 14 acrocentrics, the other with 14 acrocentrics and the two condensed Xs **147–149** *Attulus inexpectus*, showing 13 acrocentric bivalents and the sex chromosomes (26a+XaXa0), Tuva (50.6690, 92.9844) **150, 151** *Attulus* sp. (ambiguously identified, either *A. rupicola* or *floricola*), tentatively intepreted as having 24a+XaXaXaYm, Switzerland (46.9, 9.2): **151** same, sex chromosomes from another nucleus **152** *Attulus cutleri*, with 26a+XaXaYa, Canada (68.35, -133.70) **153** same, sex chromosomes from another nucleus

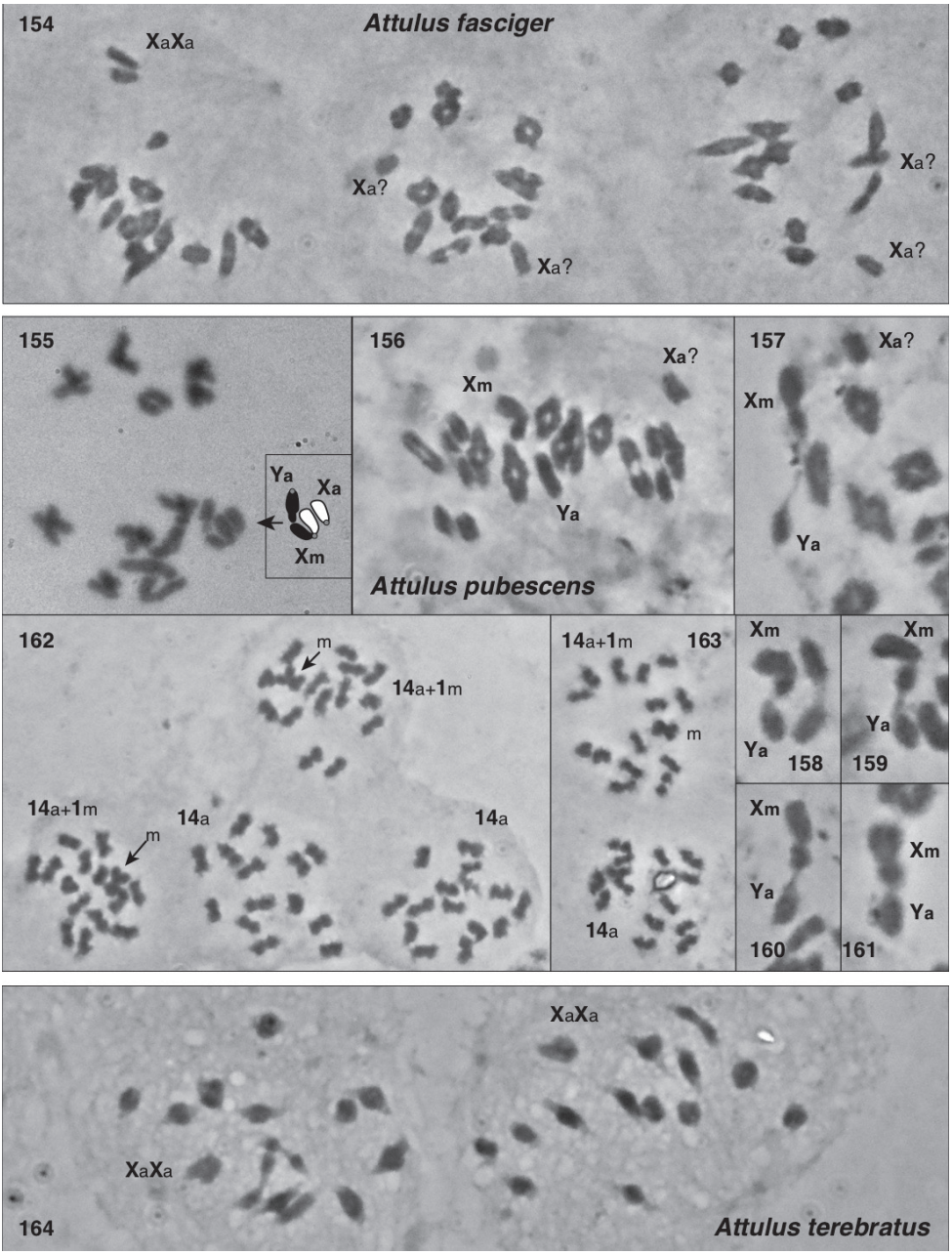

Figures 154–164. Chromosomes of meiosis of *Attulus* subgenus *Sitticus* **154** *Attulus fasciger*, three nuclei, one showing the two Xs together and toward a pole, Canada (43.351N, 79.759W) **155–163** *Attulus pubescens*, with XaXmYa sex chromosomes, Massachusetts (42.38N, 71.12W) **157–161** XmYa sex chromosomes from other nuclei; the second X is often not paired with them **162, 163** Second division nuclei, all having 14 acrocentrics, and some having in addition a metacentric (m) **164** *Attulus terebratus*, two nuclei (26a+XaXa0), Novosibirsk Oblast (53.730N, 77.866E).

notes give good evidence to consider the interpretation secure. The slides were then clear enough to score chiasma localization in the acrocentric autosomes (in 14 nuclei with at least ten autosomes scorable, the numbers of proximal vs. interstitial vs. terminal chiasmata were 76:12:50 respectively). Five of these nuclei showed a clear count of 14 acrocentric autosomes. The sex chomosomes were clear in several nuclei, consisting of a "V" shaped trivalent with a metacentric at the point of the "V", to each arm of which was paired an acrocentric. One of those acrocentrics was decondensed (heteropycnotic) in its centromeric half, and lying alongside it achiasmately was a decondensed acrocentric, thus in total making a figure of four. The achiasmate pairing and heteropycnosis suggest those acrocentrics have ancestral X material, as in the XXXY *Habronattus* (Maddison 1982, Maddison & Leduc-Robert 2013), which this resembles strongly. Three pairs of second division nuclei showed one member with 15 acrocentrics, the other with 12 acrocentrics and a metacentric. Together this points to an XaXaXaYm sex chromosome system.

Attulus (*Sitticus*) *fasciger*: 26a+XaXa0 (Fig. 154). Many clear nuclei show the classical 13 acrocentric bivalents and two acrocentric X's (heterpycnotic, side by side or apart) off toward one pole. A few division-2 nuclei are consistent with this (three nuclei with 13 similar acrocentrics; one nucleus with 13 similar and two more condensed acrocentrics).

Attulus (*Sitticus*) *finschi*: 28a+XaXa0, with one autosome much smaller. This score relies primarily on old notes, which indicate 28 acrocentric autosomes, one much smaller than the others, and two acrocentric Xs. From the Chinook Lake specimen we have been able to re-score eight nuclei in first division with 15 figures, all appearing as acrocentrics, and one much smaller than the others. The quality of those nuclei is now too poor to distinguish the Xs. However, three other metaphase nuclei in which the autosomes are not countable show clearly the two acrocentric Xs heteropycnotic and lying side by side and toward one pole.

Attulus (*Sitticus*) *pubescens*: 26a+XaXmYa (Figs 155–163). Many nuclei indicate 26 acrocentric autosomes, but relatively few show the sex chromosomes clearly, either because they are folded over themselves, or the X_2 is not clearly associated with the others. However, many first division nuclei show a peculiar figure with a metacentric (X_1) whose shorter arm is paired terminally with an acrocentric (Y). The longer arm of the X_1 is heteropycnotic, and is occasionally seen with the X_2 lying achiasmately beside it. This behaviour suggests that the metacentric and loose acrocentric are X's, and this is supported by two cases of paired second division nuclei: in each, one of the pair shows 14 all-acrocentric chromosomes, while its partner shows more than 14 chromosomes, two of which are heteropycnotic. All though the latter were not fully countable, in total 24 second division nuclei were countable, 12 with 14 acrocentrics, and 12 with 14 acrocentrics plus a metacentric. Together these point to one metacentric and one acrocentric X going to one pole, in addition to 13 acrocentric autosomes, and one acrocentric Y to the other.

Attulus (*Sitticus*) *terebratus*: 26a+XaXa0 (Fig. 164). Several well-spread first metaphase show the two acrocentric Xs side by side and off to one pole, accompa-

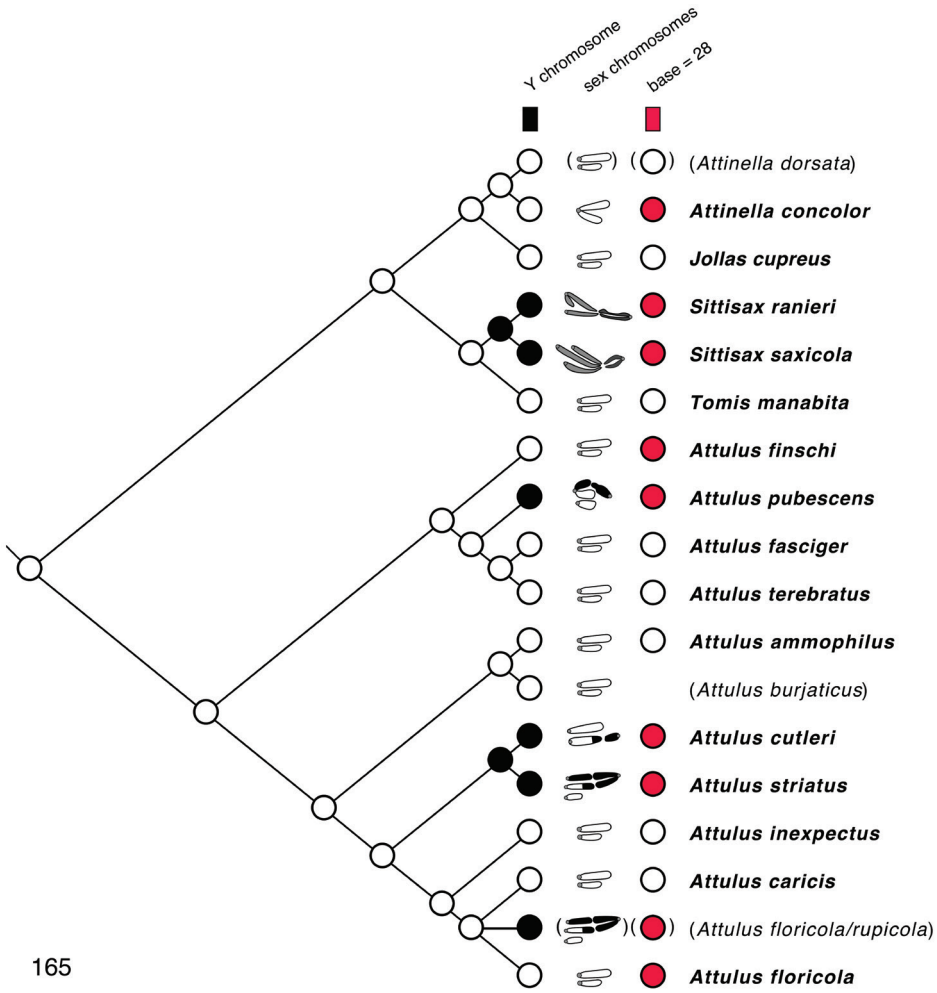

Figure 165. Chromosome evolution in sitticines. Ancestral nodes show the most parsimonious reconstruction of the evolution of Y via X-autosome fusions (black) from the X_1X_20 sex chromosome system (white). Phylogeny from Figure 48 with species added as follows: *Attinella concolor* is very similar in body and genitalia to *A. dorsata*; likewise *Sittisax saxicola* to *S. ranieri*; *Attulus caricis* position based on COI results (Fig. 96). The similar pair *A. cutleri* and *A. striatus* were placed as sisters to the *floricola* group based on their inclusion in the *floricola* group by Logunov and Kronestedt (1997) and in *Sittiflor* by Prószyński (2017a). Base chromosome number is directly the number of autosomes if the species has XX0 sex chromosomes, but is interpreted as the number of autosomes +2 if the species has XXY sex chromosomes (apparently derived by a single fusion that would have consumed an autosomal pair), or + 4 if XXXY (apparently derived by two fusions that would have consumed two pairs). Uncertain scoring is shown by parentheses (see Table 2).

nied by 13 pairs of acrocentric autosomes. Two second division nuclei show 15 acrocentrics, two of which are especially condensed (thus, the Xs), while one shows 13 normal acrocentrics.

Chromosome evolution

While salticids are fairly conservative in basic chromosome complement, with most species showing 26 acrocentric autosomes and X_1X_20 sex chromosomes (Maddison 1982; Araujo et al. 2016, Araujo et al. 2019), sitticines are striking for their diversity. The distribution of chromosome complements on the reconstructed phylogeny (Fig. 165) suggests that neo-Y chromosomes arose four separate times; the alternative, assuming a Y was ancestral, is much less parsimonious, requiring seven losses to XX0. Outgroups also favour XX0 as ancestral in sitticines: it is very much the most common sex chromosome system in salticids, and the alternatives are phylogenetically scattered, with no known Y chromosomes in other amycoids (Maddison 1982; Araujo et al. 2016, Araujo et al. 2019). Four X-autosome fusions among 18 species represents a phylogenetic density approximately as high as in *Habronattus* (Maddison and Leduc-Robert 2013), but the resulting forms of sex chromosomes are more varied in *Sitticus*.

The ancestral autosome number in sitticines is unclear. Among the species with XX0, some have 26 autosomes, others have 28. Assessing a comparable autosome number with neo-Y species requires interpretation, as the neo-Y system itself binds one or more autosomal pairs with the X chromosomes, as indicated in part by distinctive condensation patterns. If (as in *Habronattus*, Maddison and Leduc-Robert 2013) we interpret the XXY systems as having one pair of autosomes bound into the sex chromosomes, and XXXY as having two pairs, then (for example) the 26a+XaXaYa of *A. cutleri* is interpreted as having a base number of 28 (26 free and two bound). The rightmost (red and white) column of Fig. 165 shows these interpreted base numbers. The most parsimonious interpretation would then consider that red (28) is ancestral for the entire clade of *Attulus*, reverting back to the typical salticid number (26) multiple times. The ancestral node of the *Jollas-Tomis* clade, and the root of the Sitticini, could be 26 or 28 equally parsimoniously if the expected outgroup condition of 26 were not imposed.

An unanticipated but consistent correlation between base autosome number and the presence of neo-Y is seen in Fig. 165, regardless of how we interpret the ancestral state for base autosome number. The pattern is phylogenetically repeated: each of the four separate neo-Y origins occurs in a 28-autosome lineage, and for each the closest lineage with 26 has XX0. We have no suggestion as to why there might be such a correlation. This pattern is unlikely to be a tautological consequence of our counting rule that interprets XXY/XXXY systems as incorporating two/four autosomes. The counting rule is derived (partially) independently, from condensation patterns and meiotic orientation. Even lacking an independent argument within sitticines, we could import the counting rule from *Habronattus*, where such an interpretation is well supported by meiotic behaviour and chromosome counts (Maddison 1982, Maddison and Leduc-Robert 2013). We do not know how to explain a correlation between an extra pair of autosomes and the presence of neo-Y, but it is perhaps relevant that in all of the 28a+XaXa0 species, one of the chromosome pairs is especially small, half or less the size of the others.

If these small chromosomes are supernumerary (B) chromosomes, it is possible that there is considerably more variation within species than our small sample sizes can

detect. Undetected intraspecific variation in autosomes or sex chromosomes would not negate our basic evolutionary conclusions. Were we to find species variable with respect to the presence of a neo-Y chromosome, for example, it would point to even more transitions between XX0 and XXY/XXXY.

Our uncertainty about chromosome complement in some species does not strongly affect our conclusions about homoplasy or correlations, though it could affect a detailed reconstruction of the evolution of autosome number, or of particular fusions involved in a neo-Y system. For instance, if we delete autosome number for *Attinella dorsata* and *Attulus burjaticus* (the two species with uncertain counts) from Fig. 165, the ancestral states reconstructed by parsimony become ambiguously 28 or 26. Although we are uncertain about the detailed intepretation of sex chromosomes in *A. rupicola/floricola* and *Sittisax saxicola*, we conclude that they do have Y chromosomes, and thus the reconstruction of Y chromosome evolution is not affected. The scope of uncertainty allows one possible contradiction to our assessments above: should we be incorrect about the autosome count of *A. rupicola/floricola*, this may be a species in which a Y chromosome arose in the context of only 26 autosomes. Otherwise, the ambiguities do not change the interpretation of a correlation between a base number of 28 autosomes and neo-Y.

Chromosome evolution of sitticines will not be well understood, however, until a larger sample of species and specimens is obtained, given the high diversity seen in our small sample. Our data hint to the possibility of rapid evolution provoked by special mechanisms.

Acknowledgements

We are grateful to several colleagues who made special efforts to provide us access to specimens: to Galina Azarkina for greatly facilitating collecting in Siberia, to Gergin Blagoev for preparing and taking photographs of *Attulus sylvestris* specimens used for barcoding, and to Cristian Grismado for taking photographs of the holotype of *Jollas puntalara* Galiano. We thank Petra Kranebitter of the Naturmuseum Südtirol/ Museo di Scienze Naturali dell'Alto Adige for lending us the specimen of *Attulus* (*Sittilong*) *longipes*, Simone Ballini for collecting it, and Tobias Bauer for leading us to it. Laura Leibensperger and Jennifer Zaspel both helped generously in our attempts to trace what are the true types of *Attus palustris* Peckham and Peckham. Laura Leibensperger and Gonzalo Giribet of the MCZ, and Lou Sorkin and Lorenzo Prendini of the AMNH provided loans of important type material. We thank Gonzalo Giribet for kindly providing lab space and resources to sequence *Attulus longipes*. Junxia Zhang suggested euophryine identifications for two species misplaced in *Sitticus*. Helpful comments on the manuscript were provided by G.B. Edwards, D. Logunov, J. Miller, and two anonymous reviewers. We especially thank one of the anonymous reviewers for provoking us to examine our chromosome data more thoroughly. Funding was provided to WPM through an NSERC postgraduate scholarship and an NSERC Dis-

covery grant, and to DRM by the Harold E. and Leona M. Rice Endowment Fund at Oregon State University. Data collection in the Hedin lab was supported by US National Science Foundation (DEB 1754591).

References

Araujo D, Sanches MB, da Silva Gonçalves Santana Lima J, Julião do Nascimento ÉV, Marsola Giroti A, Brescovit AD, Cella DM, Schneider MC (2016) Chromosomal analyses of Salticinae and Lyssomaninae reveal a broad occurrence of the 2n♂ = 28, X_1X_20 karyotype within Salticidae. Journal of Arachnology 44: 148–152. https://doi.org/10.1636/M15-77

Araujo D, Schneider MC, Paula-Neto E, Cella DM (2019) The spider cytogenetic database, version 8.0. http://www.arthropodacytogenetics.bio.br/spiderdatabase [Accessed 2019-10-24]

Blick T, Marusik YM (2018) Three junior synonyms of jumping spider genera (Araneae: Salticidae). Arthropoda Selecta 27: 237–238. https://doi.org/10.15298/arthsel.27.3.07

Breitling R (2019) Barcode taxonomy at the genus level. Ecologica Montegrina 21: 17–37.

Castresana J (2000) Selection of conserved blocks from multiple alignments for their use in phylogenetic analysis. Molecular Biology Evolution 17: 540–552. https://doi.org/10.1093/oxfordjournals.molbev.a026334

Cutler BE (1990) Synanthropic Salticidae of the Northeast United States. Peckhamia 2: 91–92.

Derkarabetian S, Starrett J, Tsurusaki N, Ubick D, Castillo S, Hedin M (2018) A stable phylogenomic classification of Travunioidea (Arachnida, Opiliones, Laniatores) based on sequence capture of ultraconserved elements. ZooKeys 760: 1–36. https://doi.org/10.3897/zookeys.760.24937

Emerton JH (1891) New England spiders of the family Attidae. Transactions of the Connecticut Academy of Arts and Sciences 8: 220–252. https://doi.org/10.5962/bhl.part.22327

Faircloth BC (2013) illumiprocessor: a trimmomatic wrapper for parallel adapter and quality trimming. hhttps://doi.org/10.6079/J9ILL

Faircloth BC (2016) PHYLUCE is a software package for the analysis of conserved genomic loci. Bioinformatics 32: 786–788. https://doi.org/10.1093/bioinformatics/btv646

Faircloth BC (2017) Identifying conserved genomic elements and designing universal probe sets to enrich them. Methods in Ecology & Evolution 8: 1103–1112. https://doi.org/10.1111/2041-210X.12754

Galiano ME (1987) Description of *Aillutticus*, new genus (Araneae, Salticidae). Bulletin of the British Arachnological Society 7: 157–164.

Galiano ME (1989) Las especies de *Sitticus* del grupo *leucoproctus* (Araneae, Salticidae). Revista de la Sociedad Entomológica Argentina 45: 257–269.

Galiano ME (1991a) Las especies de *Sitticus* Simon del grupo *palpalis* (Araneae, Salticidae). Acta Zoologica Lilloana 40: 59–68.

Galiano ME (1991b) Revision del género *Jollas* (Araneae, Salticidae). Physis, Revista de la Sociedad Argentina de Ciencias Naturales (C) 47: 15–29.

Gertsch WJ, Mulaik S (1936) Diagnoses of new southern Spiders. American Museum Novitates 851: 1–21.

Grabherr MG, Haas BJ, Yassour M, Levin JZ, Thompson DA, Amit I, Chen Z (2011) Full-length transcriptome assembly from RNA-Seq data without a reference genome. Nature biotechnology 29: 1–644. https://doi.org/10.1038/nbt.1883

Hackman W (1948) Chromosomenstudien an Araneen mit besonderer Berücksichtigung der Geschlechtschromosomen. Acta Zoologica Fennica 54: 1–101.

Harm M (1973) Zur Spinnenfauna Deutschlands, XIV. Revision der Gattung *Sitticus* Simon (Arachnida: Araneae: Salticidae). Senckenbergiana Biologica 54: 369–403.

Hedin M, Derkarabetian S, Ramírez M, Vink C, Bond J (2018) Phylogenomic reclassification of the world's most venomous spiders (Mygalomorphae, Atracinae), with implications for venom evolution. Scientific Reports 8(1636D): 1–7. https://doi.org/10.1038/s41598-018-19946-2

ICZN (2018) Closure of Cases (3451, 3459, 3564, 3691, 3755), Bulletin of Zoological Nomenclature 75: 1–302. https://doi.org/10.21805/bzn.v75.a069

Kalyaanamoorthy S, Minh BQ, Wong TKF, von Haeseler A, Jermiin LS (2017) ModelFinder: Fast Model Selection for Accurate Phylogenetic Estimates. Nature Methods 14: 587–589. https://doi.org/10.1038/nmeth.4285

Kaston BJ (1948) Spiders of Connecticut. Bulletin of the Connecticut State Geological and Natural History Survey 70: 1–874.

Katoh D, Standley DM (2013) MAFFT multiple sequence alignment software version 7: improvements in performance and usability. Molecular Biology and Evolution 30: 772–780. https://doi.org/10.1093/molbev/mst010

Kropf C, Blick T, Brescovit AD, Chatzaki M, Dupérré N, Gloor D, Haddad CR, Harvey MS, Jäger P, Marusik YM, Ono H, Rheims CA, Nentwig W (2019) How not to delimit taxa: a critique on a recently proposed "pragmatic classification" of jumping spiders (Arthropoda: Arachnida: Araneae: Salticidae). Zootaxa 4545: 444–446. https://doi.org/10.11646/zootaxa.4545.3.10

Kumbiçak Z, Ekiz E, Çiçekli S (2014) Karyotypes of size spider species belonging to the families Gnaphosidae, Salticidae, Thomisidae, and Zodariidae (Araneae) fromTurkey. Comparative Cytogenetics 8: 93–101. https://doi.org/10.3897/compcytogen.v8i2.6065

Locket GH, Millidge AF (1951) British Spiders (Vol. I). Ray Society London, 310 pp.

Logunov DV (1993) Notes on the *penicillatus* species group of the genus *Sitticus* Simon, 1901 with a description of a new species (Araneae, Salticidae). Genus 4: 1–15.

Logunov DV (2004) Notes on new and poorly known Palaearctic species of the genera *Neon*, *Sitticus* and *Synageles* (Araneae: Salticidae). Bulletin of the British Arachnological Society 13: 33–40.

Logunov DV, Kronestedt T (1997) A new Palearctic species of the genus *Sitticus* Simon, with notes on related species in the floricola group (Araneae, Salticidae). Bulletin of the British Arachnological Society 10: 225–233.

Logunov DV, Marusik YM, Rakov SY (1999) A review of the genus *Pellenes* in the fauna of Central Asia and the Caucasus (Araneae, Salticidae). Journal of Natural History 33: 89–148. https://doi.org/10.1080/002229399300489

Logunov DV, Marusik YM (2001) Catalogue of the Jumping Spiders of Northern Asia (Arachnida, Araneae, Salticidae). KMK Scientific Press, Moscow, 300 pp.

Maddison DR, Maddison WP (2018a) Zephyr: a Mesquite package for interacting with external phylogeny inference programs. Version 2.1. http://zephyr.mesquiteproject.org [Accessed 2019-01-20]

Maddison WP (1982) XXXY sex chromosomes in males of the jumping spider genus *Pellenes* (Araneae: Salticidae). Chromosoma (Berlin) 85: 23–37. https://doi.org/10.1007/BF00344592

Maddison WP (1987) *Marchena* and other jumping spiders with an apparent leg-carapace stridulatory mechanism (Araneae: Salticidae: Heliophaninae and iodininae). Bulletin of the British Arachnological Society 7: 101–106.

Maddison WP (1996) *Pelegrina* Franganillo and other jumping spiders formely placed in the genus *Metaphidippus* (Araneae: Salticidae). Bulletin of the Museum of Comparative Zoology 154: 215–368.

Maddison WP (2015) A phylogenetic classification of jumping spiders (Araneae: Salticidae). Journal of Arachnology 43: 231–292. https://doi.org/10.1636/arac-43-03-231-292

Maddison WP, Evans SC, Hamilton CA, Bond JE, Lemmon AR, Lemmon EM (2017) A genome-wide phylogeny of jumping spiders (Araneae, Salticidae), using anchored hybrid enrichment. ZooKeys 695: 89–101. https://doi.org/10.3897/zookeys.695.13852

Maddison WP, Hedin MC (2003) Jumping spider phylogeny (Araneae: Salticidae). Invertebrate Systematics 17: 529–549. https://doi.org/10.1071/IS02044

Maddison WP, Leduc-Robert G (2013) Multiple origins of sex chromosome fusions correlated with chiasma localization in Habronattus jumping spiders (Araneae: Salticidae). Evolution. 67: 2258–2272. https://doi.org/10.1111/evo.12109

Maddison WP, Li DQ, Bodner MR, Zhang JX, Xu X, Liu QQ (2014) The deep phylogeny of jumping spiders (Araneae, Salticidae). ZooKeys 440: 57–87. https://doi.org/10.3897/zookeys.440.7891

Maddison WP, Maddison DR (2018b) Mesquite: A modular system for evolutionary analysis. version 3.6. http://www.mesquiteproject.org [Accessed 2019-01-20]

Metzner H (2019) Jumping spiders (Arachnida: Araneae: Salticidae) of the world. https://www.jumping-spiders.com [Accessed 2019-11-19]

Nguyen L-T, Schmidt HA, von Haeseler A, Minh BQ (2015) IQ-TREE: A fast and effective stochastic algorithm for estimating maximum likelihood phylogenies. Molecular Biology and Evolution 32: 268–274. https://doi.org/10.1093/molbev/msu300

Peckham GW, Peckham EG (1883) Descriptions of New or Little Known Spiders of the Family Attidae from Various Parts of the United States of North America. Milwaukee, 35 pp. https://doi.org/10.5962/bhl.title.136491

Peckham GW, Peckham EG (1909) Revision of the Attidae of North America. Transactions of the Wisconsin Academy of Sciences, Arts and Letters 16(1): 355–655.

Platnick NI (2014) The World Spider Catalog, version 15. American Museum of Natural History. http://research.amnh.org/iz/spiders/catalog [Accessed 2015-01-20]

Prószyński J (1968) Revision of the spider genus *Sitticus* Simon (Araneida, Salticidae) I. The *terebratus* group. Annales zoologici, Warszawa 26: 391–407.

Prószyński J (1971) Revision of the spider genus *Sitticus* Simon, 1901 (Araneida, Salticidae) II. *Sitticus saxicola* (C. L. Koch, 1848) and related forms. Annales zoologici, Warszawa 28: 183–204.

Prószyński J (1973) Revision of the spider genus *Sitticus* Simon, 1901 (Aranei, Salticidae), III. *Sitticus penicillatus* (Simon, 1875) and related forms. Annales zoologici, Warszawa 30: 71–95.

Prószyński J (1976) Studium systematyczno-zoogeogra czne nad rodzina Salticidae (Aranei) Regionow Palearktycznego i Nearktycznego. Wyzsza Szkola Pedagogiczna w Siedlcach Rozprawy 6: 1–260.

Prószyński J (1980) Revision of the spider genus *Sitticus* Simon, 1901 (Aranei, Salticidae), IV. *Sitticus floricola* (C.L. Koch) group. Annales zoologici, Warszawa 36: 1–35.

Prószyński J (1983) Tracing the history of a genus from its geographical range by the example of *Sitticus* (Arachnida: Araneae: Salticidae). Verhandlungen des Naturwissenschaftlichen Vereins in Hamburg 26: 161–179.

Prószyński J (2016) Delimitation and description of 19 new genera, a subgenus and a species of Salticidae (Araneae) of the world. Ecologica Montenegrina 7: 4–32.

Prószyński J (2017a) Revision of the genus *Sitticus* Simon, 1901 s. l. (Araneae: Salticidae). Ecologica Montenegrina 10: 35–50.

Prószyński J (2017b) Pragmatic classification of the world's Salticidae (Araneae). Ecologica Montenegrina 12: 1–133.

Ratnasingham S, Hebert PDN (2013) A DNA-Based Registry for All Animal Species: The Barcode Index Number (BIN) System. PLoS ONE 8(8): e66213. https://doi.org/10.1371/journal.pone.0066213

Ratnasingham S, Hebert PDN (2007) BOLD: The Barcode of Life Data System (www.barcodinglife.org). Molecular Ecology Notes 7: 355–364. https://doi.org/10.1111/j.1471-8286.2007.01678.x

Richman DB (1979) Jumping spiders of the United States and Canada: Changes in the key and list (1). Peckhamia 1: 1–125.

Ruiz GRS, Brescovit AD (2005) Three new genera of jumping spider from Brazil (Araneae, Salticidae). Revista Brasileira de Zoologia 22: 687–695. https://doi.org/10.1590/S0101-81752005000300026

Ruiz GRS, Brescovit AD (2006) *Gavarilla*, a new genus of jumping spider from Brazil, and description of two new species of the genera *Capeta* Ruiz & Brescovit and *Amatorculus* Ruiz & Brescovit (Araneae, Salticidae, Sitticinae). Revista Brasileira de Zoologia 23: 350–356. https://doi.org/10.1590/S0101-81752006000200006

Ruiz GRS, Brescovit AD, Lise AA (2007) On the taxonomy of some Neotropical species of jumping spiders described by Caporiacco (Araneae, Salticidae). Revista Brasileira de Zoologia 24: 376–381. https://doi.org/10.1590/S0101-81752007000200016

Ruiz GRS, Maddison WP (2015) The new Andean jumping spider genus *Urupuyu* and its placement within a revised classification of the Amycoida (Araneae: Salticidae). Zootaxa 4040(3): 251–279. https://doi.org/10.11646/zootaxa.4040.3.1

Stamatakis A (2014) RAxML Version 8: A tool for phylogenetic analysis and post-analysis of large phylogenies. Bioinformatics 30: 1312–1313. https://doi.org/10.1093/bioinformatics/btu033

Starrett J, Derkarabetian S, Hedin M, Bryson Jr RW, McCormack JE, Faircloth BC (2017) High phylogenetic utility of an Ultraconserved element probe set designed for Arachnida. Molecular Ecology Resources 17: 812–823. https://doi.org/10.1111/1755-0998.12621

Talavera G, Castresana J (2007) Improvement of phylogenies after removing divergent and ambiguously aligned blocks from protein sequence alignments. Systematic Biology 56: 564–577. https://doi.org/10.1080/10635150701472164

White MJD (1965) Sex chromosomes and meiotic mechanisms in some African and Australian mantids. Chromosoma (Berlin) 16: 521–547. https://doi.org/10.1007/BF00326972

World Spider Catalog (2019) World Spider Catalog Version 20.5 Natural History Museum Bern. http://wsc.nmbe.ch [Accessed on 2019-11-19]

Zerbino DR, Birney E (2008) Velvet: Algorithms for de novo short read assembly using de Bruijn graphs. Genome Research 18: 821–829. https://doi.org/10.1101/gr.074492.107

Zhang JX, Maddison WP (2013) Molecular phylogeny, divergence times and biogeography of spiders of the subfamily Euophryinae (Araneae: Salticidae). Molecular Phylogenetics and Evolution 68: 81–92. https://doi.org/10.1016/j.ympev.2013.03.017

ZooKeys 925: 55–72 (2020)
doi: 10.3897/zookeys.925.49953
http://zookeys.pensoft.net

RESEARCH ARTICLE

A peer-reviewed open-access journal
ZooKeys
Launched to accelerate biodiversity research

A remarkable new species of the millipede genus *Trachyjulus* Peters, 1864 (Diplopoda, Spirostreptida, Cambalopsidae) from Thailand, based both on morphological and molecular evidence

Natdanai Likhitrakarn[1], Sergei I. Golovatch[2], Ekgachai Jeratthitikul[3], Ruttapon Srisonchai[4], Chirasak Sutcharit[5], Somsak Panha[5]

1 *Division of Plant Protection, Faculty of Agricultural Production, Maejo University, Chiang Mai 50290, Thailand* **2** *Institute for Problems of Ecology and Evolution, Russian Academy of Sciences, Leninsky pr. 33, Moscow 119071, Russia* **3** *Animal Systematics and Molecular Ecology Laboratory, Department of Biology, Faculty of Science, Mahidol University, Bangkok 10400, Thailand* **4** *Department of Biology, Faculty of Science, Khon Kaen University, Khon Kaen, 40002 Thailand* **5** *Animal Systematics Research Unit, Department of Biology, Faculty of Science, Chulalongkorn University, Bangkok 10330, Thailand*

Corresponding author: Somsak Panha (somsak.pan@chula.ac.th)

Academic editor: D. V. Spiegel | Received 8 January 2020 | Accepted 25 February 2020 | Published 8 April 2020

http://zoobank.org/A531C6A9-F7A8-4747-B4DB-A18D00237417

Citation: Likhitrakarn N, Golovatch SI, Jeratthitikul E, Srisonchai R, Sutcharit C, Panha S (2020) A remarkable new species of the millipede genus *Trachyjulus* Peters, 1864 (Diplopoda, Spirostreptida, Cambalopsidae) from Thailand, based both on morphological and molecular evidence. ZooKeys 925: 55–72. https://doi.org/10.3897/zookeys.925.49953

Abstract

A new, giant species of *Trachyjulus* from a cave in southern Thailand is described, illustrated, and compared to morphologically closely related taxa. This new species, *T. magnus* **sp. nov.**, is much larger than all other congeners and looks especially similar to the grossly sympatric *T. unciger* Golovatch, Geoffroy, Mauriès & VandenSpiegel, 2012, which is widespread in southern Thailand. Phylogenetic trees, both rooted and unrooted, based on a concatenated dataset of the COI and 28S genes of nine species of Cambalopsidae (*Trachyjulus*, *Glyphiulus*, and *Plusioglyphiulus*), strongly support the monophyly of *Trachyjulus* and a clear-cut divergence between *T. magnus* **sp. nov.** and *T. unciger* in revealing very high average *p*-distances of the COI gene (20.80–23.62%).

Keywords

cave, diplopod, molecular-based phylogeny, morphological character, taxonomy

Introduction

In South and Southeast Asia, as well as China, the juliform millipede family Cambalopsidae Cook, 1895 is among the most diverse, common, and often highly abundant groups that clearly dominate cave millipede faunas (Golovatch 2015). Four genera are actually involved.

By far the largest genus is *Glyphiulus* Gervais, 1847 with its 60+ species ranging across China and Southeast Asia to Borneo in the east (Golovatch et al. 2007a, 2007b, 2011b, 2011c, 2012b; Jiang et al. 2017, 2018; Likhitrakarn et al. 2017; Liu and Wynne 2019; Golovatch and Liu 2020). The genus *Plusioglyphiulus* Silvestri, 1923 encompasses 28 described species ranging from northern Thailand and Laos in the west, through Myanmar and Malaysia, to Borneo in the east and southeast (Golovatch et al. 2009, 2011a; Likhitrakarn et al. 2018). Interestingly, the famous Burmese amber, 99–100 Mya, appears to contain a typical *Plusioglyphiulus* yet to be described (Wesener in litt.). This is evidence both of the very old age of this genus and its long presence *in situ* (Likhitrakarn et al. 2018).

The genus *Hypocambala* Silvestri, 1895 is the smallest, but particularly widespread, presently containing 14 species in Southeast Asia, as well as scattered across several islands of the Pacific and Indian oceans (Golovatch et al. 2011d).

The more diverse genus *Trachyjulus* Peters, 1864 is currently known to comprise 32 described species (Golovatch et al. 2012a; Likhitrakarn et al. 2018). Most of them (80%) show restricted distributions and can be assigned to short-range endemics (geographic range ca 10,000 km^2) (Harvey 2002). The genus ranges from Nepal, India, and Sri Lanka in the west, through Bangladesh and Myanmar, to Vietnam, Thailand, Peninsular Malaysia, Singapore, and Indonesia (Sumatra and Java) in the east (Golovatch et al. 2012a). Most *Trachyjulus* species have been recorded/described from a single locality/cave, but *T. ceylanicus* Peters, 1864, *T. dentatus* (Pocock, 1894), *T. singularis* (Attems, 1938), and *T. unciger* Golovatch, Geoffroy, Mauriès & VandenSpiegel, 2012 are relatively widespread, while *T. calvus* (Pocock, 1893) is nearly pantropical (Golovatch et al. 2012a).

During recent field surveys in southern Thailand, a new, unusually large *Trachyjulus* species was taken from a cave. From the first glance, it seemed to be particularly similar to the grossly sympatric *T. unciger*, but both are readily distinguished by body size and several other characters, including gonopodal structures. To better understand the species delimitations and their variations, we compare this new species to topotypes of *T. unciger* (Pung-Chang (= Tham Nam) Cave, Phang-Nga Province, Thailand) not only based on their morphological characters, but also on molecular evidence. In addition, molecular-based phylogenetic relationships within the genus *Trachyjulus* are revealed and discussed for the first time using mitochondrial cytochrome c oxidase subunit I (COI) and nuclear gene 28S rRNA sequences. These were obtained from para- or topotypes of nine species of Cambalopsidae, including not only five *Trachyjulus*, but also two *Glyphiulus* and two *Plusioglyphiulus* as outgroups. Two members of the family Harpagophoridae from the same order Spirostreptida, as well as two of the family Julidae, order Julida, are also included as more distant outgroups for tree rooting.

Material and methods

Sample collection

Specimens were collected from southern Myanmar and southern Thailand under the Animal Care and Use Protocol Review No. 1723018. The collecting sites were located by GPS by using a Garmin GPSMAP 60 CSx, and all coordinates and elevations were re-checked with Google Earth. Photographs of live animals were taken using a Nikon 700D digital camera with a Nikon AF-S VR 105 mm macro lens. The specimens collected were euthanized by a two-step method following AVMA Guidelines for the Euthanasia of Animals (AVMA 2013). Specimens were then preserved in 95% ethanol for morphological and molecular studies. Ethanol was replaced after 24 hours with fresh 95% ethanol to prevent their defensive chemicals from affecting future DNA extraction. Mostly para- or topotypes of six described species were also used for molecular analyses (Table 1).

The holotype, as well as most of the paratypes are housed in the Museum of Zoology, Chulalongkorn University (CUMZ), Bangkok, Thailand; a few paratypes have also been donated to the collections of the Zoological Museum, State University of Moscow, Russia (ZMUM) and the Natural History Museum of Denmark, University of Copenhagen, Denmark (NHMD), as indicated in the text.

Morphological study

The specimens were examined, measured, and photographed under a Nikon SMZ 745T trinocular stereo microscope equipped with a Canon EOS 5DS R digital SLR camera. Scanning electron micrographs (SEM) were taken with a JEOL, JSM-5410 LV microscope using gold-coated samples, and the material returned to alcohol upon examination. Digital images obtained were processed and edited with Adobe Photoshop CS5. Line drawings were executed based on photographs and specimens examined under a Nikon SMZ 745T trinocular stereo microscope, equipped with a Canon EOS 5DS R digital SLR camera. The terminology used and the carinotaxic formulae in the descriptions follow those in Golovatch et al. (2007a, 2007b, 2012a), while body ring counts are after Enghoff et al. (1993) and Golovatch et al. (2007a).

DNA extraction and molecular identification

Total genomic DNA was extracted from the dissected midbody ring tissues using the DNA extraction kit for animal tissue (NucleoSpin Tissue extraction kit, Macherey-Nagel, Germany), following the standard procedure of the manual. Fragments of the mitochondrial cytochrome *c* oxidase subunit I (COI, 690 bp) gene were amplified using LCO1490 (5'-GGTCAACAAATCATAAAGATATTGG-3'; Folmer et al. 1994) and hco outout (5'-GTAAATATATGRTGDGCTC; Schulmeister et al. 2002) or Nan-

Table 1. List of the species used for molecular phylogenetic analyses and their relevant information. * = paratype, ** = topotype.

Voucher number	Species	Locality	Geographical coordinates	GenBank accession numbers	
				COI	28S
CAM059*	*Trachyjulus bifidus* Likhitrakarn et al., 2018	Yae Gu Cave (River Cave), Tanintharyi, Myanmar	11°13'4.50"N, 99°10'32.33"E	MN893771	MN897820
CAM061*	*Trachyjulus bifidus* Likhitrakarn et al., 2018	Thin Bow Gu Cave (Linno Gu #2), Tanintharyi Region, Myanmar	11°11'23.0"N, 99°10'18.3"E	MN893772	MN897821
CAM027**	*Trachyjulus phylloides* Golovatch et al., 2012	Phra Kayang Cave, Ranong, Thailand	10°19'35.62"N, 98°45'53.54"E	MN893773	N/A
CAM079**	*Trachyjulus unciger* Golovatch et al., 2012	Pung-Chang Cave, Phang-Nga, Thailand	8°26'35.67"N, 98°30'57.32"E	MN893774	MN897822
CAM070*	*Trachyjulus magnus* sp. nov.	Wat Tham Khrom Wanaram, Surat Thani, Thailand	8°46'12.07"N, 99°22'6.36"E	MN893775	MN897823
CAM044*	*Trachyjulus singularis* (Attems, 1938)	Tham Kao Havot Cave, Chon Buri, Thailand	13°09'46.95"N, 101°35'51.97"E	MN893776	MN897824
CAM107**	*Trachyjulus singularis* (Attems, 1938)	Khao Loi Cave (Wat Ma Duea), Rayong, Thailand	13°03'27.00"N, 101°36'27.00"E	MN893777	MN897825
Outgroup Cambalopsidae					
CAM030*	*Glyphiulus sattaa* Golovatch et al., 2011	Tham Pum-Tham Pla Cave, Chiang Rai, Thailand	20°19'42.54"N, 99°51'50.12"E	MN893778	N/A
CAM022*	*Glyphiulus duangdee* Golovatch et al., 2011	Chan Cave, Uttaradit, Thailand	17°35'39.00"N, 100°25'18.30"E	MN893779	MN897826
CAM031*	*Plusioglyphiulus erawan* Golovatch et al., 2011	Erawan Cave, Lamphun, Thailand	18°19'37.79"N, 98°52'22.41"E	MN893780	N/A
CAM021*	*Plusioglyphiulus saksit* Golovatch et al., 2011	Tham Nennoi Cave, KhonKaen, Thailand	16°43'4.77"N, 101°53'39.08"E	MN893781	MN897826
Outgroup Harpagophoridae (Sporostreptida)					
CUMZ-D00057	*Thyropygus bearti* Pimvichai et al., 2009	Si-Chon, Nakhon Si Thammarat, Thailand	9°14'48.1"N 99°45'51.1"E	KC519519	N/A
CUMZ-D00021	*Thyropygus allevatus* (Karsch, 1881)	Siam-Nakorn-Thani village, Nakhon Si Thammarat, Thailand	8°25'23.9"N 99°58'07.0"E	KC519487	N/A
Outgroup Julidae (Julida)					
BIOUG22537	*Julus scandinavius* (Latzel, 1884)	Provincial Park, Ontario, Six Mile Lake, Canada:	44°53'52.8"N 79°45'25.2"W	MG320199	N/A
09BBMYR_083	*Brachyiulus pusillus* (Leach, 1815)	Gros Morne NP, Newfoundland and Labrador, Canada	49°25'37.2"N 57°44'20.4"W	KM611731	N/A

cy (5'-CCCGGTAAAATTAAAATATAAACTTC-3'; Bogdanowicz et al. 1993); while fragments of the nuclear 28S ribosomal RNA large subunit gene (28S) were amplified using primers 28F2-2 (5'-GCAGAACTGGCGCTGAGGGATGAAC-3') and 28SR2 GAGGCTGTKCACCTTGGAGACCTGCTGCG-3'; Passamaneck et al. 2004).

The PCR amplification was performed using a T100™ thermal cycler (BIO-RAD) with a final reaction volume of 20 µL (15 µL of EmeraldAmp GT PCR Master Mix,

1.5 µL of each primer, 10 ng of template DNA and distilled water up to 20 µL total volume). Thermal cycling was performed at 94 °C for 3 min, followed by 35 cycles of 94 °C for 30 s, annealing at 42–56 °C (depending on samples and the primer paired) for 60 s, extension at 72 °C for 90 s, and a final extension at 72 °C for 5 min. Amplification of PCR products were confirmed through 1.5% (w/v) agarose gel electrophoresis before purification by PEG precipitation. Purified PCR products were sequenced in both directions (forward and reverse) using an automated sequencer (ABI prism 3730XL). All nucleotide sequences in this study were deposited in the GenBank Nucleotide sequences database under submission numbers MN893771–MN893781 for COI, and MN897820–MN897826 for 28S. The collecting localities and submission codes of each nominal species are listed in Table 1.

Phylogenetic analyses

Our phylogenetic analyses included a specimen (paratype) of *T. magnus* sp. nov. and six individuals of four previously described species, namely *T. singularis* (Attems, 1938), *T. phylloides* Golovatch, Geoffroy, Mauriès & VandenSpiegel, 2011, *T. bifidus* Likhitrakarn, Golovatch, Srisonchai, Brehier, Lin, Sutcharit & Panha, 2018, and *T. unciger* Golovatch, Geoffroy, Mauriès & VandenSpiegel, 2011. Specimens from other genera, i.e. *Glyphiulus sattaa* Golovatch, Geoffroy, Mauriès & VandenSpiegel, 2011, *G. duangdee* Golovatch, Geoffroy, Mauriès & VandenSpiegel, 2011, *Plusioglyphiulus erawan* Golovatch, Geoffroy, Mauriès & VandenSpiegel, 2011, and *P. saksit* Golovatch, Geoffroy, Mauriès & VandenSpiegel, 2011, were utilized as outgroups (Table 1). In addition, sequences of millipedes from distant diplopod families were retrieved from the GenBank database and included as more distant outgroups for tree rooting. These were both *Thyropygus bearti* Pimvichai et al., 2009 and *Thyropygus allevatus* (Karsch, 1881), representing the family Harpagophoridae, order Spirostreptida, as well as *Julus scandinavius* (Latzel, 1884) and *Brachyiulus pusillus* (Leach, 1815), both in the family Julidae, order Julida, as even more remote relatives.

The sequences were edited and aligned using Clustal W, implemented in MEGA7 (Kumar et al. 2016). The aligned sequences were estimated for the best-fit model of nucleotide substitution for each gene separately by KAKUSAN4 (Tanabe 2011). Two phylogenetic methods, maximum likelihood (ML) and Bayesian Inference (BI), were implemented through the on-line CIPRES Science Gateway (Miller et al. 2010). The ML analysis was performed using RAxML v.8.2.10 (Stamatakis 2014) with 1,000 bootstrap replications and GTRGAMMA as the nucleotide substitution model (Silvestro and Michalak 2012). The BI analysis was performed by MrBayes 3.2.6 (Ronquist et al. 2012) using the Markov chain Monte Carlo technique (MCMC). The best-fit evolution models based on the Akaike Information Criterion (AIC: Akaike 1974) were applied: SYM+G for the 1st COI codon, and HKY85+G for the 2nd COI codon, the 3rd COI codon, and the 28S gene. Ten million generations were run with a random starting tree. The resultant trees were sampled every 1,000th generation and were used

to estimate the consensus tree topology; bipartition posterior probability (bpp) and branch lengths after the first 25% of obtained trees were discarded as burn-in. All Effective Sample Size (ESS) values sampled from the MCMC analysis were greater than 1,000 in all parameters. A neighbour-joining tree (NJ) based on K2P-distance was constructed based on the amino acid alignment of peptide sequences corresponding to the mitochondrial COI dataset. Interspecific genetic divergences based on the COI sequence were also evaluated using uncorrected *p*-distances. The NJ tree and *p*-distance were implemented in MEGA7 (Kumar et al. 2016).

Taxonomic part

Family Cambalopsidae Cook, 1895
Genus *Trachyjulus* Peters, 1864

***Trachyjulus magnus* sp. nov.**
http://zoobank.org/620CFB43-417C-4A18-A946-8DC27A5567B2
Figures 1–4

Type material. ***Holotype*** ♂ (CUMZ), Thailand, Surat Thani Province, Ban Na San District, Wat Tham Khrom Wanaram, 8°46'12.07"N, 99°22'6.36"E, 16.06.2018, leg. W. Siriwut, E. Jeratthitikul and N. Likhitrakarn.

Paratypes. 15 ♂, 20 ♀ (CUMZ), 1 ♂, 1 ♀ (ZMUM), 1 ♂, 1 ♀ (NHMD), same locality, together with holotype.

Name. To emphasize the largest body size of this species compared to all other species known in the genus.

Diagnosis. This new species differs from all other *Trachyjulus* spp. by the largest body size (43.5–64.2 mm long, 2.1–2.8 mm wide), and also from the particularly similar and grossly sympatric *T. unciger* (23–42 mm long, 1.2–2.0 mm wide) in having the tegument of rings 2 and 3 nearly smooth (vs evidently carinate), carinotaxic formulae of typical rings (11–8/11–8+I/i+2/2+m/m vs 8–6/8–6+I/i+2/2+m/m), combined with the number of ommatidia (5–6+5–6 vs 4+4), and the posterior gonopods showing medial coxosternal processes (**mcp**) subtrapezoid (vs shorter and lobe-shaped).

Description. Length of holotype ca 62.5 mm (Fig. 1A) and that of paratypes 44.1–64.3 (♂) or 43.5–64.2 mm (♀); midbody rings round in cross-section (Fig. 2I), their width (horizontal diameter) and height (vertical diameter) being similar; width of holotype 2.6 mm, of paratypes 2.1–2.7 (♂) or 2.1–2.8 mm (♀).

Coloration of live animals red-brown to yellow-brownish (Fig. 1), venter and legs brownish yellow to yellowish, antennae light to pale yellowish, eyes blackish, a thin axial line traceable; coloration in alcohol, after one year of preservation, similar, but body yellow-brownish to light brownish, vertex red-brown to light brown, eyes blackish to brownish.

Body with 80p+2a+T rings (holotype); paratypes with 68–86p+1–3a+T (♂) or 69–93p+1–4a+T (♀) rings. Eyes large, flat, ovoid, with 6(5)+6(5) ommatidia arranged

Figure 1. *Trachyjulus magnus* sp. nov., habitus, live coloration. **A** ♂ holotype **B** paratypes. Scale bars: 1 cm.

in a single vertical row (Fig. 2D). Antennae short and clavate (Figs 2A, B, D, F, 5A), extending past ring 4 laterally (♂, ♀), with four evident apical cones (Fig. 2G), antennomeres 5 and 6 each with a small distoventral group or corolla of bacilliform sensilla (Figs 2F, H, 5A). Clypeus with five teeth anteromedially (Fig. 2E). Gnathochilarium oligotrichous, mentum single (Figs 2E, 4B).

In width, head = ring 2 < ring 4 = 5 < 3 < 6 < 7 < 8 < 9 < 10 < collum = midbody ring (close to 12th to 14th); body abruptly tapering towards telson on a few posteriormost rings (Fig. 2B, O). Postcollar constriction evident, but not particularly strong (Fig. 2B).

Collum (Fig. 2A–C) smooth, only near lateral edges with 2–4 light, short, superficial striae (Fig. 2A–C). Rings 2 and 3 nearly smooth, with 6–9 light, superficial striae (Fig. 2A, B). Following metaterga clearly and rather strongly carinate (Fig. 2A, B, N, O), especially so from ring 5 on, whence porosteles commence, these being completely absent from legless rings where ozopores are missing (Fig. 2A). Porosteles large, but low, conical, round, directed caudolaterad, broader than high (Fig. 2L). Carinotaxic formula of metaterga 4, 10–11/10–11+m/m (Fig. 2A, B). Carinotaxic formulae of following rings typically 11–8/11–8+I/i+2/2+m/m (Fig. 2A, B, N, O); all crests and tubercles, including porosteles, low. Tegument smooth (Figs 1, 2A, B, N, O), shining throughout. Fine longitudinal striations in front of stricture between pro- and metazonae, remaining surface of

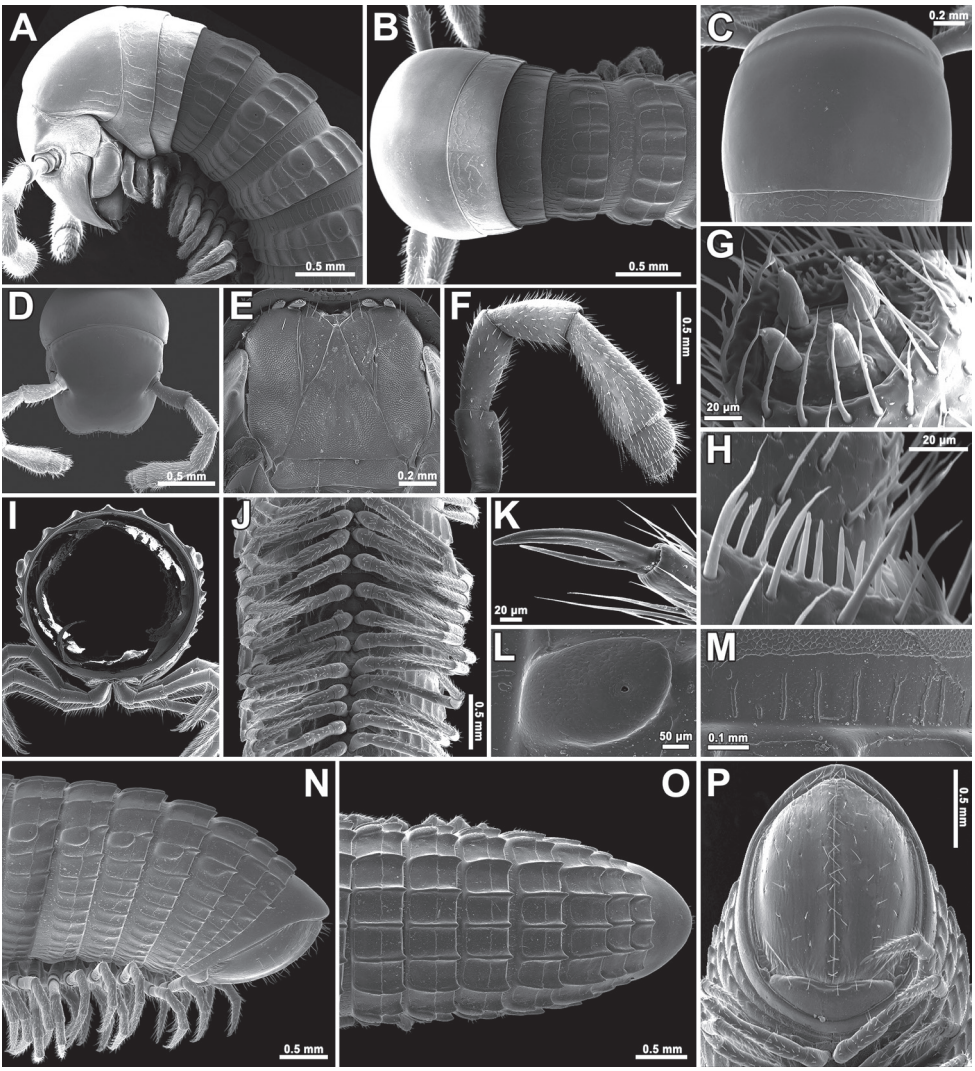

Figure 2. *Trachyjulus magnus* sp. nov., **A–C, I–P** ♀ paratype, **D–H** ♂ paratype. **A, B** anterior part of body, lateral and dorsal views, respectively **C** collum, dorsal view **D** cephalic capsule, dorsal view **E** gnathochilarium, ventral view **F** antenna, lateral view **G** tip of antenna **H** bacilliform sensilla on antennomere 5, lateral view **I** cross-section of midbody ring **J** midbody rings, ventral view **K** claw of midbody leg **L** enlarged ozopore region, lateral view **M** midbody prozona, dorsal view **N–P** posterior part of body, lateral, dorsal and ventral views, respectively.

prozonae very delicately shagreened (Fig. 2A, B, M–O). Metatergal setae absent. Rings 2 and 3 each with long pleural flaps. Midbody ring nearly round in cross-section (Fig. 2I).

Epiproct (Fig. 2N–P) simple, bare, smooth, regularly rounded caudally. Paraprocts smooth, regularly convex and densely setose (Fig. 2P). Hypoproct as usual, transversely bean-shaped, slightly concave caudally (Fig. 2P).

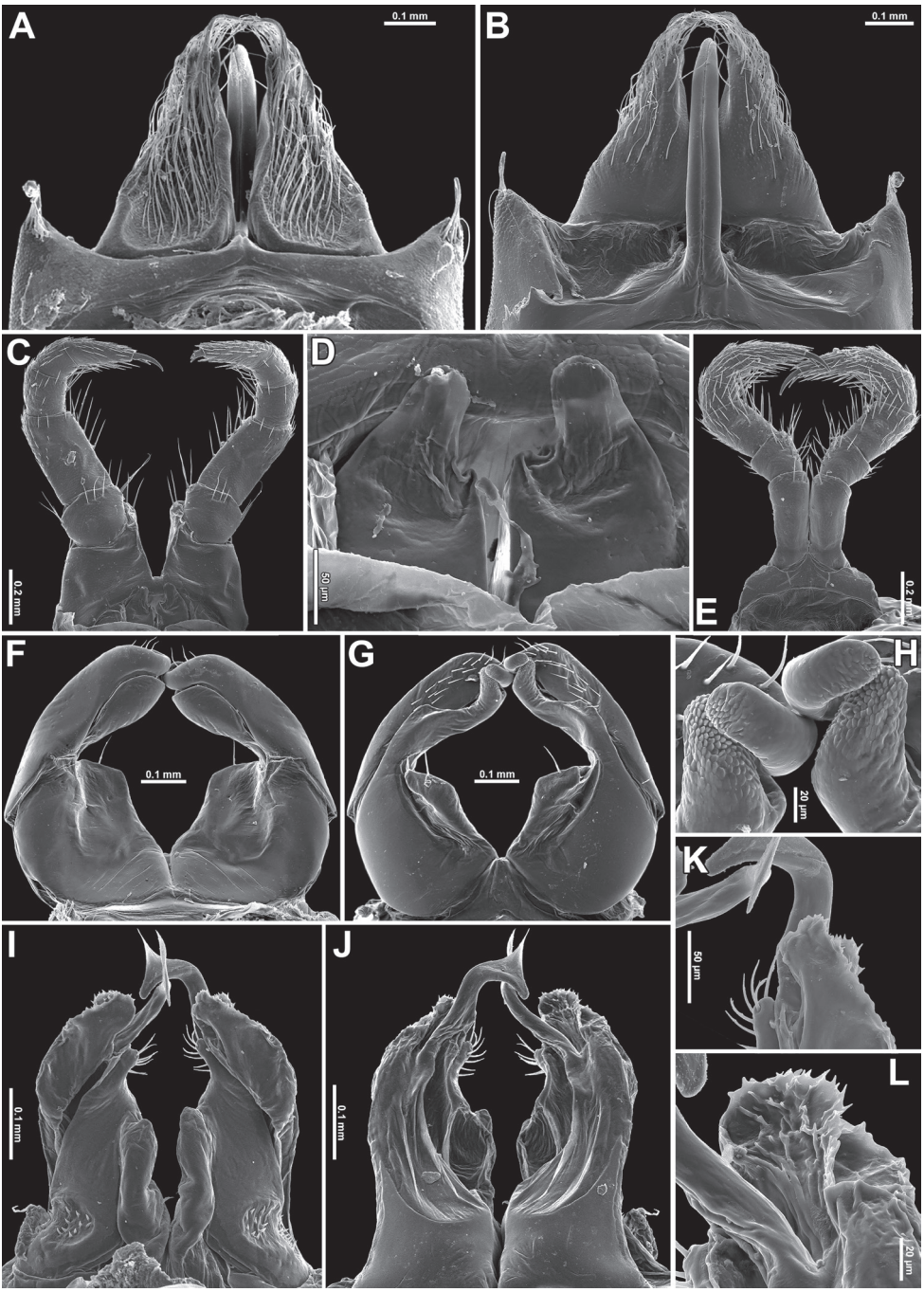

Figure 3. *Trachyjulus magnus* sp. nov., ♂ paratype. **A, B** Legs 1, frontal and caudal views, respectively **C** legs 2, caudal view **D** penes, caudal view **E** legs 3, frontal view **F, G** anterior gonopods, caudal and frontal views, respectively **H** telopodite tips of anterior gonopods **I, J** posterior gonopods, caudal and frontal views, respectively **K, L** telopodite tips of anterior gonopods, caudal and frontal views, respectively.

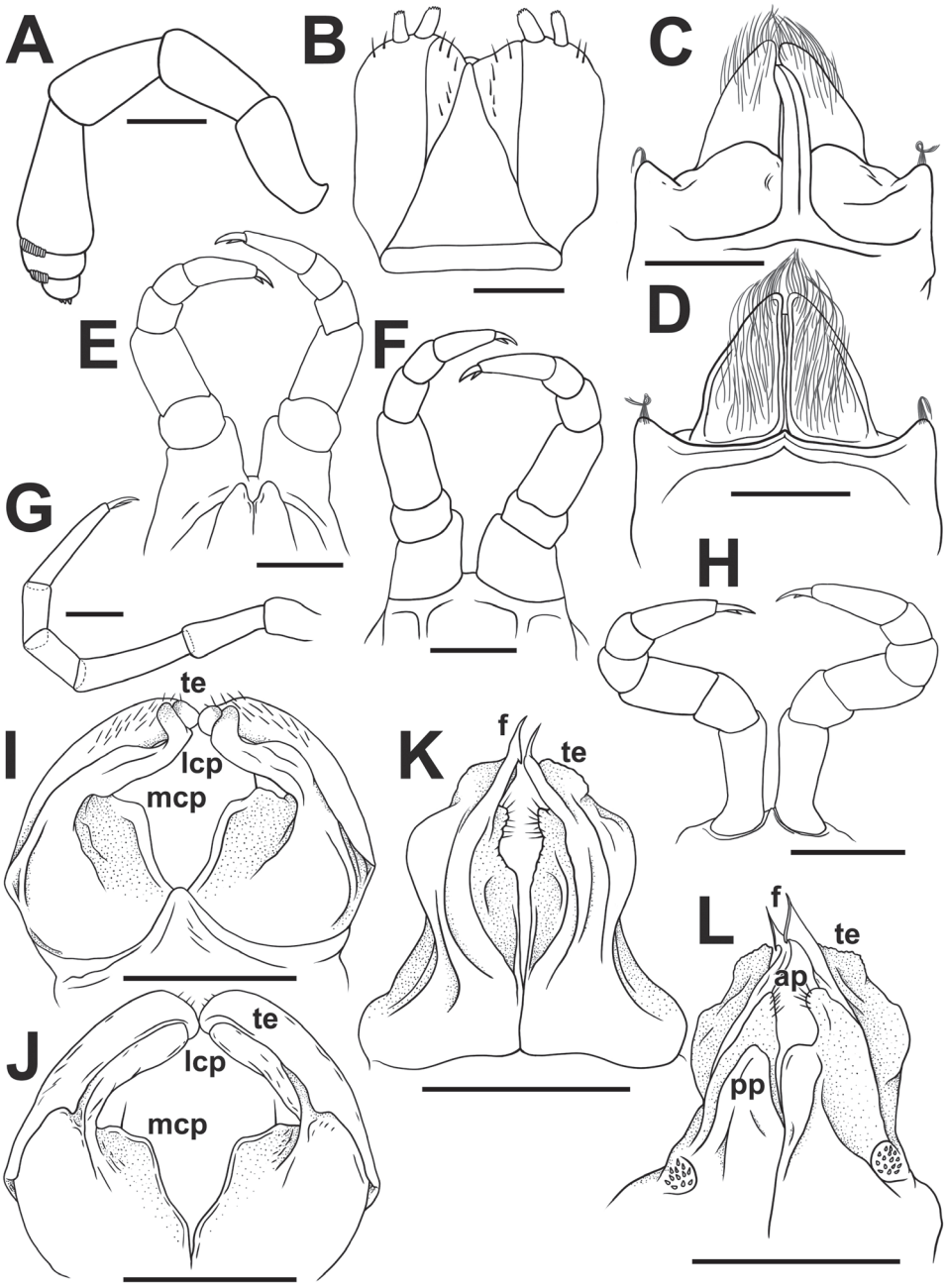

Figure 4. *Trachyjulus magnus* sp. nov., ♂ holotype. **A** Antenna, lateral view **B** gnathochilarium, ventral view **C, D** legs 1, caudal and frontal view, respectively **E, F** legs 2, caudal and frontal view, respectively **G** midbody leg, frontal view **H** legs 3, frontal view **I, J** anterior gonopods, frontal and caudal views, respectively **K, L** posterior gonopods, frontal and caudal views, respectively. Scale bars: 0.2 mm.

Ventral flaps behind gonopod aperture on ♂ ring 7 barely distinguishable as low swellings, forming no marked transverse ridge.

Legs short, on midbody rings about 2/3 (♂, ♀) as long as body height (Figs 2I, J). Claw at base with a strong accessory spiniform claw almost half as long as main claw (Fig. 2K). Tarsi and tarsal setae very delicately fringed.

♂ legs 1 highly characteristic (Figs 3A, B, 4C, D), with a strongly enlarged, long, slim, central hook (actually a pair of very tightly adjacent) curved forward (Figs 3B, C, 4C), and strong, high, densely setose, triangular, 1-ringed telopodites (Figs 3A, B, 4E, F).

♂ legs 2 (Figs 3C, D, 4E, F) slightly enlarged, with high and large coxae; telopodites hirsute on anterior face; penes subconical, rounded apically, fused at base, bare.

♂ legs 3 (Figs 3E, 4H) slightly reduced, modified in having coxae especially slender and elongate.

Anterior gonopods rather simple (Figs 3F–H, 4I, J), with 1 or 2 strong apical setae on subtrapezoid, medial, coxosternal processes (**mcp**); telopodites (**te**) club-shaped, curved, sparsely setose, nearly as high as lateral coxosternal process (**lcp**), the latter slender and long, placed basal to telopodites. Anterior parts of lateral coxal processes and telopodites rod-shaped, slender and digitiform, with apicolaterally denticulate tips (Fig. 3H).

Posterior gonopods (Figs 3I–L, 4K, L) highly compact, coxites well separated from sternum, fused only basally, with a parabasal field of coniform microsetae caudally, each with a setose, paramedian, coxal process (**pp**) (Figs 3I, 4L); telopodites (**te**) high, distally microserrate/papillate (Fig. 3K, L); anterior coxal processes (**ap**) elongate, shorter than telopodites, densely setose and rounded distally (Figs 3I–K, 4K, L); both divided by a very high, axe-shaped flagellum (**f**) (Figs 3I, J, 4K, L).

Remark. The often striking colour difference between head+collum+ring 2 and the remaining rings observed in SEM micrographs (Fig. 2) is certainly an artifact resulting from unwanted electrical charging.

Phylogenetic analysis

Our concatenated dataset contained 15 individuals, including seven *Trachyjulus* ingroup and eight outgroup species, and an alignment of approximately 1,501 base pairs (bp). We were unable to obtain sequences of the 28S gene from *T. phylloides*, *G. sattaa*, and *P. erawan*. The final alignment of the COI gene fragment yielded 690 bp (298 variable sites, 270 parsimony informative), while the 28S gene fragment comprised 811 bp (100 variable sites, 45 parsimony informative). The phylogenetic tree estimated by both ML and BI revealed equivalent topologies. As only one position within the outgroup taxa was controversial, solely a ML tree is shown in Figure 5A. The monophyly of the genus *Trachyjulus* was strongly supported (1 bpp for BI and 96% bootstrap values for ML). Within the *Trachyjulus* clade, *T. singularis* was placed in the basal part, followed by *T. magnus* sp. nov., *T. unciger*, and a sister clade

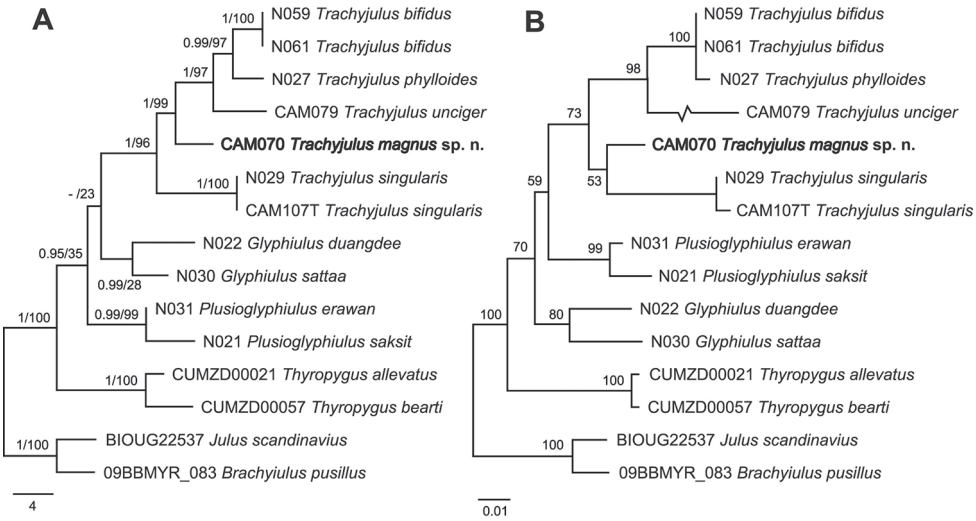

Figure 5. Phylogenetic analyses of *Trachyjulus* species and some related taxa. **A** Maximum likelihood tree based on a 1,501 bp alignment dataset of the nuclear 28S rRNA and mitochondrial COI genes. Numbers on nodes indicate bpp from Bayesian inference analysis (BI) and bootstrap values from maximum likelihood (ML), respectively **B** neighbour-joining tree (NJ) based on 230 amino acid alignments of peptide sequences corresponding to the mitochondrial COI dataset. Numbers on nodes indicate bootstrap values.

of *T. phylloides* and *T. bifidus*, respectively. All internal nodes were strongly supported (0.99–1 bpp for BI and 97–100% bootstrap values for ML). In addition, nine cambalopsid species were recovered as a monophyletic clade against the analyzed outgroups representing two other families and one order, although only the BI analysis was supported by this grouping and showed a bpp of 0.95. Within the cambalopsid clade, three genera were clustered separately as a monophyletic clade. However, no evolutionary relationship among them was revealed. The NJ tree based on the COI corresponding amino acid sequences also clearly recovered the monophyly of *Trachyjulus* (73% bootstrap values) (Fig. 5B).

The interspecific divergence of the COI uncorrected *p*-distance among these nine cambalopsid species was found to be generally high (13.48–24.49%; Table 2). Among the *Trachyjulus* species concerned, the average distance values ranged from 15.07–23.62%. *Trachyjulus singularis* showed the highest divergence from the other *Trachyjulus* species, ranging from 21.16–23.62%. The lowest divergence among *Trachyjulus* species was 15.07% between *T. bifidus* and *T. phylloides*. Five *Trachyjulus* species showed a long-distance relationship to their closely related genera, *Glyphiulus* (18.84–23.62%) and *Plusioglyphiulus* (20.00–24.49%). In addition, the average distances between the members of *Glyphiulus* and *Plusioglyphiulus* were also relatively high, ranging from 17.39–21.16%. The interspecific divergence among *Glyphiulus* and *Plusioglyphiulus* species amounted to 17.97 and 13.48, respectively.

Table 2. Matrix of the average interspecific genetic divergence (uncorrected *p*-distance: % ± SE) for the 690 bp barcoding region of the COI gene between *Trachyjulus* species and some related Cambalopsidae taxa.

Taxa	1.	2.	3.	4.	5.	6.	7.	8.
1. *Trachyjulus bifidus*								
2. *Trachyjulus phylloides*	15.07 ± 1.31							
3. *Trachyjulus unciger*	20.00 ± 1.51	19.13 ± 1.45						
4. *Trachyjulus magnus* sp. nov.	20.14 ± 1.52	20.00 ± 1.46	20.43 ± 1.52					
5. *Tachyjulus singularis*	21.16 ± 1.53	20.80 ± 1.50	23.62 ± 1.64	21.52 ± 1.54				
6. *Glyphiulus sattaa*	18.84 ± 1.50	17.68 ± 1.40	21.45 ± 1.58	18.12 ± 1.46	20.51 ± 1.53			
7. *Glyphiulus duangdee*	21.16 ± 1.51	21.16 ± 1.59	22.61 ± 1.56	23.62 ± 1.61	23.48 ± 1.59	17.97 ± 1.48		
8. *Plusioglyphiulus erawan*	21.74 ± 1.53	20.43 ± 1.46	24.49 ± 1.59	20.29 ± 1.48	21.45 ± 1.61	17.39 ± 1.40	19.42 ± 1.50	
9. *Plusioglyphiulus saksit*	20.72 ± 1.48	21.30 ± 1.44	24.06 ± 1.53	20.58 ± 1.51	20.00 ± 1.41	19.13 ± 1.43	21.16 ± 1.47	13.48 ± 1.26

Discussion

Trachyjulus magnus sp. nov. clearly represents a taxonomically valid species based on both morphological and molecular evidence. In the latest taxonomic review of *Trachyjulus*, Golovatch et al. (2012a) emphasized and listed the following primary morphological characters deemed useful to distinguishing it from the other cambalopsid genera. The genus *Trachyjulus* shows a collum which is smooth or nearly smooth at least dorsally, usually not particularly inflated compared to postcollum constrictions; midbody metazonae are strongly carinate, the carinotaxic formulae typically being 11–8/11–8+I/i+2/2+m/m; male leg 1 is strongly reduced to a broad transverse coxosternum that shows a pair of central, often completely fused coxal processes flanked by rudimentary telopodites; some structures of the gonopods are also unique. It is gonopodal structures, often highly conservative, that usually appear to be especially useful for species delimitations among congeners in the family Cambalopsidae (Golovatch et al. 2007a, 2007b, 2009, 2011a, 2011b, 2011c, 2011d, 2012b; Jiang et al. 2017; Likhitrakarn et al. 2017).

Morphologically, the new species looks especially similar to *T. unciger*, but both are clearly distinguishable (see Diagnosis above). Molecular evidence likewise reveals a sufficiently strong genetic divergence between *T. magnus* sp. nov. and *T. unciger* (*p*-distance = 20.43±1.52) (Table 2). Compared to other studies, the interspecific distances among Bavarian millipedes range from >5% among members in the same genus and up to 33.18% between the different orders, averaging 14.17% (Spelda et al. 2011). In Thailand, Pimvichai et al. (2016) reported the interspecific divergences of mitochondrial COI as ranging between 2 and 17% in the large-bodied *Thyropygus* millipedes, family Harpagophoridae. The average interspecific divergences among *Trachyjulus* species in the present study appear to be even higher than in *Thyropygus*: 15.07–23.62%. This may be accounted for by the much smaller sizes of *Trachyjulus* spp., as well as their usually more limited dispersal capacities that make them largely restricted to a particular cave or cave complex (Golovatch et al. 2007a, 2011a). High rates of interspecific genetic differentiation in small-bodied cave-dwelling species have long been reported elsewhere: 8.2–9.2% between two parapatric Callipodida millipedes from the USA, *Tetracion tennesseensis* Causey, 1959 and *T. jonesi* Hoffman, 1956 (Loria et al. 2011).

The phylogenetic trees, both rooted and inrooted, and based on the concatenated dataset, provide strong support to the monophyly of the genus *Trachyjulus* in both ML and BI analyses (bpp = 1.0 for BI and bootstrap value = 100% for ML) (Fig. 5A). In addition, the NJ tree based on the COI corresponding amino acid sequences in which the protein evolves at a slow rate (Drummond et al. 2005) clearly recovered the monophyly of *Trachyjulus* as well (73% bootstrap values) (Fig. 5B). Therefore, the molecular evidence confirms that all of the *Trachyjulus* species concerned, including the new species, do belong to the same genus. Because the unrooted phylogram totally failed to alter the topology of the rooted one, only the latter is shown in Figure 5.

Trachyjulus singularis was recovered as the basal clade of the tree. It also showed the highest genetic divergence from the other *Trachyjulus* species (21.16–23.62%). These results are in accordance with their geographic distributions, as *T. singularis* occurs

only in eastern Thailand, i.e. far away from the congeners in southern Thailand. In addition, *T. singularus* has retained the ancestral character of a divided promentum of the gnathochilarium, a trait absent from the other members of *Trachyjulus*, but present in two other related genera, *Glyphiulus* and *Plusioglyphiulus*.

In conclusion, we put on record the first results of a molecular phylogenetic study on *Trachyjulus*, a largely cavernicolous genus, using a combination of the nuclear 28S rRNA and mitochondrial CO1 genes for a total of 1,501 bp. Our results reveal high rates of interspecific divergence among *Trachyjulus* species and other closely related genera. Given that Thailand and the neighbouring countries are extremely rich in karst and karst caves, there can hardly be any doubt that additional new species of Cambalopsidae generally and *Trachyjulus* in particular still await discovery. A combination of morphological and molecular studies in Cambalopsidae seems the best to provide further insights into the taxonomy and phylogenetic relationships in this large and widespread group.

Acknowledgements

This project was partly funded through grants received from the Office of the Royal Development Projects Board (RDPB), while most of the financial support was obtained from TRF Strategic Basic Research BDG 6080011 (2017–2019) to CS and NL, and Centre of Excellence on Biodiversity (BDC-PG2-161002) to SP. We thank the members of the Animal Systematics Research Unit for their invaluable assistance in the field. One of us (SIG) was partly supported by the Presidium of the Russian Academy of Sciences, Program No. 41 "Biodiversity of natural systems and biological resources of Russia". Special thanks go to Henrik Enghoff (NHMD) for his critical review of an advanced draft that has allowed us to considerably improve the paper.

References

Akaike H (1974) A new look at the statistical model identification. IEEE Transactions on Automatic Control 19(6): 716–723. https://doi.org/10.1109/TAC.1974.1100705

AVMA (2013) AVMA guidelines for the euthanasia of animals. https://www.avma.org/KB/Policies/Documents/euthanasia.pdf [Accessed on: 2019-2-2]

Bogdanowicz SM, Wallner WE, Bell J, ODell TM, Harrison RG (1993) Asian gypsy moths (Lepidoptera: Lymantriidae) in North America: evidence from molecular data. Annals of the Entomological Society of America 86: 710–715. https://doi.org/10.1093/aesa/86.6.710

Drummond DA, Bloom JD, Adami C, Wilke CO, Arnold FH (2005) Why highly expressed proteins evolve slowly. Proceedings of the National Academy of Sciences of the United States of America 102(40): 14338–14343. https://doi.org/10.1073/pnas.0504070102

Enghoff H, Dohle W, Blower JG (1993) Anamorphosis in millipedes (Diplopoda) – the present state of knowledge with some developmental and phylogenetic considerations. Zoological Journal of the Linnean Society 109: 103–234. https://doi.org/10.1111/j.1096-3642.1993.tb00305.x

Folmer O, Black M, Hoeh W, Lutz R, Vrijenhoek R (1994) DNA primers for amplification of mitochondrial cytochrome *c* oxidase subunit I from diverse metazoan invertebrates. Molecular Marine Biology and Biotechnology 3(5): 294–299.

Golovatch SI (2009) Millipedes (Diplopoda) in extreme environments. In: Golovatch SI, Makarova OL, Babenko AB, Penev L (Eds) Species and Communities in Extreme Environments. Festschrift towards the 75th Anniversary and a Laudatio in Honour of Academican Yuri Ivanovich Chernov. Pensoft & KMK Scientific Press, Sofia–Moscow, 87–112.

Golovatch SI (2015) Cave Diplopoda of southern China with reference to millipede diversity in Southeast Asia. ZooKeys 510: 79–94. https://doi.org/10.3897/zookeys.510.8640

Golovatch SI, Liu WX (2020) Diversity, distribution patterns and faunogenesis of the millipedes (Diplopoda) of mainland China. ZooKeys (in press).

Golovatch SI, Geoffroy JJ, Mauriès JP, VandenSpiegel D (2007a) Review of the millipede genus *Glyphiulus* Gervais, 1847, with descriptions of new species from Southeast Asia (Diplopoda, Spirostreptida, Cambalopsidae). Part 1: the *granulatus*-group. Zoosystema 29(1): 7–49.

Golovatch SI, Geoffroy JJ, Mauriès JP, VandenSpiegel D (2007b) Review of the millipede genus *Glyphiulus* Gervais, 1847, with descriptions of new species from Southeast Asia (Diplopoda, Spirostreptida, Cambalopsidae). Part 2: the *javanicus*-group. Zoosystema 29(3): 417–456.

Golovatch SI, Geoffroy JJ, Mauriès JP, VandenSpiegel D (2009) Review of the millipede genus *Plusioglyphiulus* Silvestri, 1923, with descriptions of new species from Southeast Asia (Diplopoda, Spirostreptida, Cambalopsidae). Zoosystema 31(1): 71–116. https://doi.org/10.5252/z2009n1a5

Golovatch SI, Geoffroy JJ, Mauriès JP, VandenSpiegel D (2011a) The millipede genus *Plusioglyphiulus* Silvestri, 1923 in Thailand (Diplopoda: Spirostreptida: Cambalopsidae). Zootaxa 2840: 1–63. https://doi.org/10.11646/zootaxa.2940.1.1

Golovatch SI, Geoffroy JJ, Mauriès JP, VandenSpiegel D (2011b) New species of the millipede genus *Glyphiulus* Gervais, 1847 from the *granulatus*-group (Diplopoda: Spirostreptida: Cambalopsidae). Arthropoda Selecta 20(2): 65–114. https://doi.org/10.15298/arthsel.20.2.01

Golovatch SI, Geoffroy JJ, Mauriès JP, VandenSpiegel D (2011c) New species of the millipede genus *Glyphiulus* Gervais, 1847 from the *javanicus*-group (Diplopoda: Spirostreptida: Cambalopsidae). Arthropoda Selecta 20(3): 149–165. https://doi.org/10.15298/arthsel.20.3.02

Golovatch SI, Geoffroy JJ, Mauriès JP, VandenSpiegel D (2011d) Two new species of the millipede genus *Hypocambala* Silvestri, 1895 from China and Vietnam (Diplopoda: Spirostreptida: Cambalopsidae). Arthropoda Selecta 20(3): 167–174. https://doi.org/10.15298/arthsel.20.3.03

Golovatch SI, Geoffroy JJ, Mauriès JP, VandenSpiegel D (2012a) New or poorly-known species of the millipede genus *Trachyjulus* Peters, 1864 (Diplopoda: Spirostreptida: Cambalopsidae). Arthropoda Selecta 21(2): 103–129. https://doi.org/10.15298/arthsel.21.2.01

Golovatch SI, Geoffroy JJ, Mauriès JP, VandenSpiegel D (2012b) An unusual new species of the millipede genus *Glyphiulus* Gervais, 1847 from Borneo (Diplopoda: Spirostreptida: Cambalopsidae). Russian Entomological Journal 21(2): 133–137. https://doi.org/10.15298/arthsel.21.2.01

Harvey MS (2002) Short-range endemism in the Australian fauna: some examples from non-marine environments. Invertebrate Systematics 16: 555–570. https://doi.org/10.1071/IS02009

Jiang XK, Lv JC, Guo X, Yu ZG, Chen, HM (2017) Two new species of the millipede genus *Glyphiulus* Gervais, 1847 from Southwest China (Diplopoda: Spirostreptida: Cambalopsidae). Zootaxa 4323(2): 197–208. https://doi.org/10.11646/zootaxa.4323.2.3

Jiang XK, Guo X, Chen HM, Xie ZC (2018) Four new species of the *Glyphiulus javanicus* group from southern China (Diplopoda, Spirostreptida, Cambalopsidae). ZooKeys 741: 155–179. https://doi.org/10.3897/zookeys.741.23223

Kumar S, Stecher G, Tamura K (2016) MEGA7: Molecular Evolutionary Genetics Analysis Version 7.0 for Bigger Datasets. Molecular Biology and Evolution 33(7): 1870–1874. https://doi.org/10.1093/molbev/msw054

Likhitrakarn N, Golovatch SI, Inkhavilay K, Sutcharit C, Srisonchai R, Panha S (2017) Two new species of the millipede genus *Glyphiulus* Gervais, 1847 from Laos (Diplopoda, Spirostreptida, Cambalopsidae). ZooKeys 722: 1–18. https://doi.org/10.3897/zookeys.722.21192

Likhitrakarn N, Golovatch SI, Srisonchai R, Brehier F, Lin A, Sutcharit C, Panha S (2018) Two new species of the millipede family Cambalopsidae from Myanmar (Diplopoda, Spirostreptida). ZooKeys 760: 55–71. https://doi.org/10.3897/zookeys.760.24837

Liu WX, Wynne JJ (2019) Cave millipede diversity with the description of six new species from Guangxi, China. Subterranean Biology 30: 57–94. https://doi.org/10.3897/subtbiol.30.35559

Loria SF, Zigler KS, Lewis JJ (2011) Molecular phylogeography of the troglobiotic millipede *Tetracion* Hoffman, 1956 (Diplopoda, Callipodida, Abacionidae). International Journal of Myriapodology 5: 35–48. https://doi.org/10.3897/ijm.5.1891

Miller M, Pfeiffer W, Schwartz T (2010) Creating the CIPRES Science Gateway for inference of large phylogenetic trees. Proceedings of the Gateway Computing Environments Workshop (GCE), 14 November 2010, New Orleans, LA, 1–8. https://doi.org/10.1109/GCE.2010.5676129

Passamaneck YJ, Schander C, Halanych KM (2004) Investigation of molluscan phylogeny using large-subunit and small-subunit nuclear rRNA sequences. Molecular Phylogenetics and Evolution 32: 25–38. https://doi.org/10.1016/j.ympev.2003.12.016

Pimvichai P, Enghoff H, Panha S (2014) Molecular phylogeny of the *Thyropygus allevatus* group of giant millipedes and some closely related groups. Molecular Phylogenetics and Evolution 71: 170–183. https://doi.org/10.1016/j.ympev.2013.11.006

Pimvichai P, Enghoff H, Panha S, Backeljau T (2016) A revision of the *Thyropygus allevatus* group. Part V: nine new species of the extended *opinatus* subgroup, based on morphological and DNA sequence data (Diplopoda: Spirostreptida: Harpagophoridae). European Journal of Taxonomy 199: 1–37. https://doi.org/10.5852/ejt.2016.199

Ronquist F, Teslenko M, van der Mark P, Ayres DL, Darling A, Höhna S, Larget B, Liu L, Suchard MA, Huelsenbeck JP (2012) MrBayes 3.2: Efficient Bayesian Phylogenetic Inference and Model Choice Across a Large Model Space. Systematic Biology 61(3): 539–542. https://doi.org/10.1093/sysbio/sys029

Schulmeister S, Wheeler WC, Carpenter JM (2002) Simultaneous analysis of the basal lineages of Hymenoptera (Insecta) using sensitivity analysis. Cladistics 18: 455–484. https://doi.org/10.1111/j.1096-0031.2002.tb00287.x

Silvestro D, Michalak I (2012) RaxmlGUI: a graphical front-end for RAxML. Organisms Diversity and Evolution 12: 335–337. https://doi.org/10.1007/s13127-011-0056-0

Spelda J, Reip H, Oliveira Biener U, Melzer R (2011) Barcoding Fauna Bavarica: Myriapoda – a contribution to DNA sequence-based identifications of centipedes and millipedes (Chilopoda, Diplopoda). ZooKeys 156: 123–139. https://doi.org/10.3897/zookeys.156.2176

Stamatakis A (2014) RAxML version 8: A tool for phylogenetic analysis and post-analysis of large phylogenies. Bioinformatics 30(9): 1312–1313. https://doi.org/10.1093/bioinformatics/btu033

Tanabe AS (2011) Kakusan4 and Aminosan: two programs for comparing nonpartitioned, proportional and separate models for combined molecular phylogenetic analyses of multilocus sequence data. Molecular Ecology Resources 11(5): 914–921. https://doi.org/10.1111/j.1755-0998.2011.03021.x

ZooKeys 925: 73–88 (2020)
doi: 10.3897/zookeys.925.47820
http://zookeys.pensoft.net

RESEARCH ARTICLE

A peer-reviewed open-access journal
ZooKeys
Launched to accelerate biodiversity research

The complete mitochondrial genome sequence of *Scolopendra mutilans* L. Koch, 1878 (Scolopendromorpha, Scolopendridae), with a comparative analysis of other centipede genomes

Chaoyi Hu[1,*], Shuaibin Wang[1,*], Bisheng Huang[1], Hegang Liu[1], Lei Xu[1], Zhigang Hu[1,2], Yifei Liu[1]

1 *College of Pharmacy, Hubei University of Chinese Medicine, No. 1 Huangjiahu West Road, Hongshan District, Wuhan, China* **2** *Hubei Jingui Chinese Medicine Pieces Ltd., Wuhan, Hubei, China*

Corresponding author: Yifei Liu (liuyifei@hbtcm.edu.cn); Zhigang Hu (zghu0608@163.com)

Academic editor: Pavel Stoev | Received 31 October 2019 | Accepted 20 February 2020 | Published 8 April 2020

http://zoobank.org/887E26A1-28A3-4317-ACE4-9FFC507F5DC0

Citation: Hu C, Wang S, Huang B, Liu H, Xu L, Hu Z, Liu Y (2020) The complete mitochondrial genome sequence of *Scolopendra mutilans* L. Koch, 1878 (Scolopendromorpha, Scolopendridae), with a comparative analysis of other centipede genomes. ZooKeys 925: 73–88. https://doi.org/10.3897/zookeys.925.47820

Abstract

Scolopendra mutilans L. Koch, 1878 is an important Chinese animal with thousands of years of medicinal history. However, the genomic information of this species is limited, which hinders its further application. Here, the complete mitochondrial genome (mitogenome) of *S. mutilans* was sequenced and assembled by next-generation sequencing. The genome is 15,011 bp in length, consisting of 13 protein-coding genes (PCGs), 14 tRNA genes, and two rRNA genes. Most PCGs start with the ATN initiation codon, and all PCGs have the conventional stop codons TAA and TAG. The *S. mutilans* mitogenome revealed nine simple sequence repeats (SSRs), and an obviously lower GC content compared with other seven centipede mitogenomes previously sequenced. After analysis of homologous regions between the eight centipede mitogenomes, the *S. mutilans* mitogenome further showed clear genomic rearrangements. The phylogenetic analysis of eight centipedes using 13 conserved PCG genes was finally performed. The phylogenetic reconstructions showed Scutigeromorpha as a separate group, and Scolopendromorpha in a sister-group relationship with Lithobiomorpha and Geophilomorpha. Collectively, the *S. mutilans* mitogenome provided new genomic resources, which will improve its medicinal research and applications in the future.

* These authors contributed equally to this work.

Keywords
Chilopoda, Chinese medicinal materials, mitogenome, *Scolopendra mutilans*

Introduction

Animal medicine is an important part of the Chinese traditional medicine system. As a typical representative of medicinal animals, the centipede *Scolopendra mutilans* has been used for hundreds of years in China for treating many disorders, such as stroke-induced hemiplegia, epilepsy, apoplexy, whooping cough, tetanus, burns, tuberculosis, and myocutaneous disease (Ding et al. 2016). Moreover, centipedes have been described for the treatment of cardiovascular diseases in Korea, China, and other east Asian countries (Chen et al. 2014). *Scolopendra mutilans* is a venom-containing animal, which is rich in antimicrobial peptides, ion channel modulators, enzymes, and other macromolecular active substances (Yoo et al. 2014). Due to its active ingredients, it is of great interest in modern medical research. However, with the increase of medicinal applications, the wild populations of *S. mutilans* were over-exploited and declined greatly (Kang et al. 2017). Conservation and further artificial culture are needed, which in turn depends on the correct classification and molecular identification of the natural centipede taxa.

Centipedes (Chilopoda) are one of the oldest extant terrestrial arthropods. Approximately 3300 centipede species have been described (Chipman et al. 2014) and the majority of these taxa are distributed in tropical and subtropical regions. Six orders of centipedes are currently recognized, namely, Scolopendromorpha, Geophilomorpha, Lithobiomorpha, Scutigeromorpha, Craterostigmomorpha, and Devonobiomorpha (Bortolin et al. 2018). Devonobiomorpha is an extinct order represented by a single species (Shear and Bonamo 1988) and the Craterostigmomorpha only occur in Tasmania and New Zealand (Undheim et al. 2016). The remaining orders are distributed widely (Edgecombe et al. 2002), but their evolutionary relationships remain unclear on the basis of morphological traits. The Scutigeromorpha, with body respiratory openings on the back, was generally classified as class Notostigmophora, while the remaining orders with lateral spiracles were divided into another class, Pleurostigmophora (Giribet et al. 1999). However, both Scutigeromorpha and Lithobiomorpha have an anamorphic development in which the segment number increases during postembryonic life (Anamorpha). While Scolopendromorpha and Geophilomorpha have an epimorphic development in which the definitive number of body segments appears upon hatching (Epimorpha). The Craterostigmomorpha order is not strictly anamorphic, making its position unclear (Giribet et al. 1999; Edgecombe and Giribet 2007).

Previously, phylogenetic analysis on the basis of different molecular data provided support to these morphological classifications to some degree (Regier et al. 2008; Fernández et al. 2016). With a phylogenetic reconstruction based on a large number of

protein-coding nuclear genes, the Scutigeromorpha was placed as a single evolutionary branch in Chilopoda, while the other three orders were clustered together, in which the Lithobiomorpha was a sister group of the Scolopendromorpha and the Geophilomorpha showed a distant relationship to them (Regier et al. 2008). A phylogenomic reconstruction based on transcriptomic data also suggested a similar pattern, that the Scutigeromorpha order was a sister group with the other three orders. Moreover, the Scolopendromorpha order is closer to the Geophilomorpha order than the Lithobiomorpha (Fernández et al. 2016).

The mitochondrial genome (mitogenome), including those markers derived from it as well as the whole mitogenome, is the most commonly used molecule in animal studies with relation to taxonomy, population genetics, and evolutionary biology (Wolstenholme 1992; Li et al. 2018a). Generally, an animal mitogenome is a double-stranded circular molecule, ranging from 14 to 20 kb in length and containing a typical set of 37 genes, including 13 protein-coding genes (PCGs), 22 transfer RNA (tRNA) genes, and two ribosomal RNA (rRNA) genes (Taanman 1999). Functional information on replication derived from the related genomic structures has been well investigated, but the transcription features of animal mitogenomes are still limited (Chen and Du 2017). Here, we sequenced and assembled the mitogenome of *S. mutilans* and compared its genome to seven other representative centipede mitogenomes derived from Scolopendromorpha, Geophilomorpha, Lithobiomorpha, and Scutigeromorpha. We obtained the phylogenetic relationship of these centipede taxa based on the 13 PCGs and our results provide new genetic information for both conservation and sustainable use of centipedes as a medicinal resource.

Materials and methods

Sample collection and DNA extraction

Scolopendra mutilans samples were collected in August 2018 from the wild in Yichang, Hubei Province, China. The specimens used in this study were preserved in 100% ethanol and stored at -20 °C. Genomic DNA was extracted from locomotory legs by Column mtDNAout kit (Tiangen Biotech Co., China) according to the instructions and stored at -20 °C until used for sequencing. The DNA quality was measured by gel electrophoresis and the concentration was estimated using the Nanodrop ND-1000.

Sequencing, assembly, and annotation of mitochondrial genomes

Whole genome sequencing was performed on an Illumina HiSeq 2500 platform (Illumina, San Diego, CA, USA). Quality control and de novo assembly of the *S. mutilans* mitogenome were conducted based on previously described methods (Li et al. 2018b). Briefly, raw reads were first filtered to generate clean data. De novo assembly of mitog-

enomes were performed using the SPAdes v3.9.0 software package (He et al. 2018), and the gaps were filled using MITObim v1.9 (Deng et al. 2018).

The mitogenomes were annotated by combining results from both MFannot and MITOS (Bernt et al. 2013), using the genetic code 4 in both programs. The PCGs, rRNA and tRNA were initially annotated at this step. The annotated PCGs were then refined using the NCBI Open Reading Frame Finder, and further annotated with BLASTp searches against the NCBI non-redundant protein sequence database (He et al. 2018; Wang et al. 2018b). The tRNA genes were also predicted using tRNAscan-SE v1.3.1 (Zhang et al. 2018). Subsequently, graphical maps of the complete mitogenomes were drawn using OGDraw v1.2 (Wang et al. 2018a).

Repetitive element analysis

In order to identify interspersed repeats or intra-genomic duplications of large fragments throughout the mitogenomes, we performed BLASTn searches of the mitogenome against itself using an E-value of 1e-10. Tandem repeats within the mitogenome were detected by MicroSAtellite (MISA) (Shaoli et al. 2018; Thiel et al. 2003), with the following thresholds: ten, six, five, five, five, and five repeat units for mononucleotide, di-nucleotide, tri-nucleotide, tetranucleotide, penta-nucleotide, and hexa-nucleotide SSRs. Forward (direct), reverse, complemented, and palindromic (reverse complemented) repeats were identified using the REPuter software (Kurtz et al. 2001) with default settings.

The base composition of the mitogenome was determined using the DNAStar Lasergene package v7.1 (Burland 2000). The following formulae were used to assess mitogenome strand asymmetry: AT skew = [A – T] / [A + T]; GC skew = [G – C] / [G + C]. Lastly, genomic synteny of the eight mitogenomes was analyzed with Mauve v2.4.0 (Darling et al. 2004).

Phylogenetic analysis

A maximum likelihood (ML) tree was constructed using the RAxML (Stamatakis et al. 2017) based on nucleotide sequence data of 13 PCGs derived from eight centipede species among the class Chilopoda (Table 1) and a *Sphaerotheriidae* sp. (NC_018361) (Dong et al. 2012) from the class Diplopoda was used as the outgroup. The nucleotide sequences of the 13 PCGs were firstly aligned with Clustal X (Larkin et al. 2007) as implemented in MEGA7 (Kumar et al. 2008) using the default settings. The best nucleotide substitution model was determined with Jmodeltest (Posada 2008) and the GTR+G+I model was predetermined for analyses. One thousand bootstrap replicates were performed and the phylogenetic tree was illustrated using the software FigTree v1.4.2 (Lemey et al. 2010).

Table 1. Basic information of the mitogenomes for Chilopoda used in this study.

Species	Order	NCBI ID	Length (bp)
Scolopendra mutilans L. Koch, 1878	Scolopendromorpha	MN317390	15011
Scolopendra dehaani Brandt, 1840	Scolopendromorpha	KY947341.1	14538
Scolopocryptops sp.	Scolopendromorpha	KC200076.1	15119
Strigamia maritima (Leach, 1817)	Geophilomorpha	KP173664.1	14983
Cermatobius longicornis Takakuwa,1939	Lithobiomorpha	NC_021403.1	16833
Bothropolys sp.	Lithobiomorpha	AY691655.1	15139
Lithobius forficatus (Linnaeus,1758)	Lithobiomorpha	AF309492.1	15695
Scutigera coleoptrata (Linnaeus, 1758)	Scutigeromorpha	AJ507061.2	14922

Analysis of selective pressures was performed for 13 PCGs of eight centipedes using the codeml program in PAML (University College London, London, UK) (Yang 2007) by calculating the nonsynonymous (K_A) and synonymous (K_S) substitution ratio. The method reported by Yang and Nielsen (2000) was adopted to estimate the ω value ($\omega = K_A / K_S$) of every gene sequence.

Results

Gene content and composition

The full circular mitogenome of *S. mutilans* (GenBank: MN317390) was 15,011 bp in length, which was similar to those of seven other centipede mitogenomes sequenced in the class Chilopoda (Table 1) (Robertson et al. 2015; Sun et al. 2018). The *S. mutilans* mitogenome contains 29 genes, including 13 PCGs, 14 tRNA genes, and two rRNA genes (Figure 1). Most PCGs, including the cox1, cox2, cox3, nad2, nad3, nad6, atp6, atp8, and cob genes, and the majority of tRNA genes (trnI, trnM, trnW, trnK, trnD, trnG, trnA, trnS1, trnV, and trnS2) are transcribed from the plus strand, while the remaining four PCGs, two ribosomal genes, and four tRNAs are transcribed from the minus strand (Table 2). The overlapping regions between genes were in relation to three neighboring gene pairs, containing a length of 27 bp in total, with each size ranging from 2 to 18 bp. We also found a total of 2111 bp of intergenic regions on the *S. mutilans* mitogenome, accounting for 14% of the genome size.

The mitogenome size of eight centipedes ranged from 14,538 bp for *S. dehaani* Brandt, 1840 to 16,833 bp for *Cermatobius longicornis* Takakuwa,1939, with that of *S. mutilans* in the middle of the range. To identify the specific variation contributing most to the diversity of the mitogenome size in centipedes, the length variation of all PCGs, tRNA, and rRNA genes, and intergenic regions in each mitogenome was investigated. Comparatively, the length of most genes across centipede species was relatively stable except the PCGs in *L. forficatus* Linnaeus,1758 (AF309492.1), while the length of intergenic regions was the primary contributor to mitogenome size variation.

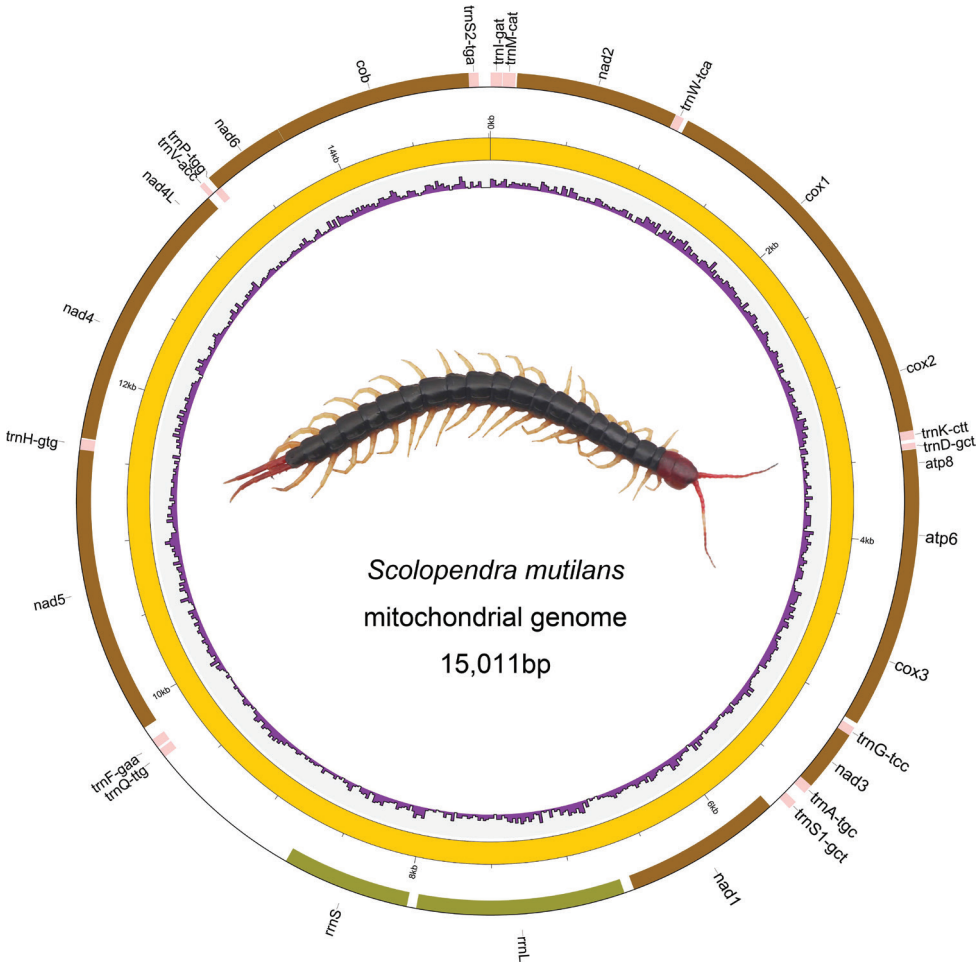

Figure 1. Mitochondrial genome map of the *Scolopendra mutilans*. Genes drawn inside the circle are transcribed clockwise, and those outside are counterclockwise. PCGs are shown as brown arrows, rRNA genes as green arrows, tRNA genes as pink arrows. The innermost circle shows the GC content. GC content is plotted as the deviation from the average value of the entire sequence.

Genomic repeats

The repeated DNA in animal mitogenomes can be divided into tandem repeats and interspersed repeats (Wu et al. 2017). In the *S. mutilans* mitogenome, 46 tandem repeats have been identified, of which the longest is 39 bp and the shortest is 9 bp. However, no interspersed repeat was found. Generally, SSRs are a group of tandem repeated sequences containing 1–6 nucleotide repeat units and are widely distributed in animal mitogenomes, and they are commonly used as molecular markers for species identification (Wang et al. 2018a). A total of nine SSRs were detected in the *S. mutilans* mitogenome, including three mono-nucleotides, five di-nucleotides, and one tri-nucleotide, as well as two compound SSRs (Table 3). Among these, only one mono-nucleotide SSR is distributed in the small subunit of one ribosomal RNA gene, while

Table 2. Organization of the *Scolopendra mutilans* mitogenome.

Gene	Start	End	Strand	Length	Start/End codon
trnI (gat)	1	65	+	65	–
trnM (cat)	69	141	+	73	–
nad2	124	954	+	831	ATT/TAA
trnW (tca)	1071	1119	+	49	–
cox1	1148	2656	+	1509	ATG/TAG
cox2	2676	3341	+	666	ATG/TAA
trnK (ctt)	3355	3405	+	51	–
trnD (gtc)	3425	3458	+	34	–
atp8	3465	3614	+	150	ATA/TAA
atp6	3620	4267	+	648	ATG/TAA
cox3	4282	5049	+	768	AYG/TAA
trnG (tcc)	5084	5137	+	54	–
nad3	5141	5488	+	348	ATT/TAG
trnA (tgc)	5487	5542	+	56	–
trnS1 (gct)	5612	5662	+	51	–
nad1	5784	6635	-	851	ATT/TAA
rrnL	6719	7937	-	1219	–
rrnS	7993	8740	-	748	–
trnQ (ttg)	9667	9720	-	54	–
trnF (gaa)	9735	9791	-	57	–
nad5	9906	11,474	-	1569	ATT/TAA
trnH (gtg)	11,556	11,619	-	64	–
nad4	11,641	12,789	-	1149	ATG/TAA
nad4l	12,939	13,181	-	243	ATA/TAA
trnV (aac)	13,230	13,262	+	33	–
trnP (tgg)	13,272	13,315	-	44	–
nad6	13,373	13,759	+	387	ATT/TAA
cob	13,773	14,873	+	1101	ATG/TAA
trnS2 (tga)	14,889	14,944	+	56	–

Table 3. Simple sequence repeats in *Scolopendra mutilans*.

Number	SSR type	SSR	Size (bp)	Start	End	Position
1	mono-nucleotide	$(A)_{11}$	11	12,790	12,800	intergenic
2	mono-nucleotide	$(A)_{12}$	12	8540	8551	rrnS
3	mono-nucleotide	$(A)_{20}$	20	12,837	12,856	intergenic
4	di-nucleotide	$(AT)_{8}$	16	8776	8791	intergenic
5	di-nucleotide	$(AT)_{8}$	17	9820	9835	intergenic
6	di-nucleotide	$(AT)_{9}$	19	3406	3423	intergenic
7	di-nucleotide	$(TA)_{11}$	22	1119	1140	intergenic
8	di-nucleotide	$(AT)_{19}$	39	14,968	15,005	intergenic
9	tri-nucleotide	$(TAA)_{5}$	17	14,954	14,968	intergenic

the other SSRs are all presented in the intergenic regions. These mitogenomic SSRs will provide additional marker information for future genetic analyses of *S. mutilans* samples and its related species.

Protein-coding genes

For all 13 PCGs identified in the *S. mutilans* mitogenome, five genes (nad2, nad3, nad1, nad5 and nad6) initiated with the start codon ATT, two genes (atp8 and nad4l) started with the ATG codon, and the remaining six genes used ATA as the start codon. The most common termination codon TAA was detected in eleven PCGs (nad2, cox2, atp8, atp6, cox3, nad1, nad5, nad4, nad4l, nad6, cob). The cox1 and nad3 genes had termination codons with TAG (Table 2). We further compared the PCGs between different centipede mitogenomes (Table 1). Across the eight centipede mitogenomes investigated, we found that the length of some PCGs was variable; for instance, the NADH dehydrogenase genes in *S. mutilans* is a little shorter than those in other centipedes, especially for both the nad2 and nad4 genes (Figure 2A). Notably, it was found that the mean length of PCG genes in the *L. forficatus* (AF309492.1) mitogenome was slightly shorter; this may be caused by post-transcriptional editing that occurs in its mitochondrial tRNAs, which may play an important role in the synthesis of subunits of ATPase in PCGs according to previous reports (Lavrov et al. 2000). Moreover, the GC content of the 13 PCGs across these mitogenomes was also different. We found two subunits of both ATPase genes (atp6 and atp8) showed the lowest GC content compared with the other PCGs in the majority of all mitogenomes. The genetic relationship is usually positively correlated with the GC content of the mitogenome of a species (Bohlin 2011). Comparatively, we found that *S. mutilans* had the lowest GC content in all investigated species at the whole genome level, and *S. dehaani*, another species of the same genus, showed the second lowest GC content of all mitogenomes we investigated (Figure 2B). Interestingly, the four NADH dehydrogenase subunits (nad1, nad4, nad4l, nad5) possessed the opposite AT skew (Figure 2C) and GC skew in the *S. mutilans* mitogenome compared with other species (Figure 2D).

Genomic arrangement analysis

By using the Mauve analysis, we identified six large genomic homologous regions (marked A–F in Figure 3). These homologous regions were commonly presented in all eight centipede mitogenomes, and their sequence lengths were variable across regions and genomes, particularly for the A and E regions, which had a relatively large fragmental size and greatly contributed to the genome size variation between centipede mitogenomes (Figure 3). Interestingly, we found the arrangement of these homologous regions was not conserved, particularly between the *S. mutilans* mitogenome and that of the other species (Figure 3). For example, *S. mutilans* contained a B-C-D-E order of four homologous regions in its mitogenome, while the majority other centipedes showed a D-E-B-C order (Figure 3). The F region was shorter and more conserved in all six homologous regions. However, there was an absence of the F region and a clearly shorter A region in the *Strigamia maritima* Leach, 1817 (KP173664.1) mitogenome. Alternatively, a large ratio of intergenic regions in the *S. maritima* mitogenome were

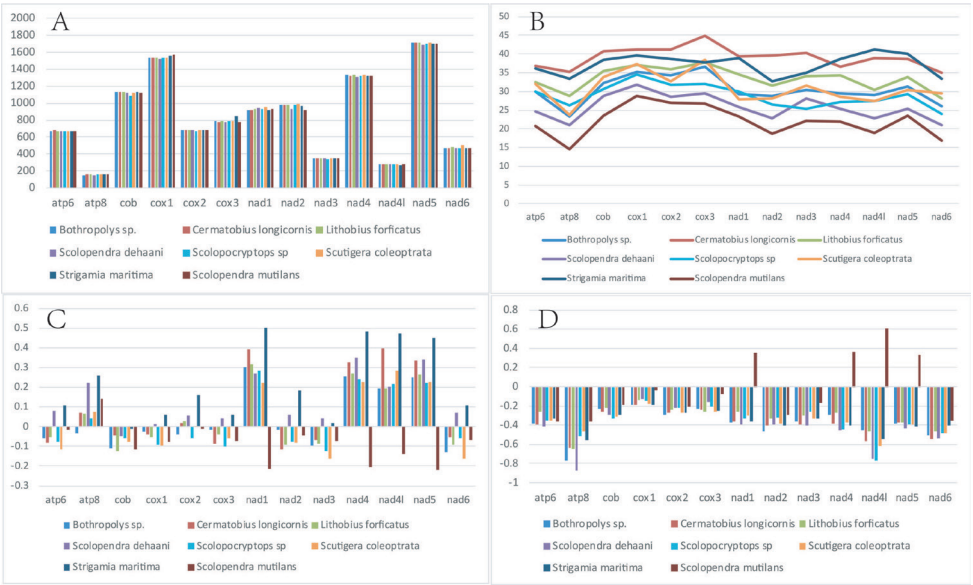

Figure 2. Variation in length and base composition of each of the 13 core protein coding genes (PCGs) among eight centipedes' mitochondrial genomes **A** PCG length variation **B** GC content across PCGs **C** AT skew **D** GC skew.

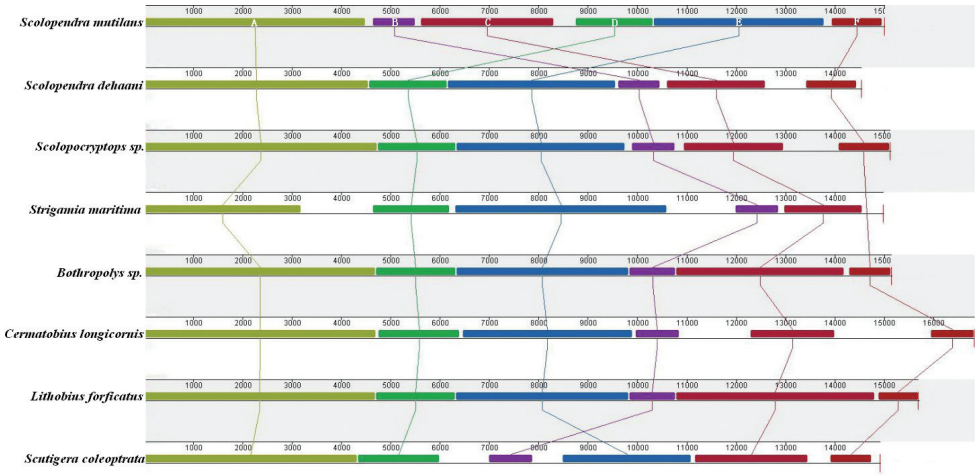

Figure 3. Mitogenome synteny among eight centipede species. Synteny analyses were generated in Mauve 2.4.0. A total of six large homologous regions were identified among the eight mitogenomes, while the sizes and relative positions of the homologous fragments varied across the mitogenomes.

identified, which was also previously reported (Chipman et al. 2014; Robertson et al. 2015). In the Lithobiomorpha order, the six homologous regions of *Bothropolys* sp. (AY691655.1) and *L. forficatus* (AF309492.1) were very similar for their length and the genomic location, while those in *C. longicornis* (NC_021403) were clearly differ-

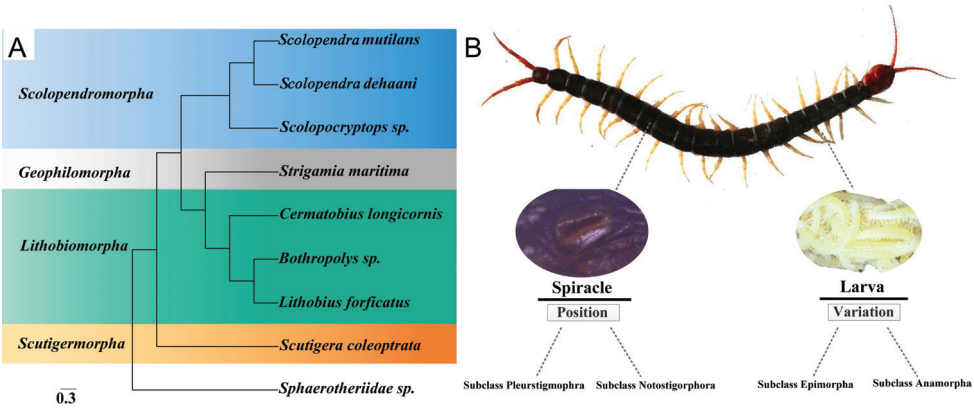

Figure 4. A Molecular phylogeny of eight centipede species based on Maximum Likelihood inference analysis of 13 protein-coding genes (PCGs) **B** Traditional morphological classification based on the position of spiracles and the variation of larvae.

ent. Comparatively, in the Scolopendromorpha order, the lengths of these homologous regions across *S. mutilans*, *S. dehaani*, and *Scolopocryptops* sp. mitogenomes were conserved, though there was a clear rearrangement among them.

Phylogenetic analysis

The constructed ML tree is presented in Figure 4. As previously expected, *S. mutilans*, together with *S. dehaani* and *Scolopocryptops* sp., was placed in one group belonging to the Scolopendromorpha order. Moreover, our phylogenetic analysis suggested that the Scutigeromorpha order (*Scutigera coleoptrata*) was a sister group with the other three centipede orders, Scolopendromorpha, Geophilomorpha (*S. maritima*) and Lithobiomorpha (*C. longicornis*, *Bothropolys* sp., and *L. forficatus*). Our analysis further showed a close relationship between the orders Geophilomorpha and Lithobiomorpha, although the traditional morphological taxonomy suggested a potentially close relationship between the Geophilomorpha and Scolopendromorpha orders due to their shared trait of a stable segment number and lateral spiracles (Fernández et al. 2014).

The ω value can be used for revealing the constraints of natural selection (Tomoko 1995). Among our calculations, the ω value of 13 PCGs were all distributed around 0.004 (Suppl. material 1: Table S1), indicated a possibly purifying selection.

Discussion

We sequenced and assembled the mitogenome of *S. mutilans*, a representative animal widely used in Chinese traditional medicine. The mitogenome is 15,011 bp in length, which is similar to the genome size of other known centipede mitogenomes,

for example, 15,119 bp in *Scolopocryptops* sp. and 15,139 bp in *Bothropolys* sp. (Table 1). The variation of the Chilopoda mitogenome size was relatively conserved, which was consistent with that reported in Diplopoda, an animal class close to Chilopoda (Dong et al. 2016). The gene distribution was mainly presented on the plus strand of the *S. mutilans* mitogenome, and only four PCGs and two rRNA genes were located on the minus strand (Figure 1). This was consistent with other centipede species, like *S. maritima* and *S. dehaani* reported in previous studies (Robertson et al. 2015; Sun et al. 2018). Comparatively, the 13 PCGs in the *S. mutilans* mitogenome revealed a relatively low GC content, which was similar to that of *S. dehaani* (Figure 2).

Our study predicted nine mitogenomic SSRs, which can provide additional genetic marker information in molecular identification of centipede species (Table 3). Generally, the identification and genetic evaluation of centipede taxa depend on the variation presented in the cox1 gene region (Chen et al. 2013). However, when samples were investigated within species or between the closely related taxa, it is difficult to identify variation at individual or population level by only using the cox1 gene information (Kang et al. 2017). Comparatively, due to the relatively high mutation rate and the potentially neutrally evolutionary trajectory of SSR loci, they are widely used in animal genetic research under the species level, including assessing genetic diversity of wild populations, accelerating the progress of genetic selection, and molecular assistant breeding (Zhang et al. 2014). Our nine mitogenome SSRs were valued for future genetic research of samples from both *S. mutilans* and its closely related taxa.

We identified six homologous regions among the eight species' mitogenomes, which revealed obviously genomic rearrangements, in particular between *S. mutilans* and some other centipedes (Figure 3). Genomic rearrangement is common and potentially randomly presented in animals' mitogenomes (Chen et al. 2016). With the increase of mitochondrial genome data of animals, it is clear that rearrangements in mitogenomes are more a matter of sampling than a product of evolution (Boore 1999). For example, Negrisolo et al. (2003) found that it is less reliable to infer phylogenetic relationships based on gene order data in Arthropoda. Genomic rearrangements also occurred randomly among different orders in Hexapoda insects, which is not directly related to the evolution of groups (Cameron et al. 2006). Nevertheless, the observed mitogenomic rearrangements of Chilopoda taxa showed information about how genes move dynamically between different mitogenomes, which may be related to each individual gene evolutionary pattern.

Previous studies revealed alternative phylogenetic relationships of different centipedes by using different molecular datasets (Regier et al. 2008; Robertson et al. 2015; Fernández et al. 2016). With the obtained whole mitogenomic information of *S. mutilans* and the comparative analysis with other representative centipede taxa, our phylogenetic tree revealed a close relationship between *S. mutilans* and *S. dehaani*, which commonly belongs to the Scolopendromorpha order together with *Scolopocryptops* sp. (Figure 4). This was consistent with previous research (Lewis et al. 2005). However, at

the order level, with increased two Scolopendromorpha samples, our analysis showed a closer relationship between Geophilomorpha and Lithobiomorpha, rather than between Geophilomorpha and Scolopendromorpha, which was slightly different to previous research (Robertson et al. 2015). Given the potentially dynamic evolutionary trajectory of different genes or between nuclear and mitochondrial genomes, this discordance may reflect the complex evolutionary history of these centipedes, including the possibility of a genetic admixture or adaptive radiations of these lineages in relation to morphological or functional specification in different geographical areas.

In conclusion, we successfully sequenced the complete mitochondrial genome of *S. mutilans* for the first time using next-generation sequencing, which will be valued for further studies in terms of the conservation, molecular identification, and evolutionary biology of diverse centipede species, improving the medicinal applications of *S. mutilans* and other closely related taxa.

Acknowledgments

We acknowledge Professor Ya'hua Zhan for identifying the materials sequenced here. Special thanks to Pavel Stoev and the reviewers for constructive comments that improved this paper. The present study was supported by the central government guides local science and technology development fund in Hubei Province (2019ZYYD063), Hubei Science Foundation for Distinguished Young Scholars (2019CFA097) and Wuhan "Yellow Crane Talent Program" Talent Project (Principal: Zhigang Hu).

References

Bernt M, Donath A, Jühling F, Externbrink F, Florentz C, Fritzsch G, Pütz J, Middendorf M, Stadler PF (2013) MITOS: improved de novo metazoan mitochondrial genome annotation. Molecular Phylogenetics Evolution 69: 313–319. https://doi.org/10.1016/j.ympev.2012.08.023

Boore JL (1999) Animal mitochondrial genomes. Nucleic Acids Research 27: 1767–1780. https://doi.org/10.1093/nar/27.8.1767

Bohlin J (2011) Genomic signatures in microbes-properties and applications. Scientific World Journal 11: 715–725. https://doi.org/10.1100/tsw.2011.70

Bortolin F, Fusco G, Bonato L (2018) Comparative analysis of diet in syntopic geophilomorph species (Chilopoda, Geophilomorpha) using a DNA-based approach. Soil Biology and Biochemistry 127: 223–229. https://doi.org/10.1016/j.soilbio.2018.09.021

Burland TG (2000) DNASTAR's lasergene sequence analysis software. Methods Molecular Biology Reports 132: 71–91. https://doi.org/10.1385/1-59259-192-2:71

Cameron SL, Beckenbach AT, Dowton M, Whiting M (2006) Evidence from mitochondrial genomics on interordinal relationships in insects. Arthropod Systematics & Phylogeny 64(1): 27–34.

Chen M, Li J, Zhang F, Liu Z (2014) Isolation and characterization of SsmTx-I, a Specific Kv2.1 blocker from the venom of the centipede *Scolopendra Subspinipes Mutilans* L. Koch. Journal of Peptide Science 20: 159–164. https://doi.org/10.1002/psc.2588

Chen S, Yao H, Han J (2013) Principles for molecular identification of traditional Chinese materia medica using DNA barcoding. China Journal of Chinese Materia Medica 38(2): 141. https://doi.org/10.4268/cjcmm20130201

Chen Z, Du Y (2016) Rearrangement of mitochondrial genome in insects. Journal of environmental insects 38(04): 843–851.

Chen Z, Du Y (2017) First Mitochondrial Genome from Nemouridae (Plecoptera) Reveals Novel Features of the Elongated Control Region and Phylogenetic Implications. International Journal of Molecular Sciences 18(5): 996. https://doi.org/10.3390/ijms18050996

Chipman AD, Ferrier DE, Brena C, Qu J, Hughes DS, Schroder R, Torres-Oliva M, Richards S (2014) The first myriapod genome sequence reveals conservative arthropod gene content and genome organisation in the centipede *Strigamia maritima*. PLos Biology 12(11): e1002005. https://doi.org/10.1371/journal.pbio.1002005

Darling C, Mau B, Blattner R, Perna T (2004) Mauve: multiple alignment of conserved genomic sequence with rearrangements. Genome research 14(7): 1394–1403. https://doi.org/10.1101/gr.2289704

Deng Y, Hsiang T, Li S, Lin L, Wang Q, Chen Q, Xie B, Ming R (2018) Comparison of the Mitochondrial Genome Sequences of Six *Annulohypoxylon stygium* Isolates suggests short fragment insertions as a potential factor leading to larger Genomic Size. Frontiers in Microbiology 9: 2079. https://doi.org/10.3389/fmicb.2018.02079

Ding D, Guo YR, Wu RL, Qi WY, Xu HM (2016) Two new isoquinoline alkaloids from *Scolopendra subspinipes mutilans* induce cell cycle arrest and apoptosis in human glioma cancer U87 cells. Fitoterapia 110: 103–109. https://doi.org/10.1016/j.fitote.2016.03.004

Dong Y, Xu JJ, Hao SJ, Sun HY (2012) The complete mitochondrial genome of the giant pill millipede, *Sphaerotheriidae* sp. (Myriapoda: Diplopoda: Sphaerotheriida). Mitochondrial DNA 23: 333–335. https://doi.org/10.3109/19401736.2012.683184

Dong Y, Zhu L, Bai Y (2016) Complete mitochondrial genomes of two flat-backed millipedes by next-generation sequencing (Diplopoda, Polydesmida). ZooKeys 637(637): 1–20. https://doi.org/10.3897/zookeys.637.9909

Edgecombe GD, Giribet G, Wheeler W (2002) Phylogeny of Henicopidae (Chilopoda: Lithobiomorpha): a combined analysis of morphology and five molecular loci. Systematic Entomology 27: 31–64. https://doi.org/10.1046/j.0307-6970.2001.00163.x

Edgecombe GD, Giribet G (2007) Evolutionary biology of centipedes (Myriapoda: Chilopoda). Annual Review of Entomology 52: 151–170. https://doi.org/10.1146/annurev.ento.52.110405.091326

Fernández R, Laumer CE, Varpu V, Silvia L, Stefan K (2014) Evaluating topological conflict in centipede phylogeny using transcriptomic data sets. Molecular Biology and Evolution 31(6): 1500–1513. https://doi.org/10.1093/molbev/msu108

Fernández R, Edgecombe GD, Giribet G (2016) Exploring phylogenetic relationships within Myriapoda and the effects of matrix composition and occupancy on phylogenomic reconstruction. Systematic Biology 65(5): 871–889. https://doi.org/10.1093/sysbio/syw041

Giribet G, Carranza S, Riutort M, Baguna J, Ribera C (1999) Internal phylogeny of the Chilopoda (Myriapoda, Arthropoda) using complete 18S rDNA and partial 28S rDNA sequences. Philosophical Transactions of the Royal Society B-Biological Sciences 354: 215–222. https://doi.org/10.1098/rstb.1999.0373

He K, Chen Z, Yu D, Zhang J (2018) The complete mitochondrial genome of *Chrysopa pallens* (Insecta, Neuroptera, Chrysopidae). Mitochondrial DNA 23: 373. https://doi.org/10.3109/19401736.2012.696631

Kang S, Liu Y, Zeng X, Deng H, Luo Y, Chen K, Chen S (2017) Taxonomy and Identification of the Genus *Scolopendra* in China Using Integrated Methods of External Morphology and Molecular Phylogenetics. Scientific Reports 7: 16032. https://doi.org/10.1038/s41598-017-15242-7

Kumar S, Nei M, Dudley J, Tamura K (2008) MEGA: a biologist-centric software for evolutionary analysis of DNA and protein sequences. Briefings in bioinformatics 9(4): 299–306. https://doi.org/10.1093/bib/bbn017

Kurtz S, Choudhuri JV, Ohlebusch E, Schleiermacher C, Stoye J, Giegerich R (2001) REPuter: the manifold applications of repeat analysis on a genomic scale. Nucleic Acids Research 29: 4633–4642. https://doi.org/10.1093/nar/29.22.4633

Larkin MA, Blackshields G, Brown NP, Chenna R, McGettigan PA, McWilliam H, Valentin F, Wallace IM, Wilm A, Lopez R (2007) Clustal W and Clustal X version 2.0. Bioinformatics 23: 2947–2948. https://doi.org/10.1093/bioinformatics/btm404

Lavrov DV, Brown WM, Boore JL (2000) A novel type of RNA editing occurs in the mitochondrial tRNAs of the centipede *Lithobius forficatus*. Proceedings of the National Academy of Sciences of the United States of America 97: 13738–13742. https://doi.org/10.1073/pnas.250402997

Lemey P, Rambaut A, Welch JJ, Suchard MA (2010) Phylogeography Takes a Relaxed Random Walk in Continuous Space and Time. Molecular Biology Evolution 27: 1877–1885. https://doi.org/10.1093/molbev/msq067

Li J, Lin RR, Zhang YY, Hu KJ, Zhao YQ, Li Y, Huang ZR, Zhang X, Geng XX, Ding JH (2018a) Characterization of the complete mitochondrial DNA of *Theretra japonica* and its phylogenetic position within the Sphingidae (Lepidoptera, Sphingidae). ZooKeys 754: 127–139. https://doi.org/10.3897/zookeys.754.23404

Li J, Zhang Y, Hu K, Zhao Y, Lin R, Li Y, Huang Z, Zhang X, Geng X, Ding J (2018b) Mitochondrial genome characteristics of two Sphingidae insects (*Psilogramma increta* and *Macroglossum stellatarum*) and implications for their phylogeny. International Journal of Biological Macromolecules 113: 592–600. https://doi.org/10.1016/j.ijbiomac.2018.02.159

Lewis JG, Edgecombe GD, Shelley RM (2005) A proposed standardised terminology for the external taxonomic characters of the Scolopendromorpha (Chilopoda). Fragmenta faunistica 48(1): 1–8. https://doi.org/10.3161/00159301FF2005.48.1.001

Posada D (2008) jModelTest: Phylogenetic Model Averaging. Molecular Biology Evolution 25: 1253–1256. https://doi.org/10.1093/molbev/msn083

Regier JC, Shultz JW, Ganley AR, Hussey A, Shi D, Ball B, Cunningham CW (2008) Resolving arthropod phylogeny: exploring phylogenetic signal within 41 kb of protein-coding nuclear gene sequence. Systematic biology 57(6): 920–938. https://doi.org/10.1080/10635150802570791

Robertson HE, Lapraz F, Rhodes AC, Telford MJ (2015) The complete mitochondrial genome of the geophilomorph centipede *Strigamia maritima*. Plos One 10: e0121369. https://doi.org/10.1371/journal.pone.0121369

Shaoli M, Hao Y, Chao L, Yafu Z, Fuming S, Yuchao W (2018) The complete mitochondrial genome of *Xizicus* (*Haploxizicus*) *maculatus* revealed by Next-Generation Sequencing and phylogenetic implication (Orthoptera, Meconematinae). ZooKeys 773: 57–67. https://doi.org/10.3897/zookeys.773.24156

Shear WA, Bonamo PM (1988) Devonobiomorpha, a new order of centipeds (Chilopoda) from the Middle Devonian of Gilboa, New York State, USA, and the phylogeny of centiped orders. American Museum Novitates 2927: 1–30.

Stamatakis A, Hoover P, Rougemont J (2017) A Rapid Bootstrap Algorithm for the RAxML Web Servers. Systematic Biology 57: 758. https://doi.org/10.1080/10635150802429642

Sun L, Yingju QI, Tian X (2018) Analysis of mitochondrial genome of *Scolopendra subspinipes dehaani*. Tianjin Journal of Traditional Chinese Medicine 35(03): 225–229.

Taanman JW (1999) The mitochondrial genome: structure, transcription, translation and replication. Biochimica Et Biophysica Acta 1410: 103. https://doi.org/10.1016/S0005-2728(98)00161-3

Thiel T, Michalek W, Varshney R, Graner A (2003) Exploiting EST databases for the development and characterization of gene-derived SSR-markers in barley (*Hordeum vulgare* L.). Theoretical Applied Genetics 106: 411–422. https://doi.org/10.1007/s00122-002-1031-0

Tomoko O (1995) Synonymous and nonsynonymous substitutions in mammalian genes and the nearly neutral theory. Journal of Molecular Evolution 40: 56–63. https://doi.org/10.1007/BF00166595

Undheim EA, Jenner RA, King GF (2016) Centipede venoms as a source of drug leads. Expert Opinion on Drug Discovery 11: 1139–1149. https://doi.org/10.1080/17460441.2016.1235155

Wang JJ, Yang MF, Dai RH, Li H, Wang XY (2018a) Characterization and phylogenetic implications of the complete mitochondrial genome of Idiocerinae (Hemiptera: Cicadellidae). International Journal of Biological Macromolecules 120: 2366–2372. https://doi.org/10.1016/j.ijbiomac.2018.08.191

Wang Y, Cao J, Murányi D, Li W (2018b) Comparison of two complete mitochondrial genomes from Perlodidae (Plecoptera: Perloidea) and the family-level phylogenetic implications of Perloidea. Gene 675: 254–264. https://doi.org/10.1016/j.gene.2018.06.093

Wolstenholme DR (1992) Animal mitochondrial DNA: structure and evolution. International review of cytology 141: 173–216. https://doi.org/10.1016/S0074-7696(08)62066-5

Wu M, Li Q, Hu Z, Li X, Chen S (2017) The Complete Amomum kravanh Chloroplast Genome Sequence and Phylogenetic Analysis of the Commelinids. Molecules 22(11): 1875. https://doi.org/10.3390/molecules22111875

Yang Z, Nielsen R (2000) Estimating synonymous and nonsynonymous substitution rates under realistic evolutionary models. Molecular biology and evolution 17: 32–43. https://doi.org/10.1093/oxfordjournals.molbev.a026236

Yang Z (2007) Paml 4: Phylogenetic analysis by maximum likelihood. Molecular biology and evolution 24, 1586–1591. https://doi.org/10.1093/molbev/msm088

Yoo WG, Lee JH, Shin Y, Shim JY, Jung M, Kang BC, Song KD (2014) Antimicrobial peptides in the centipede *Scolopendra subspinipes mutilans*. Functional & Integrative Genomics 14: 275–283. https://doi.org/10.1007/s10142-014-0366-3

Zhang D, Li WX, Zou H, Wu SG, Li M, Jakovlic I, Zhang J, Chen R, Wang GT (2018) Mitochondrial genomes of two diplectanids (Platyhelminthes: Monogenea) expose paraphyly of the order Dactylogyridea and extensive tRNA gene rearrangements. Parasites Vectors 11: 601. https://doi.org/10.1186/s13071-018-3144-6

Zhang J, Ma W, Song X, Lin Q, Gui J, Mei J (2014) Characterization and development of est-ssr markers derived from transcriptome of yellow catfish. Molecules 19(10): 16402–16415. https://doi.org/10.3390/molecules191016402

Supplementary material 1

Table S1

Authors: Chaoyi Hu, Shuaibin Wang, Bisheng Huang, Hegang Liu, Lei Xu, Zhigang Hu, Yifei Liu

Explanation note: The ω value of 13 PCGs.

Link: https://doi.org/10.3897/zookeys.925.47820.suppl1

ZooKeys 925: 89–140 (2020)
doi: 10.3897/zookeys.925.48457
http://zookeys.pensoft.net

RESEARCH ARTICLE

A peer-reviewed open-access journal
ZooKeys
Launched to accelerate biodiversity research

The genus *Vipio* Latreille (Hymenoptera, Braconidae) in the Neotropical Region

Donald L. J. Quicke[1], Scott R. Shaw[2], Mian Inayatullah[3], Buntika A. Butcher[1]

1 *Integrative Ecology Laboratory, Department of Biology, Faculty of Science, Chulalongkorn University, Phayathai Road, Pathumwan, BKK 10330, Thailand* **2** *Department of Ecosystem Science and Management, University of Wyoming, Laramie, Wyoming 82071-3354, USA* **3** *Department of Entomology, Faculty of Crop Protection Sciences, NWFP Agricultural University, Peshawer, Pakistan*

Corresponding author: Buntika A. Butcher (buntika.a@chula.ac.th)

Academic editor: C. van Achterberg | Received 15 November 2019 | Accepted 12 February 2020 | Published 8 April 2020

http://zoobank.org/A9721DD6-C551-4002-9539-AD7EB03734E0

Citation: Quicke DLJ, Shaw SR, Inayatullah M, Butcher BA (2020) The genus *Vipio* Latreille (Hymenoptera, Braconidae) in the Neotropical Region. ZooKeys 925: 89–140. https://doi.org/10.3897/zookeys.925.48457

Abstract

The genus *Vipio* Latreille is revised for the Neotropical region (south of Nicaragua). All species are fully illustrated. Thirteen species are recognised of which five (*V. boliviensis*, *V. carinatus*, *V. godoyi*, *V. hansoni*, and *V. lavignei*) are described as new, all with descriptions attributable to Inayatullah, Shaw & Quicke. All previously described Neotropical species are redescribed. A key is included for the identification of the *Vipio* species known from the Americas south of Nicaragua, and all species are illustrated.

Keywords

Isomecus, new species, re-description, South America, systematics

Introduction

The braconid genus *Vipio* Latreille is most diverse in the Holarctic Region but has a significant representation in the Neotropical Region. However, little is known of these tropical species, only a very few of which are described (Brullé 1846, Ashmead 1900, Szépligeti 1906, Bréthes 1909, 1913), nor are there any host records for the species from this part of the world. Because of a recent upsurge in Hymenoptera studies in South America, the publication of keys to the genera of New World Braconidae

(Wharton et al., 1997), and a growing number of biodiversity studies, there is a need to provide identification keys to the Neotropical fauna. Here we present a revision of the nine *Vipio* species now known to occur in South America and southern Central America (south of Nicaragua), which includes descriptions of four new species, and redescriptions of the five previously described ones whose original descriptions do not mention many important characters. An illustrated key to the species is also provided. The Nearctic species were revised (Inayatullah et al., 1997) and since then only one additional New World species, *V. porteri* Inayatullah et al., 2015, has been described. Species from northern Central America, Mexico, and the Caribbean are diverse and comprise a complex assemblage that will be treated in a subsequent paper.

Materials and methods

Terminology and collections

Terminology follows van Achterberg (1979, 1988) except for the relative heights of eye (EH) and malar space (MS) follow Inayatullah (1992) and Inayatullah et al. (2012), and wing venation nomenclature which follows Sharkey & Wharton (1997); see also fig. 2.2 in Quicke (2015) for comparison of wing venation naming systems. Sculpture terminology follows Harris (1979). The following abbreviations are used to save space:

EH eye height;
FH face height measured between anterior margin of antennal socket and anterior tentorial pit;
FW face width;
HH head height as least distance between base of mandible and lateral ocellus (inclusive), in lateral view;
HW head width;
HL head length:
ITD inter-tentorial distance;
LMC labiomaxillary complex;
LRC length of radial cell measured between apex of pterostigma and 3RSb;
MS malar space;
PL pterostigma length;
PW maximum width of pterostigma;
T tergite;
TOD tentorio-ocular distance**.**

Collections from where specimens were borrowed are abbreviated as follows:

BMNH Natural History Museum, London, U.K.;
CNCI Canadian National Collection of Insects, Ottawa;
EMUS Entomology Museum, Utah State University, Logan (formerly American Entomological Institute, Gainesville);
ESUW Entomology Section, University of Wyoming, Laramie, WY;
HNHM Hungarian Natural History Museum, Budapest;
IFML Tucuman, Instituto Fundación Miguel Lillo, Argentina;
MACN Museo Argentino de Ciencias Naturales, Buenos Aires;

MCZC Museum of Comparative Zoology, Harvard University, Cambridge, Massachussetts;
MNHN Museum national d'Histoire naturelle, Paris;
USNM United States National Museum, Washington D.C..

Images were captured with a 3 MP Leica video camera on a Leica M205C stereomicroscope running Leica Application Suite (LAS) software (Leica Microsystems GmbH, Wetzlar, Hesse, Germany), and focus-stacked using the same software. Some minor adjustments in images and plate preparation were performed in Adobe Photoshop version CS6 (Adobe Systems Inc., San Jose, California, United States of America).

Taxonomy

Vipio Latrielle, 1804

Vipio Latreille, 1804. Nouv. Dict. Hist. Nat. 24: 173. Type-species: *Ichneumon desertor* Fabricius. Desig. by Foerster, 1862.
Isomecus Kriechbaumer, Prog. Staats-Gym. Pola, 1895: 12. Type-species: *Isomecus schlettereri* Kriechbaumer, 1895. Synon. by Quicke & Sharkey (1989).
Zavipio Viereck, 1914. U. S. Natl. Mus. Bull. 83: 156. Type-species: *Vipio marshalli* Schmiedeknecht (Orig. desig.); unnecessary replacement name for *Vipio*.

Remarks. Members of the genus *Vipio* can be recognised using the keys to genera of Quicke (1987, 1997) or Quicke & Sharkey (1989).

Key to females of Neotropical species of *Vipio*

1 Claw with small, rounded basal lobe, at most with very small angulation, but never protruding (a) **2**

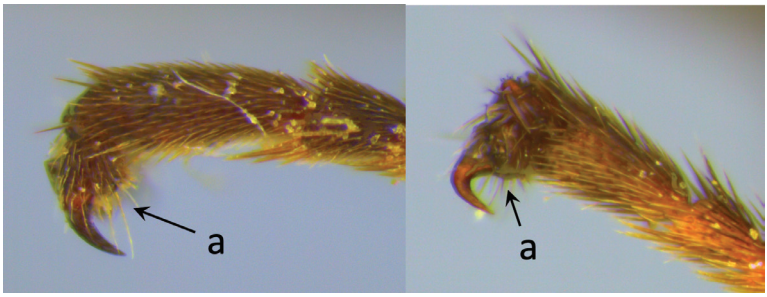

– Claw with large, acutely pointed or square basal lobe (b) **5**

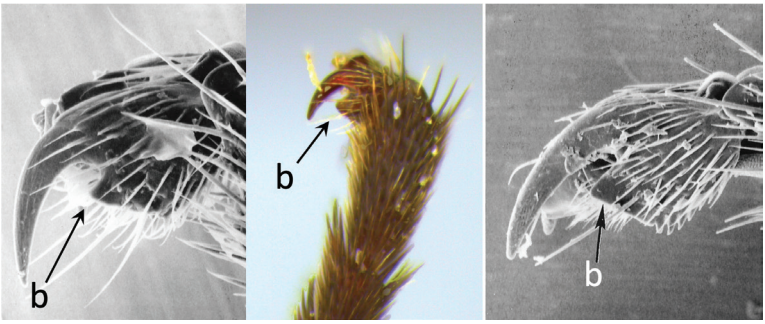

2 Ovipositor long, exserted part, always more than 0.9 × length of fore wing (a) **3**

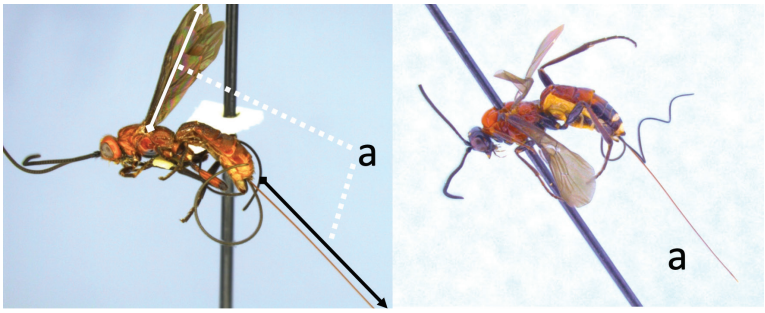

– Ovipositor shorter, exserted part less than 0.7 × length of fore wing, usually less than 0.5 × (aa) **4**

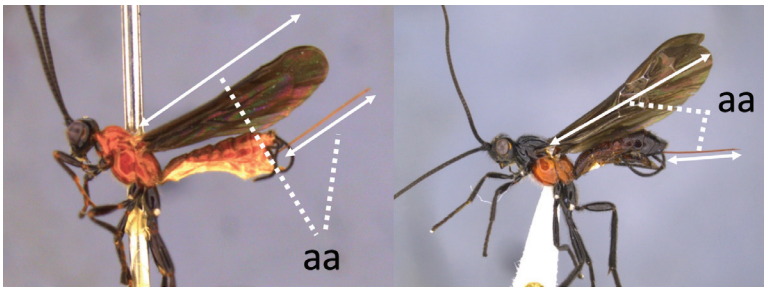

3 Head largely black (a); base of metasomal T II with 3 smooth triangular areas margined posteriorly by sharp carinate borders (b); hypopygium short, not or hardly extending beyond apex of metasomal tergites (c) .... ***V. boliviensis* sp. nov.**

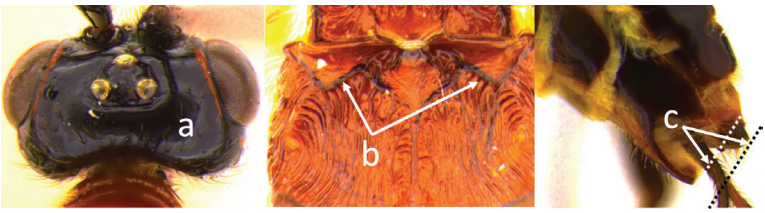

– Head orange-red (aa); base of metasomal T II and III without such distinct triangular areas, posterior borders not so evenly or completely carinate, and inside areas of triangles more roughly sculptured, not completely smooth (bb); hypopygium extending beyond apex of metasoma by 0.3–0.7 mm (cc)..... ..... ***V. belfragei*** **(Cresson)**

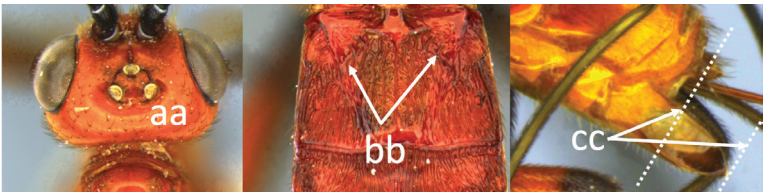

4 Face largely smooth with weak corrugation (a); second metasomal suture occupying approximately one third length of T III (b); pronotum, mesoscutum and metasomal tergites orange-red (c)..... ***V. hansoni*** **sp. nov.**

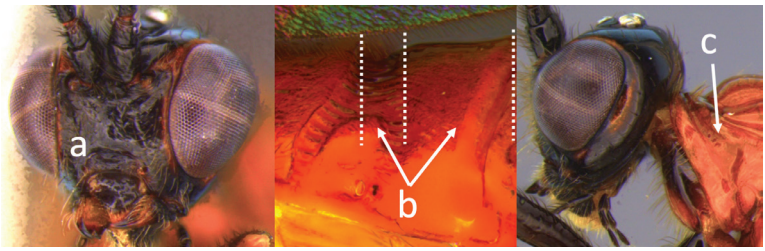

– Face strongly sculptured, rugose punctate (aa); 2nd metasomal suture very wide occupying approximately half length of T III (bb); pronotum, mesoscutum and posterior metasomal tergites piceous or black (cc)..... ..... ***V. lavignei*** **sp. nov.**

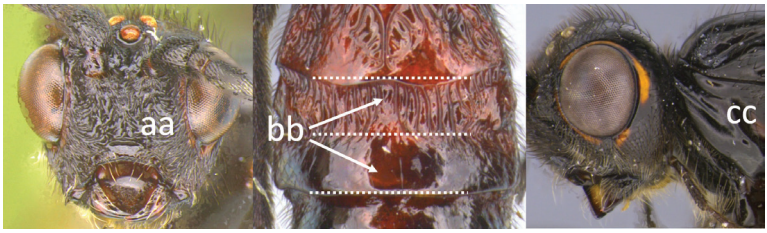

5 Ovipositor shorter than fore wing (a) **6**

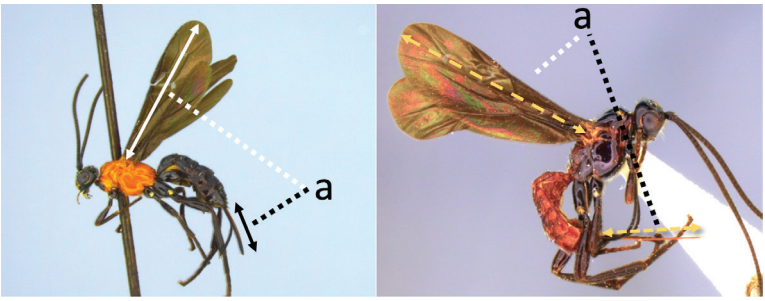

– Ovipositor at least 1.3 × fore wing length (aa) **10**

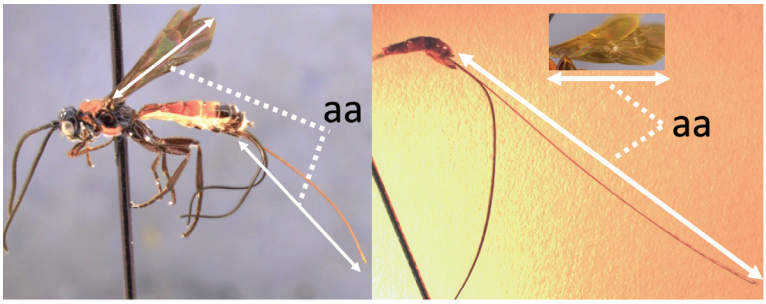

6 Metasoma entirely black (a) ..... ***V. quadrirugulosus*** **(Enderlein)**

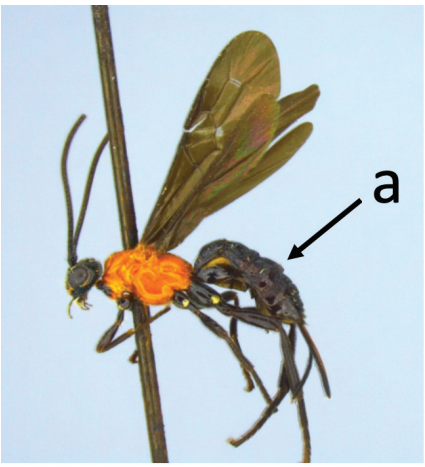

– Metasoma largely red (aa) **7**

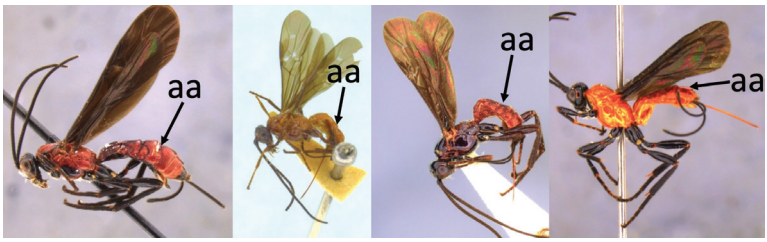

7 Propodeum with a single, mid-longitudinal anteriorly blunt carina and only a short pair of submedial carinae posteriorly (a) ..... ***V. carinatus* sp. nov.**

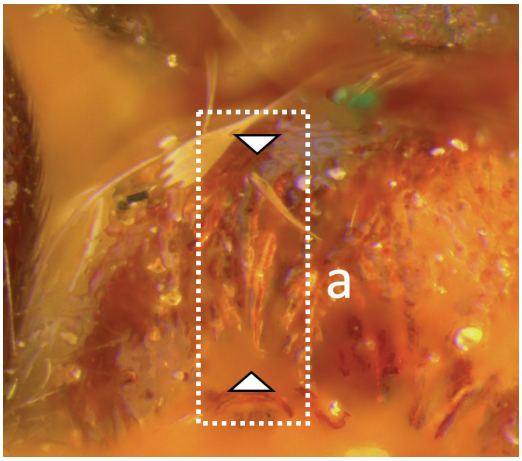

– Propodeum smooth (aa) or with numerous anteriorly diverging carinae on posterior half (aaa) **8**

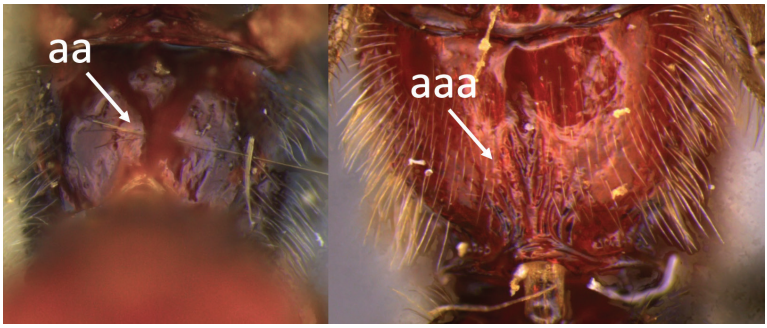

8 Propodeal spiracle large, > 0.5 (0.56) diameter of median ocellus (a); spiracle of metasomal T III large, > 0.5 (0.57) diameter of median ocellus; dorsolateral carinae of metasomal T I strongly lamelliform (b) ..... ***V. godoyi* sp. nov.**

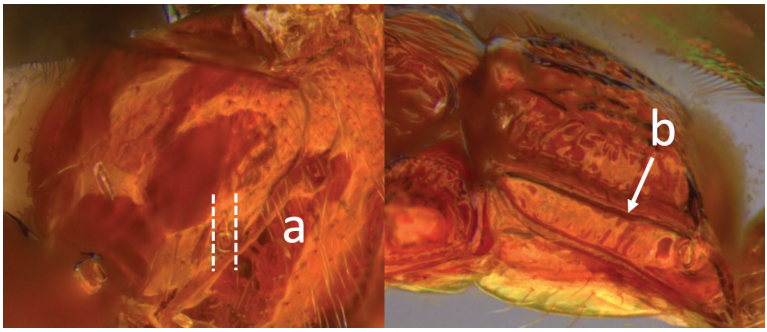

– Propodeal and metasomal spiracles smaller (aa); dorsolateral carinae of metasomal T I relatively less developed (bb) **9**

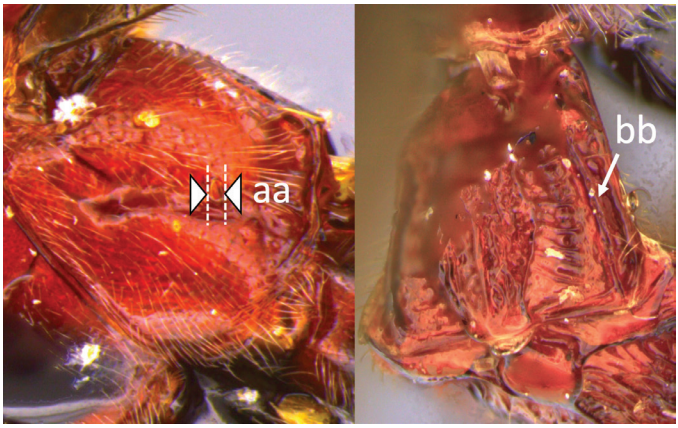

9 Propodeum with prominent striations posteriorly (a); mesonotum largely reddish (b) ..... ***V. strigator* (Bréthes)**

– Propodeum smooth (aa); mesoscutum and most of mesosoma reddish black (bb) ..... ***V. thoracica* (Ashmead)**

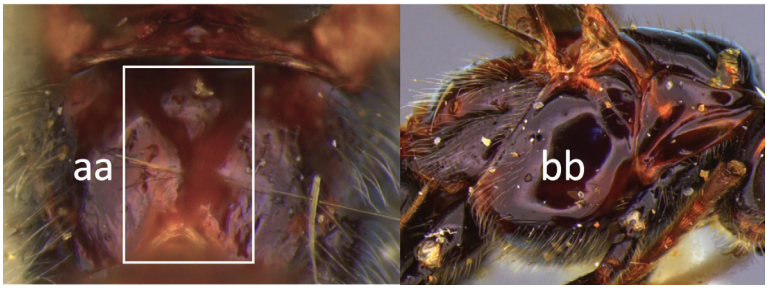

10 Propodeum with a short median longitudinal wide carina anteriorly (a); ovipositor 1.1–1.4 × body length (b) ..... ***V. paraguayensis* Szépligeti**

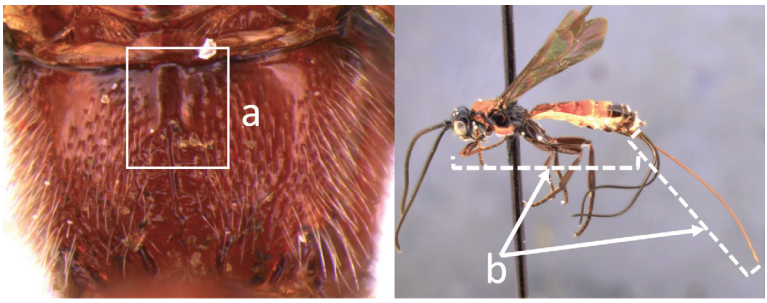

– Propodeum without median longitudinal carina anteriorly, with reticulate to areolate rugose sculpture posteriorly (aa, aaa); ovipositor > 1.55 × body length (bb) **11**

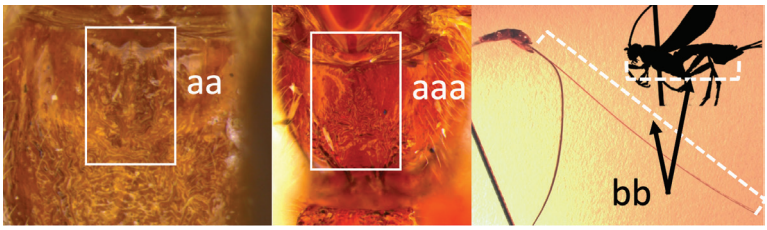

11 Head yellow or reddish yellow (a) ..... ***V. fiebrigi* Bréthes**

– Head black or with extensive black markings dorsally (aa, aaa, aaaa) **12**

12 Ovipositor less than 1.9 × body length (range 1.5–1.85); MS less than 0.35 (> 0.31) × maximum eye height in lateral view (a) .... ***V. porteri*** **Inayatullah et al.**

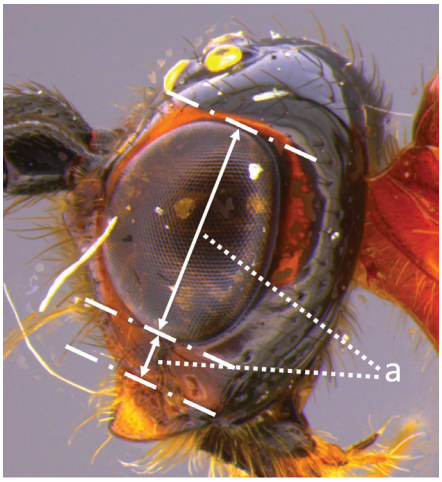

– Ovipositor more than 1.9 × body length (range 1.94–2.34); MS more than 0.35 (0.4) × maximum eye height in lateral view (aa)..... ..... ***V. melanocephalus*** **Brullé**

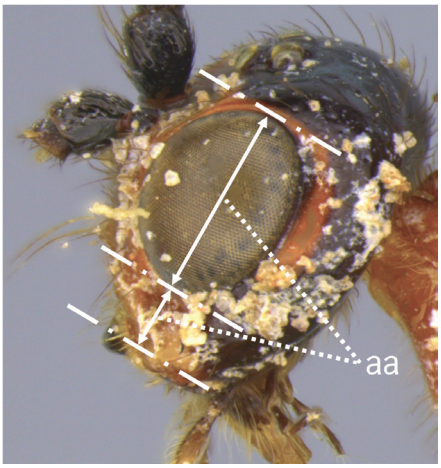

***Vipio belfragei* (Cresson, 1872)**
Figures 1, 2

Bracon belfragei Cresson, 1872: 186; *Vipio belfragei*: Pierce, 1908: 44; Shelefelt, 1978: 1843; Inayatullah et al., 1998: 125–127, figs 3, 25; López-Martínez et al. 2009: 215; *Zavipio belfragei*: Sattertwait, 1932: 1003.

Type material. Holotype ♀, **USA**, Texas, (no date), W. Belfrage (USNM type No. 1610) (examined).

Comments. Additional material examined is summarised in Inayatullah et al. (1998) who re-described it. It is fully illustrated here for the first time. This is a common, widespread, and rather variable (Inayatullah et al. 1998) species in the USA and Mexico with a range extending as far south as Costa Rica and Panama.

***Vipio boliviensis* sp. nov.**
http://zoobank.org/30868A9A-2247-4249-B01A-78FC9612222D
Figures 3, 4

Type material. Holotype ♀, **Bolivia**: Comarapa, 18 m., 14.xii.1984 (L. Pena) (EMUS). Paratype: **Argentina:** 1 ♀, Pronunciamiento Entre Rios, xii.1965 (CNCI); 1 ♀, E. Rios, xii.1972, Feliciano Fritz col. (EMUS).

Diagnosis. Can be distinguished from other Neotropical *Vipio* species by the combination of a hypopygium ending at apex of metasoma and a long ovipositor (ovipositor length/body length 1.17). Additionally, it has claws without basal lobe, ovipositor longer than fore wing.

Description. Female. Length of body 5.4 mm; of fore wing 5.6 mm; of ovipositor (part exserted beyond apex of abdomen) 6.4 mm.

Head. Antenna robust, with 37–41 flagellomeres; terminal flagellomere blunt and distinctly laterally compressed; median flagellomeres as long as wide, more distal flagellomeres becoming thicker; first flagellomere 1.5 × longer than second, 3.3 × longer than wide; second flagellomere 2.2 × longer than wide; head transverse; HL 0.78 × HH; clypeus rugulose; clypeal guard setae typical; face slightly punctate; remainder of head smooth and shiny; HW/HH 0.96; FH/FW 0.5; EH/HH 0.73; EH/FW 1.0; ITD 2.25 × TOD; MS 0.25 × EH; LMC slightly less than 0.5 × HH; third segment of maxillary palpus 5 × longer than wide.

Mesosoma. Length of mesosoma 1.43 × height. Pronotum carinate antero-laterally. Notauli smooth. Propodeum rugulose medially, with a blunt and short median longitudinal carina not reaching posterior end, and with a pair of short, longitudinal, anteriorly diverging submedial carinae not reaching middle of propodeum; remainder of mesosoma laterally smooth and shiny.

Wings. Fore wing: length of fore wing 1.03 × body length; PL/LRC 0.75; PW/PL 0.19; length of vein 1M 0.71 × length of (RS+M)a; length of vein 3RSb 0.82 × combined length of r-rs and 3RSa; vein 3RSa reaching wing margin 0.55 × distance

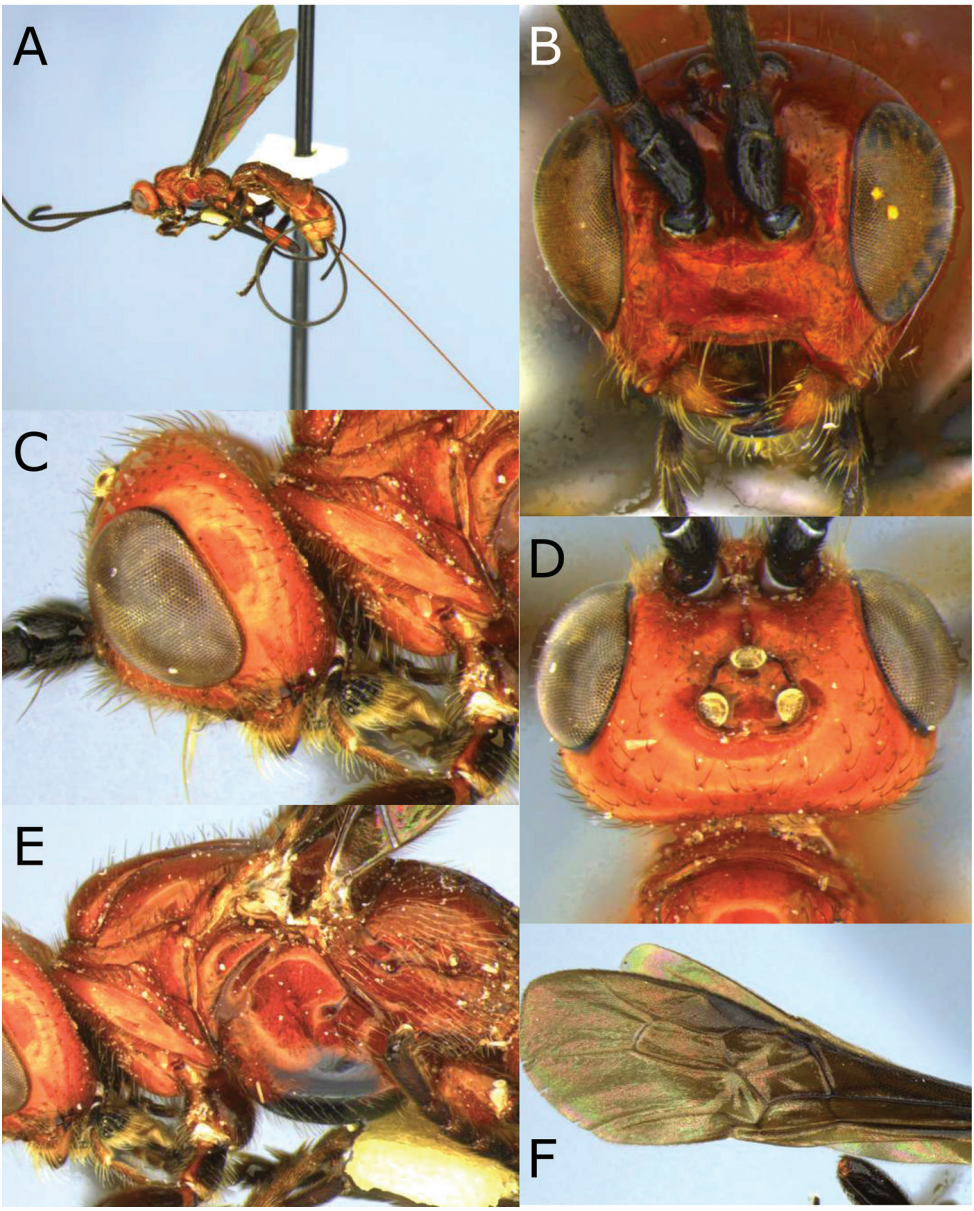

Figure 1. Montaged light micrographs of *Vipio belfragei* female. **A** Habitus, lateral view **B** face **C** head and anterior mesosoma, lateral view **D** head, dorsal view **E** mesosoma, lateral view **F** wings **G** claw.

between apex of pterostigma and wing tip. Hind wing: with a glabrous area distal to cu-a; apex of C+SC+R with one basal hamule

Legs. Claw without pointed basal lobe.

Metasoma. First metasomal tergite 1.20 × longer than wide, raised median area of T I oval, rugose, with a median longitudinal carina posteriorly, surrounding area with

Figure 2. Montaged light micrographs of *Vipio belfragei* female. **A** Mesosoma, dorsal view **B** propodeum **C** metasomal tergite I, near dorsal view **D** metasomal tergites II–IV, dorsal view.

short, transverse carinae, dorso-lateral carina present; T II 1.5 × wider than long medially, longitudinally striate, basal areas rugulose, oblique furrow strongly impressed; T III 1.45 × wider than long medially, anteriorly with longitudinal striations running

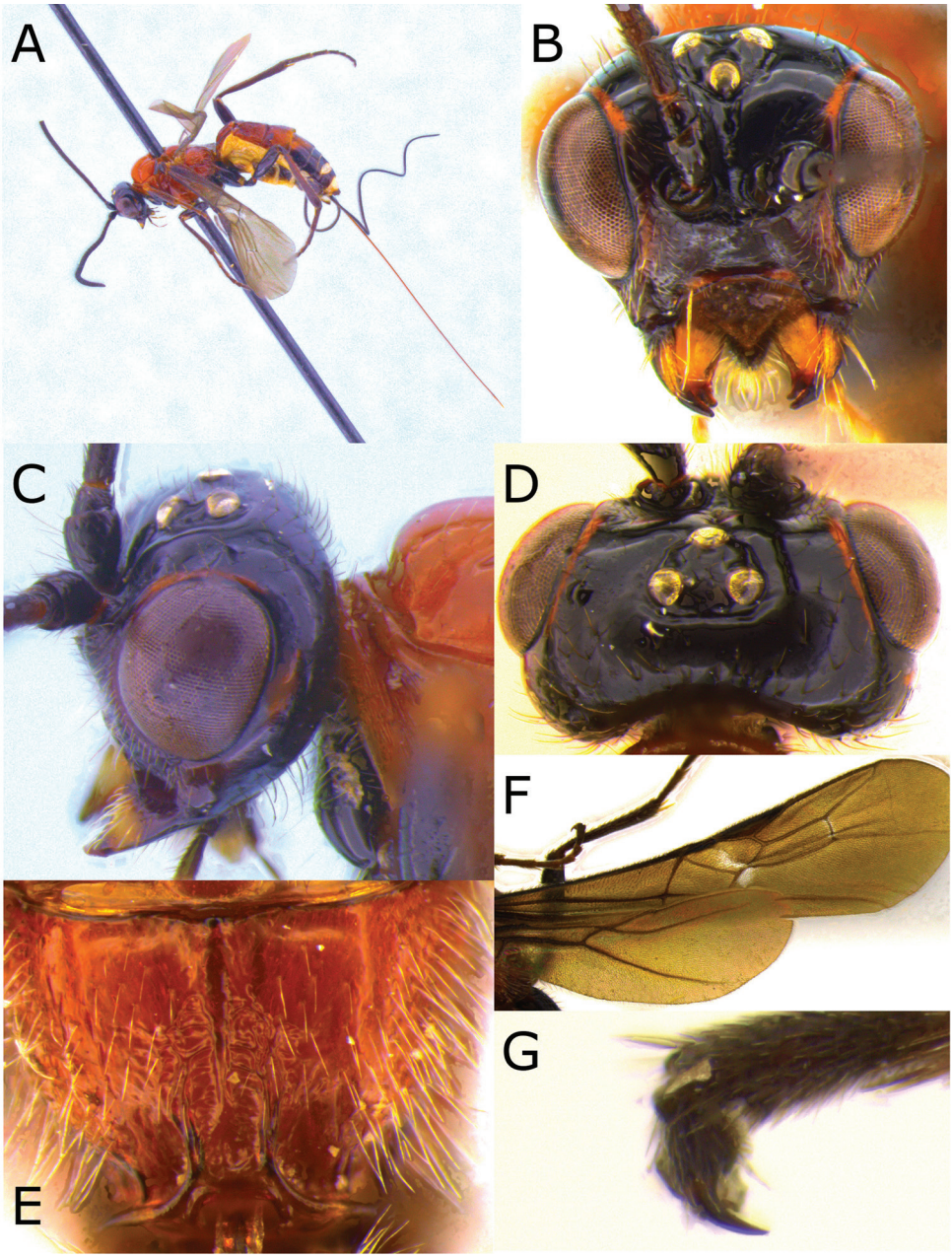

Figure 3. Montaged light micrographs of *Vipio boliviensis* sp. nov. **A** Holotype, habitus lateral view **B** head, front view **C** head, oblique view **D** head, dorsal view **E** propodeum **F** wings **G** claw.

postero-laterally, and with transverse striations posteriorly; T IV entirely with transverse striation but not reaching lateral margin which is smooth and shiny; T V–VII smooth and shiny; hypopygium short, ending at apex of metasoma; ovipositor sheath with sparse setae; ovipositor 1.17 × body length.

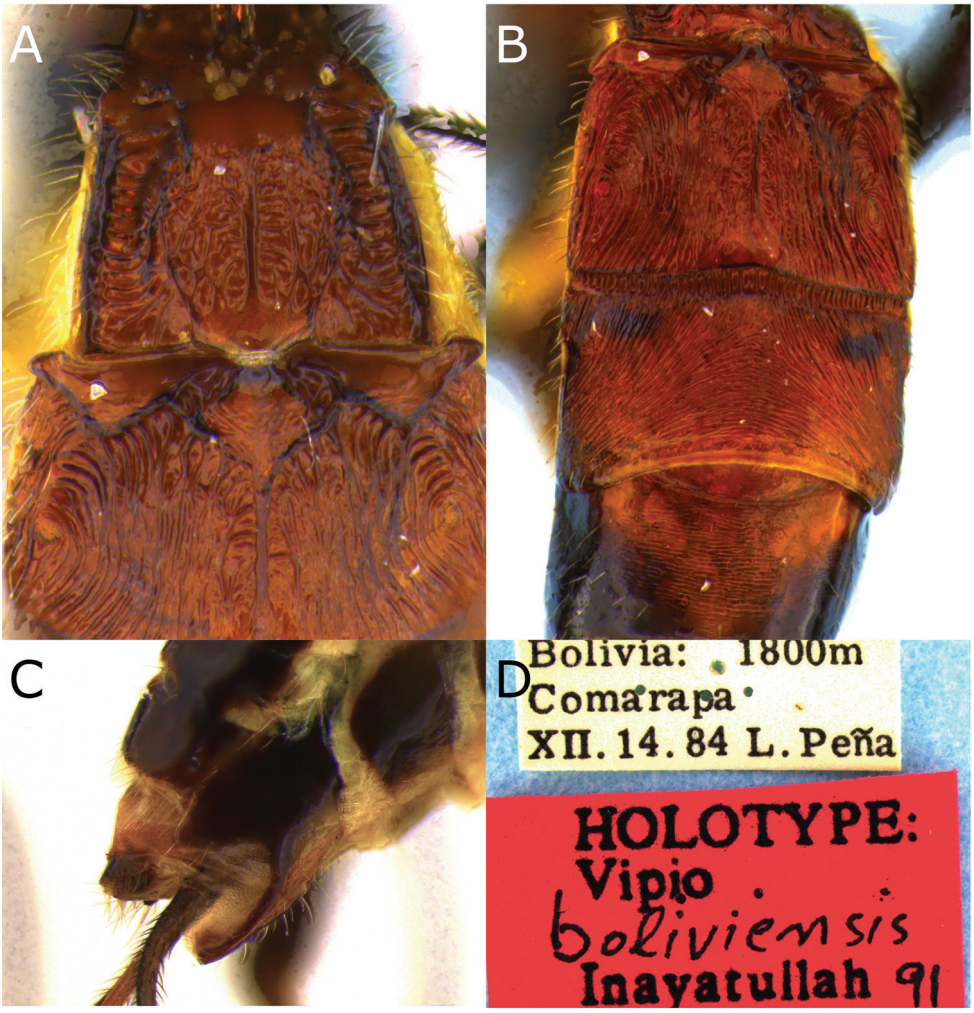

Figure 4. Montaged light micrographs of *Vipio boliviensis* sp. nov. **A** Metasomal tergites I and II **B** metasomal tergites II–IV **C** apex of metasoma, lateroventral view **D** holotype specimen labels.

Colour. Yellowish red except head, antenna, palpi, prosternum, T IV posteriorly, and T V–VII, metasomal laterotergites and ovipositor sheath black. Wings smoky.

Male. Unknown.

Remarks. This species appears to be closely related to *V. paraguayensis* Szépligeti, because of the presence of a median longitudinal carina on propodeum and similar sculpture of T1 and T2. *Vipio boliviensis* can be distinguished by the carinate pronotum (smooth and shiny in *paraguayensis*), absence of pointed basal lobe on the claw (present in *paraguayensis*), transverse striations on T III and T IV (longitudinal in *paraguayensis*), and short hypopygium (long in *paraguayensis*).

Etymology. Named after the country of Bolivia, where the holotype was collected. We have retained this name despite the recent discovery of a specimen from Argentina because of its use in Inayatullah's MS thesis (1992).

***Vipio carinatus* sp. nov.**
http://zoobank.org/B63E1D1A-8159-4C1D-9DBC-D8B0EE61D5B4
Figures 5, 6

Type material. Holotype ♀, **Bolivia:** Sara (no date), (Steinbach) (MCZC). Paratypes: **Bolivia:** Santa Cruz, 1 ♀, 28.i–ii.1964 (Z. Golbach) (IFML); 1 ♂, (no date) (J. Steinbach) (MCZC). **Argentina:** 1 ♂, Chaco, Colonia, Benítez, 10.xii.1948 (R. Golbach) (IFML).

Diagnosis. Ovipositor shorter than fore wing, propodeum with an anteriorly blunt but complete mid-longitudinal carina, claw with pointed basal lobe, ovipositor approximately half length of fore wing, body except head, predominantly yellow.

Description. Holotype ♀ length of body 4.6–5.0 mm, of fore wing 4.6–5.0 mm and of ovipositor (part exserted beyond apex of abdomen) 2.5 mm.

Head. Antenna robust, 1.1 × body length, with 42 flagellomeres; first flagellomere 1.4 × longer than second, 1.1 × longer than wide; second flagellomere 1.2 × longer than wide; flagellomeres beyond the fifth 1.1–1.2 × longer than wide; median flagellomeres slightly shorter than wide; terminal flagellomere sharply pointed apically; head transverse; HL 0.79 × HH; clypeal guard setae consist of one long and one short seta near each anterior tentorial pit; clypeus rugulose; face rugulose, with a median and slightly raised triangular area above the clypeus; remainder of head smooth and shiny; HW/HH 0.77; FH/FW 0.55; EH/HH 0.65; EH/FW 0.92; EW/EH = 0.75; ITD 1.85 × TOD; MS 0.37–0.42 × EH (Fig. 5B); LMC 0.5 × HH; third segment of maxillary palpus 6 × longer than wide.

Mesosoma. Length of mesosoma 1.71 × height; pronotal furrow crenulate dorsally and dorso-laterally; notauli smooth; propodeum slightly rugulose with an anteriorly blunt median longitudinal carina and one short longitudinal carina lateral to the median longitudinal carina posteriorly.

Wings. Fore wing : length of fore wing 1.0 × body length; PL/LRC 0.89; PW/PL 0.28; length of vein 1M 0.67 × length of (RS+M)a; length of vein 3RSb 1.0 × combined length of r-rs and 3RSa; vein 3RSa reaching anterior wing margin 0.61 × distance between apex of pterostigma and wing tip. Hind wing: uniformly setose; apex of C+SC+R with 1 basal hamule.

Legs. Claw with pointed basal lobe.

Metasoma. First metasomal tergite 1.2 × longer than wide, raised median area oval, slightly rugulose, with a blunt and irregular dorso-lateral carinae which are more pronounced anteriorly, surrounding area with short transverse carinae, dorso-lateral carina present; T II-IV longitudinally striate (Fig. 6C); T II 1.8 × wider than medially long, basal areas smooth and shiny, oblique furrow impressed; T III 1.7 × wider than medially long; T V–VII smooth and shiny; hypopygium ending at same level as tergites; ovipositor 0.47–0.5 × body length.

Colour. Predominantly yellow to orange-yellow, head and antenna black, except maxillary palp, face laterally, and basal half of mandible blackish red, legs blackish red except fore tibia and tarsi yellow (Fig. 5A). Wings brown with dark brown venation, pterostigma entirely dark brown (Fig. 6A).

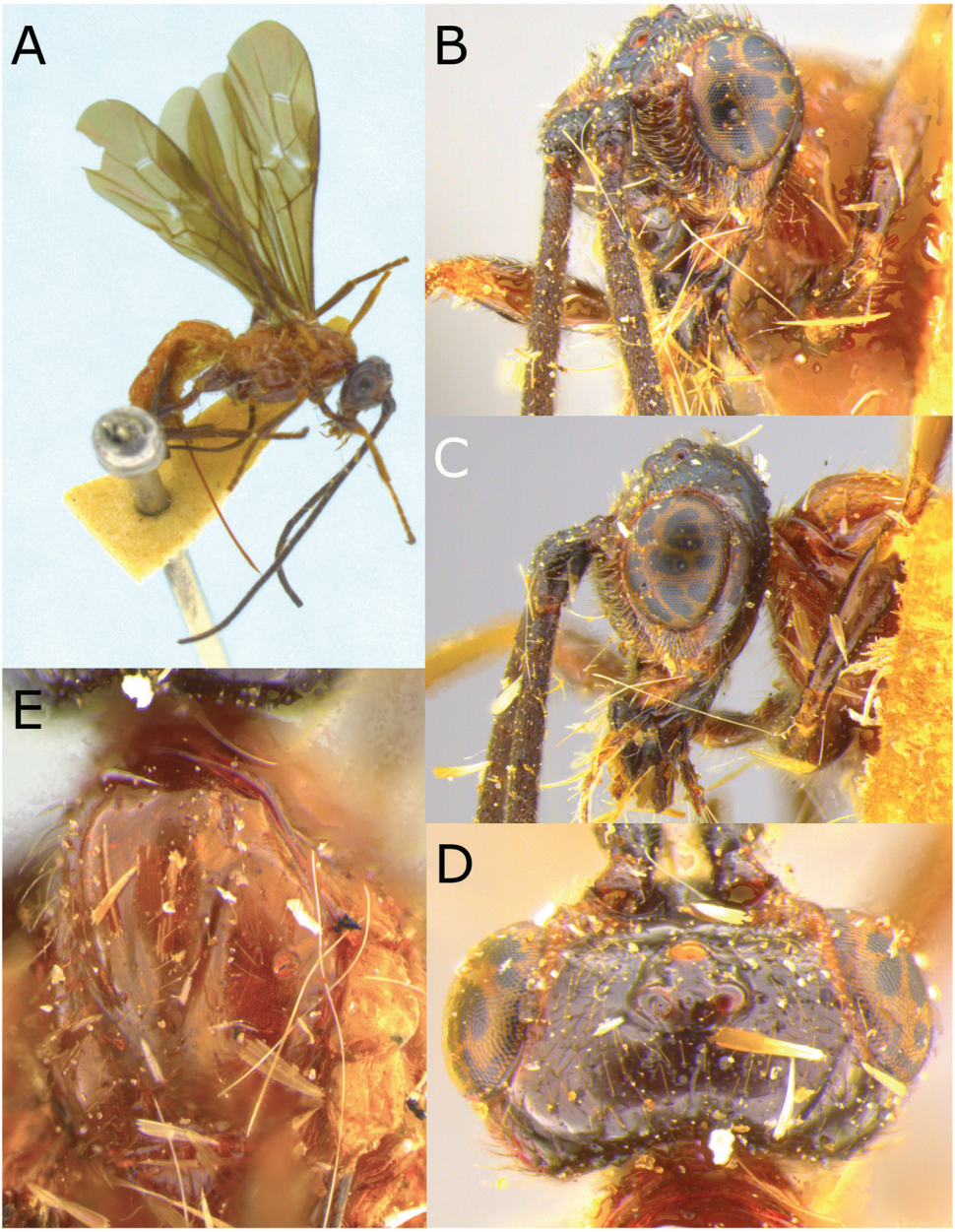

Figure 5. Montaged light micrographs of *Vipio carinatis*. **A** Holotype, habitus lateral view **B** face, oblique view **C** head, lateral view **D** head, dorsal view **E** mesoscutum, oblique dorsal view.

Variation. Female paratype as in holotype, except EH/HH 0.68; FH/FW 0.61; EH/FW 1.0; ITD 1.6 × TOD; mesosoma red. Male paratypes (Fig. 6D) as in female, except length of body 6.2–6.5 mm; length of fore wing/body length 0.74–0.82; HL 0.8–0.82 × HH; EH/HH 0.69–0.71; EW/EH 0.70–0.73; EH/FW 1.0–1.04; ITD

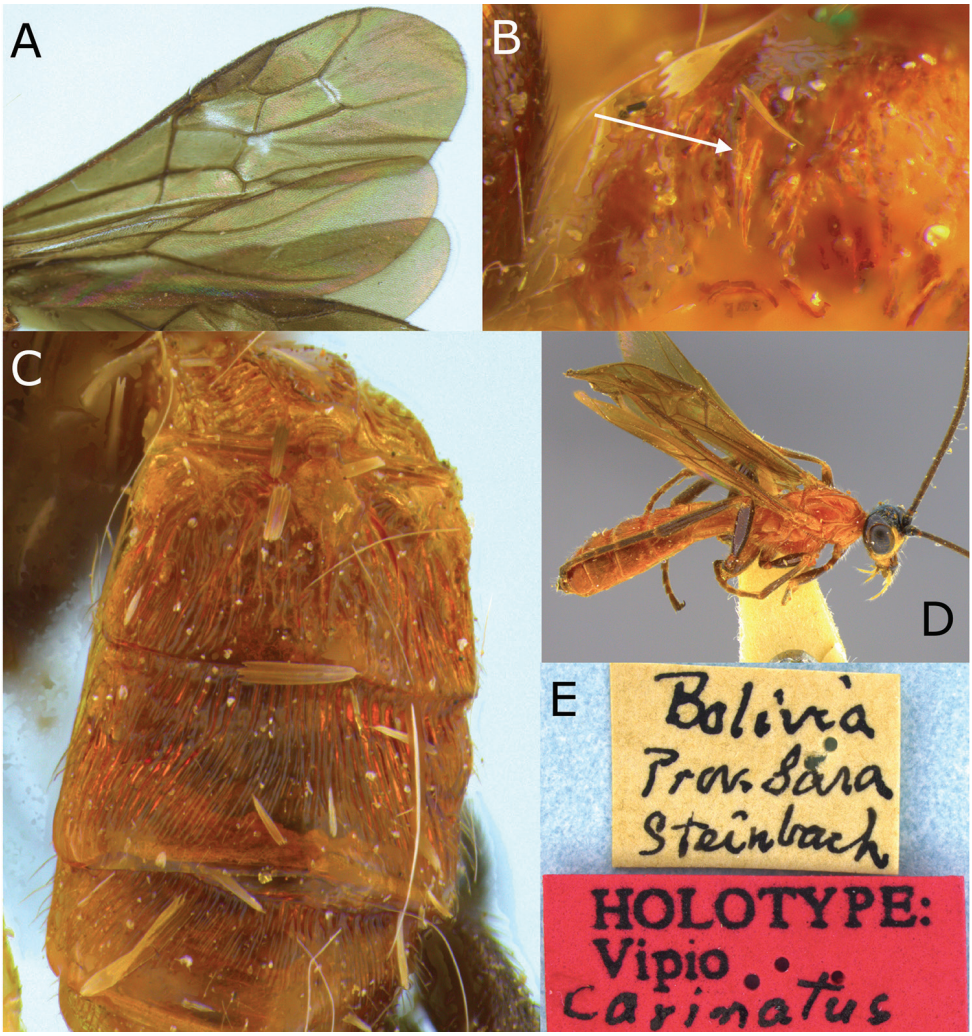

Figure 6. Montaged light micrographs of *Vipio carinatus*. **A** Wings **B** propodeum **C** metasomal tergites I–III, oblique dorsal view **D** paratype male, oblique dorsal habitus **E** holotype specimen labels.

1.6–1.9 × TOD; MS 0.28–0.30 × EH. Face yellowish white with a black spot above clypeus; carinae on propodeum more pronounced than in female.

Etymology. Named for the presence of distinctive carinae on the propodeum which are diagnostic.

Comments. Based on the presence of a raised area on face, strongly striate metasoma, and short hypopygium, this species is most closely related to *V. rugator* (Say). The presence of carinae on the propodeum and the long ovipositor (ovipositor length/body length 0.47–0.5) distinguish *V. carinatus* from *V. rugator*, which lacks the carinae on the propodeum and has a shorter ovipositor (ovipositor length/body length 0.29–0.37).

***Vipio fiebrigi* Bréthes, 1909**
Figures 7, 8

Vipio fiebrigi Bréthes, 1909: 231; Shenefelt, 1978: 1849; Quicke & Genise, 1994: 44.

Type material. Holotype ♀, *Vipio fiebrigi* Bréthes, 1909, **Paraguay:** San Bernardino (no date) (Fiebrig) (MACN).

Additional specimens examined. Argentina: 1 ♀, Chaco, Las Brecias (no date, collector) (USNM); 1 ♀, Chaco, Montevidio So. Amer. Paras lab, No. 674.20, v.1942 (Berry) (USNM); 1 ♂, Chaco, Colonia Benintez, 10.xii.1948 (R. Golbach) (IFML); 3 ♂, Tucuman, Aráoz, Estacion, 8.i.1927 (no collector) (IFML).

Diagnosis. This species can be distinguished from other Neotropical species with very long ovipositors (> 2.0 × body length) by having a yellow-red head, densely striate metasoma and a pointed basal lobe to the claw.

Description. Holotype♀, length of body 8.5–12.3 mm, of fore wing 6.5–9.0 mm, and of ovipositor (part exserted beyond apex of abdomen) 21.5–30.0 mm.

Head. Antenna robust, 0.94–0.97 × body length, with 62–68 flagellomeres; remaining 0.92–1.0 × longer than wide; first flagellomere 1.4 × longer than second; first flagellomere 2.7 × longer than wide; second flagellomere 1.4 × longer than wide; median flagellomeres 1 × longer than wide; terminal flagellomere (missing); head transverse to sub-transverse; clypeus higher in profile, slightly rugulose, clypeal guard setae typical; face sparsely punctate or rugulose; remainder of head smooth and shiny; HL 0.79–0.84 × HH; HW/HH 0.79–0.84; FH/FW 0.42–0.45; EH/HH 0.62–0.64; EH/FW 0.75–0.78; EW/EH 0.7–0.75; ITD 1.5–1.65 × TOD; MS 0.42–0.46 × EH; LMC 0.4 × HH; third segment of maxillary palp 4 × wider than long.

Mesosoma. Length of mesosoma 1.70–1.81 × height; pronotum smooth and shiny or transversely carinate dorso-laterally, smooth and shiny or crenulate at furrow dorso-laterally; notauli smooth, mesonotal lobes well defined; metapleuron smooth to slightly punctate; propodeum strongly reticulate or areolate-rugose postero-medially, smooth or punctate on basal and lateral margins.

Wings. Fore wing: length of fore wing/body length 0.72–0.76; PL/LRC 0.89–0.94; PW/PL 0.21–0.28; length of vein 3RSb 0.82–0.87 × combined length of r-rs and 3RSa; length of vein 1M 0.78–0.80 × length of (RS+M)a; vein 3RSa reaching wing margin 0.52–0.59 × distance between apex of pterostigma and wing tip. Hind wing: with basal glabrous area and/or with sparse basal setosity (Fig. 7E); apex of vein C+SC+R with one basal hamule.

Legs. Claw with strong pointed basal lobe.

Metasoma. First metasomal tergite 1.32–1.34 × longer than wide, rectangular, slightly narrowing anteriorly; raised median area oval, areolate-rugose; basal smooth area narrowing and continuing posteriorly as median longitudinal carina reaching small smooth raised area at the apex of tergum; surrounding area with short transverse carinae; dorso-lateral carina present, area below crenulate; T II 1.15–1.25 × wider than medially long, depressed, baso-lateral areas sub-triangular, smooth and shiny, me-

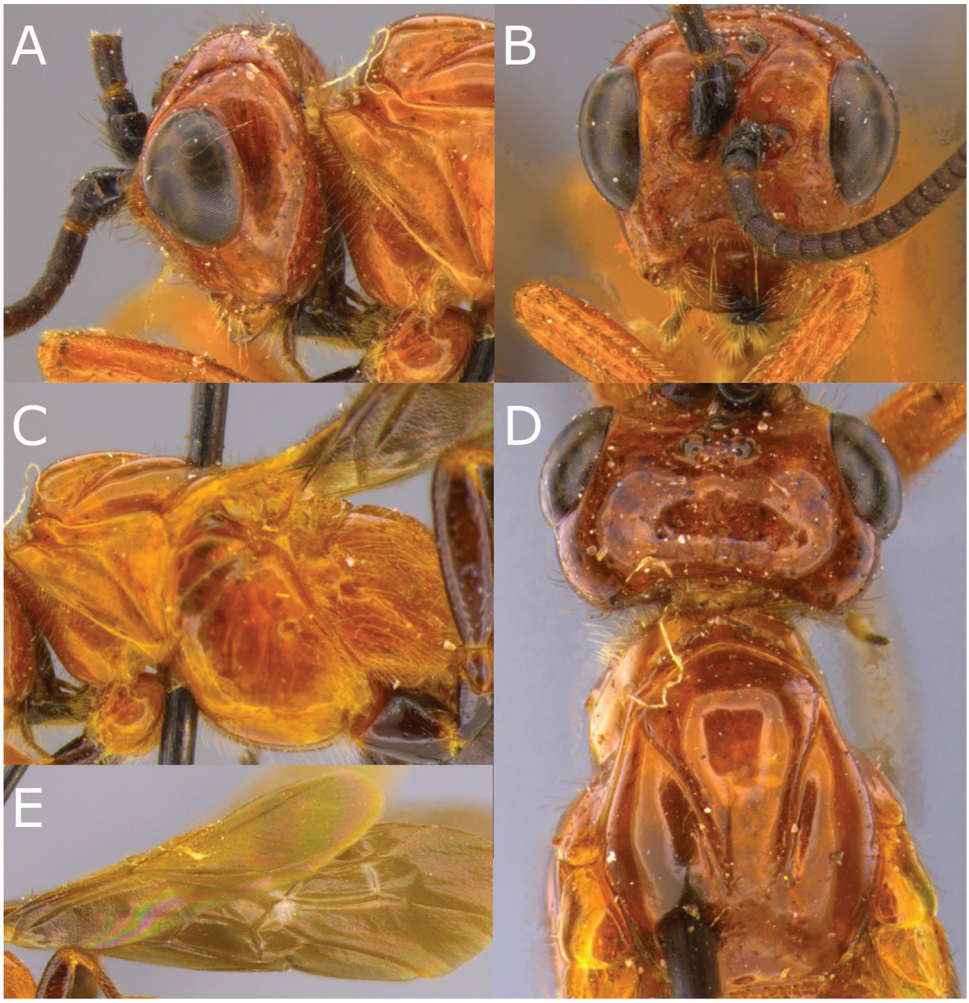

Figure 7. Montaged light micrographs of *Vipio fiebrigi* sp. nov. **A** Head, posterolateral view **B** face **C** mesosoma lateral view **D** head and mesoscutum, dorsal view **E** wings.

diobasal area smooth and shiny, continuing posteriorly as median longitudinal carina, remainder of tergum longitudinally striate, oblique furrow strongly impressed, striate; T III 1.4 × wider than medially long, longitudinally striate, baso-lateral area well defined; T IV longitudinally striate, baso-lateral area short and transverse; T V–VII smooth and shiny; hypopygium extending 0.4–1.0 mm beyond apex of metasoma, ovipositor 2.2–2.6 × body length.

Colour. Yellow to reddish yellow, except tip of mandible, labial palp, basal two segments of maxillary palp, labio-maxillary complex, antenna basally, fore trochanter, middle and hind legs and ovipositor sheath black. slightly smoky to dark brown, pterostigma black, yellow basally.

Male. Unknown.

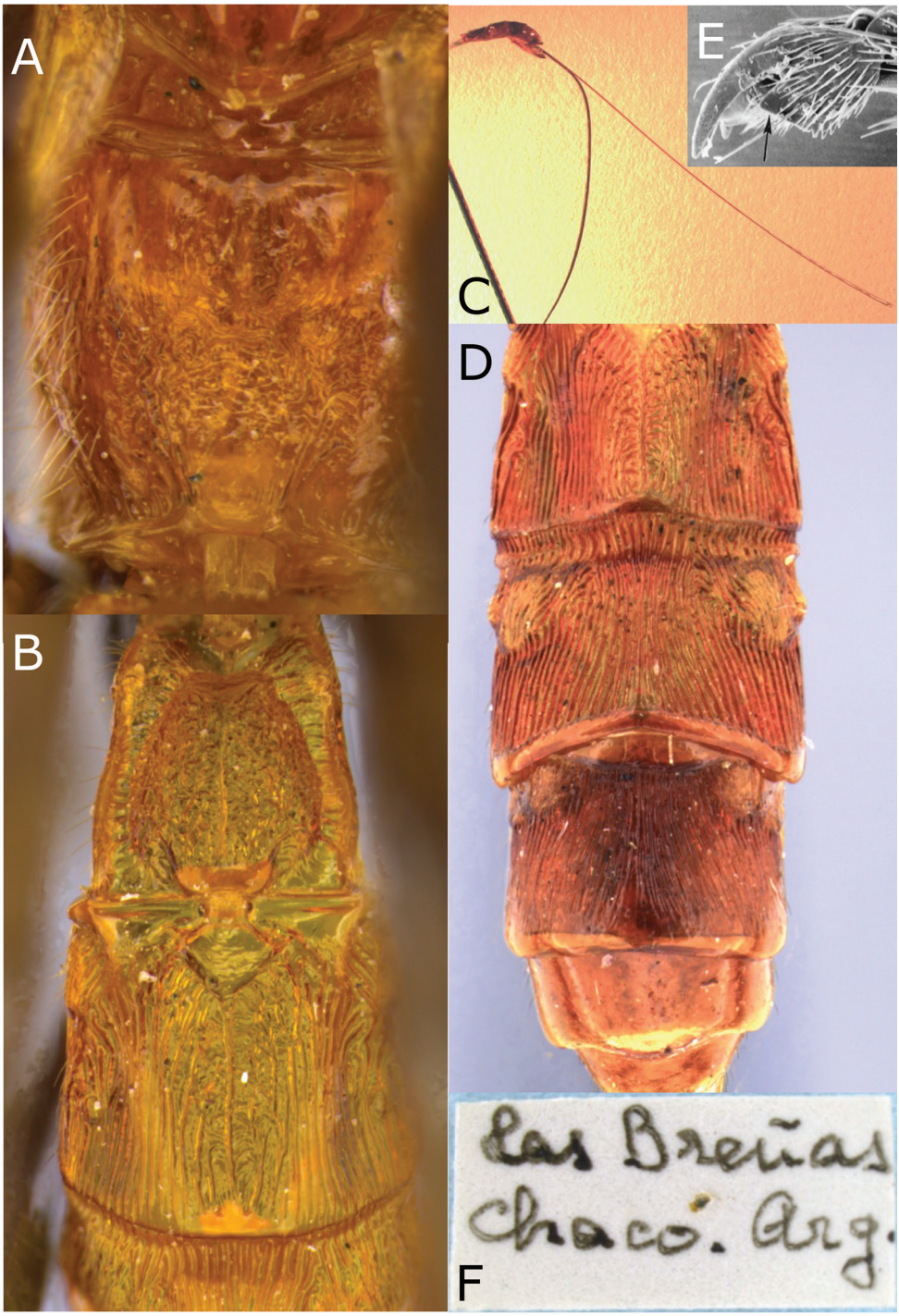

Figure 8. Montaged light and scanning electron micrographs of *Vipio fiebrigi* sp. nov. **A** Propodeum **B** metasomal tergites I and II **C** metasoma, lateral view, showing relative length of ovipositor **D** metasomal tergites II–VI **E** SEM of claw **F** data label of holotype.

Remarks. Based on the long body, ovipositor length, similar propodeal and metasomal sculpture, this species is closely related to *V. melanocephalus* Brullé. The longer MS (0.42–0.46 × EH) and yellow head in *fiebrigi* will separate it from *melanocephalus*, in which the MS/EH ratio is 0.39–0.41 and the head is black.

***Vipio godoyi* sp. nov.**
http://zoobank.org/80C332E5-D2BC-455A-972C-433FDF88E0E8
Figures 9, 10

Type material. Holotype ♀, **Costa Rica**, Heredia, Chilamate, 75 m, 25.i.-1989 (Hanson & Godoy) (ESUW). Paratypes: **Costa Rica**: 1 ♂, same data as holotype, except 25.iii.1989. 1 ♂, Alajuela, Rio-Laguna Arenal, 500 m, 14.viii.1988 (Paul Hanson). 2 ♂♂, Limon, Rio Toro Amarillo nr. Guapiles, 19.viii.1964 (G.C. Eickwort); 1 ♂, (same data) (USNM); 1 ♂, Heredia, La Selva Res. Sta., 11–17.vi.1986 (W. Hanson, G. Bohart) (EMUS); 1 ♀, same locality, ii-iv.1993 (P. Hanson), huertos Malaise trap set by G. Wright (ESUW). **Honduras**: 1 ♂, Suyapa MorÀzan, 3.xi.1965 (N.L.H. Krauss) (USNM). **Nicaragua**: 1 ♂, Zelaya, El Recreo, x.1984 (no collector) (MCZC). **Panama**: 1 ♂, C.Z. (Canal Zone) Summit, ix.1946 (N.L.H. Krauss) (ESUW); 1 ♂, same data, except (USNM).

Diagnosis. *Vipio godoyi* can be recognised by the combination of large propodeal (Fig. 10A) and metasomal spiracles (Fig. 10C), claw with large pointed basal lobe, strongly laminate T1 dorso-lateral carinae, and short ovipositor and hypopygium.

Description. Holotype ♀ length of body 7.1 mm; fore wing 7.1 mm and of ovipositor 3.8 mm.

Head. Antenna, broken, with 47 flagellomeres remaining, median flagellomeres longer than wide; first flagellomere 2.5 × longer than wide, 1.3 × longer than second, the latter 2.0 × longer than wide; clypeus rugulose, clypeal guard setae typical; face minutely punctate, smooth and shiny; head 0.87 × longer than high; HW/HH 0.8; FH/FW 0.59; EH/HH 0.71; EH/FW 1.04; EW/EH 0.77; ITD 1.8 × TOD; MS 0.3 × EH; third segment of maxillary palpus 3.3 × longer than wide; LMC 0.4 × HH.

Mesosoma. Length of mesosoma 1.7 × height; smooth and shiny; notauli smooth; propodeum smooth, spiracle large, 0.56 × diameter of median ocellus.

Wings. Length of fore wing: 1.0 × body length; PL/LRC 0.8; PW/PL 0.25; length of vein 3RSb 0.88 × combined length of r-rs and 3RSa; length of vein 1M 0.7 × length of (RS+M)a; vein 3RSa reaching anterior wing margin 0.71 × distance between apex of pterostigma and wing tip. Hind wing: uniformly setose; apex of vein C+SC+R with two basal hamules.

Legs. Claw with pointed basal lobe.

Metasoma. First tergite 1.1 × longer than posteriorly wide; raised median area oval, rugulose, with a median longitudinal ridge posteriorly, surrounding area smooth and shiny; dorso-lateral carina laminate, area below smooth and shiny, carina absent above spiracle; T II 1.75 × wider than medially long, longitudinally striate, basal areas smooth and shiny, oblique furrows impressed, striate; T III 1.9 × wider than medially

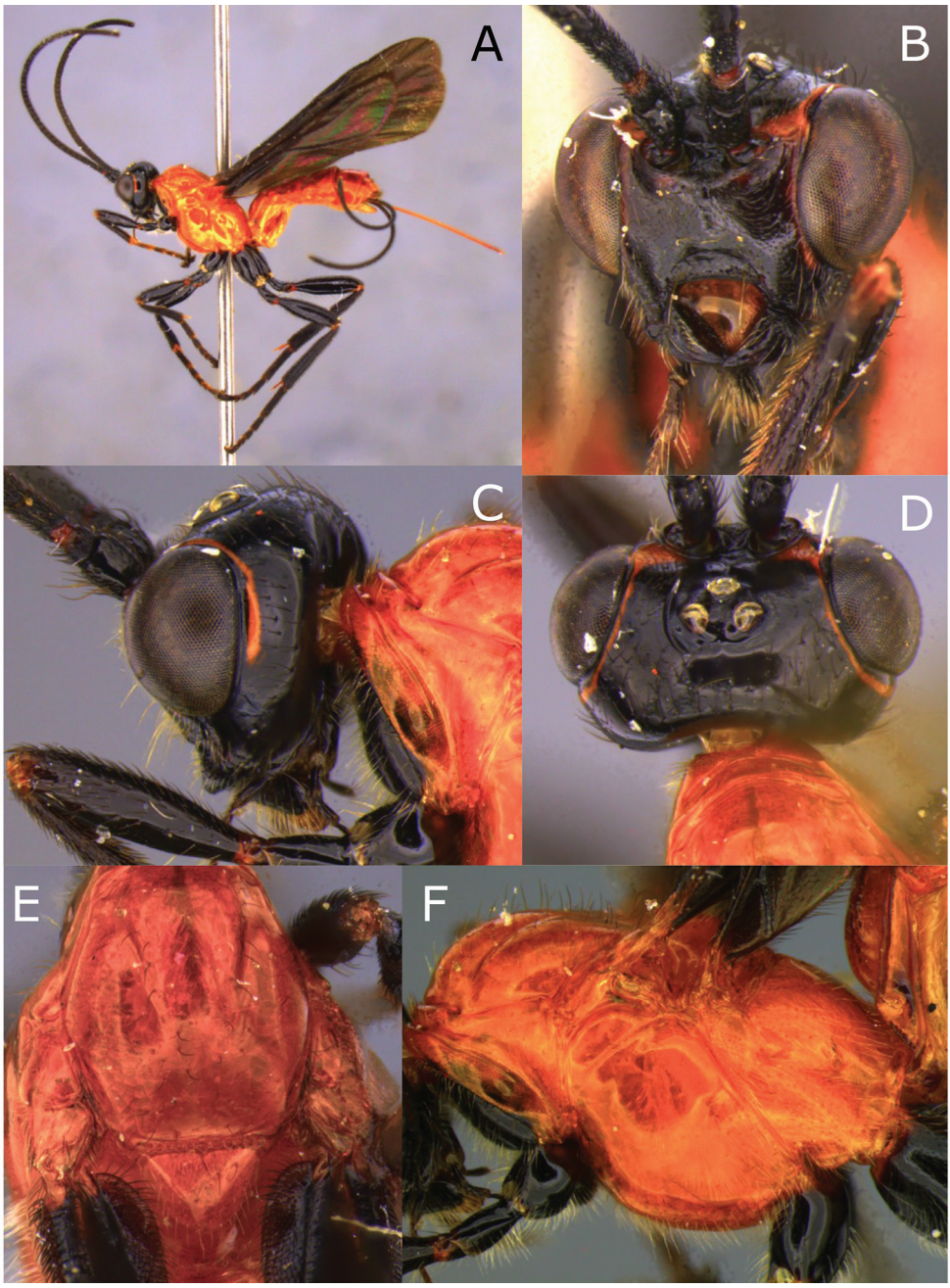

Figure 9. Montaged light micrographs of *Vipio godoyi* sp. nov. **A** Habitus lateral view **B** face **C** head and anterior mesosoma, postero-lateral view **D** head, dorsal view **E** anterior mesosoma, dorsal view **F** mesosoma, lateral view.

long, longitudinally striate except apex smooth, anterolateral area smooth; all metasomal spiracles large, those of T III 0.57 × the diameter of median ocellus; T IV with short longitudinal striae at base and posterior to anterolateral area, remainder of ter-

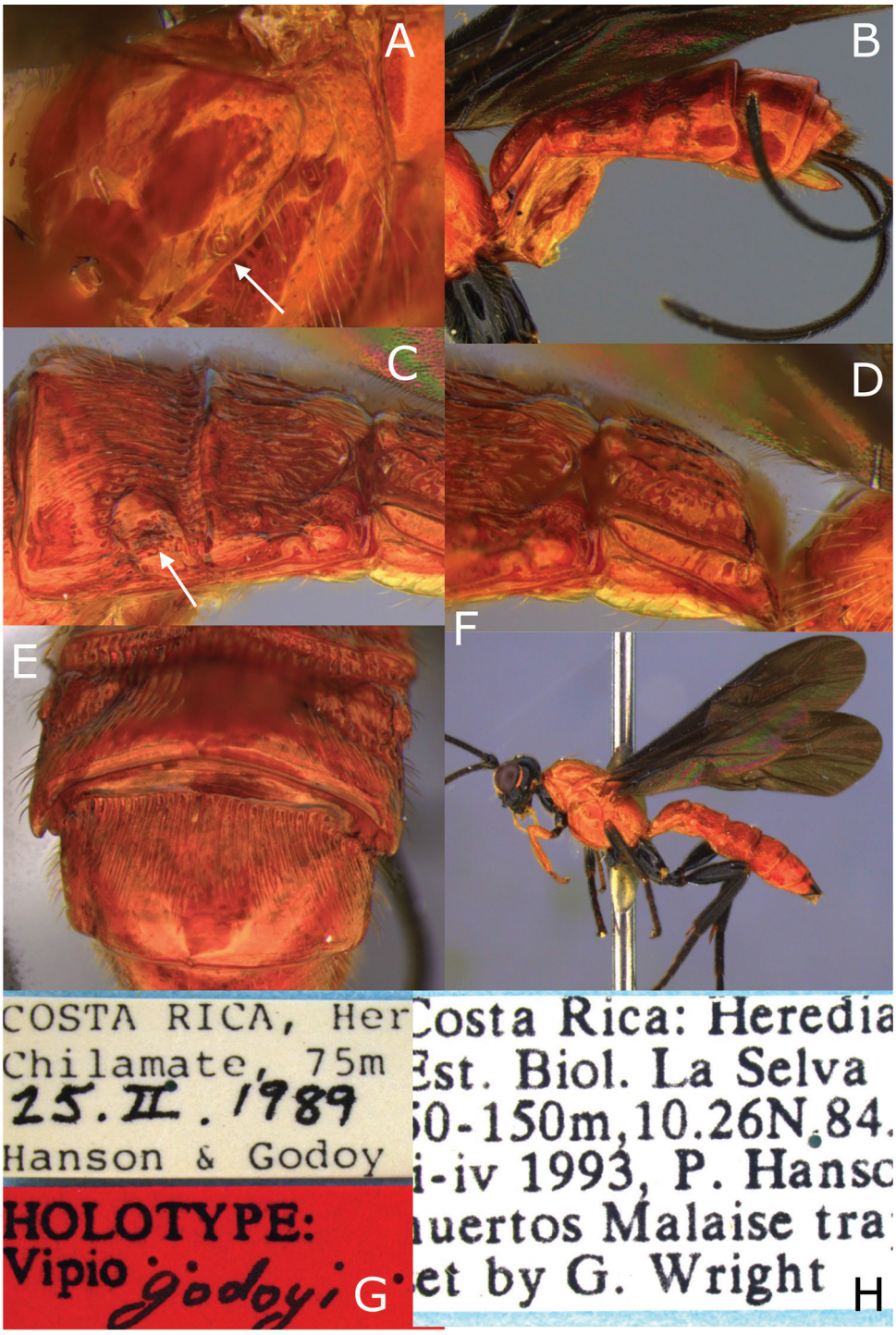

Figure 10. Montaged light micrographs of *Vipio godoyi* sp. nov. **A** Propodeum, oblique dorsal view **B** metasoma, lateral view **C** metasomal tergites II–III, dorso-lateral view **D** metasomal tergite I, dorso-lateral view **E** metasomal tergites III–IV, postero-dorsal view **F** male paratype, lateral habitus **G** holotype labels **H** labels.

gum, smooth and shiny; T V–VII smooth and shiny, mostly retracted; hypopygium barely extending beyond apex of metasoma (Fig. 10B); ovipositor 0.54 × body length.

Colour. Reddish yellow, except head, including mouthparts and antenna, legs and ovipositor sheath black. Wings black.

Variation. Paratype males (*N* = 10) as in female, except body length 7.5–7.9 mm; FWL/BL 0.76–0.83; AL/BL 0.8–0.95; HL/HH 0.8–0.85; EH/HH 0.59–0.62; FH/FW 0.76; EH/FW 0.0.87–0.90; EW/EH 0.75–0.77; ITD 1.64–1.79 × TOD; MS 0.38 × EH; first five flagellomeres 1.8–3.4 × longer than wide; remaining flagellomeres 1.2–1.4 × longer than wide; terminal flagellomere acutely pointed; face smooth and shiny, yellowish white with a black spot above clypeus; third segment of maxillary palpus swollen, 1.9–2.1 × longer than wide; T II-V densely longitudinally striate, striations sometimes absent on posterior part of T V; spiracle of T III of males 0.6–1.0 × the diameter of median ocellus; T VI minutely punctate. Paratype female (*N* = 1) with terminal flagellomere acutely pointed.

Biology. Unknown.

Distribution and seasonality. Costa Rica, Honduras, Nicaragua and Panama. Recorded flying from February through August in Costa Rica, November in Honduras and Panama, and October in Nicaragua. May occur sympatrically with *V. hansoni* sp. nov. (in one case, specimens of both species were taken from the same Malaise trap sample).

Comments. *Vipio godoyi* is apparently closely related to *V. hansoni* sp. nov. based on similar body colour, stout antennae, smooth and shiny propodeum, lamelliform dorsolateral carinae of T I, deeply impressed oblique furrows, oval and posteriorly narrowed raised median area of T I, short hypopygium, and short ovipositors in both species. Females of *V. godoyi* sp. nov. can be separated from those of *V. hansoni* sp. nov. by the presence of a pointed basal lobe on claw (absent in *hansoni*), and the setosity of ovipositor sheath (Fig. 10B). Males of *V. godoyi* have visibly larger and broader spiracles on metasomal T I-III as compared with those of other species. The diameter of spiracle on T III in males of *V. godoyi* is 0.6–1.0 × the diameter of median ocellus (0.35 × in *hansoni*).

Etymology. *Vipio godoyi* is named after Ms. Carolina Godoy, currently of the Instituto Nacional de Biodiversidad (INBio), who assisted with collection of the holotype specimen.

***Vipio hansoni* sp. nov.**

http://zoobank.org/E83AADC3-672A-4A18-A82D-1406A0959557
Figures 11, 12

Type material. Holotype ♀, **Costa Rica**: Limon, Bribri, 4 km NE, ix.1989 (Paul Hanson) (ESUW). Paratypes: **Costa Rica:** 1 ♂, Alajuela, Sta. Clara de San Carlos, 400', 17.ii.1964 (H.E. Evans) (MCZC); 1 ♂, Heredia, Chilamate, 75 m, 25.iii.1989, (Hanson & Godoy) (ESUW); 1 ♀, Heredia, F. La Selva, 3 km S. Pto. Viejo, 10°26'N, 84°01'W, 31.iii.1980 (H.A. Hespenheide) (ESUW); 1 ♀, same locality, ii-iv.1993 (P. Hanson), huertos Malaise trap set by G. Wright (ESUW).

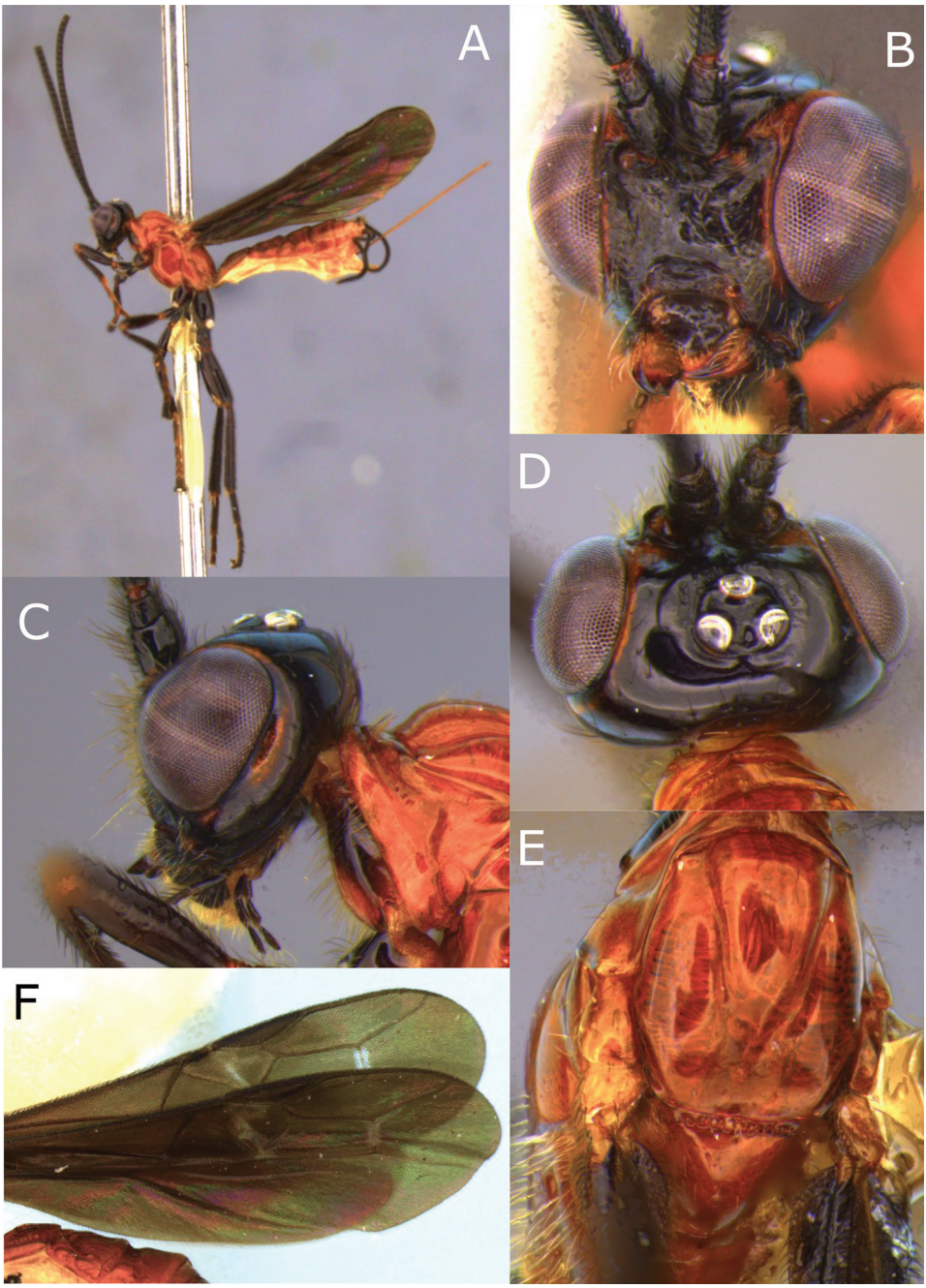

Figure 11. Montaged light micrographs of *Vipio hansoni* sp. nov. **A** Female habitus, lateral view **B** face **C** head and anterior mesosoma, lateral view **D** head, dorsal view **E** anterior mesosoma, dorsal view **F** wings, **G** claw.

Diagnosis. *Vipio hansoni* sp. nov. can be recognised by the combination of the predominantly reddish yellow colour, claw with rounded basal lobe, and the presence of two anterior carinae on raised median area of first metasomal tergite.

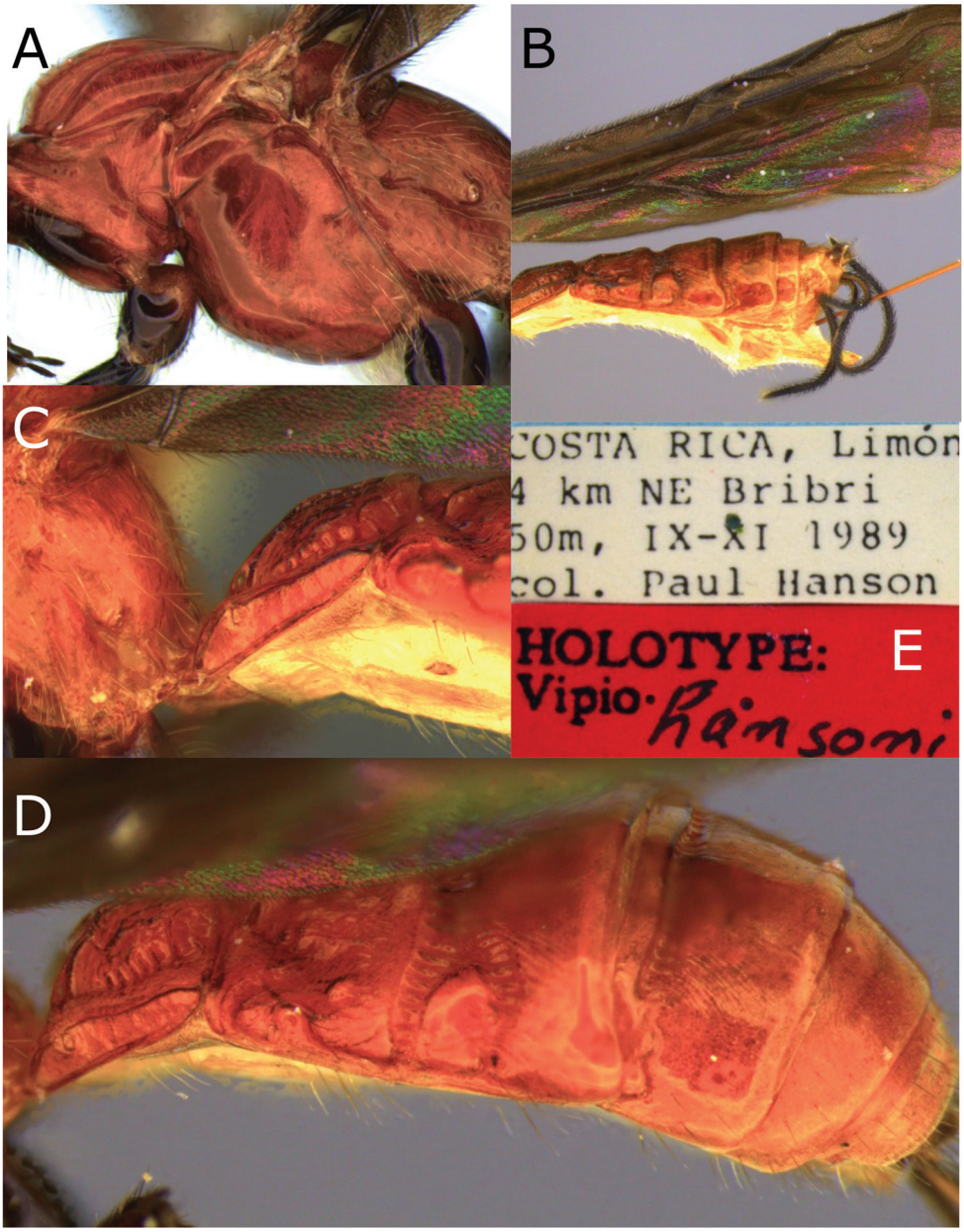

Figure 12. Montaged light micrographs of *Vipio hansoni* sp. nov. **A** Mesosoma, lateral view **B** wings and metasoma, lateral view **C** propodeum and metasomal tergite I, lateral view **D** metasoma, oblique dorsal view **E** holotype labels.

Description. Holotype ♀ length of body 5.5 mm, of fore wing 5.5 mm and of ovipositor 2.9 mm.

Head. Antenna stout, incomplete with 30 flagellomeres remaining; first flagellomere 4.0 × longer than wide; second flagellomere 3.0 × longer than wide; median

flagellomeres 1.15–1.2 × longer than wide; first flagellomere 1.5 longer than second; head transverse; face slightly rugulose; clypeus rugulose; clypeal guard setae typical; HL/HH 0.78; HW/HH 0.87; FH/FW 0.69; EH/HH 0.7; EH/FW 1.15; EW/EH 0.8; ITD 1.65 × TOD; MS 0.23 × EH; LMC 0.3 × HH; third segment of maxillary palpus 4.0 × longer than wide.

Mesosoma. Length of mesosoma 1.74 × height; smooth and shiny; notauli smooth; propodeum mostly smooth except slightly rugose posteromedially.

Wings. Fore wing: length of fore wing 1.0 × body length. PL/LRC 0.87; PW/PL 0.18; length of vein 3RSb 0.88 × combined length of r-rs and 3RSa; length of vein 1M 0.61 × length of (RS+M)a; vein 3RSa reaching anterior wing margin 0.67 × distance between apex of pterostigma and wing tip. Hind wings: uniformly setose; apex of vein C+SC+R with one basal hamule.

Legs. Claw with small, rounded basal lobe.

Metasoma. First tergite 1.1 × longer than posteriorly wide, raised median area oval, rugulose, anteriorly with two carinae joining posteriorly and becoming a single median longitudinal carina reaching apex of disc; surrounding area with short transverse carinae; dorso-lateral carina present, area below rugulose; T II 1.7 × wider than long, longitudinally striate, basal areas smooth and shiny, oblique furrow impressed, striate; T III 1.15 × wider than medially long, longitudinally striate, baso-lateral areas smooth and shiny for the most part; T IV longitudinally striate, T V–VII smooth and shiny; hypopygium ending at the apex of metasoma; ovipositor 0.53 × body length.

Colour. Reddish yellow except head, legs, propleuron, and ovipositor sheath black. Wings dark brown.

Variation. Paratype males (n = 2) as in female, except body length 3.3–3.5 mm; antenna with 32 flagellomeres, gradually shortening and widening distally becoming slightly clavate beyond 25th; a small and short median longitudinal carina present on face below antennae; HL/HH 0.88–0.91; EH/HH 0.74–0.76; EH/FW 1.24–1.27; EW/EH 0.72; ITD 2.8–3.1 × TOD; MS 0.16–0.20 × EH; T II–V densely longitudinally striate; fore wing length equal to body length; face yellow with a median black spot above clypeus, third segment of maxillary palpus, antenna basally, fore and middle legs yellow. Paratype females (*N* = 2) with terminal flagellomere acutely pointed.

Host. Unknown.

Distribution and seasonality. So far recorded only from Limon, Alajuela, and Heredia Provinces in Costa Rica. Specimens were collected in March, April, and September.

Remarks. This species is closely related to *V. godoyi* the explanation given under *godoyi* distinguishes both species. This species also is similar to *V. lavignei* sp. nov., but the comments given under *lavignei* separate these species.

Etymology. *Vipio hansoni* is named after Professor Paul Hanson, of the Universidad de Costa Rica, who collected the holotype specimen.

***Vipio lavignei* sp. nov.**
http://zoobank.org/C069146D-118E-4BB8-BA8C-DA4CCBB12299
Figures 13, 14

Type material. Holotype ♀, **Peru:** Tingo Maria 620, 5–12.x.1964 (C.C. Porter) (MCZC). Paratypes: **Peru:** 1 ♀, Tingo Maria, 20–27.i.1968 (A. Garacia and C. Porter) (USNM). **Argentina:** 1 ♂, Tucuman, Horco, Molle, 18–21.iii.1968 (C.C. Porter) (MCZC); 1 ♂, Tucuman, Orán Abra, Grande, 18.iv–5.v.1969, (C.C. Porter) (MCZC).

Diagnosis. *Vipio lavignei* can be recognised by the black head and pronotum, rugo-punctate face, and rectangular, dorso-laterally carinate raised median area of first metasomal tergite.

Description. Holotype and paratype ♀, length of body 9.0–9.2 mm, of fore wing 8.2–8.8 mm, of ovipositor (part exserted beyond apex of abdomen) 3.3 mm, and of antenna 8.8 mm.

Head. Antenna as long as body, with 49 flagellomeres, median flagellomeres 1.2–1.3 × longer than wide, tapering distally; first flagellomere 4.0 × longer than wide, and 1.2 × longer than second, the latter 3.0 × longer than wide; head sub-transverse; clypeus rugose, carinate dorsally; guard setae typical; face rugo-punctate with a small short ridge below antennae; frons rugulose; remainder of head smooth and shiny; HL 0.85 × HH; HW/HH 0.93; FH/FW 0.64; EH/HH 0.6; EH/FW 0.99. EW/EH 0.8; ITD 1.25 × TOD; MS 0.47–0.5 × EH; LMC 0.3 × HH; third segment of maxillary palpus 4.0 × longer than wide.

Mesosoma. Length of mesosoma 1.8 × height. smooth and shiny, except pronotal furrow, crenulate dorsally; notauli smooth; propodeum smooth and shiny.

Wings. Fore wing: length of fore wing 0.96 × body length; PW/PL 0.28; PL/LRC 0.71; length of vein 3RSb 1.1 × combined length of r-rs and 3RSa; length of vein 1M 0.82 × length of (RS+M)a; vein 3RSa reaching anterior wing margin 0.74 × distance between apex of pterostigma and wing tip. Hind wing: uniformly setose; apex of vein C+SC+R with one basal hamule.

Legs. Claw without pointed basal lobe;

Metasoma. First metasomal tergite 1.14 × longer than wide; raised median area rectangular with dorso-lateral carina; slightly rugulose, surrounding area with widely spaced transverse carinae, dorso-lateral carina laminate, area below smooth and shiny; T II 1.8 × wider than long, sparsely longitudinally striate; basal areas smooth and shiny; OF wide, deep, and striate; posterior of tergum smooth; second metasomal suture wide, striate; T III 1.9 × wider than medially long, smooth and shiny posteriorly, baso-lateral areas smooth and shiny for the most part with surrounding area strongly striate; T IV smooth and shiny, except for crenulate transverse basal groove; remainder of metasoma smooth and shiny; hypopygium short, ending at apex of metasoma; ovipositor 0.37 × body length.

Colour. Head, including antenna and palpi, prothorax, mesonotum and legs black; a narrow strip surrounding the eye and a small spot behind each eye yellow; metasomal T I–III red with black tinge; T IV–VII reddish black. Wings smoky;

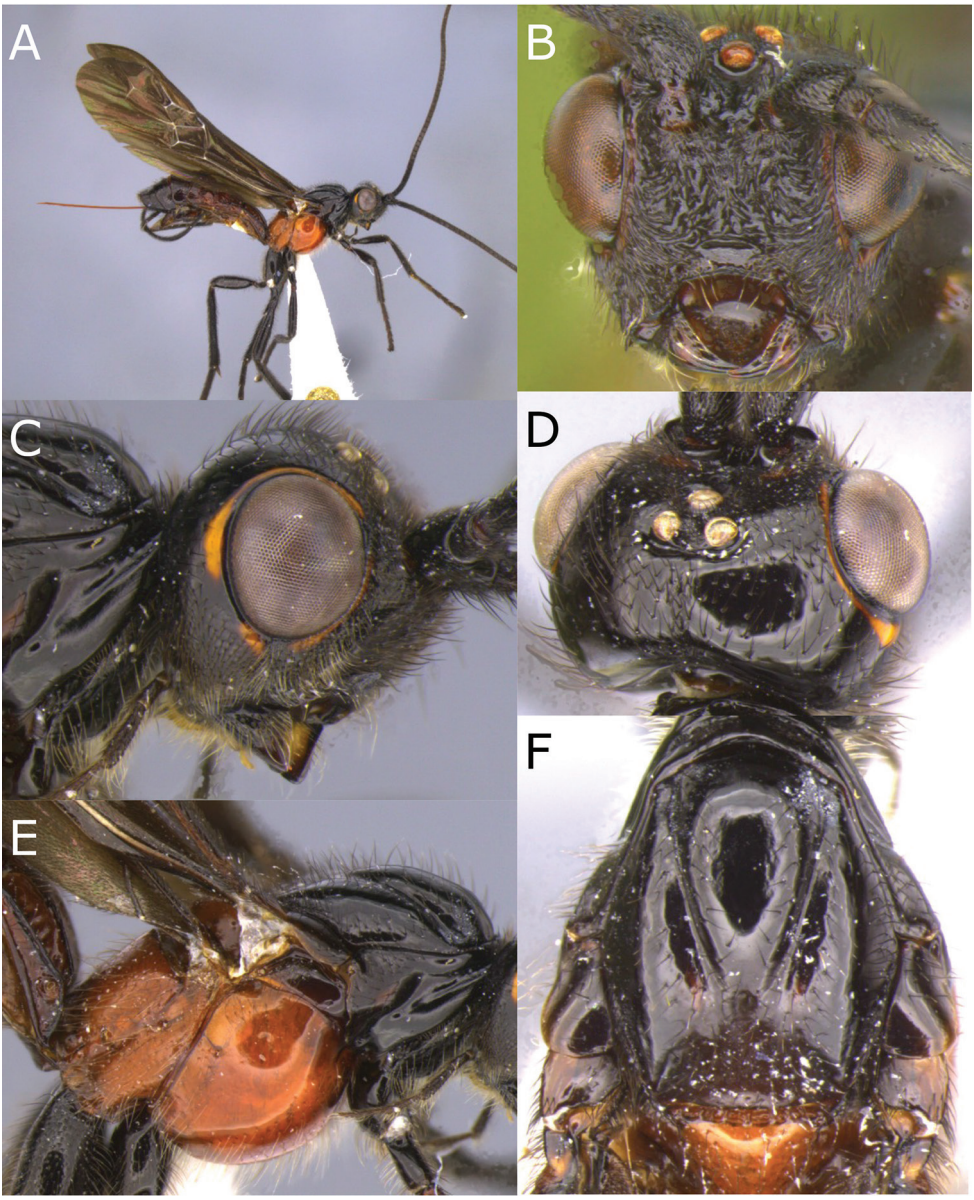

Figure 13. Montaged light micrographs of *Vipio lavignei* sp. nov. **A** Female habitus, lateral view **B** face **C** head and anterior mesosoma, lateral view **D** head, near dorsal view **E** mesosoma and metasomal tergite I, lateral view **F** mesoscutum and scutellum, dorsal view.

Variation. Paratype female as in holotype except, length of body 9.2 mm, of fore wing 8.2 mm; face strongly rugose; EH/FW 0.70; HW/HH 0.91; ITD 1.3 × TOD; mesosoma 1.64 × longer than high; length of fore wing 0.88 × body; PL/LRC 0.94; PW/PL 0.24; length of vein 1M 0.75 × length of (RS+M)a; length of vein 3RSb 1.1 ×

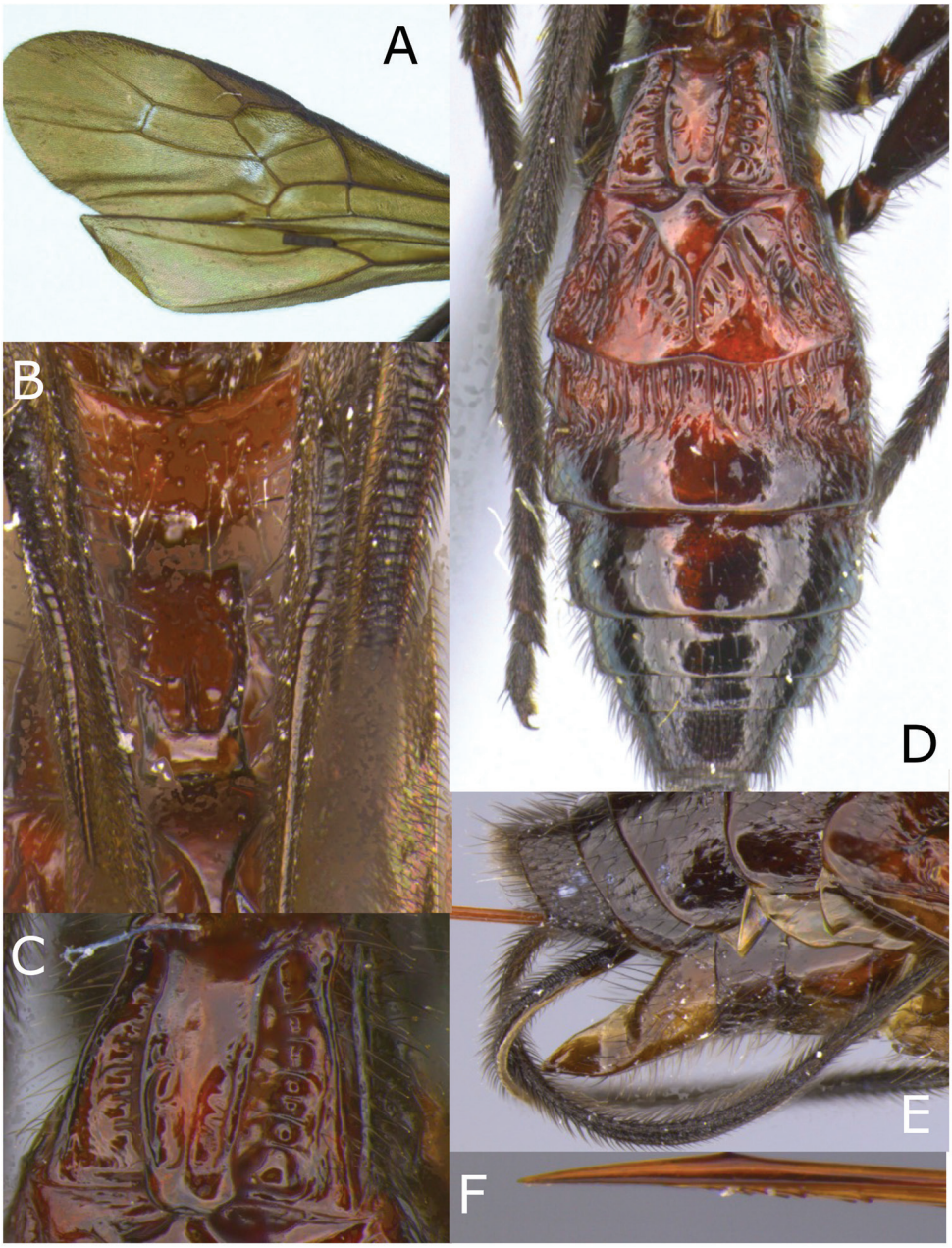

Figure 14. Montaged light micrographs of *Vipio lavignei* sp. nov. **A** Wings **B** propodeum and metasomal tergite I, dorsal view **C** metasomal tergite I, near dorsal view **D** metasoma, dorsal view **E** apex of metasoma, lateral view **F** apex of ovipositor, lateral view.

combined length of r-rs and 3RSa; 3RSa reaching anterior wing margin between apex of pterostigma and wing apex at distance 0.67; T I 1.23 × longer than wide; T II 2.1 × wider than long; T III 2.3 × wider than medially long; yellow spot behind antenna

absent;. Paratype males (*N* = 2) as in female, except length of body 7.2 mm; length of fore wing 0.89 × body length; antenna 1.0–1.1 × body length; with 38 or 39 flagellomeres; HL 0.89–0.90 × HH; FH/FW 0.67; EH/HH 0.62–0.64; EW/EH 0.79; EH/FW 0.95; ITD 1.7 × TOD; MS 0.39 × EH; T II–IV uniformly longitudinally striate.

Distribution and seasonality. Argentina and Peru. Two specimens from Argentina were collected in March and May and two from Peru in October.

Etymology. Named after UW Professor Emeritus Robert J. Lavigne, in honour of his diverse contributions to entomological research and his role in promoting the insect systematics program at the University of Wyoming.

Remarks. This species is apparently closely related to *V. hansoni* sp. nov. because of its strongly sclerotised metasoma, and wide, deep 2nd metasomal suture. *V. lavignei* can be separated by the rugo-punctate face (smooth and shiny in *hansoni* sp. nov.), the black mesonotum (yellow in *hansoni*), and the rectangular T I raised median area (oval in *hansoni*).

Vipio melanocephalus **Brullé, 1846**

Figures 15, 16

Vipio melanocephalus Brullé, 1846: 445; Shenefelt, 1978: 1853.

Type material. Holotype ♀, *Vipio melanocephalus* Brullé, 1846, **Brazil**: del Rio-Grande (no other data) (MNHN).

Additional specimens examined. Bolivia:1 ♀, 3 ♂, Sara (no date) (Steinbach) (MCZC).

Diagnosis. *Vipio melanocephalus* can be recognised by the combination of its size (body length > 1cm), ovipositor length (≥ 2 × body length), largely black head and claw with large, acutely pointed basal lobe.

Description. Females, length of body 10.8–11.5 mm, of fore wing 7.1–7.3 mm, and of ovipositor (part exserted beyond apex of abdomen) 21.0–27.0 mm.

Head. Antenna stout; first flagellomere 2.7 × longer than wide, 1.6 × longer than second, the latter 1.4 × longer than wide; (data could not be recorded for other antennal characters because the only available specimen with antenna was dirty and broken); head transverse; clypeal guard setae typical; face slightly rugulose laterally; remainder of head smooth and shiny; HL 0.72–0.74 × HH; HW/HH 0.77–0.79; EH/HH 0.59–0.61; EH/FW 0.81; EH/HH; EW/EH 0.81; 0.59–0.60; ITD 1.65 × TOD; MS 0.39–0.40 × EH; LMC 0.4 × HH; third segment of maxillary palp 4 × wider than long.

Mesosoma. Length of mesosoma 1.79–1.81 × height; smooth and shiny, except pronotum rugulose dorso-laterally; notauli smooth; propodeum rugose medially, slightly rugulose laterally, smooth or punctate on basal and lateral margins.

Wings. Fore wing: length of fore wing 0.61–0.67 × body length; PL/LRC 0.75–0.80; length of vein 1M 0.69–0.73 × length of (RS+M)a; length of vein 3RSb 0.83–0.90 × combined length of r-rs and 3RSa; vein 3RSa reaching anterior wing margin between apex of pterostigma and wing apex at distance 0.5–0.53. Hind wing: with glabrous area basally; with one basal hamule.

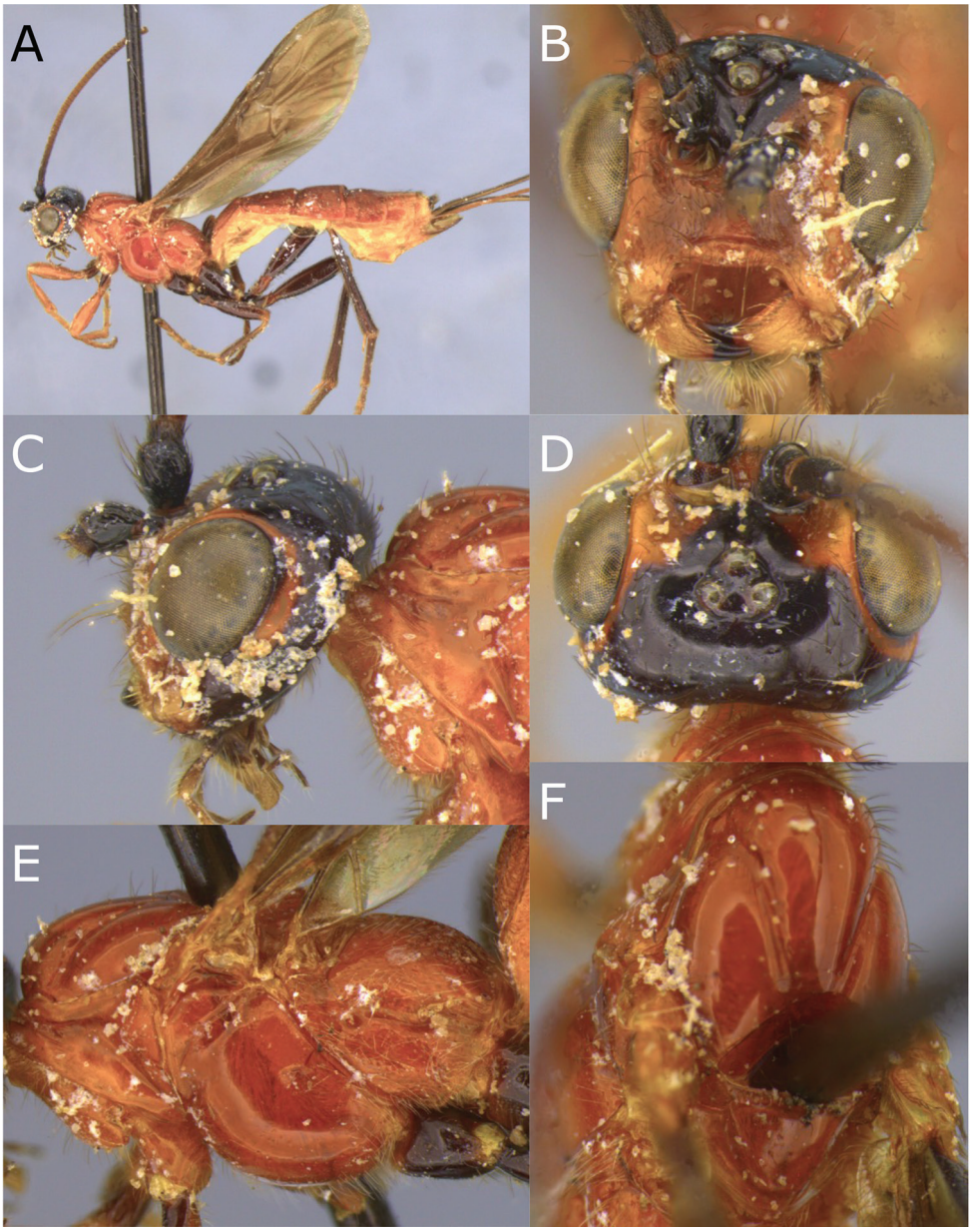

Figure 15. Montaged light micrographs of *Vipio melanocephalus*. **A** Female habitus, lateral view **B** face **C** head and anterior mesosoma, lateral view **D** head, dorsal view **E** mesosoma, lateral view **F** anterior mesosoma, dorsal view.

Legs. Claw with pointed basal lobe.

Metasoma. First tergite 1.4–1.42 × longer than wide, raised median area oval, rugulose, with smooth anterior area continuing posteriorly as median longitudinal carina, surrounding area with transverse carinae, dorso-lateral carina present; T II –IV longitudinally striate; T II 1.1 × wider than long, basal areas smooth, medio-basal

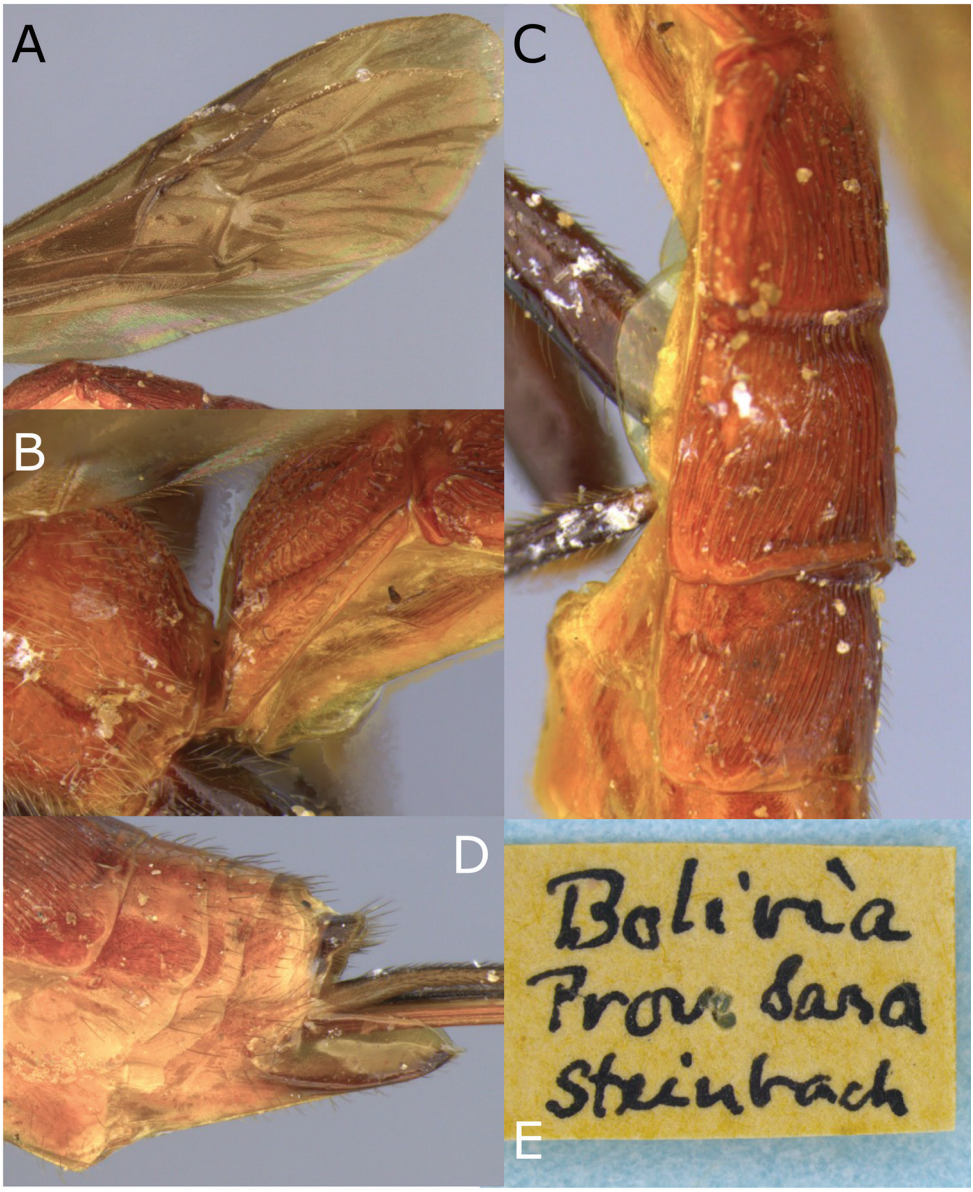

Figure 16. Montaged light micrographs of *Vipio melanocephalus*. **A** Wings **B** propodeum and metasomal tergite I, near dorsal view **C** metasomal tergites II–V, lateral view **D** apex of metasoma and hypopygium, lateral view **E** data label.

area continuing posteriorly as a median longitudinal carina, oblique furrows strongly impressed; T III 1.2 × wider than medially long, baso-lateral areas present; remainder of metasoma smooth and shiny; hypopygium extending 1.0 mm beyond apex of metasoma; ovipositor 2.0–2.3 × body length.

Colour. Predominantly orange; head largely black, face sometimes orange; frons sometimes yellow laterally; antenna rufous or black; labial and maxillary palp reddish black; legs black or reddish black, except fore legs beyond trochanter and middle tarsi orange.

Variation. Paratype males (*N* = 3) as in female, except length of body 6.5 mm; median flagellomeres longer than wide (antenna broken beyond F43); HL 0.86–0.88 × HH; EH/HH 0.72–0.73; EW/EH 0.80; EH/FW 1.03–1.06; FH/FW 0.5–0.52; ITD 2.5 × TOD; MS 0.18 × EH; punctation on pronotal furrow sometimes extends laterally; T V striate; face yellowish or reddish white with a reddish brown triangular spot above clypeus; frons yellow, remainder of head black; legs yellow to black;.

Remarks. This species is similar to *V. fiebrigi* Bréthes, but can be readily separated by the characters discussed under *V. fiebrigi*.

Vipio paraguayensis Szépligeti, 1906

Figures 17–19

Vipio paraguayensis Szépligeti, 1906: 157; Shenefelt, 1978: 1857.

Type material. Holotype ♀, *Vipio paraguayensis* Szépligeti 1906, **Paraguay,** Villa Encarnacion, 7.xii.1904 (Schrottky) (HNHM type No. 832).

Additional material examined. Argentina: 1 ♀, Buenos Aires, 1.i.1950 (J. Foerster) (USNM); 1 ♀, Buenos Aires, San Clement del Tuyu, xi.1950 (J. Foerster) (CNCI); 1 female, Pronunciamiento Entre Rios, ii.1965 (CNCI); 1 ♀, Tucuman, Va. Padro Monte-R. Nio, 25.iv.1966 (C.C. Porter) (USNM); 1 ♀, La Plata, Fac., Agronomia, 22.xii.1968 (C.C. Porter) (USNM). **Bolivia:** 3 ♀♀, Corolco (HNHM); 1 ♂, Corolco, 1800 m, 3–8.xii.1955 (L.E. Pena) (CNCI). **Brazil:** 3 ♀♀, Nova Teutonia 27°11'S, 52°23'W 300–500 m, vii-xi.1968 (F. Plaumann) (CNCI). **Chile:** 1 ♀, Conesa, Rio Negro, i.1954 (F.H. Waltz) (USNM). **Colombia:** 1 ♀, Cundinamarca Monterredondo, 10.xii.1958 (J. Foerster) (USNM). **Trinidad:** 1 ♂, Port of Spain (W.S. Brooks); 1 ♀, "1–9" Maracas, xii.1977, malaise trap (CNCI); 3 ♀, Curepe, 10.iii.1978, 28.iii.1978, 6.xii.1967; 1 ♀, San Andrew, nr. Valencia 23.iii.1985 (G.F. & J.F. Hevel) (CNCI); 1 ♀, Cocos Bay, 28–29.vi.1982 (J.M. Carpenter & J.S. Edgerly) (USNM); 1 ♀, Caranege, 14.x.1918 (Harold & Morrison) (USNM); 1 ♀, St. Augustine, 2.iii.1953 (F.J. Simmonds) (USNM); 1 ♂, Aripo Savana, 26.x.1918 (Harold & Morrison) (USNM); 2 ♂, Aripo Cumuto (R. Thaxter) (USNM). **Venezuela:** 1 ♂, El Tucuco, 200 m 19.iv.1981 (L. Masner) (USNM).

Diagnosis. May be distinguished from other Neotropical *Vipio* species by the combination of long ovipositor (1.5–1.9 × body length), presence of an acutely pointed basal lobe to claw and a short mid-anterior, rather wide, carina on the propodeum.

Description. Females, length of body 5.6–8.4 mm, of fore wing 4.6–6.8 mm, of ovipositor (part exserted beyond apex of abdomen) 6.4–10.2 mm and of antenna 4.5–7.0 mm.

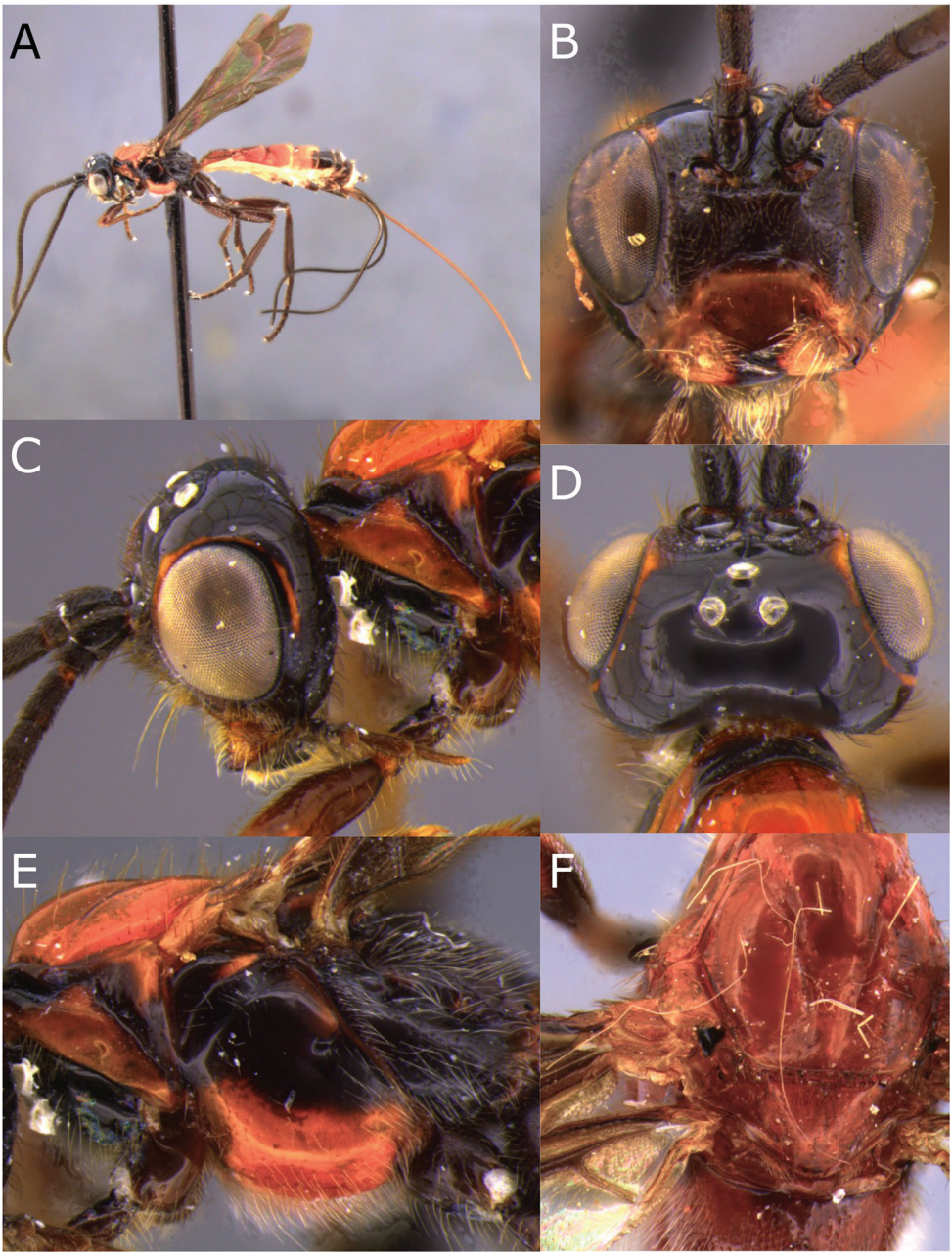

Figure 17. Montaged light micrographs of *Vipio paraguayensis*. **A** Female habitus, lateral view **B** face **C** head and anterior mesosoma, dorso-lateral view **D** head, dorsal view **E** mesosoma, lateral view **F** mesoscutum and scutellum, dorsal view.

Head. Antenna robust, 0.85–0.87 × body length, with 42–48 flagellomeres; first flagellomere 1.5–1.6 × longer than second, 2.0 × longer than wide; second flagellomere 1.6 × longer than wide; median flagellomeres quadrate; distal flagellomeres wider than

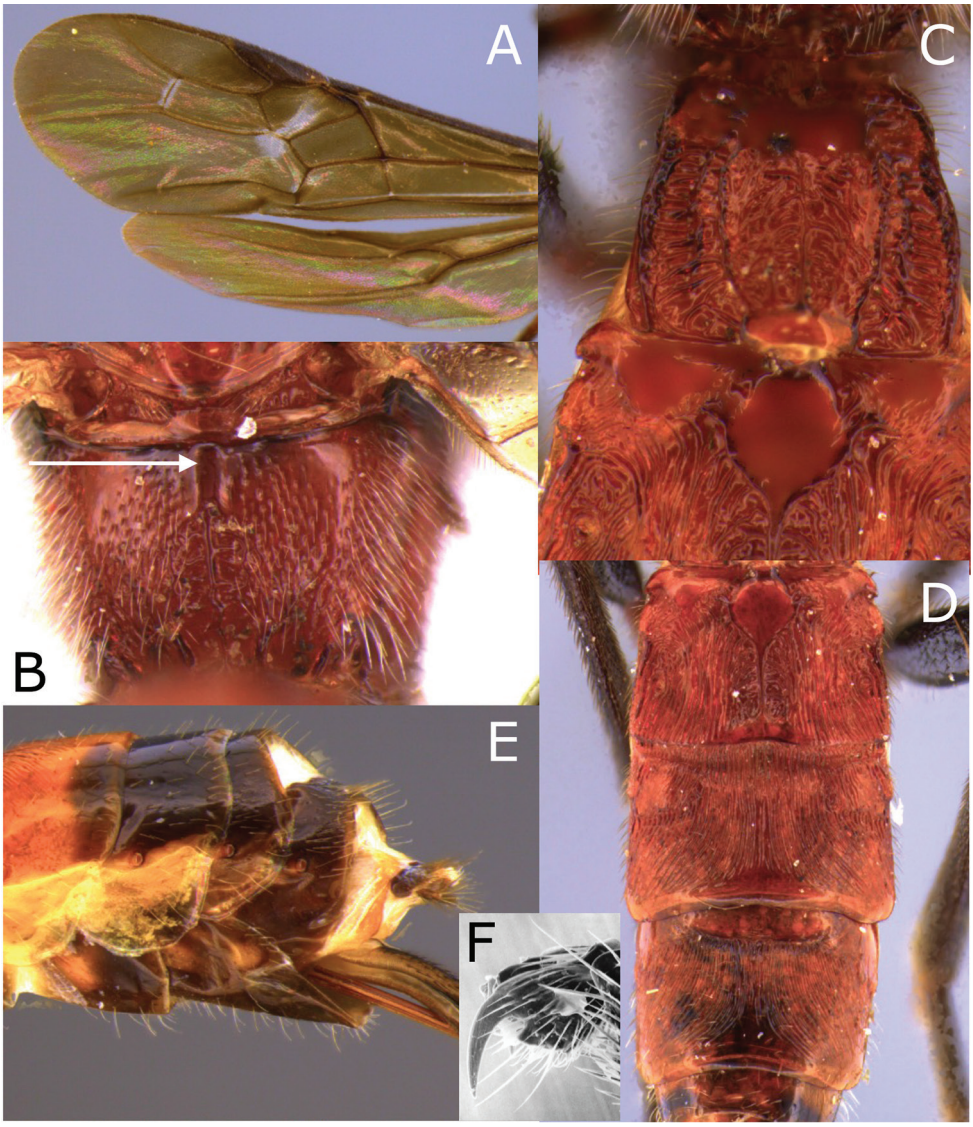

Figure 18. Montaged light and scanning electron micrographs of *Vipio paraguayensis*. **A** Wings **B** propodeum **C** metasomal tergites I and II, dorsal view **D** metasomal tergites II–IV, dorsal view **E** apex of metasoma and hypopygium, lateral view **F** SEM of claw.

long, except terminal flagellomere longer than wide, with apex bluntly rounded; head sub-transverse; face uniformly punctate, rarely rugulose laterally, remainder of head smooth and shiny; clypeus higher in profile, slightly rugulose, clypeal guard setae typical; HL 0.8–0.87 × HH; HW/HH 0.87–0.9; FH/FW 0.47–0.49; EH/HH 0.67–0.70; EH/FW 0.70–0.94; EW/EH 0.78–0.8; ITD 1.7 × TOD; MS 0.3–0.35 × EH; LMC 0.3 × HH; third segment of maxillary palpus 4.0 × longer than wide.

Mesosoma. Length of mesosoma 1.78–1.8 × height; pronotum smooth and shiny, except at furrow, punctate dorso-laterally; notauli smooth; propodeum

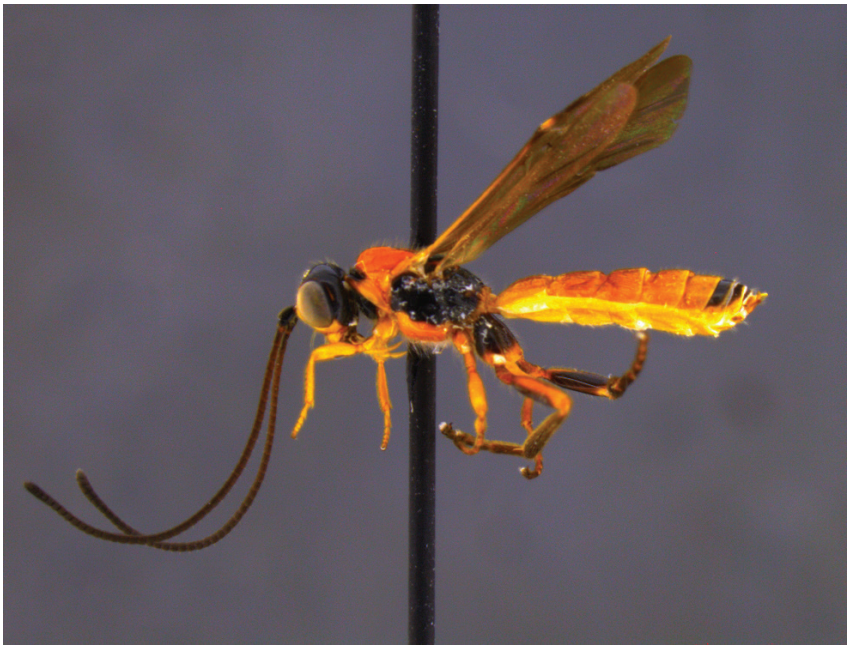

Figure 19. *Vipio paraguayensis* male, lateral habitus.

smooth and punctate laterally with a shallow median furrow, having a basally smooth median longitudinal carina.

Wings. Fore wing: length of fore wing 0.75–0.80 × body length; PL/LRC 0.92–0.94, PW/PL 0.24–0.27; length of vein 3RSb 0.91–0.95 × combined length of r-rs and 3RSa; length of vein 1M 0.62–0.64 × length of (RS+M)a; 3RSa reaching anterior wing margin between apex of pterostigma and wing apex at distance 0.53–0.57. Hind wing: uniformly setose or with sparse setosity basally; apex of C+SC+R with one basal hamule.

Legs. Claw with pointed basal lobe.

Metasoma. T I 1.34–1.38 × longer than wide, raised median area oval, anterior smooth area narrowing posteriorly, becoming a median longitudinal carina with short transverse carinae posteriorly; carinate at lateral margin; surrounding area with short transverse striae; dorso-lateral carina present, area below crenulate; T II 1.35–1.50 × wider than long, baso-lateral areas smooth and triangular; baso-medial area becoming a median longitudinal carina posteriorly and reaching a small raised smooth area at the apex of tergum; remainder of the tergum longitudinally striate, oblique furrows impressed, striate; T III 1.3–1.7 × wider than medially long longitudinally striate, baso-lateral areas distinct; T IV longitudinally striate with small baso-lateral area; T V–VII smooth and shiny; hypopygium extending 0.4–0.7 mm beyond apex of metasoma; ovipositor 1.1–1.4 × body length.

Colour. Black and reddish yellow; face black or reddish black; base of mandible, and a narrow strip around eyes yellow; remainder of head black; pronotum dorsally

(sometimes), propleuron (sometimes), mesopleuron, scutellum (except edges), propodeum, metapleuron, legs, metasomal T V–VII, ovipositor sheath black; remainder of body reddish yellow. Wings smoky, pterostigma yellowish brown.

Male. As in female, except length of body 4.3–6.4 mm, of fore wing 0.89–0.94 × body length; antenna with 36–46 flagellomeres, all flagellomeres longer than wide, except distal 5 or 6 which gradually become clavate (Fig. 19); HL 0.83–0.87 × HH; EH/HH 0.88–0.90; EH/FW 0.85–0.87; FH/FW 0.56–0.59; ITD 3.0 × TOD; MS 0.14–0.16 × EH; EW/EH 0.61; face smooth and shiny, yellowish white with a black spot above clypeus; segments 2 and 3 of maxillary palp distinctly expanded.

Remarks. *Vipio paraguayensis* can be easily recognised by the combination of the presence of a pointed basal lobe on the claw, the presence of a median longitudinal carina on the propodeum, the densely striate T II–IV, and the long ovipositor. Based on the presence of the median longitudinal carina on propodeum, this species may be closely related to *V. boliviensis* sp. nov. However, the presence of a pointed basal lobe on the claw, longitudinal striations on the metasoma, and longer hypopygium in *paraguayensis* separate it from *boliviensis* sp. nov. (in which the basal lobe of the claw is rounded, T III and IV are transversely striated, and the hypopygium is short). Males of this species can be confused with males of *V. belfragei* because of the expanded third and fourth maxillary segments, but the clavate antenna in *paraguayensis* (as opposed to a filiform antenna in *belfragei*) readily separate these two species. Another useful character is the presence of a median longitudinal carina on the propodeum in this species, as opposed to several short carinae posteriorly in *belfragei*.

Vipio porteri **Inayatullah, Sabahatullah & Ain Tahira, 2015**
Figure 20

Vipio porteri Inayatullah, Sabahatullah & Ain Tahira, 2015: 132–133, fig. 4 (note that the SEM figures published therein are distorted by approximately 1.3:1.0).

Type material. Holotype ♀, **Argentina,** Tucuman, Las Cejas, 8.iii–11.iv.1968 (C.C. Porter) (MCZC). Paratypes: **Argentina**: 9 ♀, 2 ♂, Tucuman, Las Cejas, 8.iii–11.iv.1968 (C.C. Porter) (MCZC); 3 ♀, 2 ♂, 22.ii–13.iii.1968 (C.C. Porter) (MCZC); 1♀, 1♂, same data, except 21.i–21.ii, 1968; 1 ♂, same data, except 1–21.i.1968; 1 ♀, same data, except 2.iv.1966; 3 ♀, near Las Cejas, 20.iv.1968 (C.C. Porter) (MCZC); 2 ♀, 5 ♂, Las Cejas, 11 km W, 1–16.xi.1967 (C.C. Porter) (MCZC); 1 ♀, same data, except 1.xi.1967; 2 ♀, same data, except 18.xi–4.xii.1967; 1 ♀, same data, except 27.v–14.viii.1968; 1 ♀, same data, except 24.ix–17.x.1968; 1 ♀, same data, except xii.1967; 4 ♀, 1 ♂, same data, except 24.ix–17.x.1968 (ESUW); 1 ♀, Las Cejas, 11 km. W, 12.iv–5.v.1968 (L. Stange) (EMUS).

Distribution and seasonality. Known only from Argentina. Specimens collected between September and May.

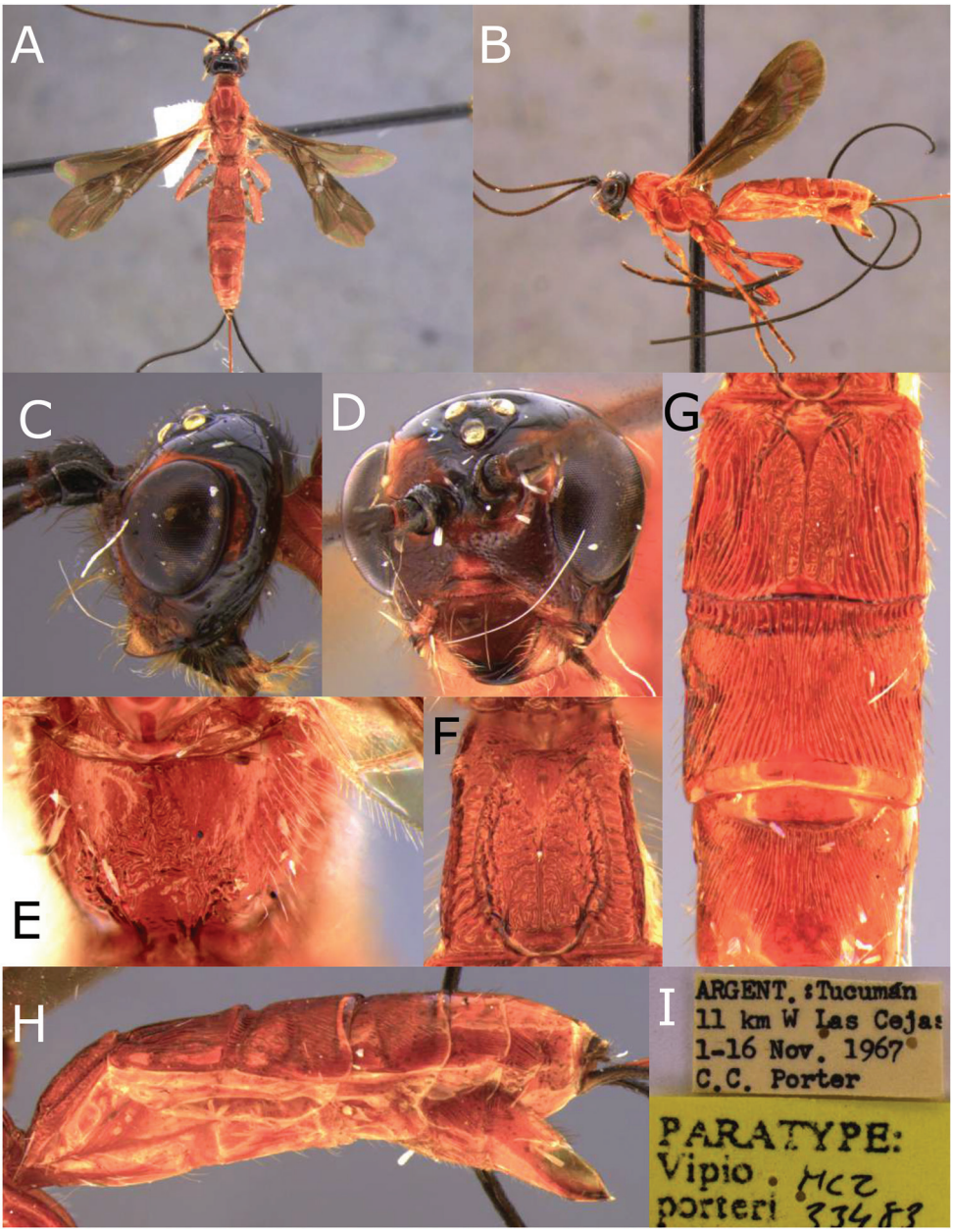

Figure 20. Montaged light micrographs of *Vipio porteri* paratype female. **A** Habitus, dorsal view **B** habitus, lateral view **C** head, lateral view **D** face **E** propodeum **F** metasomal tergite I **G** metasomal tergites II–IV, dorsal view **H** metasoma lateral view **I** labels.

Vipio quadrirugulosus **(Enderlein)**
Figures 21, 22

Craspedolcus quadrirugulosus Enderlein, 1920: 94; Shenefelt, 1978: 1673; *Isomecus quadrirugulosus*: Quicke & van Achterberg, 1990: 253, 256; *Vipio quadrirugulosus* Yu et al., 2016.

Type material. Holotype♀, *Craspedolcus quadrirugulosus* Enderlein, 1920, **Ecuador**, Bucay, (no additional data) (APSW).

Additional material examined. Costa Rica: 1♀, Alajuela, Rio-Laguna de Arenal, 500 m, 14.iii.1988 (P. Hanson) (RMSEL); 1 ♀, Guanacaste, Hacind, La Pacifica, Canas, 3 km N, 24.i.1972 (G. Frankie) (TAMU). **El Salvador**: 1 ♀, Quezaltepeque, 20.vi.1961 (M.E. Irwin) (USNM). **Guatamala**: 1 ♀, Yepocopa, v.1948, (H.T. Dalmat) (USNM). **Honduras**: 1 ♀, Mt. Pine Ridge, 2–6.vii.1967 (Porter) (USNM). **Mexico**: 2 ♀, Chiapas, Pichucalco, 11.6 mi. SE, 3.viii.1980, (Schaffner, Weaver, Freidlander) (TAMU); 1 ♀, Chiapas, Huixtla, 20 mi. N, 3000', 1.vi.1969 (W.R.M. Mason) (TAMU); 1 ♀, Chiapas, Pichucalco, 9.5 mi. NW, 3.viii.1980 (TAMU); 1 ♀, Chiapas, Campostela Rio de Marcos, 42.7 mi. SW, 100', 1.i.1942, (R.R & H.E. Murray) (TAMU). 1 ♀, Chiapas, No 2154 (C.F. Baker), 1 ♀, Morelos, Cuernavaca, iii.1945 (N.L.H. Krauss) (USNM); 1 ♀, Tabasco, Cardina, 8.ix.1974, (G. Bohart & W. Hanson) (USU). **Panama**: 1 ♀, Canal Zone, Albrook Field, 25.x.1937 (USNM); 1 ♀, Panama City, Bella Vista, 7.viii.1924, (N. Banks) (USNM); 1 ♀, Canal Zone, Ft. Clayton, xii.1946 (N.L.H. Krauss) (USNM).

Diagnosis. This species can be easily recognised from all other species by the black metasoma. Additionally, T II–V are densely striate longitudinally and the claws have a pointed basal lobe.

Description. Females (N = 17) length of body 4.8–9.3 mm; of fore wing 5.3–8.3 mm, of ovipositor 2.3–2.6 mm, and of antenna 4.6–8.5 mm.

Head. Antenna 0.94–1.0 × body length; with 39–47 flagellomeres; first flagellomere 1.4 × longer than second, 2.5 × longer than wide; second flagellomere 2.0 × longer than wide; median flagellomeres 1.0–1.4 × longer than wide; antenna gradually tapering towards apex; terminal flagellomere acutely pointed apically; head transverse; clypeus rugulose; clypeal guard setae consist of one seta above each anterior-tentorial pit; face smooth and shiny or sparsely punctate; remainder of head smooth and shiny; HL/HH 0.76–0.78; HW/HH 0.75–0.78; FH/FW 0.6–0.62; EH/HH 0.63–0.67; EH/FW 0.99–1.1; EW/EH 0.72–0.74; ITD 1.35–1.7 × TOD; MS 0.32–0.35 × EH; LMC 0.3 × HH; third segment of maxillary palpus 4.0 × longer than wide.

Mesosoma. Length of mesosoma 1.5–1.64 × height; smooth and shiny, except dorsally crenulate pronotal furrow; pronotum usually carinate antero-laterally; notauli smooth; propodeum mostly smooth except slight rugose apically.

Wings. Fore wing: length of fore wing 1.0–1.1 × body length; PL/LRC 0.9–1.0; PW/PL 0.19–0.24; length of vein 3RSb 0.77–0.82 × combined length of r-rs and 3RSa; length of vein 1M 0.66–0.71 × length of (RS+M)a; 3RSa reaching wing margin

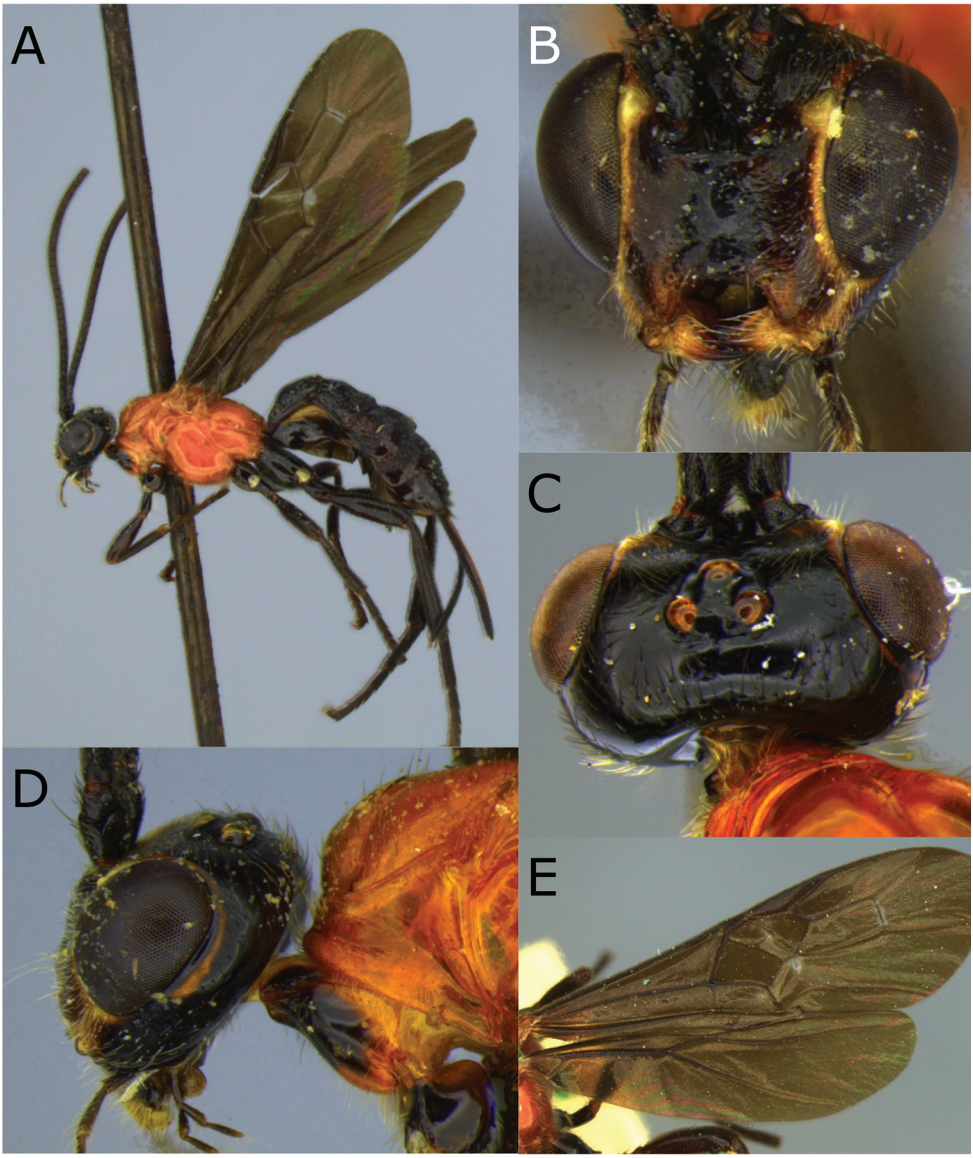

Figure 21. Montaged light micrographs of *Vipio quadrirugulosus*. **A** Female habitus, lateral view **B** face **C** head, dorsal view **D** head and anterior mesosoma, lateral view **E** wings.

0.63–0.65 distance between apex of pterostigma and wing apex. Hind wing: basally uniformly setose; apex of vein C+SC+R with one or two basal hamules.

Legs. Claw with wide pointed basal lobe.

Metasoma. First tergite 1.2 × longer than posteriorly wide; raised median area oval, smooth or rugulose anteriorly with or without a complete median longitudinal carina; always with a median longitudinal carina and areolate-rugose posteriorly; surrounding area with transverse carinae; dorso-lateral carina lamelliform; T II–V longitudinally

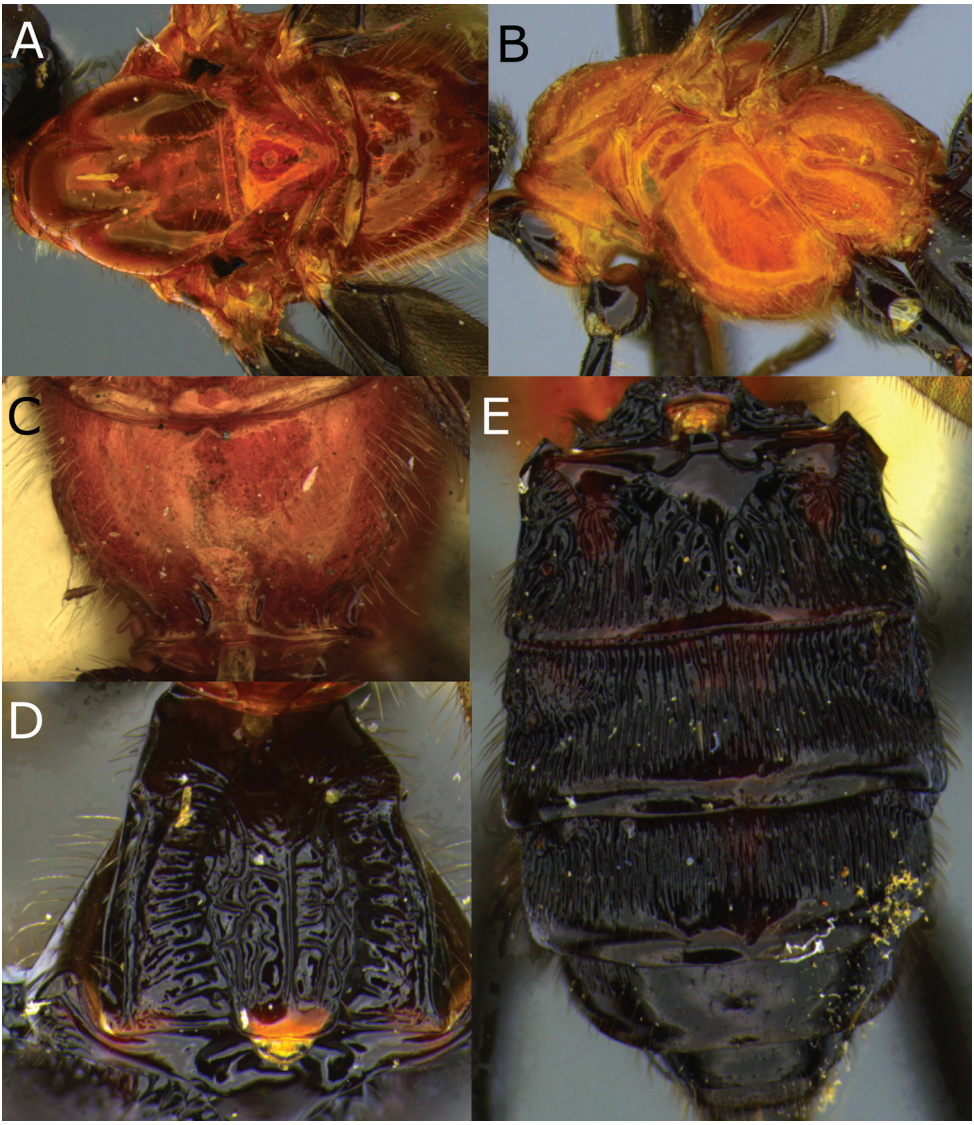

Figure 22. Montaged light micrographs of *Vipio quadrirugulosus*. **A** Mesosoma, dorsal view **B** mesosoma, lateral view **C** propodeum **D** metasomal tergite I, dorsal view **E** metasomal tergites II–VI.

striate; T II 2.0–2.1 × wider than long, basal areas smooth and shiny oblique furrow strongly impressed, striate; T III 2.2–2.5 × wider than medially long, baso-lateral areas usually carinate-rugulose; T IV baso-lateral area rugulose; T V smooth and shiny, rarely striate; remainder of metasoma smooth and shiny; hypopygium short, ending at apex of metasoma; ovipositor 0.35–0.48 × body length.

Colour. Head black, except a yellowish red and/or yellowish stripe surrounding the eye and basal half mandible reddish yellow to yellow; antenna, maxillary and labial palpi, prosternum, propleuron, legs, and metasoma black. Wings brownish black, pterostigma black.

Distribution and seasonality. Ranging from northern Mexico southwards to Ecuador (with records from Costa Rica, El Salvador, Ecuador, Guatemala, Honduras, Mexico and Panama). Specimens from Costa Rica were collected from January through March, June in El Salvador, May in Guatemala, July in Honduras, August through December in Panama, and from June through September in Mexico.

Remarks. *Vipio quadrirugulosus* appears closely related to the Nearctic *V. rugator* because of presence of a raised median area on the face, a strongly sclerotised and densely longitudinally striate metasoma, short ovipositor, and the presence of a pointed basal lobe on the claw. However, the black metasoma and the presence of carinae on the raised median area in *V. quadrirugulosus* will readily separate this species from *V. rugator* in which the metasoma is yellow or reddish yellow and the raised median area of the first tergite is areolate and rugose and lacks such a carina.

Vipio strigator **(Bréthes, 1913)**

Figures 23, 24

Iphiaulax strigator Bréthes, 1913: 79; Shenefelt, 1978: 1797; *Vipio strigator*: Quicke & Genise, 1994: 44.

Type material. Holotype, ♀, *Iphiaulax strigator* Bréthes, 1913, **Argentina:** "Potrerillo", Mendoza, (no date) 4000' (IFML).

Additional material examined. Argentina: 1 ♀, Misiones Panamb, 24.xi.1954 (Monro's, Willink); 1 ♀, Misiones San Pedro, 15.xi.1973 (Tomsic, Willink); 1 ♀, Misiones Bernardino de Irigoyen 12.xi.1973 (Tomsic, Willink); 1 ♂, Misiones San Pedro, 16.xi.1973 (Willink, Tomsic); 2 ♀, Misiones Iguazo, 30.i–13.iii.1945 (Hayward, Willink, & Golbach) (IFML). **Brazil:** 5 ♀, 11 ♂, Nova Teutonia, 27°11'S, 52°23'W, 300–500 m, i.1965 (F. Plaumann) (CNCI); 16 ♀, same data, except xi.1966; 12 ♀, xi.1968; 3 ♀, xi.1964; 2 ♀, xii.1966; 2 ♀, same data, except 20.xii.1955, 2.xi.1962. **Paraguay:** 1 ♀, Villarrica, ii.1951 (Pfannl) (IFML). **Peru:** 1 ♀, Valle Chanchamayo, 800 m, 13.viii.1951 (Weyrauch) (IFML).

Diagnosis. Ovipositor less than 0.5 × body length, predominantly red, head black; face with raised triangular area; propodeum with raised stub-like area and with four or five carinae postero-medially that usually reach the middle of propodeum; claw with strong pointed basal lobe.

Description (**Females,** *N* = 51). Length of body 6.0–10.1 mm, of fore wing 6.6–11.1 mm, of ovipositor (part exserted beyond apex of abdomen) 2.4–3.2 mm, and of antenna 6.0–9.5 mm.

Head. Antenna 0.74–0.97 × body length, with 43–50 flagellomeres; first flagellomere 2.5 × longer than wide, 1.4 × longer than second, the latter 2.0 × longer than wide; median flagellomeres as quadrate; terminal flagellomere acutely pointed apically; clypeus rugulose, clypeal guard setae typical; face smooth to sparsely punctate, with a raised triangular area above clypeus; remainder of head smooth and shiny; HL 0.76–

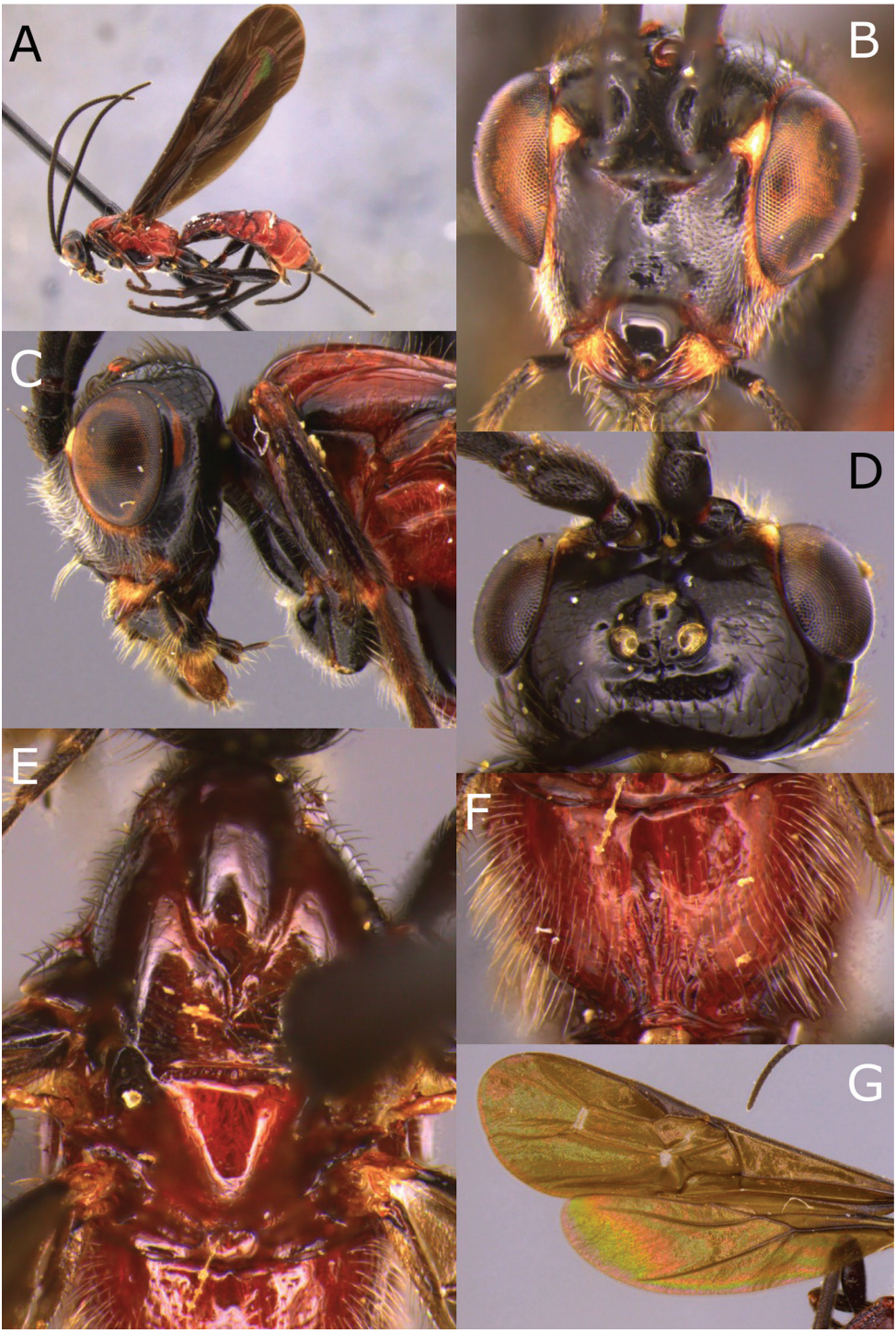

Figure 23. Montaged light micrographs of *Vipio strigator*. **A** Habitus lateral view **B** face **C** head and anterior mesosoma, lateral view **D** head, dorsal view **E** mesoscutum and scutellum, dorsal view **F** propodeum **G** wings.

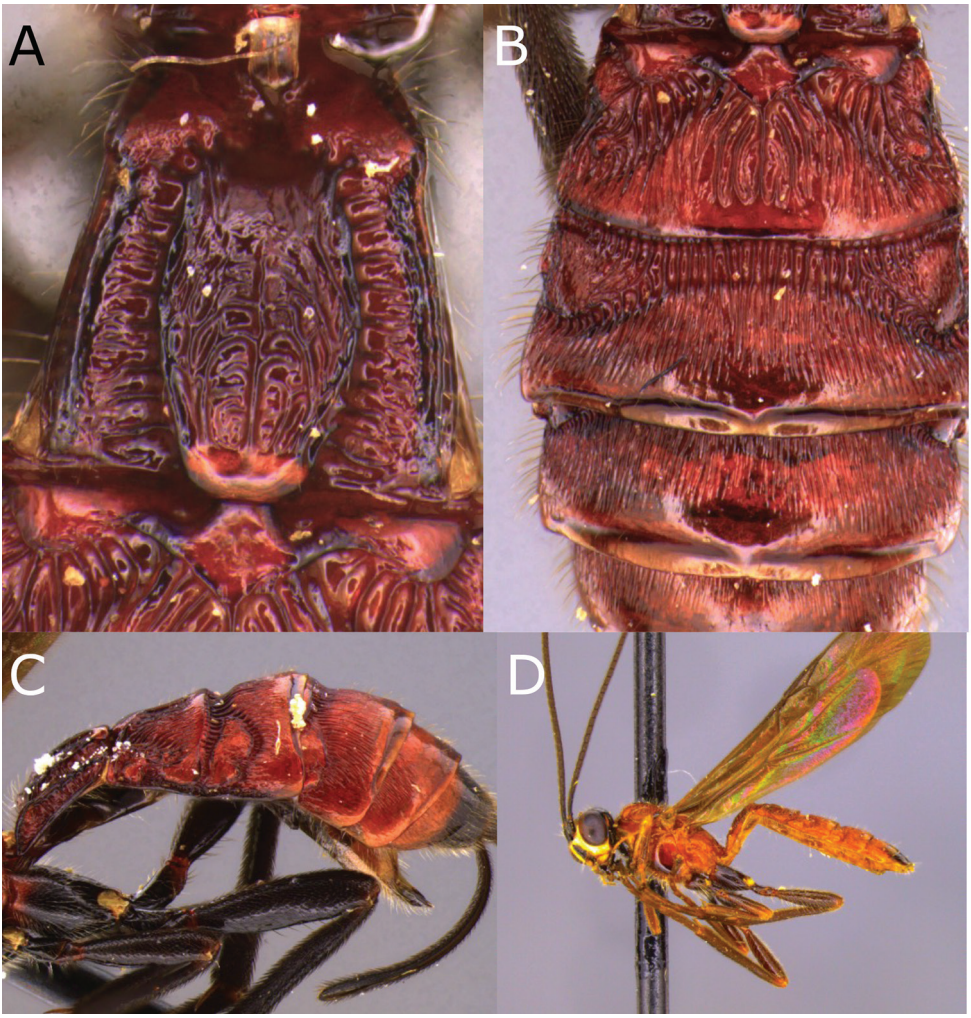

Figure 24. Montaged light micrographs of *Vipio strigator*. **A** Metasomal tergite I, dorsal view **B** holotype, metasomal tergites II–V **C** metasoma lateral view **D** male habitus, lateral view.

0.86 × HH; HW/HH 0.69–0.88; FH/FW 0.61–0.69; EH/HH 0.64–0.72; EH/FW 1.0–1.1; EW/EH 0.68–0.7; ITD 1.15–1.3 × TOD; MS 0.36–0.42 × EH; LMC 0.3 × HH; third segment of maxillary palpus 4.0 × longer than wide.

Mesosoma. Length of mesosoma 1.54–1.7 × height; smooth and shiny; propodeum with a raised postero-medially area with 4–5 longitudinal carinae reaching almost the middle of propodeum.

Wings. Fore wing: length of fore wing1.0–1.1 × body length; PW/PL 0.25–0.35; PL/LRC 1.0–1.05; length of vein 3RSb 0.84–0.87 × combined length of r-rs and 3RSa; length of vein 1M 0.6–0.7 × length of (RS+M)a; vein 3RSa reaching wing margin at distance 0.59–0.62 between apex of pterostigma and wing apex. Hind wing: uniformly setose basally; apex of vein C+SC+R with one or two basal hamules.

Legs. Claw with strong pointed basal lobe.

Metasoma. First metasomal tergite 1.1–1.15 × longer than wide, raised median area oval, gradually narrowing posteriorly, pointed anteriorly, carinate rugose, surrounding area with short transverse carinae, dorso-lateral carina lamelliform; T II–V longitudinally striate; T II 2.0–2.25 × wider than long, medio-basal area smooth and shiny, oblique furrows strongly impressed, striate; T III 2.6–2.9 × wider than medially long; baso-lateral areas of T III and IV rugulose; T VI–VIII smooth and shiny; hypopygium short, ending at apex of abdomen; ovipositor 0.3 × body length.

Colour. Largely red; head, including antenna and palpi, black except basal half of mandible reddish yellow and a yellow or yellowish red stripe surrounding the eye; pronotum reddish black with pronotal furrow red; prosternum, propleuron, basal 0.8 of mesopleuron, middle and lateral lobe of mesonotum laterally, scutellum apically, legs, and ovipositor sheath black. Wings brownish-black.

Male (*N* = 12). As in female, except length of body 4.6–6.5 mm, fore wing as long as body length; antennae 1.0–1.1 × body length; HL 0.84–0.89 × HH; EH/HH 0.71–0.76; EH/FW 1.34–1.4; FH/FW 0.77–0.82; EW/EH 0.71–0.75; ITD 1.6–1.7 × TOD; MS 0.21–0.27 × EH.

Remarks. *Vipio strigator* can be recognised by the combination of reddish black markings on the mesosoma, the short hypopygium, and the short ovipositor. This species is similar to the Nearctic *V. rugator* because of the presence of a raised area on face, short hypopygium, and short ovipositor in both species. However, the red coloration with reddish black markings on the mesosoma and a carinate propodeum in *strigator* will readily separate it from *rugator* (in which the mesosoma lacks black markings and propodeum lacks such carinae).

Vipio thoracica (Ashmead), 1900

Figures 25, 26

Glyptomorpha thoracica Ashmead, 1900: 295; Szépligeti, 1904: 15; *Vipio thoracica*: Shenefelt, 1978: 1863.

Type material. Holotype, ♀, *Glyptomorpha thoracica* Ashmead, 1900, **Grenada**: W.I. Chantilly Est. (Windward side) (no date) (H.H. Smith) (BMNH 3.c.540).

Additional material examined. Venezuela: 1 ♀, Puerto Cabello, 10.i.1940 (P. Anduze) (USNM).

Diagnosis. Raised area present on the face; T I with strong dorso-lateral carina; metasoma widely ovate and densely striate; hypopygium short; ovipositor length/body length 0.5; mesosoma dark reddish black.

Description. (females). Length of body 4.8–6.2 mm, of fore wing 5.2–6.2 mm, of ovipositor (part exserted beyond apex of abdomen) 2.4–3.1 mm and of antenna 5.1–6.2 mm.

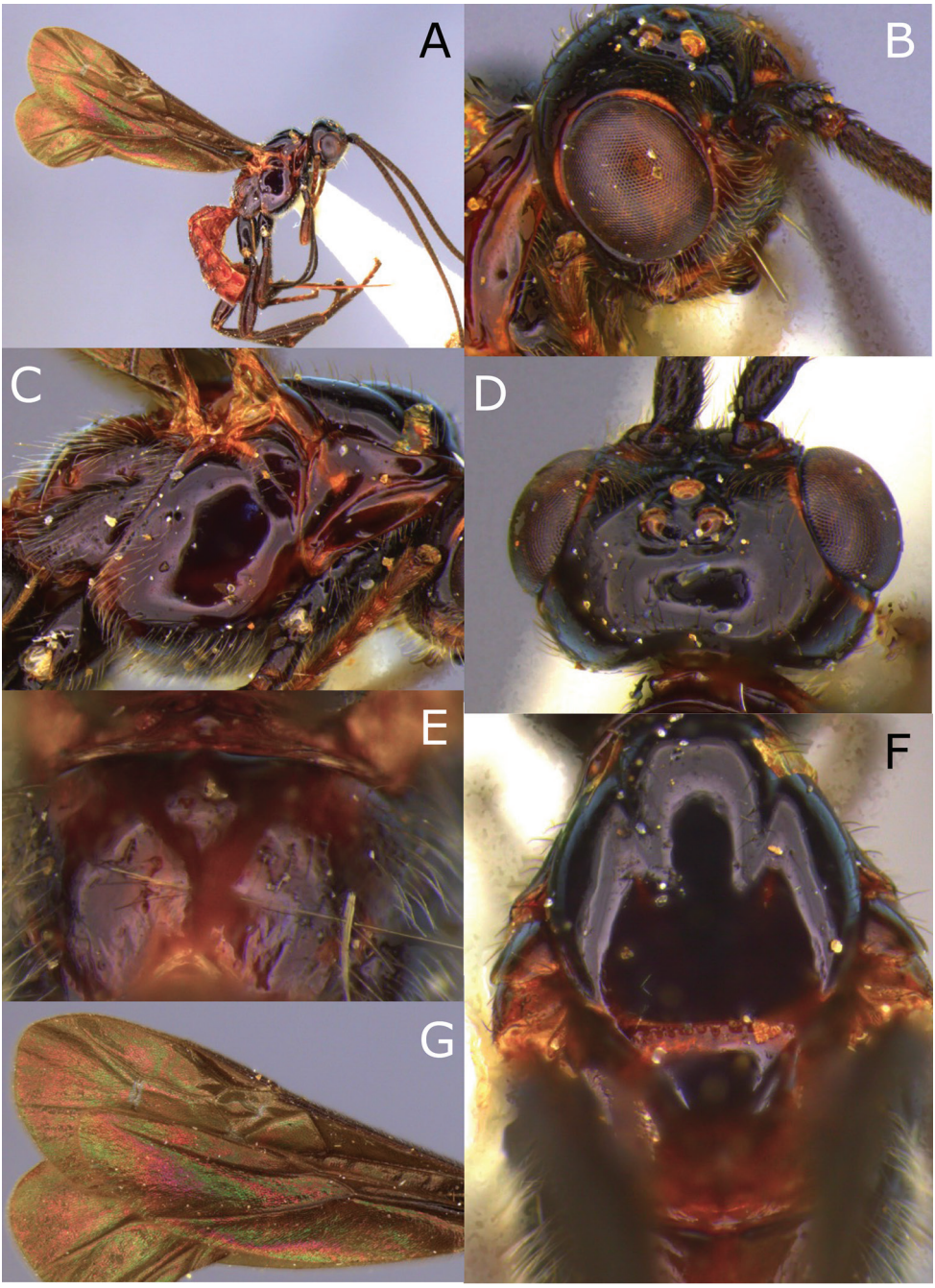

Figure 25. Montaged light micrographs of *Vipio thoracica*. **A** Holotype, habitus lateral view **B** head, oblique view **C** mesosoma, lateral view **D** head, dorsal view **E** propodeum **F** mesoscutum and scutellum, dorsal view **G** wings.

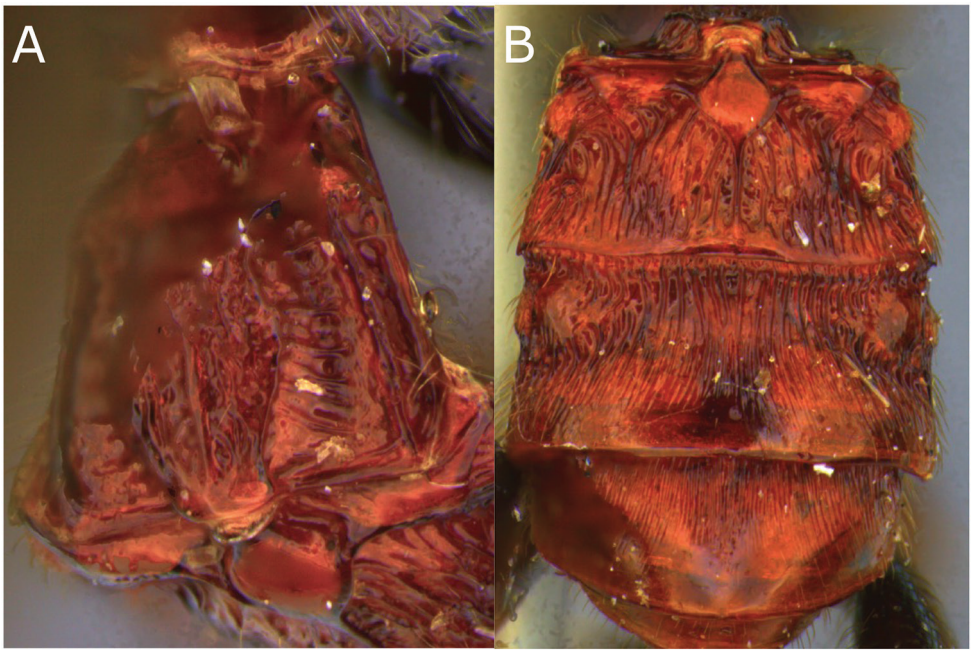

Figure 26. Montaged light micrographs of *Vipio thoracica*. **A** Holotype, metasomal tergite I, oblique dorsal view **B** holotype, metasomal tergites II–IV.

Head. Antenna 1.0–1.1 × body length, with 39–45 flagellomeres; first flagellomere 2.0 × longer than wide, 1.5–1.6 × longer than 2nd, the latter 1.7 × longer than wide; median flagellomeres quadrate; terminal flagellomere acutely pointed apically; head transverse; face smooth; smooth and shiny; clypeus slightly rugulose, clypeal guard setae typical; HL 0.72–0.76 × HH; HW/HH 0.72–0.74; FH/FW 0.56–0.62; EH/HH 0.66–0.69 EH/FW 1.0–1.1; EW/EH 0.70–0.71; ITD 1.61–1.7 × TOD; MS 0.23–0.33 × EH; LMC 0.3 × HH; third segment of maxillary palpus 4.0 × longer than wide.

Mesosoma. Length of mesosoma 1.74–1.8 × height; smooth and shiny; notauli smooth; propodeum smooth.

Wings. Fore wing: length of fore wing 1.0–1.1 × body length; PL/LRC 0.84–0.97; PW/PL 0.22–0.27; length of vein 3RSb 0.86–0.97 × combined length of r-rs and 3RSa; length of vein 1M 0.68–0.71 × length of (RS+M)a; vein 3RSa reaching wing margin 0.69–0.71 × distance between apex of pterostigma and wing tip. Hind wing: uniformly setose; apex of C+SC+R with one basal hamule.

Legs. Claw with pointed basal lobe.

Metasoma. Metasoma widely ovate. First metasomal tergite 0.8–1.3 × longer than wide, raised median area oval, rugose; dorso-lateral carina laminate; T II 2.0–2.25 × wider than long, basal areas smooth, oblique furrows strongly impressed, crenulate; T III 2.2–2.6 × wider than medially long; T III–V longitudinally striate, T III and IV with anterolateral areas; T V–VII smooth and shiny; hypopygium ending at apex of abdomen; ovipositor 0.5 × body length.

Colour. Face yellow, except a black, raised median area; palpi, tip of mandible, vertex, temple, occiput, and antenna black; metasoma reddish yellow to black. Wings smoky.

Male. Unknown.

Remarks. This species resembles the Nearctic species *V. rugator* because of the presence of a raised area on the face, strong dorso-lateral carina of T I, widely ovate and densely striate metasoma, and short hypopygium. The relatively longer ovipositor (ovipositor length/body length 0.5) and reddish black mesosoma separate *thoracica* from *rugator*, in which the ovipositor is shorter (ovipositor length/body length 0.29–0.35) and the metasoma is yellow or reddish yellow.

Conclusions

The genus *Vipio* in the Neotropics is generally uncommon and most of the material available for examination is rather old. It can be noted that at the time of writing, not one Neotropical *Vipio* barcode sequence is listed on The Barcode of Life Data System (BOLD) (www.barcodinglife.org) (Ratnasingham and Hebert 2007) despite extensive Malaise trapping in Costa Rica, French Guiana, and Honduras, and examination of various other Neotropical samples. Currently, the BOLD database contains only 13 specimens of *Vipio*, one from a European Malaise trap and the remainder from an extremely extensive sampling of North America (Young et al. 2012, Steinke et al. 2017, Global Malaise Trap Program 2019). New and freshly collected material would be desirable for carrying out molecular investigation including DNA barcoding to test the current morphological taxonomic hypotheses.

Acknowledgements

We would like to thank the following for the loans of specimens in their care: D. Azuma (ANSP), H.D. Blocker (KSU), R.M. Bohart (USU), R.W. Brooks (SEMC), C.B. de Fernández (IFML), J.F. Genise (MACN), S. Heydon (UCD), T. Huddleston (BMNH), E. Kierych (APSW), Frank Koch (MNHB), B. C. Kondratieff (CSU), J. K. Liebherr (CU), K. C. McGiffen (INHS), P.M. Marsh (USNM), J. Papp (HNHM), M. J. Sharkey and H. Goulet (CNCI), D. Ubick (CAS), D. Wahl (EMUS), F.G. Werner (UA), J. C. Weulersse (MNHN), R.A. Wharton (TAMU), J. Wiley (FSC), and E.O. Wilson (MCZC). Sincere appreciation and gratitude are expressed to Robert J. Lavigne, James K. Wangberg, Jack E. Lloyd (deceased), and Ronald L. Hartman (deceased) for valuable suggestions and critical reading of early versions of this manuscript. Funding for this project was provided by the US-AID TIPAN Project, and the NERC Initiative in Taxonomy. Imaging equipment and additional funding was provided by National Science Foundation grants DEB-10-20751 and DEB 14-42110 (Dimensions of Biodiversity Program). Research support for SRS was partly provided by McIntire-Stennis Grant Project number WYO-530-14, Studies of Parasitoid Wasps of Forest Ecosystems, and McIntire-Stennis Grant Project number WYO-553-15, Studies of Parasitoid Wasps of Associated with the Mountain Pine Beetle. We are grateful to the Rachadaphiseksomphot Fund, Graduate

School, Chulalongkorn University, for the award of a Senior Postdoctoral Fellowship to DLJQ, Office of Higher Education Commission (BDCPG2-160007) and RSPG to BAB. Finally, special thanks to Sadaf for patience, understanding, and support. Any opinions, findings, and conclusions expressed are those of the authors and do not necessarily reflect the views of the National Science Foundation.

References

Ashmead WH (1900) Report on the aculeate Hymenoptera of islands of St. Vincent and Grenada with additions to the parasitic Hymenoptera and a list of the described Hymenoptera of the West Indies. Transactions of the Entomological Society of London 1900: 207–367. https://doi.org/10.1111/j.1365-2311.1900.tb02379.x

Bréthes J (1909) Hymenoptera Paraguayensis. Anales del Museo Nacional de Buenos Aires 19: 225–256.

Bréthes J (1913) Hymenoptera de La America Meridional. Anales del Museo Nacional de Historia Natural de Buenos Aires 24: 35–169.

Brullé A (1846) Suites a' Buffon: Histoire naturelle des insectes: Hymenopteres, vol. 4. Lepeletier de St. Fargeau. Roret, Paris, 689 pp.

Enderlein G (1920) Zur Kenntnis aussereuropäischer Braconiden. Archiv für Naturgeschichte 84A: 51–224. https://doi.org/10.5962/bhl.part.13627

Global Malaise Trap Program (2019) Global Malaise Trap Program. https://biodiversitygenomics.net/projects/gmp/ [accessed 21.ii.2020]

Harris RA (1979) A glossary of surface sculpture. Occasional papers of the Bureau of Entomology of the California Department of Food and Agriculture, Division of Plant Industry 28: 1–31.

Inayatullah M (1992) A systematic study of the genus *Vipio* Latreille. (Ph. D. dissertation in Entomology) University of Wyoming, Laramie, USA.

Inayatullah M, Shaw SR, Quicke DLJ (1998) The genus *Vipio* Latreille (Hymenoptera: Braconidae) of America north of Mexico. Journal of Natural History 32: 117–148. https://doi.org/10.1080/00222939800770071

Inayatullah M, Sabahatullah M, Ain Tahira Q, Ullah R, Haq F (2013) Phylogeny of genus *Vipio* Latrielle (Hymenoptera: Braconidae) and the placement of *moneilemae* group of *Vipio* species based on character weighting. International Journal of Biosciences 3: 115–120. https://doi.org/10.12692/ijb/3.3.115-120

Inayatullah M, Sabahatullah M, Ain Tahira Q (2015) A new species of genus *Vipio* Latreille *Vipio porteri* sp. nov. (Hymenoptera, Braconidae) from Argentina. Journal of Entomology and Zoology Studies 3(2): 131–133.

López-Martínez V, Saavedra-Aguilar M, Delfín-González H, Figueroa-De la Rosa JI, de J García-Ramírez M (2009) New Neotropical distribution records of braconid wasps (Hymenoptera: Braconidae). Neotropical Entomology 38(2): 213–218. https://doi.org/10.1590/S1519-566X2009000200008

Pierce WD (1908) Studies on parasites of the cotton boll weevil. Bulletin of the Bureau of Entomology of the U.S. Department of Agriculture, No. 73, 63 pp. https://doi.org/10.5962/bhl.title.65126

Quicke DLJ (1987) Old world genera of braconine wasps (Hymenoptera: Braconidae). Journal of Natural History 21: 43–157. https://doi.org/10.1080/00222938700770031

Quicke DLJ (1997) Subfamily Braconinae. In: Wharton RA, Marsh PM, Sharkey MJ (Eds) Identification manual to the New World genera of Braconidae. Special Publication of the International Society of Hymenopterists, Washington DC 1: 1148–174.

Quicke DLJ (2015) Biology, Systematics, Evolution and Ecology of Braconid and Ichneumonid Parasitoid Wasps. Wiley Blackwell, Chichester, UK, 681 pp. https://doi.org/10.1002/9781118907085

Quicke DLJ, Genise JF (1994) Reclassification of the Braconinae types described by Bréthes housed in Buenos Aires. Entomologists' Monthly Magazine 130: 35–45.

Quicke DLJ, Sharkey MJ (1989) A key to and notes on the genera of Braconinae (Hymenoptera: Braconidae) from America North of Mexico with description of two new genera and three new species. Canadian Entomologist 121: 337–361. https://doi.org/10.4039/Ent121337-4

Quicke DLJ, van Achterberg C (1990) The type specimens of Enderlein's Braconinae (Hymenoptera: Braconidae) housed in Warsaw. Tijdschrift voor Entomologie 133: 251–264.

Ratnasingham S, Hebert PDN (2007) The Barcode of Life Data System (www.barcodinglife.org). Molecular Ecology Notes 7: 355–364. https://doi.org/10.1111/j.1471-8286.2007.01678.x

Satterthwait AF (1932) How to control bill bugs destructive to cereal and forage crops. Farmers Bulletin of the U.S. Department of Agriculture, No. 1003 (rev. 22), 22 pp.

Sharkey MJ, Wharton RA (1997) Morphology and terminology. In: Wharton RA, Marsh PM, Sharkey MJ (Eds) Identification manual to the New World genera of Braconidae. Special Publication of the International Society of Hymenopterists Washington DC 1: 19–37.

Shenefelt RD (1978) Braconidae 10. Braconinae, Gnathobraconinae, Mesestoinae, Pseudodicrogeniinae, Telengainae, Ypsistocerinae, plus Braconidae in general, major groups, unplaced genera and species. Hymenopterorum Catalogus (nova editio) 15: 1425–1872.

Steinke D, Breton V, Berzitis E, Hebert PDN (2017) The School Malaise Trap Program: coupling educational outreach with scientific discovery. PLoS Biology 15(4): e2001829. https://doi.org/10.1371/journal.pbio.2001829

Szépligeti GV (1904) Hymenoptera. Fam. Braconidae. Genera Insectorum 22: 1–253.

Szépligeti GV (1906) Braconiden aus der Sammlung des Ungarischen National Museums. Annales Historico-Naturales Musei Nationalis Hungarici, Budapest 4: 547–618.

van Achterberg C (1979) A revision of the subfamily Zelinae auct. (Hym., Braconidae). Tijdschriftz voor Entomologie 122: 241–479.

Wharton RA, Marsh PM, Sharkey MJ (1997) Identification manual to the New World genera of Braconidae. Special Publication. The International Society of Hymenopterists, Washington DC 1: 1148–174.

Young MR, Behan-Pelletier VM, Hebert PDN (2012) Revealing the hyperdiverse mite fauna of subarctic Canada through DNA barcoding. PLoS ONE 7(11): e48755. https://doi.org/10.1371/journal.pone.0048755

Yu DSK, van Achterberg C, Horstmann K (2016) Taxapad 2016, Ichneumonoidea 2015. Database on flash-drive, Nepean, Ontario. http://www.taxapad.com

ZooKeys 925: 141–161 (2020)
doi: 10.3897/zookeys.925.49503
http://zookeys.pensoft.net

RESEARCH ARTICLE

A peer-reviewed open-access journal
ZooKeys
Launched to accelerate biodiversity research

New morphological and molecular data for *Xystretrum solidum* (Gorgoderidae, Gorgoderinae) from *Sphoeroides testudineus* (Tetraodontiformes, Tetraodontidae) in Mexican waters

Andrés Martínez-Aquino[1], Jhonny Geovanny García-Teh[2], Fadia Sara Ceccarelli[3], Rogelio Aguilar-Aguilar[4], Víctor Manuel Vidal-Martínez[2], M. Leopoldina Aguirre-Macedo[2]

1 *Facultad de Ciencias, Universidad Autónoma de Baja California, Carretera Transpeninsular 3917, Fraccionamiento Playitas, Ensenada, Baja California 22860, México* **2** *Laboratorio de Patología Acuática, Departamento de Recursos del Mar, Centro de Investigación y de Estudios Avanzados del Instituto Politécnico Nacional, Unidad Mérida, Cordemex, Carretera Antigua a Progreso Km. 6, Mérida, Yucatán, 97310, México* **3** *Departamento de Biología de la Conservación, CONACYT-Centro de Investigación Científica y de Educación Superior de Ensenada, Carretera Ensenada-Tijuana, Ensenada, Baja California, 22860, México* **4** *Departamento de Biología Comparada, Facultad de Ciencias, Universidad Nacional Autónoma de México, Circuito Exterior s/n, Ciudad Universitaria, 04510, Ciudad de México, México*

Corresponding author: M. Leopoldina Aguirre-Macedo (leopoldina.aguirre@cinvestav.mx)

Academic editor: D. Gibson | Received 19 December 2019 | Accepted 21 February 2020 | Published 8 April 2020

http://zoobank.org/2286D72A-5213-4CA3-AA7F-F2EEA2D48133

Citation: Martínez-Aquino A, García-Teh JG, Ceccarelli FS, Aguilar-Aguilar R, Vidal-Martínez VM, Aguirre-Macedo ML (2020) New morphological and molecular data for *Xystretrum solidum* (Gorgoderidae, Gorgoderinae) from *Sphoeroides testudineus* (Tetraodontiformes, Tetraodontidae) in Mexican waters. ZooKeys 925: 141–161. https://doi.org/10.3897/zookeys.925.49503

Abstract

Adults of trematodes in the genus *Xystretrum* Linton, 1910 (Gorgoderidae, Gorgoderinae) are parasites found exclusively in the urinary bladders of tetraodontiform fishes. However, limited and unclear morphological data were used to describe the type species, *X. solidum* Linton, 1910. Here, we present the first detailed morphological information for a member of *Xystretrum*. Morphological characters were described using light and scanning electron microscopy (SEM) of *Xystretrum* specimens from *Sphoeroides testudineus* (Linnaeus) (Tetraodontiformes, Tetraodontidae), collected at six localities off the northern Yucatan Peninsula coast of the Gulf of Mexico. We also compared sequence fragments of the 28S (region D1–D3) ribosomal DNA and mitochondrial Cytochrome c oxidase subunit 1 (COI) gene with those available for

other gorgoderine taxa. We assigned these *Xystretrum* specimens to *X. solidum*, despite the incompleteness of published descriptions. The data provide a foundation for future work to validate the identities of *X. solidum*, *X. papillosum* Linton, 1910 and *X. pulchrum* (Travassos, 1920) with new collections from the type localities and hosts. Comparisons of 28S and COI regions described here also provide an opportunity to evaluate the monophyletic status of *Xystretrum*.

Keywords

COI, molecular phylogenetics and systematics, parasites of marine fishes, scanning electron micrographs, 28S

Introduction

Linton (1910) proposed the genus *Xystretrum* Linton, 1910 (Gorgoderidae, Gorgoderinae) to include two new trematode species, *X. solidum* Linton, 1910 (type species) and *X. papillosum* Linton, 1910, which, as adults, are parasites of tetraodontiform fishes of the families Balistidae (*Balistes capriscus* Gmelin [as *B. carolinensis*] from off Bermuda) and Ostraciidae (*Lactophrys triqueter* (Linnaeus) from Dry Tortugas, Florida, USA). Unfortunately, the original descriptions of both species are incomplete and unclear. This has resulted in taxonomic confusion when new species have been proposed. Several *Xystretrum* species have subsequently been reported, synonymized and later resurrected by some (but not all) authors, while the validity of others remain doubtful (Linton 1907; MacCallum 1917; Manter 1947; Yamaguti 1971; Siddiqi and Cable 1960; Nahhas and Cable 1964; Overstreet 1969).

The most reliable list of species of *Xystretrum* available is the public resource database of the World Register of Marine Species (WoRMS 2020), which lists 14 accepted species. Of these species, *X. solidum* and *X. papillosum*, along with *X. pulchrum* (Travassos, 1920) Manter 1947, are reported from the Northwest Atlantic Ocean and Gulf of Mexico (Linton 1910; Travassos 1922; Manter 1947; Mendoza 2016). However, *X. pulchrum* was also inadequately described from *Sphoeroides testudineus* (Linnaeus) (Tetraodontiformes, Tetraodontidae) collected in the southwestern Atlantic Ocean (Manquinhos State, southeastern Brazil) (Travassos 1922; Manter 1947) and its incomplete description has generated synonyms (e.g., Siddiqi and Cable 1960; Overstreet 1969). *Xystretrum pulchrum* was reported from the type locality of *X. papillosum* (i.e., Tortugas, Florida) and from the North Pacific Ocean (Hawaii), but the morphological data used to separate the two species are questionable (Travassos 1922; Manter 1947; Hanson 1955; Yamaguti 1970). Thus, the morphological descriptions of *X. solidum*, *X. papillosum* and *X. pulchrum* remain incomplete.

Despite the scarce taxonomic information from the western Atlantic, Overstreet et al. (2009) reported *X. solidum* parasitizing the kidneys and urinary bladder of five tetraodontiform fish species from four families (i.e., *B. capriscus* [Balistidae], *L. triqueter* [Ostraciidae], *S. spengleri* Bloch, *S. testudineus* [Tetraodontidae] and *Stephanolepis hispidus* (Linnaeus) [Monacanthidae]) distributed from Bermuda, the Caribbean Sea and the North Gulf of Mexico to the Atlantic coast of South America.

Cutmore et al. (2013) provided the first genetic sequence data for an Atlantic species, tentatively identified as *X. solidum*, from *S. testudineus* collected in the Florida Keys near (200 km in an approximately straight line) Dry Tortugas, the type locality of *X. papillosum*. Recently, Pérez-Ponce de León and Hernández-Mena (2019) provided a second genetic sequence published as *X. solidum* from *Balistes vetula* (Linnaeus) (Balistidae) from Puerto Morelos, Quintana Roo, Mexico, from the Mexican Caribbean.

Several *S. testudineus* from the coasts and lagoons of the Northern Yucatan Peninsula, Mexico were examined for parasites between 1995 and 2013. Gorgoderids were recovered from the urinary bladder of these hosts and preliminarily identified as *Phyllodistomum* sp. (Tello 1999; Pech et al. 2009; Sosa-Medina et al. 2014, 2015). Following a study program to fully characterize parasite biodiversity (Pérez-Ponce de León and Nadler 2010; Nadler and Pérez-Ponce de León 2011), DNA sequences of the 28S gene were obtained from these "*Phyllodistomum* sp." and compared to GenBank sequences available for gorgoderines. A high similarity (BLAST scores) between the "*Phyllodistomum* sp." and trematodes tentatively identified as *X. solidum* by Cutmore et al. (2013) suggests that records for these *Phyllodistomum* should be reassigned to the genus *Xystretrum*.

As Nadler and Pérez-Ponce de León (2011) pointed out, phylogenetic analyses are essential for correctly characterizing a species (including cryptic species) and data from morphological approaches; e.g., morphology, morphometry and microphotographs of scanning electron microscopy (SEM) should be corroborated using molecular-based results. Both morphological and molecular information are lacking for three species of *Xystretrum* found in the Atlantic Ocean (i.e., *X. solidum*, *X. papillosum* and *X. pulchrum*). The intention here is to provide morphological descriptions to support the reassignment of trematodes previously identified as *Phyllodistomum* to *Xystretrum* and to provide new morphological and sequence data to facilitate future revisions of the genus *Xystretrum*.

Materials and methods

Collection of hosts and trematodes

Trematode specimens in this study were collected from the urinary bladder of *Sphoeroides testudineus*. Hosts were collected between 1998 and 2016 (collection permit PPF/DGOPA-070/16 issued by Comisión Nacional de Acuacultura y Pesca, Mexico) at six localities in and off the northern Yucatan Peninsula, Mexico: Celestún tropical lagoon (20°45'N, 90°22'W, June 2005, August 2012, January 2016), Chelem lagoon (21°15'N, 89°45'W, August 2005, March 2007), Ría Lagartos lagoon (21°22'N, 87°30'W, July 2005), Chuburna port (coastal area) (21°15'N, 89°48'W, March 2005), Progreso port (coastal area) (21°16'N, 89°39'W, August 2006), and Chicxulub port (coastal area) (21°17'N, 89°36'W, June 2009) (Fig. 1). Specimens were fixed in 4% hot formalin for morphological treatment or scanning electron micrographs (SEM), or in absolute ethanol for molecular analyses.

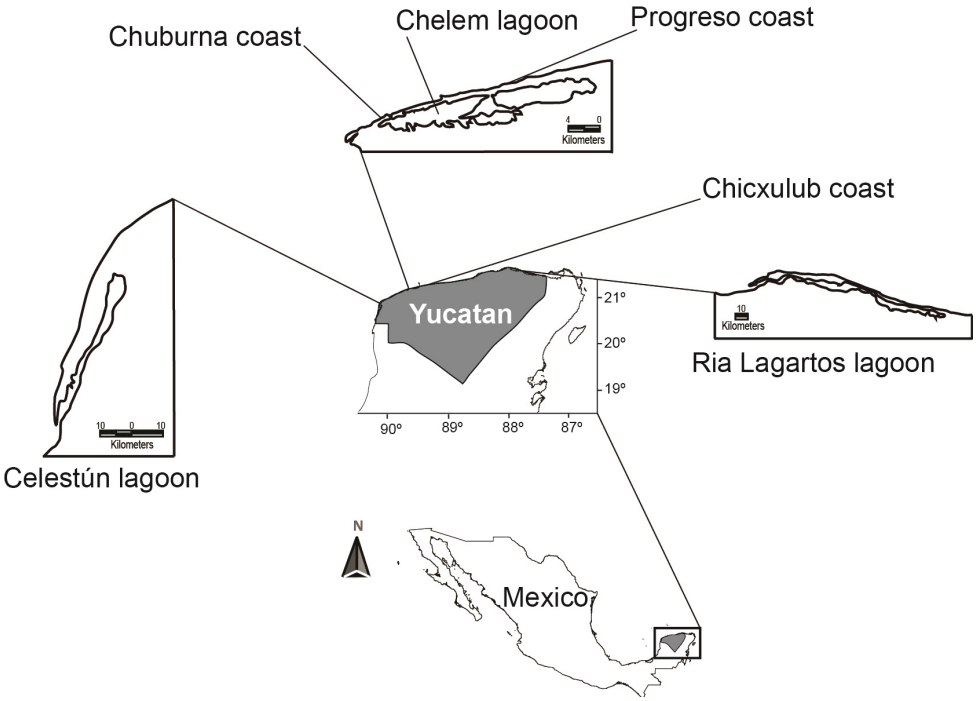

Figure 1. Northern Yucatan Peninsula, Mexico, showing localities where the specimens of *Xystretrum solidum* were collected.

Morphological data and morphometric analyses

Unflattened trematode specimens were stained with Mayer's paracarmine and mounted on permanent slides using Canada balsam. Specimens were measured, and drawings were made with the aid of a drawing tube attached to an Olympus BX50 microscope; measurements are presented in micrometres (µm) as ranges followed by the means in parentheses. For the SEM study, specimens were dehydrated through a graded series of ethyl alcohols and critical point dried with carbon dioxide. Specimens were mounted on metal stubs with silver paste, then coated with gold and examined in a Philips XL30 ESEM for variable pressure SEM at 10 kV. Trematodes were identified following/contrasting the taxonomic criteria of Linton (1907; 1910), Travassos (1922), Manter (1947; 1972), Winter (1959), Overstreet (1969), Yamaguti (1971), Campbell (2008) and Madhavi and Bray (2018). Holotype, labelled as *X. papillosum* (No. 1321174; now in the Smithsonian Institution National Museum of Natural History (NMNH) (ex USNM Helm. Coll. No. 8426) from *Lactophrys triqueter* from Dry Tortugas, Florida, USA, was studied to compare with the newly collected specimens. The *X. solidum* holotype described by Linton in 1907 was not found in the scientific collections in the USA, Europe or Australia, and should be considered lost. Several specimens collected for morphological analysis were deposited as voucher specimens in the Colección Helmintológica del CINVESTAV (CHCM), Departamento de Recursos del Mar, Centro de Investigación y de Estudios Avanzados del Instituto Politécnico

Nacional, Unidad Mérida, Yucatán, Mexico (Tab. 1). Morphological measurements obtained in this study were compared with those of the 14 congeneric *Xystretrum* spp. (Suppl. material 1: Tab. S1).

DNA extraction, PCR amplification and sequencing

Deoxyribonucleic acid (DNA) was extracted from individual adult trematodes; DNA extraction was performed using the DNeasy blood and tissue extraction kit (Qiagen, Valencia, CA, USA) following the manufacturer's instructions. Partial sequences of the 28S (region D1–D3) ribosomal DNA were amplified by Polymerase Chain Reaction (PCR) (Saiki et al. 1988) using 28sl fwd (5´-AAC AGT GCG TGA AAC CGC TC-3´) (Palumbi 1996) and LO rev (5´-GCT ATC CTG AG(AG) GAA ACT TCG- 3´) (Tkach et al. 2000). The primers JB3 fwd (5´-TTT TTT GGG CAT CCT GAG GTT TAT- 3´) (Morgan and Blair 1998) and CO1R trema rev (5´ -CAA CAA ATC ATG ATG CAA AAG G- 3´) (Miura et al. 2005) were used for the COI fragment. The reactions were prepared using the Green GoTaq Master Mix (Promega). This procedure was carried out using an Axygen Maxygen thermocycler. The PCR cycling conditions were as follows: for COI, an initial denaturing step of 3 min at 94 °C, followed by 35 cycles of 92 °C for 30 sec, 47 °C for 45 sec and 72 °C for 90 sec, and a final extension step at 72 °C for 10 min; for 28S, an initial denaturing step of 5 min at 94 °C, followed by 35 cycles of 92 °C for 30 sec, 50 °C for 45 sec and 72 °C for 90 sec, and a final extension step at 72 °C for 10 min. The PCR products were analyzed by electrophoresis in 1% agarose gel using the TAE 1X buffer and observed under UV light using the QIAxcel Advanced System. The purification and sequencing of the PCR products were carried out by Genewiz, South Plainfield, NJ, USA (https://www.genewiz.com/).

Molecular data and phylogenetic reconstruction

To obtain the consensus sequences of specimens of *Xystretrum*, we assembled and edited the chromatograms of forward and reverse sequences using the Geneious Pro

Table 1. Localities sampled (from east to west) for *Sphoeroides testudineus*, the host species of *Xystretrum solidum*, from the Yucatan Peninsula, Yucatan, Mexico. LM = Total number of measured individuals of *X. solidum* used for morphometric studies on light microscope slides. SEM = Total number of individuals of *X. solidum* used for scanning electron micrograph studies. CHCM = Voucher number from the Colección Helmintológica del CINVESTAV (CHCM) for specimens studied in this work.

Localities	LM	SEM	CHCM
Celestún	4	1	529
Chuburna	3	4	530
Chelem	1	1	531
Progreso	6	2	532
Chicxulub	1	–	533
Ría Lagartos	2	3	534

v.5.1.7 platform (Kearse et al. 2012). The 28S and COI partial sequences generated during this study were aligned with sequences of gorgoderids and representative outgroup sequences of members of the Allocreadiidae, Callodistomidae, Dicrocoeliidae and Encyclometridae (see GenBank accession numbers in Figs 2, 3) used previously

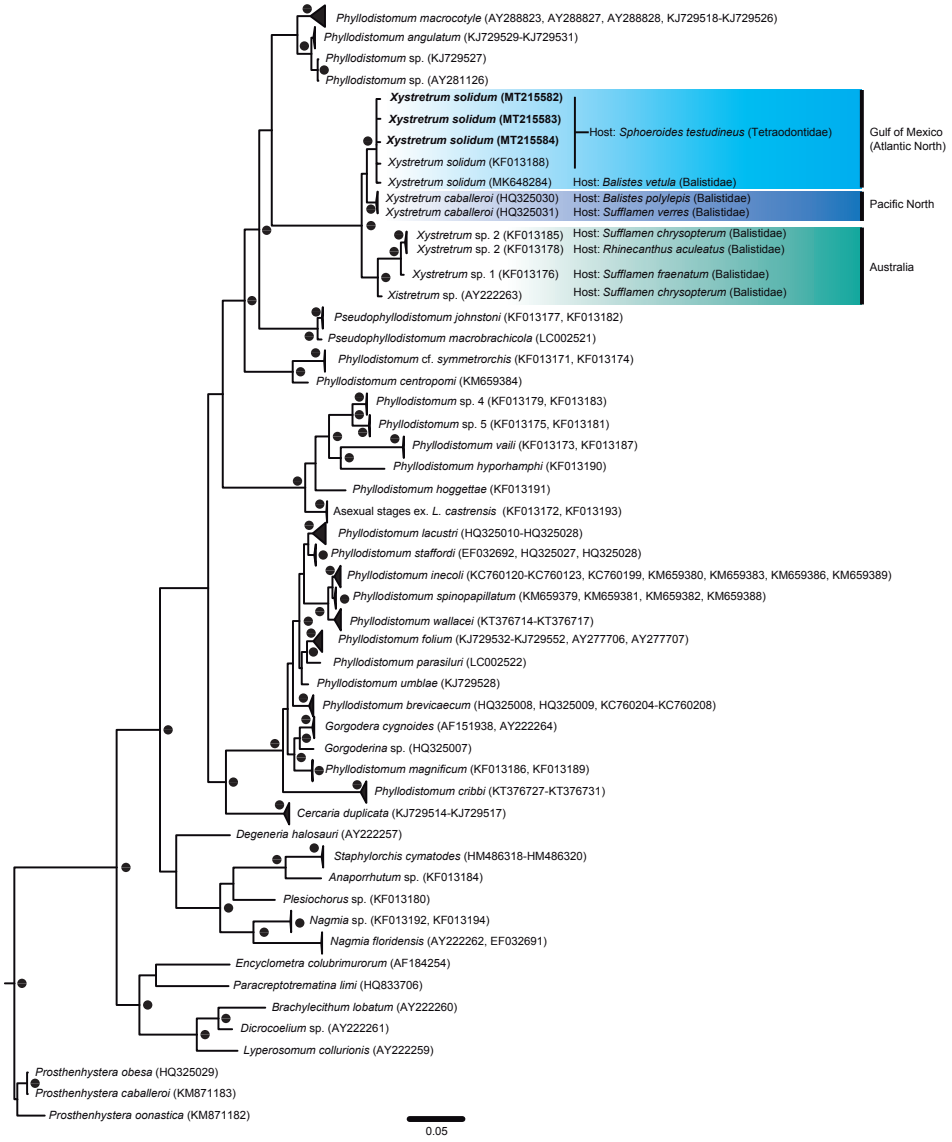

Figure 2. Phylogenetic tree obtained using Bayesian inference for the 28S rRNA dataset. The scale bar represents the number of nucleotide substitutions per site. GenBank accession numbers of the new sequences of *Xystretrum solidum* are shown in bold. Filled circles above/below branches and at the nodes represent Bayesian Posterior Probability ≥ 0.95.

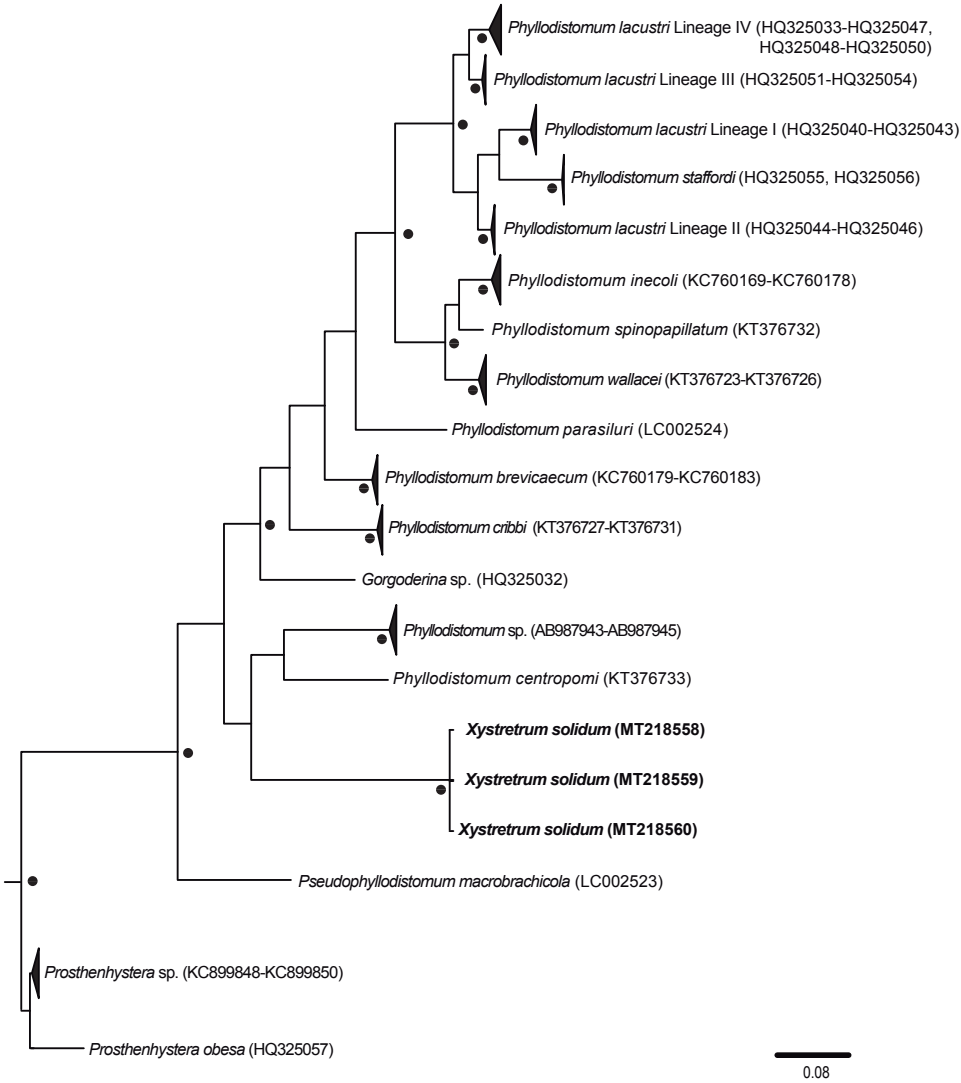

Figure 3. Phylogenetic tree obtained using Bayesian inference for the COI dataset. The scale bar represents the number of nucleotide substitutions per site. GenBank accession numbers of the new sequences of *Xystretrum solidum* are shown in bold. Filled circles above/below branches and at the nodes represent Bayesian Posterior Probability ≥ 0.95.

by Cutmore et al. (2013), Martínez-Aquino et al. (2013), Petkevičiūtė et al. (2015) and Urabe et al. (2015), using an interface available in MAFFT v.7.263 (Katoh and Standley 2016), an "auto" strategy and a gap-opening penalty of 1.53 with Geneious Pro, and a final edition by eye in the same platform. The Gblocks Website v.0.91b (Castresana 2000; Talavera and Castresana 2007) was used to remove ambiguously aligned regions of 28S. To evaluate the sequence and molecular marker utility for phylogenetic analyses at the intended taxonomic level (family level for the complete-

outgroup dataset and genus level for the *Xystretrum* dataset), we tested the nucleotide composition homogeneity within each data alignment (28S and COI matrix data), using chi-squared metric provided in the program TreePuzzle v.5.3.rc (Schmidt et al. 2002). The software jModelTest v.2.1.3 (Darriba et al. 2012) was used to select evolution models through the Bayesian Information Criterion (BIC) (Schwarz 1978) for each dataset separately (28S and COI). The nucleotide substitution model that best fit the 28S dataset was TVM+I+G (Posada 2003). The COI dataset was partitioned into first-, second- and third-codon positions with the appropriate nucleotide substitution model implemented for each codon position (TrN+I for the first [Tamura and Nei 1993]; TPM3uf+I for the second [Kimura 1981]; and HKY+I for the third codon position [Hasegawa et al. 1985]). Furthermore, the net evolutionary distances between *Xystretrum* taxa, using *p*-value with variance estimation, with the Bootstrap method (500 replicates) and with a nucleotide substitution (transitions + transversions) uniform rate, were estimated for the 28S fragment in MEGA v.7.0 (Kumar et al. 2016).

Phylogenetic trees were reconstructed for each gene separately (28S and COI), to test the monophyly of *X. solidum* analyzed in this study. Phylogenetic tree reconstructions were carried out using Bayesian Inference (BI) in MrBayes v.3.2.3 (Ronquist et al. 2012), with two parallel analyses of Metropolis-Coupled Markov Chain Monte Carlo (MCMCMC) for 20×10^6 generations each. Topologies were sampled every 1000 generations and the average standard deviation of split frequencies was observed to be less than 0.01, as suggested by Ronquist et al. (2012). A majority consensus tree with branch lengths was reconstructed for the two runs after discarding the first 5000 sampled trees. The robustness of the clades was assessed using Bayesian Posterior Probability (PP), where PP > 0.95 was considered strongly supported. The Bayesian phylogenetic reconstructions were run through the CIPRES Science Gateway v.3.3 (Miller et al. 2010).

Results

Specimens analyzed were assigned to *Xystretrum solidum* (Figs 4, 5 and Suppl. material 2: Fig. S1). Measurements are of 17 individuals from six localities, and details of the body surface are of 11 gravid specimens from five localities (Tab. 1). New taxonomic and morphometric data: Body flask-shaped, with smooth lateral margins in forebody, 1870–3520 (2750) long, 1020–2100 (1550) wide. Forebody long, narrow, sub-cylindrical, 800–1600 (1170) long, 420–900 (730) wide, representing 35–47% (43%) of total body length. Tegument without spines. Forebody tapered anteriorly. Surface of forebody with elongated and rosette-type papillae (Fig. 5A, B and Suppl. material 2: Fig. S1C). Inner margin of oral sucker covered by fringe arrangement of elongated papillae (Fig. 5C, and Suppl. material 2: Fig. S1A, D, J). Subterminal oral sucker rounded, 200–500 (360) long, 230–450 (330) wide, bearing 14 pairs of well-developed rosette-type papillae, arranged in five pairs on interior margin surrounding mouth;

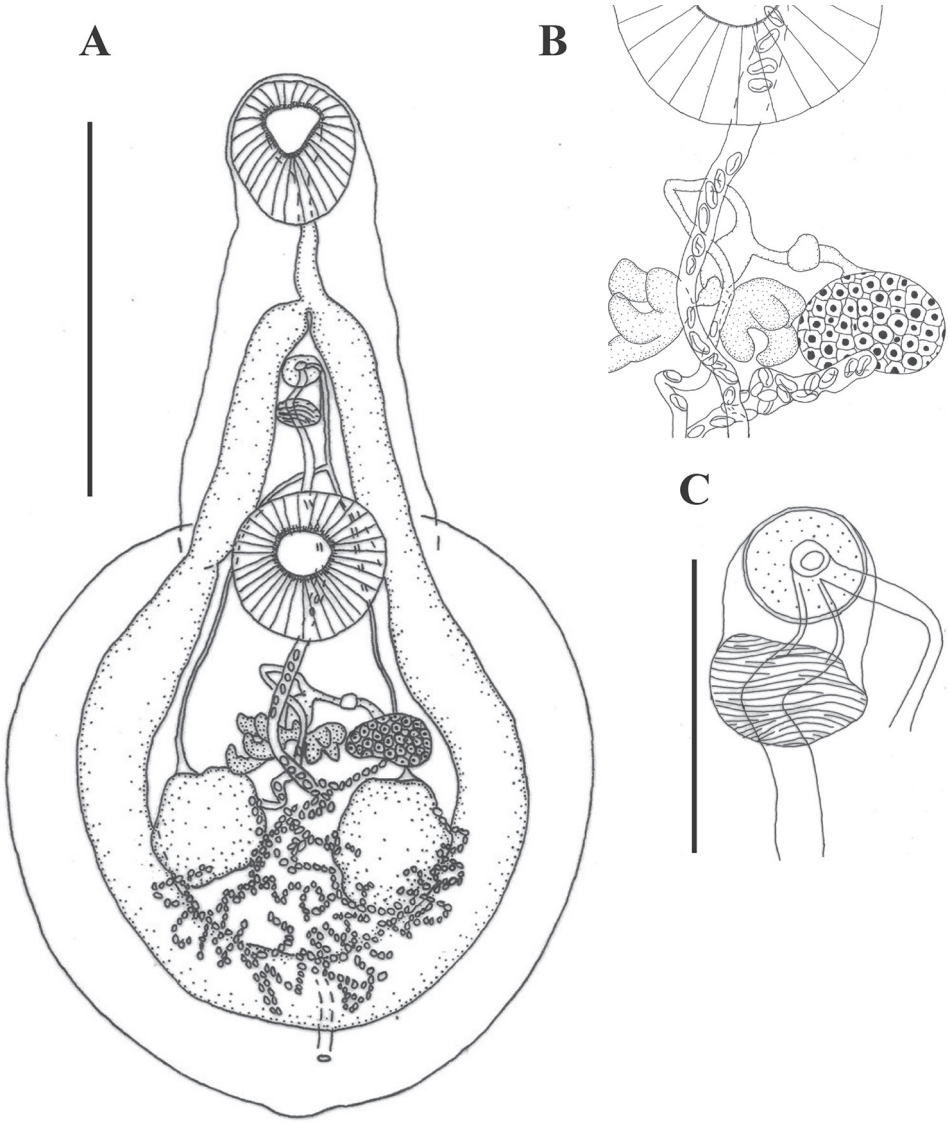

Figure 4. Line drawings of the 532 CHCM-voucher of *Xystretrum solidum* from the urinary bladder of *Sphoeroides testudineus* **A** whole specimen (ventral view) **B** details of reproductive organs **C** details of genital atrium. Scale bars: 1000 µm (**A**); 250 µm (**B–D**).

one pair on posterolateral on interior margin; three pairs on anterolateral to interior margin; two pairs on stylet scar; one pair lateral to stylet scar; one pair on posterior external margin of oral sucker; and one pair inside mouth (Fig. 5C; Suppl. material 2: Fig. S1A, B, D, E, J). Ventral region between oral and ventral suckers with six pairs of robust papillae, arranged in two columns, plus several pairs of small papillae (between six and 10) at the lateral borders of this region, and six to seven additional pairs

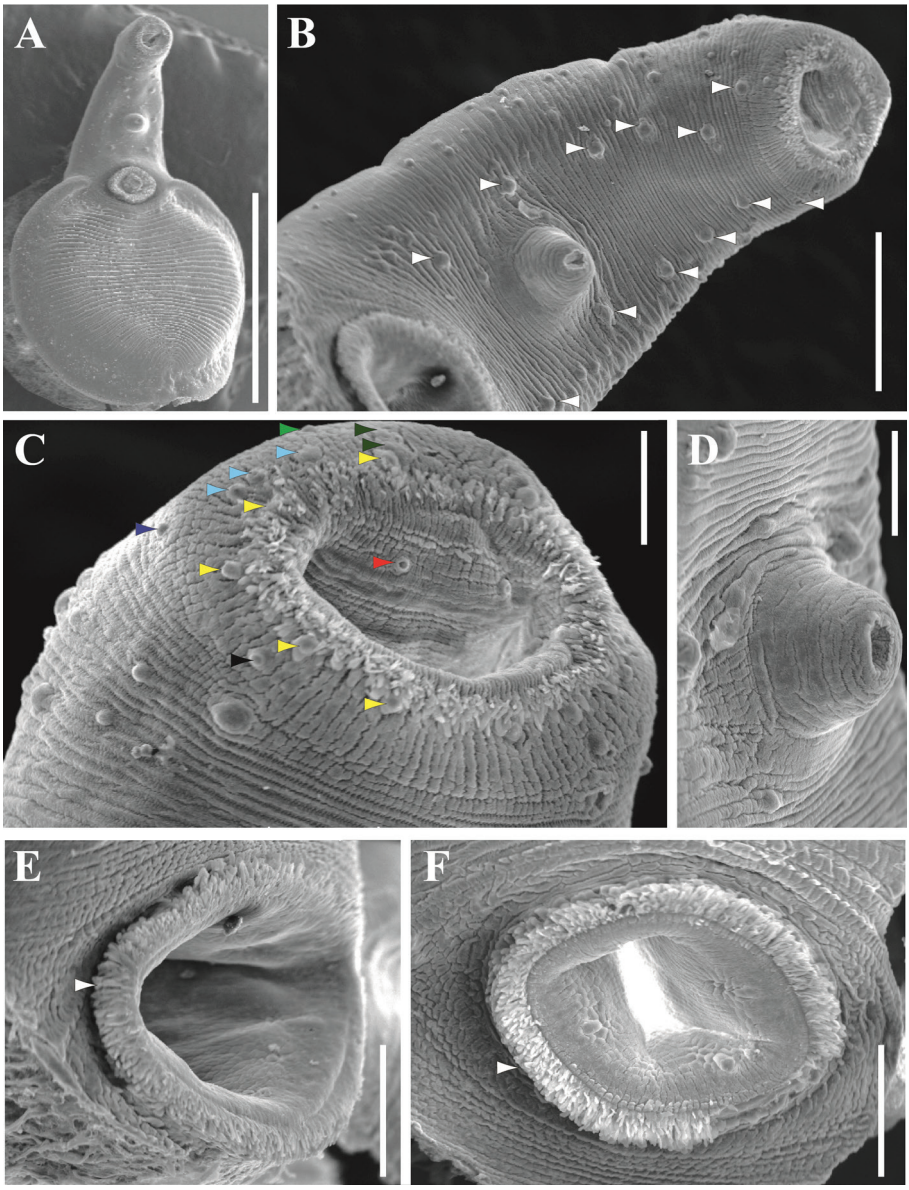

Figure 5. Scanning electron microscopy (SEM) images of *Xystretrum solidum* (from three specimens collected at Progreso Port, Yucatan, Mexico) **A** whole adult specimen (ventral view) with scattered rosette papillae on forebody **B** forebody, showing 6 pairs of robust papillae (white arrowhead) **C** oral sucker, showing 13 pairs of papillae: 5 on interior margin surrounding mouth (yellow arrowhead); one posterolateral to interior margin (dark blue arrowhead); three anterolateral to interior margin (light blue arrowhead); 2 on stylet scar (dark green arrowhead); one lateral to stylet scar (light green arrowhead); one on posterior external margin of oral sucker (black arrowhead); one inside of mouth (red arrowhead) (only right hand side papillae are indicated) **D** genital atrium detail **E** ventral sucker (side view), showing long papillae on inner margin (white arrowhead) **F** ventral sucker (ventral view), showing long papillae on inner margin (white arrowhead). Scale bars: 1000 µm (**A**); 200 µm (**B**); 500 µm (**C, D**); 100 µm (**E, F**). For more details of observed characters by SEM from other localities analyzed in this study, see Suppl. material 2: Figure S1.

distributed heterogeneously (Figs. 5B and Suppl. material 2: Fig. S1C). Hindbody oval in outline, foliaceus, corrugated and demarcated by folds, 1000–2050 (1590) long, 1020–2100 (1550) wide; papillae absent in this region, except for long papillae covering inner margin of ventral sucker, but marked grooves are present (Fig. 5E, F and Suppl. material 2: Fig. S1G, H). Ventral sucker muscular, slightly pre-equatorial, 270–560 (430) long, 300–580 (450) wide. Sucker ratio 1:1.30 (1.05–1.89). Pharynx absent. Oesophagus 150–260 (200) long, 50–130 (90) wide. Intestinal bifurcation in first third of body, 360–690 (530) from anterior end. Caeca long, narrow, running laterally into hindbody, joining close to posterior extremity of body forming cyclocoel, 3190–6130 (4580) long, 90–210 (160) wide; post-caecal space 120–330 (200) long. Testes two, irregular, slightly symmetrical, rounded, inter-caecal in middle of hindbody; left testis 210–420 (300) long, 140–460 (310) wide; right testis 210–460 (300) long, 240–480 (330) wide. Efferent ducts anterior to ventral sucker, forming *vas deferens*. Seminal vesicle tubular, posterior to intestinal bifurcation, 120–360 (220) long, 80–130 (100) wide. Pseudosinus-sac present. Genital pore immediately posterior to intestinal bifurcation, 450–980 (690) from anterior extremity. Ovary smooth, oval, sinistral, anterior to right testis, 110–190 (150) long, 140–300 (200) wide. Oviduct connected to common vitelline duct. Vitellarium in two symmetrical, lobed masses (3–4 lobes), conspicuous vitelloduct intersections present in terminal part of second third of the body; masses 140–280 (180) long, 80–290 (160) wide. Uterus distributed in inter-caecal area, forming several loops, sometimes overlapping caeca slightly at level of middle and posterior part of body (Fig. 4A). Eggs elliptical, 30–60 (50) long, 20–30 (20) wide. Excretory vesicle I-shaped; excretory pore subterminal, dorsal, 90–250 (160) from posterior end of body.

Host: *Sphoeroides testudineus* (Tetraodontidae).

Site: Urinary bladder.

Localities: Dry Tortugas, Florida, USA (Gulf of Mexico). New localities from the Northern Yucatan Peninsula, Mexico: Celestún tropical lagoon (20°45'N, 90°22'W), Chelem lagoon (21°15'N, 89°45'W), Ría Lagartos lagoon (21°22'N, 87°30'W), Chuburna port (coastal area) (21°15'N, 89°48'W), Progreso port (coastal area) (21°16'N, 89°39'W), Chicxulub port (coastal area) (21°17'N; 89°36'W).

GenBank accession numbers: 28S rDNA sequences: MT215582–MT215584; COI mtDNA sequences: MT218558–MT218560.

DNA sequences and dataset analyses

In total, 12 bi-directional 28S and COI sequences were obtained from three individual adults of *X. solidum*. The final lengths (in number of base-pairs) of the 28S ribosomal sequence fragment were 892 (for two sequences) and 899 (for one sequence), with zero genetic variation, either among the new sequences or in the published 28S sequences of *X. solidum* (GenBank accession numbers MK648284 and KF013188). The total alignment length following the Gblocks exclusion was 814 bp. Nucleotide sequence variation in the 28S alignment from gorgoderids (excluding the outgroup taxon) in-

cluded 330 conserved sites, 483 variable sites, 410 parsimony-informative sites and 73 singleton sites. The COI dataset consisted of 309 bp with a genetic distance of 0.3% between the three mitochondrial sequences. Nucleotide sequence variation (excluding the outgroup taxa) for each partition from COI (first, second and third codon positions) was 70/92/12 conserved, 33/11/91 variable, 29/7/79 parsimony-informative and 4/4/12 single sites, respectively.

Phylogenetic reconstructions

We inferred the phylogenetic relationships from the 28S and COI sequence matrices separately. The 28S gene dataset contained 46 taxa (150 sequences) and the COI contained 18 taxa (63 sequences). Figures 2 and 3 show the phylogenetic topologies resulting from 28S and COI dataset analyses, respectively. The 28S tree shows that the sequences generated in this study form a clade with the sequences from the material tentatively identified as *X. solidum* (sequence KF013188) by Cutmore et al. (2013) and *X. solidum* (sequence MK648284) from *B. vetula* in the Gulf of Mexico (see below). Furthermore, in the 28S tree, species of *Xystretrum* form a monophyletic group, with high nodal support values (PP ≥ 0.95) (Fig. 2). The COI tree shows that all sequences of *X. solidum* form a clade (Fig. 3). Based on the phylogenetic trees constructed from the 28S dataset, the taxa most closely related to *Xystretrum* spp. are members of the genus *Phyllodistomum* (i.e., *Phyllodistomum angulatum* Linstow, 1907, *P. macrocotyle* Lühe, 1909 and *Phyllodistomum* sp.), whereas the relatives of the species *X. solidum*, based on the COI dataset, were *Phyllodistomum centropomi* Mendoza-Garfias & Pérez-Ponce de León, 2005 and *Phyllodistomum* sp. (Fig. 3). The differences in topology between the two trees are most likely due to the differences in the taxa included in the two datasets. The genetic distance values from the 28S dataset of *X. solidum*, when compared with *Xystretrum* spp., were 2.74 %, 3.50 %, 5.02 % and 5.02 % for *X. caballeroi*, *Xystretrum* sp., *Xystretrum* sp. 1 and *Xystretrum* sp. 2, respectively.

Discussion

The morphologies of the trematodes examined in this study are consistent with those of the genus *Xystretrum* provided by Campbell (2008); i.e., intestinal caeca forming a cyclocoel, presence of a pseudosinus-sac, and a corrugated hindbody demarcated by folds. This study adds detail to those descriptions by providing new morphological and morphometric data and revealing characters not previously described, such as the number of papillae on the tegument and oral sucker. However, the published descriptions for the species of *Xystretrum* are very basic, particularly from the American Atlantic, i.e., *X. solidum*, *X. papillosum* and *X. pulchrum*. Body size range (i.e., length) is the primary character used to distinguish these three species. *Xystretrum solidum* is the smallest (i.e., 1750), *X. papillosum* is intermediate (i.e., 2100) (a size that corre-

sponds to the samples analyzed in this study) and *X. pulchrum* is the largest (i.e., 4500). However, since there are no data on intraspecific morphological variation for the three species, it is impossible to decide whether body size is sufficient for the correct identification of our specimens. There are several impediments to species-level identification, including: 1) scarce morphological data from congeners, and particularly the limited measurements for *X. solidum* and *X. papillosum*, 2) voucher material (holotype) apparently lost for *X. solidum*, and 3) incongruences in the host specificity patterns previously reported for *Xystretrum* spp. at family level. For these reasons and based on the genetic similarities and the phylogenetic relationships obtained in this study, we agree with the proposal of Cutmore et al. (2013) and identify our samples as *X. solidum*.

Based on the observation of material from this study, plus the holotype of *X. papillosum* (voucher 1321174), we found that *X. solidum* presents a fluted tegument on the hindbody and that along the dorsoventral margin there are short dense fringe papillae (only readily visible using SEM, see Suppl. material 2: Fig. S1I), which were referred to as "hair-like spines" by Manter (1947; page 330) but without mentioning their exact location. The material examined in this study shows a relatively broad range of polymorphism.

It is necessary to collect new *X. solidum* specimens from the original host (i.e., *B. capriscus*) and the type locality (i.e., off Bermuda) to compare their morphological measurements with our samples. Also, it is necessary to explore the possible presence of *X. papillosum* from *L. triqueter* co-distributed with *B. capriscus* off Bermuda, as part of a taxonomic revision of the genus *Xystretrum*, taking into consideration the morphological data presented here. In parallel, future revisions should seek to distinguish or synonymize *X. solidum*, *X. papillosum* and *X. pulchrum*, while being sensitive to the potential presence of cryptic species.

To date, 14 species of the genus *Xystretrum* are considered valid (WoRMS 2020). From a purely biogeographical standpoint, most of these species are non-conspecific with our material, as they have been reported from unique marine regions other than the Gulf of Mexico. This gives them a set of host-associations and biogeographical differences with respect to the remaining species. Thus, species such as *X. chauhani* Ahmad, 1982, *X. manteri* Ahmad, 1982, *X. overstreeti* Ahmad, 1982, *X. srivastavai* Ahmad, 1982 and *X. thapari* Ahmad, 1982 appear to be confined to the Arabian Sea; *X. abalistis* Parukhin, 1964 occurs in the Gulf of Tonkin (South China Sea); *X. triacanthi* Ahmad & Gupta, 1985 occurs off the Indian coast of the Bay of Bengal (Indian Ocean) (Madhavi and Bray 2018); *X. moretonense* Manter, 1972 and *X. plicoporatum* Manter, 1972 inhabit Australian waters (Manter 1972); and *X. caballeroi* Bravo-Hollis, 1953 and *X. hawaiiense* Yamaguti, 1970 are distributed in various parts of the Pacific Ocean (Bravo-Hollis 1953; Winter 1959; Parukhin 1964; Yamaguti 1970; Arthur and Te 2006; Mendoza 2016). An additional marine region, extending through the Western Atlantic from Brazil to Bermuda and the Gulf of Mexico, harbors the species *X. solidum*, *X. papillosum* and *X. pulchrum* described from members of the Balistidae, Ostraciidae and Tetraodontidae, respectively. The fact that the latter species are geographically sympatric and were described some time ago, resulting in a confused taxo-

nomic characterization, suggests that the published records may indicate incorrect host assignments and host localities.

In the phylogenetic tree obtained from the 28S dataset, all members of the genus *Xystretrum* included in the analysis formed a well-supported clade, but without nodal support with their sister clade. A similar result has been reported in previous phylogenetic analyses carried out for similar taxa using the same gene (e.g., Cutmore et al. 2013; Razo-Mendivil et al. 2013; Pérez-Ponce de León et al. 2015; Petkevičiūtė et al. 2015; Urabe et al. 2015; Stunžėnas et al. 2017). Cutmore et al. (2013) detected that the species of *Xystretrum* genus are not closely related to marine representatives of the family Gorgoderidae. At the present time, species of *Xystretrum* appear related to the freshwater *Phyllodistomum* spp. Even though the *Xystretrum* clade did not exhibit a high nodal support based on the 28S dataset in this study, a phylogenetic relationship with freshwater phyllodistomid trematodes was observed, e.g., *Phyllodistomum* sp., *P. angulatum* and *P. macrocotyle* (see also Stunžėnas et al. 2004; Petkevičiūtė et al. 2015). Because of the incomplete dataset of gene sequences for *Xystretrum* spp., the phylogenetic relationships of this genus remain unclear. Based on the 28S phylogenetic tree topology, *X. solidum* (found in Tetraodontidae and Balistidae) seems to be related to *X. caballeroi* (although lacking nodal support). Current phylogenetic information confirms another sub-clade, which includes samples of *Xystretrum* associated with the Balistidae from the Coral Sea, Australia and the Indian Ocean off Western Australia (as *Xystretrum* sp., *Xystretrum* sp. 1 and *Xystretrum* sp. 2 in Cutmore et al. [2013]).

The COI phylogenetic topology shows a clade with *X. solidum* from this study, and the clade formed by the freshwater taxa *P. centropomi* + *Phyllodistomum* sp. (from Urabe et al. [2015]) as sister, although this relationship does not have nodal support. However, based on COI phylogenetic topology plus 28S, it is possible to suggest a diversification of the most recent common ancestor of *Xystretrum* from freshwater to marine environments, and a subsequent diversification in tetraodontiforms via host-switching events. A similar evolutionary process of transition from freshwater to marine environments has also been suggested for other platyhelminth groups (e.g., Álvarez-Presas et al. 2008; Van Steenkiste et al. 2013; Martínez-Aquino et al. 2017).

As indicated by Cutmore et al. (2013), *Xystretrum* occurs only in marine fishes of the order Tetraodontiformes; however, patterns of host specificity at the family level for each species of *Xystretrum* are not currently well-defined. For example, in the reported cases of *X. solidum* from the American Atlantic, Overstreet et al. (2009) recorded *X. solidum* associated with five tetraodontiform fish species included in four families, including the host species from which *X. papillosum* and *X. pulchrum* were described, i.e., *L. triqueter* and *S. testudineus*, respectively. Furthermore, the recently published sequence by Pérez-Ponce de León and Hernández-Mena (2019) (sequences MK648284) suggests that *X. solidum* is associated with both the Tetraodontidae and Balistidae. Although there are efforts to build molecular libraries of parasite biodiversity (Pérez-Ponce de León and Nadler 2010; Nadler and Pérez-Ponce de León 2011), DNA sequences of parasites with little or no morphological support continue to be generated, primarily due to incomplete taxonomic descriptions. Here, we pro-

vide molecular sequences supported by detailed morphological description, which can provide a foundation for future comparisons and revisions within *Xystretrum* and the Gorgoderidae.

Acknowledgments

Our thanks go to the staff of the laboratory of the Patología Acuática: Gregory Arjona-Torres, Francisco Puc-Itzá, Clara Vivas and Nadia Herrera Castillo from CINVESTAV-IPN, Unidad Mérida, Mexico. We are indebted to Dr. José Q. García-Maldonado for lending us space for sequencing and to MSc. Abril Gamboa-Muñoz for technical assistance in the molecular lab. We are grateful to Anna Philips and Freya Goetz, Museum Technician and Curator of the Clitellata and Parasitic Worms at the Smithsonian Institution National Museum of Natural History, USA, for the loan of the *X. papillosum* holotype. Dr. Cristina Damborenea (Curator of Colección Helminthológica of Museo de La Plata, Argentina [MLP-He]), Dr. Fabiana B. Drago (MLP-He), Dr. Melissa Q. Cárdenas (Laboratório de Helmintos Parasitos de Peixes, Instituto Oswaldo Cruz, Brasil), and Dr. Carlos Mendoza-Palmero (Institute of Parasitology, Czech Republic) kindly helped with the literature on *Xystretrum* spp. Our thanks also go to Dr. John Mclaughlin and the editor Dr. David Gibson for reviewing the manuscript and greatly improving the style and grammar. Special thanks are due to Beatriz Heredia-Cervera and Ana Ruth Cristobal Ramos, at the CLSM and SEM unit at CINVESTAV-IPN-Unidad Mérida, Mexico. AM-A thanks Dr. Juan Tapia, Director of the Facultad de Ciencias, UABC, for invaluable support during the writing of the present work. JGG-T thanks CONACyT for a scholarship to accomplish his MSc degree within the Posgrado en Biología Marina, CINVESTAV–IPN, Mérida, Yucatán, Mexico. Financial support for AM-A at the Laboratory of Aquatic Pathology, CINVESTAV–IPN came from Grant No. 201441 SENER Hidrocarburos–CONACYT.

References

Álvarez-Presas M, Baguñà J, Riutort M (2008) Molecular phylogeny of land and freshwater planarians (Tricladida, Platyhelminthes): from freshwater to land and back. Molecular Phylogenetics and Evolution 47: 555–568. https://doi.org/10.1016/j.ympev.2008.01.032

Arthur JR, Te BQ (2006) Checklist of the Parasites of Fishes of Vietnam. FAO Fisheries Technical Paper 369/2, Rome, 133 pp.

Bravo-Hollis M (1953) Dos nuevos tremátodos digéneos de peces de las costas del Pacífico Anales del Instituto de Biología, Universidad Nacional Autónoma de México 24: 415–424.

Campbell RA (2008) Family Gorgoderidae Looss, 1899. In: Bray RA, Gibson DI, Jones A (Eds) Keys to the Trematoda (Vol. 3). CAB International, Wallingford, 191–213. https://doi.org/10.1079/9780851995885.0191

Castresana J (2000) Selection of conserved blocks from multiple alignments for their use in phylogenetic analysis. Molecular Biology and Evolution 17: 540–552. https://doi.org/10.1093/oxfordjournals.molbev.a026334

Cutmore SC, Miller TL, Curran SS, Bennett MB, Cribb TH (2013) Phylogenetic relationships of the Gorgoderidae (Platyhelminthes: Trematoda), including the proposal of a new subfamily (Degeneriinae n. subfam.). Parasitology Research 112: 3063–3074. https://doi.org/10.1007/s00436-013-3481-5

Darriba D, Taboada GL, Doallo R, Posada D (2012) jModelTest 2: more models, new heuristics and parallel computing. Nature Methods 9: 1–772. https://doi.org/10.1038/nmeth.2109

Hanson ML (1955) Some digenetic trematodes of plectognath fishes of Hawaii. Proceedings of the Helminthological Society of Washington 22: 76–87.

Hasegawa M, Kishino H, Yano T (1985) Dating of the human-ape splitting by a molecular clock of mitochondrial DNA. Journal of Molecular Evolution 22: 160–174. https://doi.org/10.1007/BF02101694

Katoh K, Standley DM (2016) A simple method to control over-alignment in the MAFFT multiple sequence alignment program. Bioinformatics 32: 1933–1942. https://doi.org/10.1093/bioinformatics/btw108

Kimura M (1981) Estimation of evolutionary distances between homologous nucleotide sequences. Proceedings of the National Academy of Sciences 78: 454–458. https://doi.org/10.1073/pnas.78.1.454

Kearse M, Moir R, Wilson A, Stones-Havas S, Cheung M, Sturrock S, Buxton S, Cooper A, Markowitz S, Duran C, Thierer T, Ashton B, Meintjes P, Drummond A (2012) Geneious Basic: an integrated and extendable desktop software platform for the organization and analysis of sequence data. Bioinformatics 28: 1647–1649. https://doi.org/10.1093/bioinformatics/bts199

Kumar S, Stecher G, Tamura K (2016) MEGA7: Molecular Evolutionary Genetics Analysis version 7.0 for bigger datasets. Molecular Biology and Evolution 33: 1870–1874. https://doi.org/10.1093/molbev/msw054

Linton E (1907) Notes on parasites of Bermudas fishes. Proceedings of the United States National Museum 23: 85–126. https://doi.org/10.5479/si.00963801.33-1560.85

Linton E (1910) Helminth fauna of the Dry Tortugas. II. Trematodes. Papers of the Tortugas Laboratory of the Carnegie Institute of Washington 4: 11–98.

MacCallum GA (1917) Some new forms of parasitic worms. Zoopathology 1: 43–75.

Madhavi R, Bray RA (2018) Superfamily Gorgoderoidea Looss, 1899. In: Madhavi R, Bray RA (Eds) Digenetic Trematodes of Indian Marine Fishes. Crown, 551–565. https://doi.org/10.1007/978-94-024-1535-3_17

Manter HW (1947) The digenetic trematodes of marine fishes of Tortugas, Florida. American Midland Naturalist 38: 257–416. https://doi.org/10.2307/2421571

Manter HW (1972) Two new species of *Xystretrum* Linton, 1910 (Trematoda: Gorgoderidae) from fishes of Queensland, Australia. Anales del Instituto de Biología, Universidad Nacional Autónoma de México 41: 93–98.

Martínez-Aquino A, Ceccarelli SF, Pérez-Ponce de León G (2013) Molecular phylogeny of the genus *Margotrema* (Digenea: Allocreadiidae), parasitic flatworms of goodeid freshwater fish-

es across central Mexico: species boundaries, host-specificity, and geographical congruence. Zoological Journal of the Linnean Society 168: 1–16. https://doi.org/10.1111/zoj.12027

Martínez-Aquino A, Vidal-Martínez VM, Aguirre-Macedo ML (2017) A molecular phylogenetic appraisal of the acanthostomines *Acanthostomum* and *Timoniella* and their position within Cryptogonimidae (Trematoda: Opisthorchioidea). PeerJ 5: e4158. https://doi.org/10.7717/peerj.4158

Mendoza M (2016) Infracomunidad parasitaria de *Balistes polylepis* Steindachner, 1876 (Tetraodontiformes: Balistidae) en tres localidaes del municipio de La Paz, Baja California Sur, México. BSc thesis, La Paz, Baja California Sur, Mexico: Universidad Autonóma de Baja California Sur.

Miller MA, Pfeiffer W, Schwartz T (2010) Creating the CIPRES Science Gateway for Inference of Large Phylogenetic Trees. Proceedings of the Gateway Computing Environments Workshop (GCE) November 2010. IEEE, New Orleans, 8 pp. https://doi.org/10.1109/GCE.2010.5676129

Miura O, Kuris AM, Torchin ME, Hechinger RF, Dunham EJ, Chiba S (2005) Molecular-genetic analyses reveal cryptic species of trematodes in the interdial gastropod, *Batillaria cumingi* (Crosse). International Journal for Parasitology 35: 793–801. https://doi.org/10.1016/j.ijpara.2005.02.014

Morgan JAT, Blair D (1998) Relative merits of nuclear ribosomal internal transcribed spacers and mitochondrial CO1 and ND1 genes for distinguishing among *Echinostoma* species (Trematoda). Parasitology 116: 289–297. https://doi.org/10.1017/S0031182097002217

Nadler S, Pérez-Ponce de León G (2011) Integrating molecular and morphological approaches for characterizing parasite cryptic species: implications for parasitology. Parasitology 138: 1688–1709. https://doi.org/10.1017/S003118201000168X

Nahhas FM, Cable RM (1964) Digenetic and aspidogastrid trematodes from marine fishes of Curaçao and Jamaica. Tulane Studies in Zoology and Botany 11: 167–228. https://doi.org/10.5962/bhl.part.7052

Overstreet RM, Cook JC, Heard RH (2009) Trematoda (Platyhelminthes) of the Gulf of Mexico. In: Felder DL, Camp DK (Eds) Gulf of Mexico – Origins, Waters, and Biota. Biodiversity. Texas A&M University Press, College Station, 419–486.

Overstreet RM (1969) Digenetic trematodes of marine teleost fishes from Biscayne Bay, Florida. Tulane Studies in Zoology and Botany 15: 119–176. https://digitalcommons.unl.edu/parasitologyfacpubs/867

Palumbi SR (1996) Nucleic acids II: the polymerase chain reaction. In: Hillis DM, Moritz C, Mable BK (Eds) Molecular Systematics. Sinauer Associates, Sunderland, 205–247.

Parukhin AM (1964) A new trematode of the family Gorgoderidae Looss, 1901. Helminthologia 5: 123–124.

Pech D, Vidal-Martínez VM, Aguirre-Macedo ML, Gold-Bouchot G, Herrera-Silveira J, Zapata-Pérez O, Marcogliese DJ (2009) The checkered puffer (*Sphoeroides testudineus*) and its helminths as bioindicators of chemical pollution in Yucatan coastal lagoons. Science of the Total Environment 407, 2315–2324. https://doi.org/10.1016/j.scitotenv.2008.11.054

Pérez-Ponce de León G, Hernández-Mena DI (2019) Testing the higher-level phylogenetic classification of Digenea (Platyhelminthes, Trematoda) based on nuclear rDNA sequences

before entering the age of the 'next-generation' Tree of Life. Journal of Helminthology 93: 260–276. https://doi.org/10.1017/S0022149X19000191

Pérez-Ponce de León G, Nadler S (2010) What we don't recognize can hurt us: a plea for awareness about cryptic species. Journal of Parasitology 96: 453–464. https://doi.org/10.1645/GE-2260.1

Pérez-Ponce de León G, Martinez-Aquino A, Mendoza-Garfias B (2015) Two new species of *Phyllodistomum* Braun, 1899 (Digenea: Gorgoderidae), from freshwater fishes (Cyprinodontiformes: Goodeidae: Goodeinae) in central Mexico: an integrative taxonomy approach using morphology, ultrastructure and molecular phylogenetics. Zootaxa 4013: 87–99. https://doi.org/10.11646/zootaxa.4013.1.6

Petkevičiūtė R, Stunžėnas V, Stanevičiūtė G, Zhokhov AE (2015) European *Phyllodistomum* (Digenea, Gorgoderidae) and phylogenetic affinities of *Cercaria duplicata* based on rDNA and karyotypes. Zoologica Scripta 44: 191–202. https://doi.org/10.1111/zsc.12080

Posada D (2003) Using MODELTEST and PAUP* to select a model of nucleotide substitution. In: Baxevanis AD, Davison DB, Page RDM, Petsko GA, Stein LD, Stormo GD (Eds) Current Protocols in Bioinformatics. John Wiley & Sons, New York, 6.5.1–6.5.14. https://doi.org/10.1002/0471250953.bi0605s00

Razo-Mendivil U, Pérez-Ponce de León G, Rubio-Godoy M (2013) Integrative taxonomy identifies a new species of *Phyllodistomum* (Digenea: Gorgoderidae) from the twospot livebearer, *Heterandria bimaculata* (Teleostei: Poeciliidae), in Central Veracruz, Mexico. Parasitology Research 112: 4137–4150. https://doi.org/10.1007/s00436-013-3605-y

Ronquist F, Teslenko M, van der Mark P, Ayres DL, Darling A, Höhna S, Larget B, Liu L, Suchard MA, Huelsenbeck JP (2012) MrBayes 3.2: efficient Bayesian phylogenetic inference and model choice across large model space. Systematic Biology 61: 539–542. https://doi.org/10.1093/sysbio/sys029

Saiki RK, Gelfand DH, Stoffel S, Scharf SJ, Higuchi R, Horn GT, Mullis KB, Erlich HA (1988) Primer-directed enzymatic amplification of DNA with a thermostable DNA polymerase. Science 239: 487–491. https://doi.org/10.1126/science.239.4839.487

Schmidt HA, Strimmer K, Vingron M, von Haeseler A (2002) Tree-Puzzle: Maximum likelihood phylogenetic analysis using quartets and parallel computing. Bioinformatics 18: 502–504. https://doi.org/10.1093/bioinformatics/18.3.502

Schwarz G (1978) Estimating the dimension of a model. Annals of Statistics 6: 461–464. https://doi.org/10.1214/aos/1176344136

Siddiqi AH, Cable RM (1960) Digenetic trematodes of marine fishes of Puerto Rico. Scientific Survey of Porto Rico and the Virgin Islands 17: 257–369.

Sosa-Medina T, Vidal-Martínez VM, Aguirre-Macedo ML (2014) Comunidades de macroparásitos de la mojarra *Eucinostomus gula* y el pez globo *testudines*. In: Euán-Ávila JI (Ed.) La costa del estado de Yucatán, un espacio para la reflexión sobre la relación sociedad-naturaleza en el contexto de su ordenamiento ecológico territorial (Vol. I). CONABIO, México, 311–321.

Sosa-Medina T, Vidal-Martínez VM, Aguirre-Macedo ML (2015) Metazoan parasites of fishes from the Celestun coastal lagoon, Yucatan, Mexico. Zootaxa 4007: 529–544. https://doi.org/10.11646/zootaxa.4007.4.4

Stunžėnas V, Cryan JR, Molloy DP (2004) Comparison of rDNA sequences from colchicine treated and untreated sporocysts of *Phyllodistomum folium* and *Bucephalus polymorphus* (Digenea). Parasitology International 53: 223–228. https://doi.org/10.1016/j.parint.2003.12.003

Stunžėnas V, Petkevičiūtė R, Poddubnaya LG, Stanevičiūtė G, Zhokhov AE (2017) Host specificity, molecular phylogeny and morphological differences of *Phyllodistomum pseudofolium* Nybelin, 1926 and *Phyllodistomum angulatum* Linstow, 1907 (Trematoda: Gorgoderidae) with notes on Eurasian ruffe as final host for *Phyllodistomum* spp. Parasites and Vectors 10: 1–286. https://doi.org/10.1186/s13071-017-2210-9

Talavera G, Castresana J (2007) Improvement of phylogenies after removing divergent and ambiguously aligned blocks from protein sequence alignments. Systematic Biology 56: 564–577. https://doi.org/10.1080/10635150701472164

Tamura K, Nei M (1993) Estimation of the number of nucleotide substitutions in the control region of mitochondrial DNA in humans and chimpanzees. Molecular Biology and Evolution 10: 512–526. https://doi.org/10.1093/oxfordjournals.molbev.a040023

Tello GE (1999) Comparación de la helmintofauna de tres especies de peces en la laguna costera Río lagartos, Yucatán. BSc Thesis, Mérida, Mexico: Universidad Autonóma de Yucatán.

Tkach V, Pawlowski J, Mariaux J (2000) Phylogenetic analysis of the suborder Plagiorchiata (Platyhelminthes, Digenea) based on partial lsrDNA sequences. International Journal for Parasitology 30: 83–93. https://doi.org/10.1016/S0020-7519(99)00163-0

Travassos L (1922) Contribuições para o conhecimento da fauna helmintolojica brasileira XVII. Gorgoderidae brasileiras. Memórias do Instituto Oswaldo Cruz 15: 220–234. https://doi.org/10.1590/S0074-02761922000200015

Urabe M, Ishibashi R, Uehara K (2015) The life cycle and molecular phylogeny of a gorgoderid trematode recorded from the mussel *Nodularia douglasiae* in the Yodo River, Japan. Parasitology International 64: 26–32. https://doi.org/10.1016/j.parint.2014.09.003

Van Steenkiste N, Tessens B, Willems W, Backeljau T, Jondelius U, Artois T (2013) A comprehensive molecular phylogeny of *Dalytyphloplanida* (Platyhelminthes: Rhabdocoela) reveals multiple escapes from the marine environment and origins of symbiotic relationships. PLoS ONE 8: e59917. https://doi.org/10.1371/journal.pone.0059917

Winter (1959) Algunos tremátodos digéneos de peces marinos de aguas del Océano Pacífico del sur de California, USA y del litoral mexicano. Anales del Instituto de Biología, Universidad Nacional Autónoma de México 30: 183–225.

WoRMS (2020) *Xystretrum* Linton, 1910. http://www.marinespecies.org/aphia.php?p=taxdetails&id=416151 [2020-02-19]

Yamaguti S (1970) Digenetic Trematodes of Hawaiian Fishes. Keigaku Publishing Co.,Tokyo, 436 pp.

Yamaguti S (1971) Synopsis of Digenetic Trematodes of Vertebrates (Vol. 1). Keigaku Publishing Co., Tokyo, 1074 pp.

Yamanoue Y, Miya M, Matsuura K, Katoh M, Sakai H, Nishida M (2008) A new perspective on phylogeny and evolution of tetraodontiform fishes (Pisces: Acanthopterygii) based on whole mitochondrial genome sequences: Basal ecological diversification? BMC Evolutionary Biology 8: 1–212. https://doi.org/10.1186/1471-2148-8-212

Supplementary material 1

Table S1

Authors: Andrés Martínez-Aquino, Jhonny Geovanny García-Teh, Fadia Sara Ceccarelli, Rogelio Aguilar-Aguilar, Víctor Manuel Vidal-Martínez, Ma. Leopoldina Aguirre-Macedo

Explanation note: Comparative data of relevant taxonomic characters of *Xystretrum solidum* from this study, in contrast to the 14 congeneric *Xystretrum* spp.

Link: https://doi.org/10.3897/zookeys.925.49503.suppl1

Supplementary material 2

Figure S1

Authors: Andrés Martínez-Aquino, Jhonny Geovanny García-Teh, Fadia Sara Ceccarelli, Rogelio Aguilar-Aguilar, Víctor Manuel Vidal-Martínez, Ma. Leopoldina Aguirre-Macedo

Explanation note: Scanning electron microscopy (SEM) images of *Xystretrum solidum* (from five specimens collected in the Northern Yucatan Peninsula, Mexico). (**A**) Oral sucker, showing 13 pairs of papillae surrounding margin of oral sucker (locality: Chelem). (**B**) Stylet scar, showing 2 pairs of surrounding papillae and one lateral (dark and light green arrowhead, respectively) (locality: Ría Lagartos). (**C**) Forebody, showing 6 pairs of robust papillae (white arrowhead) (locality: Chuburna). (**D**) Oral sucker, showing 13 pairs of papillae surrounding anterolateral margin (locality: Chuburna). (**E**) Oral sucker, showing single pair in upper region inside oral sucker (red arrowhead) (locality: Chuburna). (**F**) Genital pore detail (locality: Chuburna). (**G**) Ventral sucker, showing long papillae on inner margin (white arrowhead) (locality: Chuburna). (**H**) Details of hindbody corrugation and demarcation of folds (locality: Chuburna). (**I**) Details of "pseudopapilles" on smooth lateral margins of hindbody (white arrowhead) (locality: Chuburna). (**J**) Oral sucker, showing 13 pairs of papillae surrounding margin of oral sucker (locality: Celestún). Colors of arrowheads in A, D and J as follows: Yellow arrowhead = 5 pairs of papillae on interior margin, surrounding mouth; Dark blue arrowhead = one pair of papillae posterolateral to interior margin; Light blue arrowhead = three pairs of papillae anterolateral to interior margin; Dark green arrowhead = 2 pairs of papillae on stylet scar; Light green arrowhead = one pair of papillae lateral to stylet scar; Black arrowhead = one pair of papillae on posterior external margin of oral

sucker. Scale bars: 100 μm (**A, J**); 50 μm (**B, D, E, F, G**); 200 μm (**C, I**); 20 μm (**H**); 200 μm (**I**).

Link: https://doi.org/10.3897/zookeys.925.49503.suppl2